Identifying the diverse functionalities and characteristics of the RNAi response against arthropod-borne viruses in mosquitoes

Dissertation

Christina Scherer

Hamburg

2021

Identifying the diverse functionalities and characteristics of the RNAi response against arthropod-borne viruses in mosquitoes

---

Dissertation

submitted in fulfillment of the requirements for the degree of

doctor rerum naturalium (Dr. rer. nat.)

Faculty of Mathematics, Informatics and Natural Sciences

Department of Biology

Universität Hamburg

&

Department of Molecular Entomology

Bernhard Nocht Institute for Tropical Medicine

Christina Scherer

Hamburg

2021

Thesis committee

Thesis supervisor
Prof. Dr. E. Schnettler
Group leader ‘Molecular Entomology’ at Bernhard Nocht Institute for Tropical Medicine, Hamburg
Universität Hamburg / BNITM

Thesis co-supervisor
Prof. Dr. I. Bruchhaus
Group leader ‘Protozoology’ at Bernhard Nocht Institute for Tropical Medicine, Hamburg
Universität Hamburg / BNITM

Day of oral defense: 02.07.2021

This research project was conducted as a member of the Leibniz Center Infection Graduate School “Infection”.

"The single biggest threat to man's continued dominance on the planet is a virus."

Joshua Lederberg

The Nobel Prize in Physiology or Medicine 1958

Table of contents

Abstract

Mosquitoes are known as important vectors of several arthropod-borne (arbo)viruses causing severe diseases in humans like West Nile Virus, Dengue virus or Zika virus. Although they often cause severe clinical manifestations in their vertebrate hosts, no apparent pathology is seen in their mosquito vector despite high viral replication levels, indicating an effective immune response against arboviruses in the mosquito vector. However, arbovirus infection generally result in a persistent infection, indicating the inability of the mosquito immune response to clear these viral infections.

The mechanism of RNA interference (RNAi) is a sequence-specific RNA degradation system that is known to act antiviral in a variety of organisms like plants and invertebrates. Three different pathways based on different classes of small RNAs are associated with RNAi: the microRNA, small-interfering RNA (siRNA) and PIWI-interacting RNA (piRNA) pathway. The exogenous siRNA (exo-siRNA) pathway is believed to be the main antiviral defense in arthropods, including mosquitoes and has been shown to be linked to vector competence.

Recently, evidence towards an antiviral activity of the piRNA pathway has emerged. Moreover, the formation of virus-derived cDNA (vcDNA), which subsequently is being incorporated into the vector mosquito genome as non-retroviral integrated RNA virus sequences (NIRVS) was reported; this results in the production of piRNAs from these incorporated genomic sequences, targeting actively replicating viral RNA.

The role of small RNAs in controlling arbovirus infection in mosquitoes and in shaping vector competence is widely recognized but the underlying mechanisms remain unknown. It also seems to be highly specific with regard to the virus species and the stage of infection. This study was designed to investigate the characteristics of the RNAi response against different arbovirus infections in vector mosquitoes during the acute and persistent infection phase.

In order to study the antiviral role of Argonaute-2 (Ago2) and Dicer-2 (Dcr2) as key players of the exo-siRNA pathway, two novel Ago2 knockout cell lines based on Aag2-AF5 cells (*Ae. aegypti*) were characterized and used together with a previously produced Dcr2-deficient cell line. Knockout of these key proteins also allows the general study of the function of the piRNA pathway without the interference of the siRNA pathway. Furthermore, characteristics of acute and persistent infection of various arboviruses with regard to small RNA production and functions of RNAi key proteins were explored with different approaches, including silencing of target proteins and small RNA sequencing. To elucidate the biological activity of virus-derived small RNAs, sensor constructs expressing viral sequences were employed. Eventually, an experimental set up was successfully created to investigate the formation of vcDNA, NIRVS and corresponding small RNAs as well as the (possible) generation of an adaptive immunity.

Overall, experiments confirmed the exo-siRNA pathway as the major antiviral defense mechanism in mosquitoes for all tested arboviruses with the exception of ZIKV. It was shown that the RNAi response highly varies related to the viral species infecting the mosquito. Moreover, the piRNA pathway is contributing to the antiviral immunity during *Bunyamwera orthobunyavirus* (BUNV) infection. Further experiments indicated, that an initial infection with Semliki Forest virus (SFV) or BUNV is able to confer an adaptive immunity in cells challenged with a recurring infection most likely mediated by the piRNA pathway.

The described experiments deliver new information and fundamental knowledge about the piRNA pathway and its wide-ranging responsibilities, interactions and functions. This study broadens the knowledge about the complex interactions of arboviruses and their arthropod vectors and implies further research topics and directions. Understanding the nature of virus-host interactions is of great medical and scientific importance. Discerning vector competence and identifying determinants behind antiviral responses in vector mosquitoes can aid to the development of intervention strategies to reduce arbovirus transmission and infection.

Zusammenfassung

Stechmücken sind als wichtige Vektoren verschiedener durch Arthropoden übertragener (Arbo-)Viren bekannt, die beim Menschen schwere Krankheiten verursachen wie das West-Nil-Virus, das Dengue-Virus oder das Zika-Virus. Obwohl sie in ihren Wirbeltier-Wirten oft schwere klinische Manifestationen verursachen, wird in ihrem Moskito-Vektor trotz hoher Virusreplikationsraten keine offensichtliche Pathologie beobachtet, was auf eine effektive Immunantwort gegen Arboviren im Moskito-Vektor hinweist. Eine Infektion mit Arboviren führt jedoch normalerweise zu einer persistenten Arbovirusinfektion, was auf die Unfähigkeit der Immunantwort der Stechmücke hinweist, diese viralen Infektionen zu beseitigen.

Der Mechanismus der RNA-Interferenz (RNAi) ist ein sequenzspezifisches RNA-Abbausystem, von dem bekannt ist, dass es in einer Vielzahl von Organismen wie Pflanzen und Invertebraten antiviral wirkt. Drei verschiedene Wege, die auf unterschiedlichen Klassen von kleinen RNAs basieren, werden mit RNAi in Verbindung gebracht: der microRNA, der small-interfering RNA (siRNA) und der PIWI-interacting RNA (piRNA) Weg. Es wird angenommen, dass der exogene siRNA (exo-siRNA) Weg die wichtigste antivirale Abwehr in Arthropoden, einschließlich Moskitos, darstellt und dass er im Zusammenhang mit der Vektorkompetenz steht.

In letzter Zeit wurden vermehrt Hinweise auf eine antivirale Aktivität des piRNA-Wegs gefunden. Darüber hinaus wurde über die Bildung von viraler cDNA (vcDNA) berichtet, die als nicht-retrovirale integrierte RNA-Virus-Sequenzen (NIRVS) in das Genom der Vektormücke eingebaut wird; dies führt zur Produktion von piRNAs aus diesen eingebauten genomischen Sequenzen, die sich gegen aktiv replizierende virale RNA richten.

Die Rolle von kleinen RNAs bei der Kontrolle der Arbovirus-Infektion in Moskitos und bei der Gestaltung der Vektorkompetenz ist weithin anerkannt, aber die zugrunde liegenden Mechanismen bleiben unbekannt. Sie scheint darüber hinaus spezifisch zu sein in Bezug auf die Virusart und das Stadium der Infektion. In dieser Studie wurden die Eigenschaften der RNAi-Antwort gegen verschiedene Arbovirus-Infektionen in Vektormücken während der akuten und persistenten Infektionsphase untersucht.

Um die antivirale Rolle von Argonaute-2 (Ago2) und Dicer-2 (Dcr2) als Schlüsselproteine des exogenen siRNA-Wegs zu untersuchen, wurden zwei neuartige Ago2-Knockout-Zelllinien auf Basis von Aag2-AF5-Zellen (*Ae. aegypti*) charakterisiert und zusammen mit einer zuvor hergestellten Dcr2-defizienten Zelllinie verwendet. Der Knockout dieser Schlüsselproteine erlaubt darüber hinaus auch die generelle Untersuchung der Funktion des piRNA Wegs ohne die Interferenz des siRNA Wegs. Darüber hinaus wurden die Charakteristika der akuten und persistenten Infektion verschiedener Arboviren im Hinblick auf die Produktion kleiner RNAs und die Funktionen der beteiligten RNAi-Proteine mit verschiedenen Ansätzen untersucht, einschließlich Silencing von Zielproteinen und Sequenzierung kleiner RNAs. Zur Aufklärung der biologischen Aktivität von viralen, kleinen RNAs wurden Sensor-Konstrukte eingesetzt, die virale Sequenzen exprimieren. Schließlich wurde erfolgreich ein Versuchsaufbau erstellt, um die Bildung von vcDNA, NIRVS und entsprechenden kleinen RNAs sowie die (mögliche) Generierung einer adaptiven Immunität zu untersuchen.

Insgesamt bestätigten die Experimente den exo-siRNA-Weg als den wichtigsten antiviralen Abwehrmechanismus in Mücken für alle getesteten Arboviren mit Ausnahme von ZIKV. Es konnte gezeigt werden, dass die RNAi-Antwort in Abhängigkeit von der Virusspezies, die die Mücke infiziert, stark variiert. Darüber hinaus trägt der piRNA-Signalweg zur antiviralen Immunität während einer Infektion mit dem Bunyamwera orthobunyavirus (BUNV) bei. Weitere Experimente zeigten, dass eine Erstinfektion mit Semliki Forest Virus (SFV) oder BUNV in der Lage ist, eine adaptive Immunität in Zellen zu induzieren, die eine Zweitinfektion abmildert. Diese adaptive Immunität ist wahrscheinlich mit Hilfe des piRNA-Signalweges entstanden.

Die beschriebenen Experimente liefern neue Informationen und grundlegendes Wissen über den piRNA-Signalweg und seine weitreichenden Aufgaben, Interaktionen und Funktionen. Diese Studie

erweitert das Wissen über die komplexen Interaktionen von Arboviren und ihren Vektoren und impliziert weitere Forschungsthemen.

Das Verständnis der Natur der Virus-Wirt-Interaktionen ist von großer medizinischer und wissenschaftlicher Bedeutung. Die Identifizierung von Determinanten hinter antiviralen Reaktionen in Vektormücken kann bei der Entwicklung von Interventionsstrategien zur Reduzierung der Arbovirusübertragung und -infektion helfen.

Abbreviations

Table 1: General abbreviations.

%	percent
(RT-)qPCR	(reverse transcription) quantitative PCR
Ae.	*Aedes*
approx.	approximately
arbovirus	arthropod-borne virus
as	antisense
BNITM	Bernhard Nocht Institute for Tropical Medicine
bp	basepair
BSL	biosafety level
C	capsid protein
CPE	cytopathic effect
CT	Cycle treshold
Cx.	*Culex*
D.	*Drosophila*
dd	double-distilled
DMEM	Dulbecco's Modified Eagle Medium
DNA	deoxyribonucleic acid
dNTP	deoxynucleotide triphosphate
dpi	days post infection
dpt	days post transfection
dsRNA	double-stranded ribonucleic acid
eGFP	enhanced green fluorescent protein
FBS/FCS	fetal bovine serum / fetal calf serum
GMEM	Glasgow Minimum Essential Medium
hpi	hours post infection
hpt	hours post transfection
kb	kilobase
L-15	Leibovitz L-15 medium
miRNA	microRNA
MOI	multiplicity of infection
mRNA	messenger RNA
n	number
ns	non-significant
nsP	non-structural protein
nt	nucleotide
p	p-value
PBS	Phosphate-buffered saline
PCR	polymerase chain reaction
PFU	plaque forming units
piRNA	PIWI-interacting RNA
PIWI	P-element induced Wimpy testis
pmol	picomol
RNA	ribonucleic acid
RT	room temperature
s	sense
siRNA	small interfering RNA

ssRNA	single-stranded ribonucleic acid
TCID50	50 % tissue culture infective dose
Tm	melting temperature
TPB	Tryptose phosphate broth
UTR	untranslated region

Table 2: Virus abbreviations.

BUNV	Bunyamwera orthobunyavirus
CFAV	Cell fusing agent virus
CHIKV	Chikungunya virus
CYV	*Culex* Y virus
DENV	Dengue virus
FHV	Flock House virus
ISV	Insect-specific virus
LACV	La Crosse orthobunyavirus
PCLV	Phasi Charoen-like phasivirus
RVFV	Rift Valley fever virus
SBV	Schmallenberg orthobunyavirus
SFV	Semliki Forest virus
SINV	Sindbis virus
WNV	West Nile virus
YFV	Yellow fever virus
ZIKV	Zika virus

1. Introduction

1.1. Viruses and pathology

Viruses have been accompanying all domains of life like plants, animals, bacteria and also humans for around 3-4 billion years [1]. The earth's virome is carefully estimated with 10^{31} viral particles of which most species are yet to be discovered [2, 3]. Viruses are often recognized as harmful pathogens, but the knowledge about viruses is expanding. Nowadays viruses are also used as cell therapy tools or vaccine delivery agents in a beneficial way. Evidence is also provided that viruses can act in a mutualistic way conferring drought tolerance in plants [4] or slowing down disease progression of HIV-infected patients co-infected with GB virus C (*Pegivirus C*) [5, 6].

Nevertheless, viruses are well known for their role as pathogens infecting all kinds of organisms and thereby having a tremendous effect on public health causing social and economic damage in all parts of the world, which is actually being demonstrated by the current pandemic caused by the severe acute respiratory syndrome-related coronavirus type 2 (SARS-Cov-2).

Global outbreaks caused by vector-borne viruses and their further geographical expansion due to the dispersal of their carriers have shown how important it is, to understand virus-host interactions and determinants of vector competence. Besides surveillance of recent outbreaks and vector population control tools, research focuses on the development of vaccines or antiviral medication to be able to prevent and control future vector-borne epidemics.

1.2. Arthropod-borne viruses and their distribution

Earlier outbreaks of viruses have shown how dangerous viral infections can be and how fast they are distributed especially when transmitted by biting arthropods such as ticks, mites, midges and mosquitoes. Those viruses are called arthropod-borne viruses (arboviruses). Transmitting arthropods serve as vectors and natural reservoir, maintaining the virus and thereby increasing the risk of recurring outbreaks. A lot of these arboviruses are zoonotic and have been responsible for millions of human infections with significant mortality and severe illness. Clinical manifestations of infection often include arthritis, hemorrhagic fever or encephalitis [7-9]. Moreover, these viruses do not only pose a risk to humans, but also to livestock all over the world endangering food security. Around 1880, first reports came up announcing the ability of mosquitoes to vector human pathogens, transmitting filarial worms and yellow fever virus [10-12]. To date, mosquitoes are seen as one of the major arboviral vectors being responsible for the transmission of many medically important arboviruses. Until now, countermeasures against most arboviruses have included reduction of severity of symptoms, vaccine development and controlling the mosquito vector.

Outbreaks of Zika virus (ZIKV; family *Flaviviridae*, genus *Flavivirus*) disease have been reported in Africa, the Americas, Asia and the Pacific region from time to time. Recent outbreaks were recorded some years ago, starting from Micronesia and French Polynesia in 2007, culminating in a large outbreak in Brazil in 2015 drawing more attention towards ZIKV and raising research efforts. Soon, ZIKV infection was identified as a cause of microcephaly and was found to be associated with Guillain-Barré syndrome [13, 14].

Another arbovirus causing estimated 390 million infections per year is dengue virus (DENV; family *Flaviviridae*, genus *Flavivirus*) of which around 100 million people suffer with clinical manifestations of mild or severe symptoms. Cases of DENV infection have tremendously increased from only 9 countries with severe dengue epidemics in 1970 to 100 countries where DENV is endemic nowadays. The threat of a possible outbreak of dengue is now also present in Europe with autochthonous cases reported in France and Croatia [15, 16]. Other arboviruses like West Nile virus (WNV; family *Flaviviridae*, genus

Flavivirus) or Chikungunya virus (CHIKV; family *Togaviridae*, genus *Alphavirus*) are also on the rise in Europe with autochthonous transmission reported for CHIKV in France and Italy and cases reported for WNV in Germany [17, 18].

The majority of these arboviruses belong to four different families:*Togaviridae*, *Bunyaviridae*, *Flaviviridae* and *Reoviridae* [19-21]. Two of the main vectors of medically important mosquito-borne viruses are the anthropophilic mosquitoes *Aedes aegypti* and *Ae. albopictus* (order *Diptera,* family *Culicidae*).

Figure 1 displays a map of the global distribution of the two species: *Ae. albopictus* is originally native to the forests of Southeast Asia [22], whereas *Ae. aegypti* as the main vector for yellow fever virus (YFV; family *Flaviviridae*, genus *Flavivirus*), DENV and CHIKV emerged from the sub-Saharan Africa [23]. *Ae. albopictus* is also a known vector for CHIKV and DENV and has just recently started to invade the Americas and particularly Europe. Conversely, *Ae. aegypti* has not established stable populations in Europe yet [19].

The map indicates that both species are rapidly invading new areas via shipping routes and along human movement like travel, speeded up by globalization. Arboviral emergence is also accelerated by the extensive urbanization of rural areas, leading to an extending habitat for *Aedes* mosquitoes following human colonization. In addition to this, climate change facilitates vector spread into more temperate regions and establishment of constant populations. The presence and ongoing dispersal to almost every continent is accompanied by the vectorial capacity for arboviruses, which are concurrently adapting to new environmental conditions of their hosts [7, 24-26].

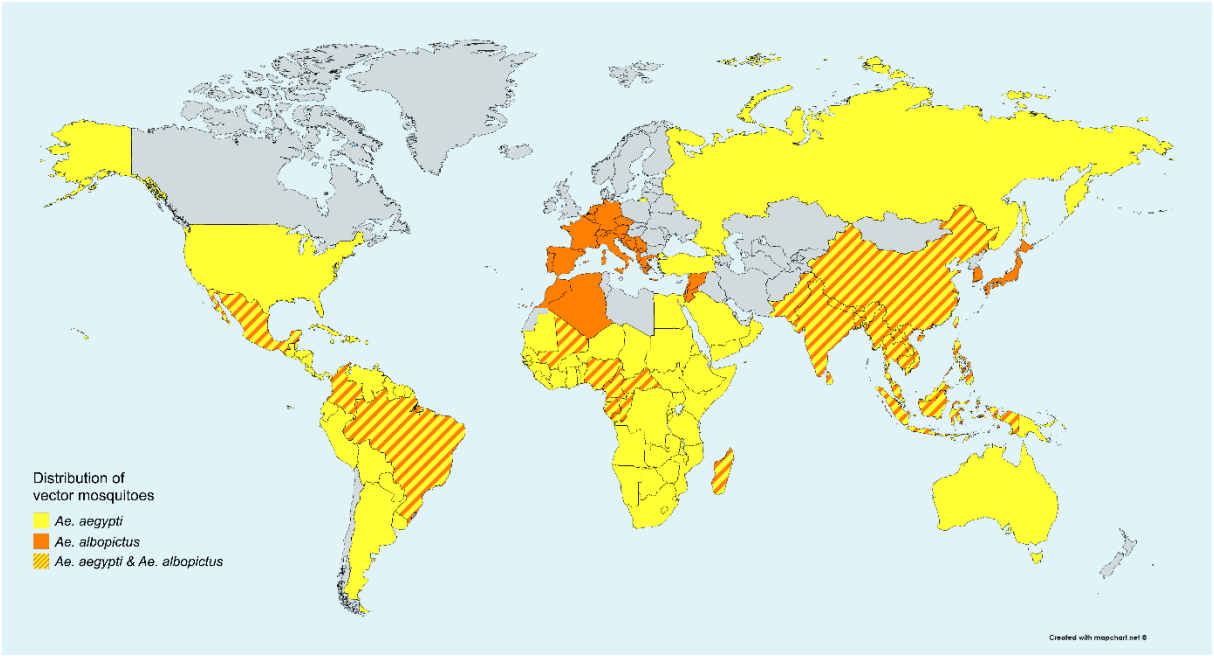

Figure 1: Worldwide distribution of vector mosquitoes Ae. aegypti (yellow) and Ae. albopictus (orange) [27-31]. *Countries in which populations of both vector mosquitoes were reported are depicted by combined yellow and orange stripes.*

The distribution of some important arboviruses transmitted by mosquitoes such as CHIKV, Rift Valley fever virus (RVFV; order *Bunyavirales*, family *Phenuiviridae*) and ZIKV is shown in Figure 2. Diversity of virus species around sub-Saharan Africa is well known and standing out. Mainly due to the effects of climate change, vector mosquitoes are also dispersing to more temperate regions like Europe or North America, increasing the risk of infections with to date tropical viruses. The congruence between vector distribution shown in Figure 1 and the incidence of various arbovirus infections underlines the close relation between vector dispersal and vectorial capacity as carriers of arboviruses.

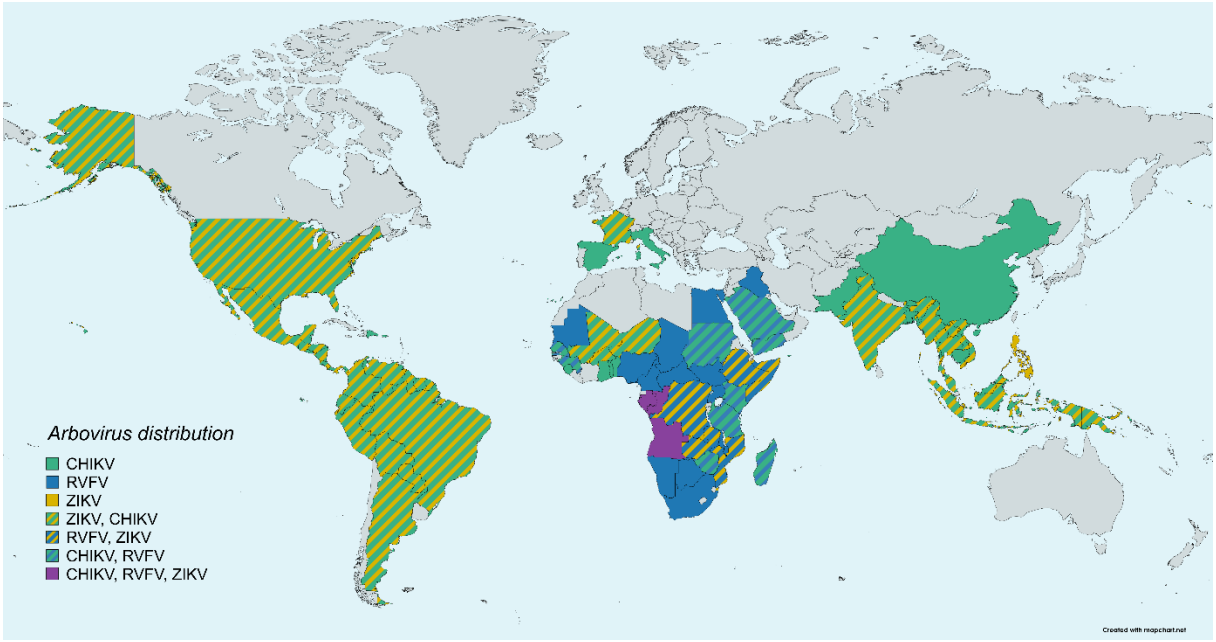

Figure 2: Worldwide distribution of CHIKV (green), RVFV (blue) and ZIKV (yellow).
Stripes indicate the common presence of two arboviruses in the same country. Purple labeling indicates countries in which CHIKV, RVFV and ZIKV are present altogether [32-39].

RVFV (family *Phenuiviridae*, genus *Phlebovirus*) is a zoonotic viral disease mainly seen in ruminants in sub-Saharan Africa but also infects humans. The clinical signs of RVFV infection include mild symptoms like fever, back pain or dizziness but also more severe symptoms like hemorrhagic fever and encephalitis. RVFV was identified in 1951 in South Africa [40] and periodic outbreaks have occurred throughout the African continent from time to time. In 2000, RVFV emerged in the Middle East with outbreaks in Saudi Arabia and Yemen causing the estimated death of 40,000 animals. To date, no vaccine is approved for the use in humans, but three veterinary vaccines are licensed although with limitations to the use in endemic regions [39].

CHIKV (family *Togaviridae,* genus *Alphavirus*) is a member of the Semliki Forest virus antigenic complex and infection has been reported to cause non-specific flu-like symptoms like high fever, headache, myalgia and arthralgia, but can also cause encephalitis [41]. In 2004, a large CHIKV epidemic dispersed from Kenya to India and Southeast Asia boosted by a glycoprotein mutation, which enhanced transmission by *Ae. albopictus [42]*. With its flu-like symptoms a diagnosis of CHIKV infection is difficult and the lack of a treatment protocol or vaccine makes it difficult to fight and manage the disease. Until today no licensed vaccine is available for CHIKV but several potential candidates are in clinical trial phases [43].

ZIKV (family *Flaviviridae*, genus *Flavivirus*) was first discovered in Uganda in 1947 [44] and is transmitted mainly by the yellow fever mosquito *Ae. aegypti*. The potential of this virus as a threat to humans became clearer in connection with a major outbreak in 2007 starting at the Pacific islands of Micronesia, having spread further to the Americas and Africa by 2015. The combination of efficient transmission in *Aedes* mosquitoes and further spread through mobility and travel raised the interest and research efforts on this virus. Several vaccines are under development but the decline of ZIKV infection reduces the effort in fighting the virus hence, no vaccine or drug is licensed to prevent ZIKV infection or treat it [45, 46].

1.3. Vector mosquitoes

Ae. aegypti and Ae. albopictus

Ae. aegypti and *Ae. albopictus* are mostly mammalian and anthropophilic feeders whereby only females show a blood-feeding behaviour. Hematophagy is a common feeding behaviour and until today around 14,000 species of hematophagous arthropods are known. Historically it has been shown that sand flies were already blood feeding on vertebrates around 100 millions of years ago thereby transmitting leishmanial parasites [47]. This indicates a long evolutionary development maybe also in conjunction with the transmission of arboviruses.

Ae. aegypti is a globally distributed vector accounting for 23 % of vector-borne diseases worldwide. It is the principal vector of DENV, CHIKV, ZIKV and YFV [48]. *Ae. albopictus*, the Asian tiger mosquito is a day-time biting insect with an aggressive biting strategy that has been playing a major role next to *Ae. aegypti* in the recent DENV and CHIKV outbreaks [22, 30, 49].

Mosquitoes use heat, CO_2 production, or different body odours to locate their potential hosts [50]. Female mosquitoes are required to feed on blood for the development of eggs. After egg deposition above the waterline, eggs hatch after the water level rises, as larvae and pupae of both mosquitoes are aquatic. It takes about 7-10 days for an egg to develop into an adult mosquito [22, 50].

Ae. aegypti has become a significant research tool as a vector for the above named arboviruses being able to easily adapt to diverse ecological conditions. For both species a high plasticity in ecological, physiological and genetic terms is known as both lay drought-resistant eggs, adapt easily to colder temperatures and have a high generation rate with 5-17 generations per year aiding them in quickly developing a resistance to insecticides [49, 50]. Availability of the whole genome sequence makes *Ae. aegypti* one of the most studied arthropods in arbovirus research and with it also the cell lines derived from it [50, 51].

1.4. Cell culture systems of vector mosquitoes

In vitro studies using cell culture systems faithfully represent essential aspects of virus-vector interactions and can provide preliminary evidence for further research *in vivo*. Continuous cell lines have been established also for vectors like *Ae. aegypti* and *Ae. albopictus* like Aag2 (*Ae. aegypti*) [52], C6/36 [53] and U4.4 cells (*Ae. albopictus*) and are extensively used as research tools. These tissue cultures are suggested to provide a more homogenous, sensitive and reproducible modelling system for mosquito immunity than live mosquitoes.

The Aag2 cell line was first derived from a pool of *Ae. aegypti* embryos and has been shown to be immunocompetent and the cell line genome was recently published [54-56]. Aag2 cell culture exhibits rather diverse morphologies, which was attributed to the presence of a wide variety of embryonic and

differentiated cell types [57]. Providing a more homogenous cell culture system, single-cell sorted cell lines and clones were generated [58, 59]. Many studies also use the C6/36 cell line which is derived from *Ae. albopictus,* but is limited in application as it has been shown to be defective in the antiviral immunity [60].

1.5. The arbovirus transmission cycle

Arboviruses are characterized by the unique trait of transmission by blood-sucking arthropods, which is also called ‚biological transmission'. This kind of transmission involves three individual and essential components: virus, vector and host. Furthermore, also non-biological transmission mechanisms like vertical transmission passing the infection on to the offspring, direct transmission through contact with infected tissues or mechanical transmission by contaminated mouth parts of the mosquito can occur [61].

Most arboviruses are zoonotic and maintain an enzootic sylvatic transmission cycle involving birds, rodents or non-human primates as reservoir hosts. Some arboviruses expand their range by entering rural epizootic cycles including domestic animals, which brings them closer to the human environment increasing the risk of spillover events. For example DENV has changed its host range from non-human primates as reservoirs to humans, becoming one of the most important arboviral pathogens for humans (urban epidemic cycle, Figure 3) [19, 62].

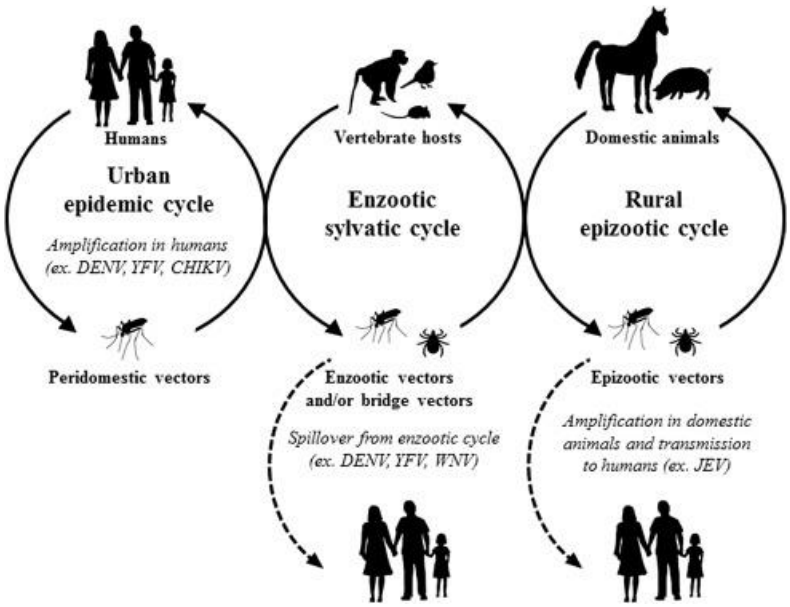

Figure 3: Arbovirus transmission cycles [62].
Arboviruses are initially maintained in enzootic sylvatic life cycle characterized by the reciprocal transmission to vertebrate hosts including birds, rodents or non-human primates. Spillover occurs through incidental feeding on humans. Some arboviruses might also adapt to domestic animals establishing a rural epizootic life cycle, which can also lead to epizootic cycle infecting humans. If the host range is altered by enzootic vectors, which switch from non-human primates to humans, an urban epidemic cycle can be established leading to adaptation and viral replication also in human hosts. YFV: yellow fever virus, JEV: Japanese encephalitis virus, DENV: dengue virus, CHIKV: Chikungunya virus, WNV: West Nile virus.

1.6. Transmission of arboviruses - the mosquito host

Efficient transmission of viruses between susceptible hosts is needed to ensure further viral replication and persistence. After ingestion of an infectious blood meal, the virus particles enter the midgut (Figure 4). From here, the virus has to pass the first physical barrier and enter the midgut epithelial cells in order to start replication. This midgut infection barrier (MIB) can prevent the virus from dissemination into other tissues and the establishment of a systemic infection in non-competent hosts. However, once the virus has set up its replication in the midgut epithelial cells, it has to pass the second physical barrier: the basal lamina which surrounds the midgut. Crossing this so-called midgut escape barrier (MEB), the virus is able to spread into other mosquito tissues like the fat body, hemocytes or nerve and muscle tissue via the hemolymph. In order to infect a vertebrate host, the virus is required to reach the salivary glands and pass the salivary gland infection barrier (SGIB). Upon infection of the salivary gland cells, the newly produced virions are stored in apical cavities of the acinar cells waiting to be transmitted during the next blood meal. If the virus can not be transmitted during the blood meal, this is referred to as the salivary gland escape barrier (SGEB) [63, 64].

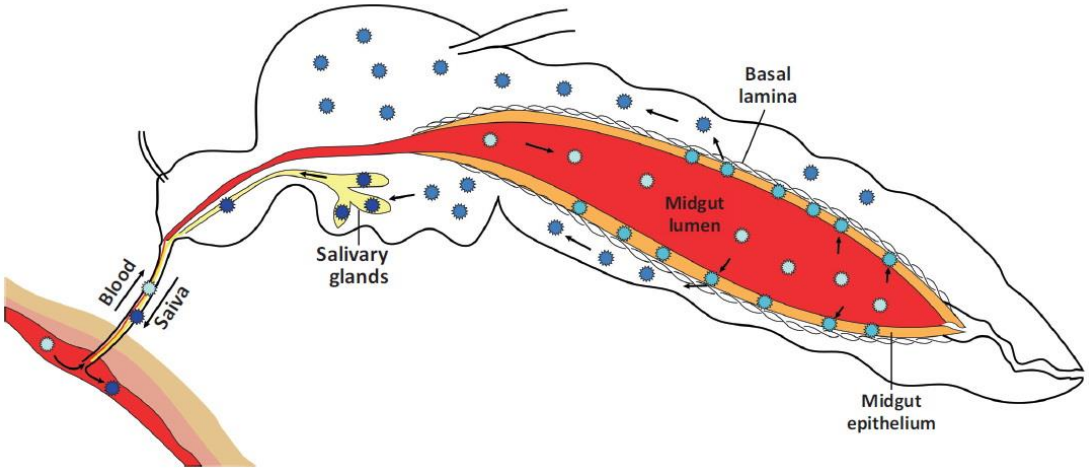

Figure 4: Virus infection of vector mosquitoes [64].
After ingestion of an infectious blood meal, the virus infects the midgut epithelium cells where it replicates. It subsequently passes the basal lamina surrounding the midgut and disseminates into various tissues of the mosquito establishing a systemic infection. The virus finally infects the salivary glands from where it can be transmitted to the next host during a blood meal. The dissemination of the virus through the mosquito is obstructed by various physical infection and escape barriers such as midgut infection and escape barrier and salivary gland infection and escape barrier [32].

1.7. Vector control strategies

Actual vector control strategies include larvicides, insecticides, insect repellents, mosquito nets and the desiccation and prevention of breeding sites. All of these measures contribute to the control of vector mosquitoes, but they have clear limitations. Mosquitoes like *Ae. aegypti* and *Ae. albopictus* can breed in very small amounts of water, which renders the control of breeding sites a Sisyphean task. As both species are also day-biting insects, mosquito nets have a limited impact as well. On top of that, the resistance to insecticides is increasing worldwide and poses the question whether their use is sustainable [65]. Several new vector-control strategies are therefore being developed, like the use of the endosymbiont *Wolbachia spp.*. These bacteria are found in many insects and were shown to be able to prevent DENV and CHIKV transmission [66-71]. Mating of *Wolbachia*-infected males with uninfected females leads to sterile eggs and population suppression thereby limiting arbovirus dispersion [66, 72]. The sterile insect technique using radiation which leads to sterile eggs has been used for a long time to control mosquito population, similar to the *Wolbachia*-based approach [73].

Other novel control studies involve the genetic manipulation of mosquitoes, being pushed by the recent advances in mosquito genetics and the CRISPR/Cas9 technology. This includes attempts to create immunity in female mosquitoes against arbovirus infection or inducing death upon infection. First reports of a genetically modified *Ae. aegypti* mosquito termed OX513A released in areas of Brazil, with a high incidence of DENV and ZIKV cases, indicated significant reductions in vector abundance. The OX513A is carrying a self-limiting gene, which renders mating between modified males and wild-type females unproductive [74]. However, introducing genetically modified mosquitoes into the wild harbours various risks. Ensuring it is not leading to further ecological damage is challenging, but can provide novel strategies to control arbovirus outbreaks.

1.8. Replication and genome structure of model arboviruses

Genetically related viruses from the same family are often determined by similar core viral traits such as genome length and organization, encoded proteins and viral life cycle and transmission. Although sharing structural and genomic similarities, not all arboviruses from the same family pose a major threat to human and animal health. Instead, related model viruses can be useful tools to study general characteristics shared by other representatives of the same family or genus. Model viruses of different arbovirus families are widely used in studies like SFV or Sindbis virus (SINV; family *Togaviridae*, genus *Alphavirus*). The model viruses used in this study are introduced below giving an overview of general characteristics.

1.8.1. Semliki Forest virus

Semliki Forest virus (SFV; family *Togaviridae*, genus *Alphavirus*) was first discovered in 1942 in Uganda [75] and is known to cause disease mainly in rodents but also in other mammals. SFV is extensively used in biological research as a model virus for other representatives of the *Alphavirus* genus like CHIKV, SINV, Mayaro virus or various equine encephalitis viruses.

The virion is enveloped with a spherical, icosahedral structure, approximately 65-70 nm in diameter and possesses a positive-sense, single-stranded RNA genome ((+)ssRNA) of 11 - 12 kb, which is capped at the 5‘ end and polyadenylated at the 3‘ end.

Upon attachment of the viral glycoproteins to a host receptor, the virion is endocytosed into the host cell via clathrin-mediated endocytosis. After fusion with the host endosomal membrane, the viral RNA genome is released into the cytoplasm of the host cell [76, 77]. The (+)ssRNA genomic strand of SFV serves both as template for viral replication and viral mRNA and encodes two open reading frames (ORFs) that in turn are translated into polyproteins, which are processed and cleaved by host and viral proteases (Figure 5). The non-structural polyprotein, encoded in the first ORF of the viral genome, is processed into proteins essential for RNA synthesis, like genome replication and transcription. The RNA-dependent RNA polymerase (RdRp) is expressed by suppression of termination at the end of the polyprotein coding sequence. Replication takes place in the cytoplasm at the surface of endosomes by synthesis of new (+)ssRNA genomes via the intermediate production of the negative-sense single-stranded RNA ((-)ssRNA) of SFV. In the late phase of infection, the subgenomic RNA is transcribed from the second ORF, leading to the production of the structural polyprotein, which is processed into the capsid protein, glycoproteins and further structural proteins needed for virion assembly. After capsid assembly in the cytoplasm, the newly produced virion is enveloped by budding at the plasma membrane and is released from the cell [78-80].

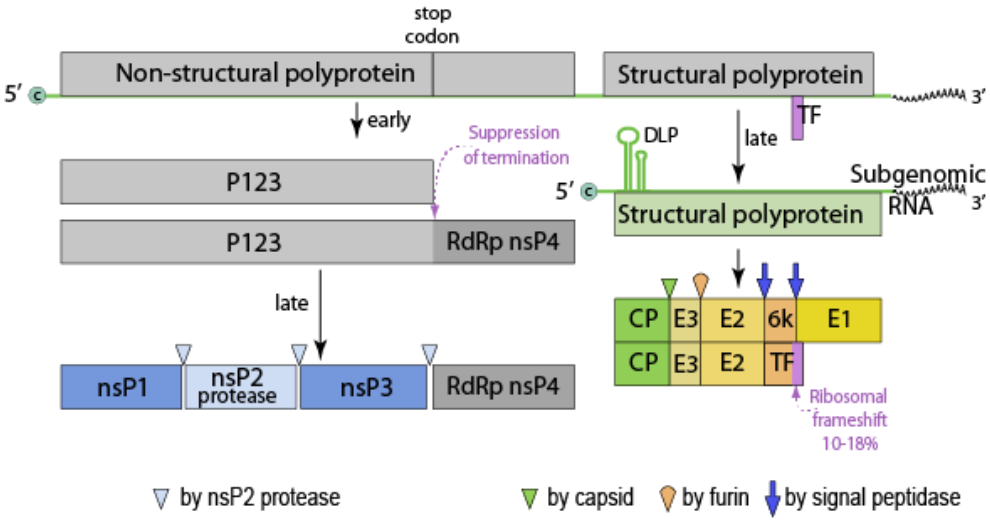

Figure 5: Alphavirus genome structure.
The non-structural proteins are translated from a polyprotein precursor encoded by the first ORF of the alphavirus genome while the structural proteins are translated from a sub-genomic RNA. The ns-polyprotein is processed and cleaved by host and viral proteases while the viral RdRp is expressed by suppression of termination at the end of the non-structural polyprotein. After establishment of replication components, the structural polyprotein is expressed and further processed into the capsid protein (CP), glycoproteins E3 and E2 and additional proteins 6k, TF and E1. (ViralZone, SIB Swiss Institute of Bioinformatics; 2021)

1.8.2. Bunyamwera orthobunyavirus

Bunyamwera orthobunyavirus (BUNV, order *Bunyavirales*, family *Peribunyaviridae*) was first discovered in 1943 in Uganda and can infect humans and animals by transmission via the *Ae. aegypti* mosquito [81, 82]. New emerging bunyaviruses like the severe fever thrombocytopenia syndrome virus (family *Bunyaviridae*, genus *Phlebovirus*) [83] are an increasing threat due to the expanding range of vectors and targeted hosts inducing a diverse host pathogenicity affecting humans and livestock and being suspected to cause major epidemics. Although BUNV does not constitute a major threat to humans and animal health, it is an ideal model to study segmented (-)ssRNA viruses like the medically important RVFV, Oropuche virus or La Crosse orthobunyavirus (LACV; order *Bunyavirales*, family *Peribunyaviridae*).

The BUNV virion is enveloped with a spherical structure and a diameter of 80 - 120 nm. Its genome is tripartite with the L-segment (approx. 6.9 kb) encoding the viral RdRp, while the M segment (approx. 4.5 kb) encodes for the viral glycoproteins Gn and Gc as well as the non-structural protein NSm. The small S-segment (approx. 1 kb) encodes the N and the non-structural NSs protein which are translated from overlapping ORFs [84] (Figure 6). The coding regions of all segments are flanked by 3‘ and 5‘ untranslated regions (UTR), which serve as promoters for transcription and replication. Moreover, they provide a signal for encapsidation by the N protein to form ribonucleic particles and are also suggested to play a role in the packaging of virions.

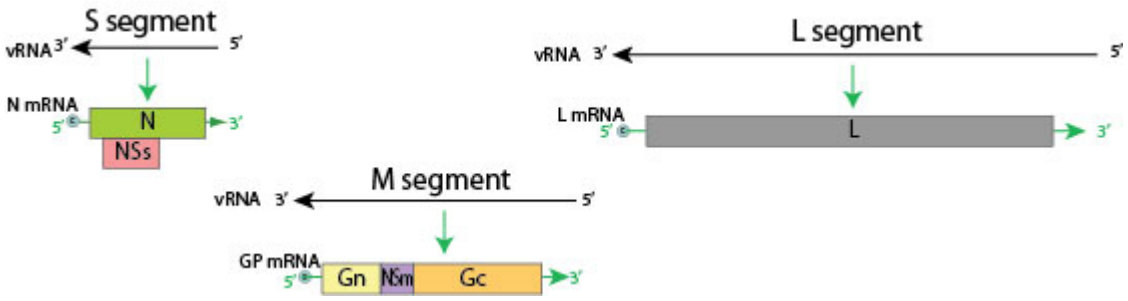

Figure 6: Bunyamwera orthobunyavirus genome.
The three segments L, M and S encode for six viral proteins. The L-segment encodes the viral RdRp, while the M-Segment expresses the glycoproteins Gn and Gc and the non-structural protein NSm required for virus assembly [85]. The S-segment codes for the N protein, which encapsidates genomic RNA to form ribonucleoproteins (RNPs) and the non-structural NSs protein by leaky ribosomal scanning using an alternative AUG start codon [86]. (ViralZone, SIB Swiss Institute of Bioinformatics; 2021)

The BUNV virion attaches to host cell receptors through its glycoprotein heterodimers (Gn-Gc) and is endocytosed into vesicles through clathrin-dependent endocytosis into the host cell (Figure 7). After vacuolar acidification, the virus membrane fuses with the vesicle membrane and the encapsidated segments are released into the cytoplasm. The viral RdRp binds to the promoter on each segment and transcribes the mRNA from the negative-sense viral RNA. mRNAs are already capped by the polymerase using cap snatching. After their synthesis, the glycoproteins form a heterodimer in the endoplasmatic reticulum (ER) and transit to the Golgi apparatus to be packed. Simultaneously, the negative-stranded RNA genome of BUNV is replicated via positive-sense intermediates. The newly produced ribonucleoproteins are then transported to the Golgi apparatus to be assembled into virions, which are budding into Golgi membrane-derived vesicles and are shuttled to the cell membrane. The vesicle membrane fuses with the plasma membrane and releases the viral particles from the cell [84, 85, 87].

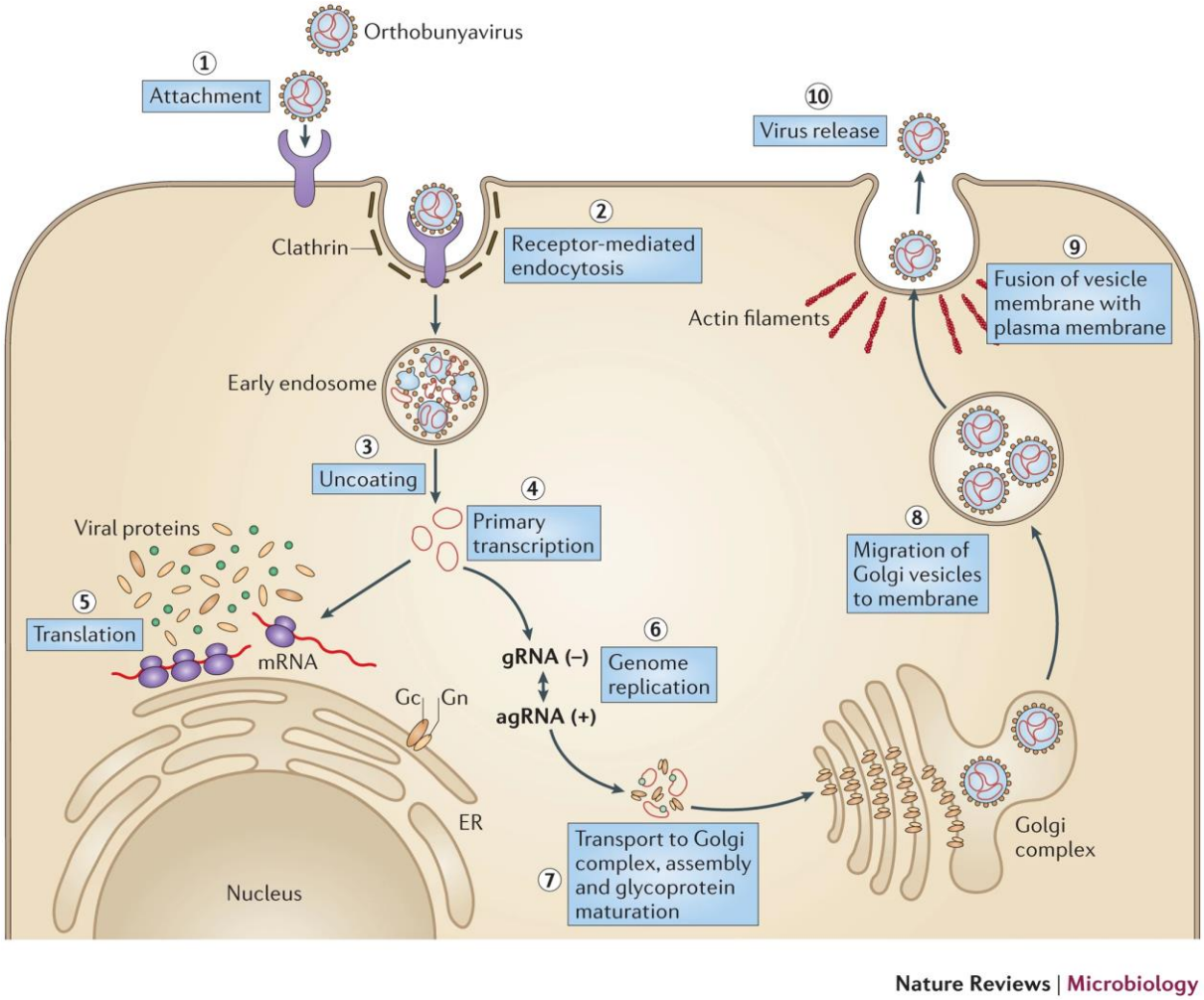

Figure 7: Orthobunyavirus replication cycle.

Entry of the BUNV virion is mediated by clathrin-dependent endocytosis (2) upon binding of the BUNV glycoproteins to host cell receptors (1). Acidification of the endosome leads to virion uncoating (3) and fusion of the viral membrane with the endosomal membrane releasing the viral RNA into the cytoplasm. The viral RdRp catalyses the primary transcription of viral mRNAs (4). Following translation of the mRNAs (5), the glycoproteins Gn and Gc dimerize in the ER and transit to the Golgi apparatus for packaging using a signal in the transmembrane domain of Gn. Additionally, the negative-strand RNA genome of BUNV (gRNA (-)) is replicated producing positive-sense antigenomes (agRNA (+)) for further genome replication in the virus factory (6). The produced ribonucleoproteins (RNPs) are then transported to the Golgi complex where virus particles are assembled and bud into Golgi membrane-derived vesicles (7). Golgi vesicles containing virions are trafficked to the cell surface (8) where the vesicle membrane fuses with the plasma membrane to release the viral particles (9) under participation of actin filaments [86].

1.8.3. Zika virus

Zika virus (ZIKV, family *Flaviviridae*, genus *Flavivirus*) was first isolated in 1947 from a rhesus monkey (*Macaca mulatta*) in Uganda, Africa. It has gained more attention and research efforts were increased after a major outbreak in Brazil in 2015 [88]. ZIKV is an enveloped virus with a spherical structure and a virion size of about 50 nm in diameter.

ZIKV has a (+)ssRNA genome structure similar to SFV and a genome size of ~ 11 kb. The 5‘ end of the genome has a methylated cap structure, but it is not polyadenylated at the 3‘ end. Instead, a loop structure is leading to the formation of a subgenomic flavivirus RNA (sfRNA). The positive-sense RNA genome serves both as mRNA and template for replication, expressing a single polyprotein (Figure 8).

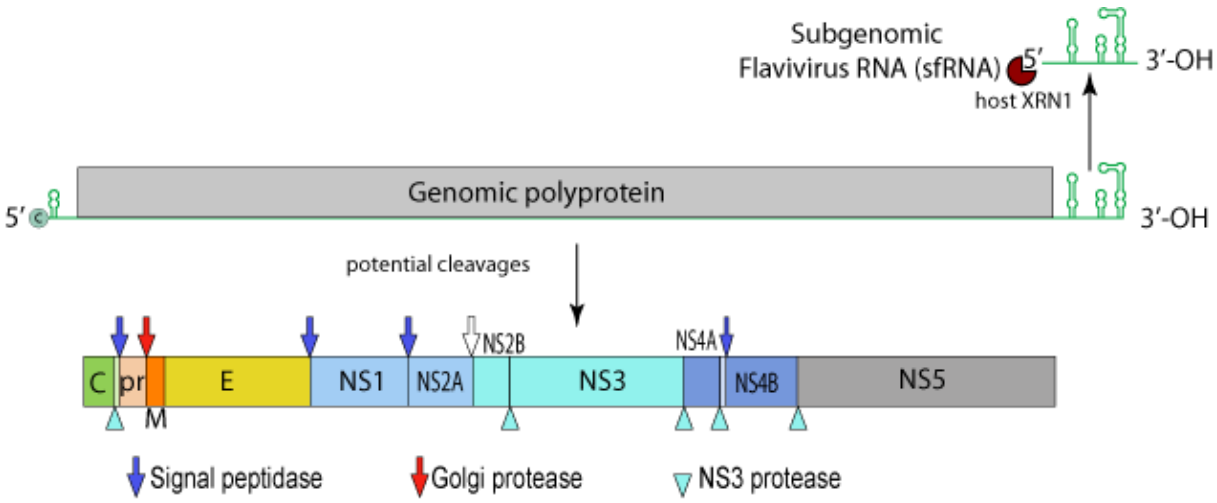

Figure 8: ZIKV genome structure.
ZIKV is a (+)ssRNA virus with a cap structure at the 5‘ end. The RNA is translated into a single polyprotein, which is cleaved into three structural (C, prM, E) and seven non-structural proteins (NS1, NS2A, NS2B, NS3, NS4A, NS4B, NS5). The structural proteins form the viral particle with the capsid protein (C), membrane protein (pr-M) and surface glycoprotein E, while the non-structural proteins assist in replication and packaging of the genome. The polyprotein is cleaved by host and viral proteases as assigned by red and blue arrows and triangles, respectively [89]. (ViralZone, SIB Swiss Institute of Bioinformatics; 2021)

After attachment of the viral glycoprotein E to host receptors, the virus enters the cell via clathrin-dependent endocytosis, followed by membrane fusion and release of the viral genome [90]. The positive-sense RNA genome is translated into a single polyprotein, which is cleaved by host and viral proteases into 10 structural and non-structural proteins [91]. Replication and virus assembly takes place at the surface of the endoplasmic reticulum (ER) in specialized viral compartments. The virion then buds from the ER and is transported to the Golgi apparatus for maturation and subsequent release of the viral particle through exocytosis [89].

1.9. Vector competence

Transmission of many viruses is dependent on complex relationships that exist between virus, vector and host. Arthropod-borne viruses are transmitted by vectors such as ticks, mites, midges and mosquitoes, whereas this study focuses on mosquitoes. Hence, vector competence describes the ability of a mosquito to acquire an arbovirus, replicate it and transmit it to the next host.

Extrinsic factors such as environmental conditions, proximity of vector and host populations and their density and composition determine whether a vector mosquito will come in contact with a suitable vertebrate host [24]. Intrinsic factors such as genetic diversity, host immune response and the presence of interacting microbes influence the ability of mosquitoes to become infected with an arbovirus after an infectious blood meal and to subsequently transmit the virus successfully to a naïve, susceptible host. In addition, also environmental conditions such as temperature influences intrinsic factors by affecting viral replication and genetic expression of determinants for vector competence in the mosquito [24].

As vector competence is a complex phenotype that always evolves depending on the virus-host interactions, it is not surprising that variability in vector competence is reported. Differences do not only exist between geographic distributions or species of mosquitoes but also in the same population between different viruses and viral strains [92]. Despite their huge impact as vectors, little is known about the specific factors and mechanisms controlling vector competence in mosquitoes, specifically for arboviruses. Most knowledge comes from *Ae. aegypti* where the reported susceptibility to arboviral infections varies strongly. So far, it has been shown that almost every population of *Ae. aegypti* is naturally susceptible to some kind of arbovirus infection. Some are even completely susceptible to ZIKV, DENV or CHIKV infections [92].
Genetic variation especially of RNA viruses is highly dynamic and is shaped by selection pressure and bottlenecks like the physical infection and escape barriers setup by the midgut or the salivary gland barriers. High mutation rates of single-stranded RNA viruses and adaptation to replicate in different hosts strongly shapes variations in vector competence [92]. Even a single point mutation was shown to confer increased infectivity in *Ae. albopictus* for CHIKV [93, 94].

Mosquito-associated microbiota play an important role in nutrition and digestion of mosquitoes and maturation of the innate immune system of insects, but studies have also shown that some bacteria can aid in controlling mosquito populations like *Bacillus thuringiensis* or copepods as natural enemies of mosquito larvae. Some *Wolbachia* strains have been shown to reduce or even confer resistance to arboviral transmission, specifically in *Ae. aegypti* shown for DENV or CHIKV infection [49, 66, 95, 96].

Once ingested via blood meal, arboviruses are not only challenged by physical barriers, but are confronted with the primary immune components of the mosquito in the form of hemocytes. These hemolymph cells are involved in processes such as pathogen recognition, phagocytosis or the production of lytic enzymes initiating diverse antiviral pathways and mechanisms. The genetic makeup and host immune response of a mosquito species and the interplay with the arbovirus thereby strongly contributes to vector competence [97].

1.10. Antiviral immune pathways and cellular processes in insects

Insects seem to lack the classical adaptive immune system of vertebrates shaped by pathogen-specific interactions and creation of an immunological memory. The innate immune system of insects typically comprises physical barriers such as the midgut infection and escape barriers, cellular and humoral responses which are launched depending on the invading pathogen [94, 98, 99]. To characterize antiviral immunity, the model organism *D. melanogaster* has been used widely and revealed a conserved but highly dynamic immune system with mechanisms evolving in dipterans and especially *Ae. aegypti*.

Typically cellular and humoral responses are activated upon a pathogen crossing the physical barriers. The cellular response is engaged almost immediately and comprises actions such as nodulation, encapsulation, phagocytosis, apoptosis and autophagy. During nodulation, invading pathogens are recognized and entrapped by aggregation of transformed hemocytes. Encapsulation refers to the binding of hemocytes to larger targets to entrap them while phagocytosis leads to destruction of the pathogen upon recognition and engulfment by plasmatocytes or granulocytes [99, 100].

The humoral response is activated later than the cellular mechanisms, although there is an effective cross-talk between both immune types in insects. Typically, it induces the production of antimicrobial peptides (AMP) upon infection by activating signaling pathways that release those AMPs into the hemolymph like defensins, cecropins, attacins and drosomycins [101, 102].

Figure 9 shows an overview of the different pathways involved in antimicrobial and antiviral immunity in dipteran insects.

Toll and Imd pathway

Toll and Imd are both nuclear factor κB (NF-κB) pathways which are triggered mainly by bacteria or fungi and in the end release the NF-κB transcription factor which relocates into the nucleus inducing the transcription of various immune effectors like AMPs [103] (Figure 9). Although it was suggested for Toll and Imd pathways to act antiviral against CHIKV and DENV in *Ae. aegypti* [104], side effects of AMP-release and underlying mechanisms are not fully understood [94].

JAK-STAT pathway

The Janus kinase - signal transducer and activator of transcription (JAK-STAT) pathway is a conserved mechanism found in mammals and insects. It does not only regulate developmental processes but also orchestrates the mammalian immune response and confers antiviral immunity, which was suggested for DENV and ZIKV [105-109]. Upon cytokine binding to the extracellular domain of the Domeless receptor, phosphorylation and resulting dimerization of Stat92E is induced further downstream and its translocation into the nucleus and the transcription of several JAK-STAT dependent genes [110] (Figure 9). It was also suggested that Dicer 2, a key protein of the exogenous small interfering RNA (siRNA) pathway, mediates expression of Vago, a cytokine that is secreted upon infection with WNV and DENV in *Drosophila* and *Culex* mosquitoes. Vago in turn is suggested to activate the JAK-STAT pathway to support antiviral measures of the mosquito, although no expression was reported in Aag2 cells recently [103, 111, 112]. Although it is known that the JAK-STAT pathway and the RNAi response are important antiviral defense mechanisms in mosquitoes, it is not fully understood how they communicate with each other.

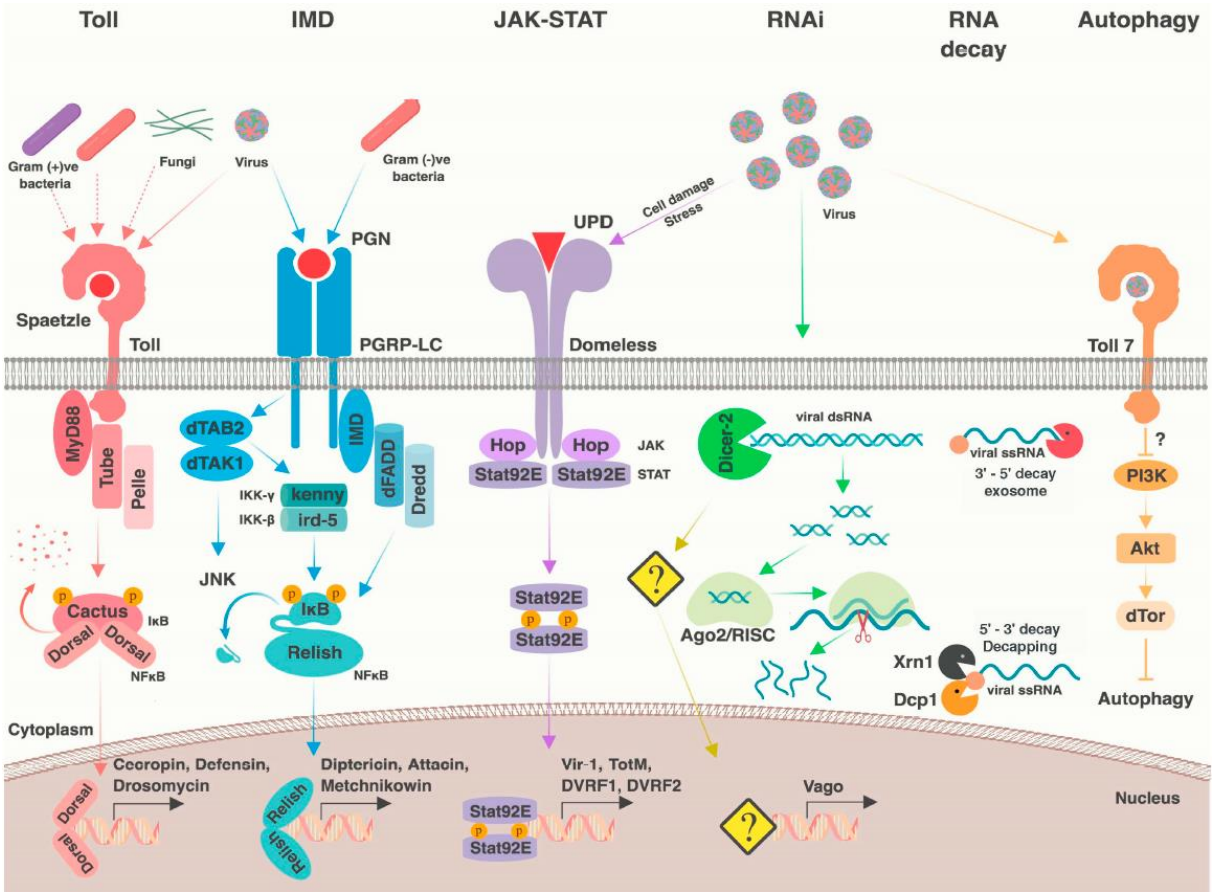

Figure 9: Antiviral innate immune pathways in dipteran insects.
***Toll pathway**: Detection of pathogen-associated molecular patterns (PAMPs) by pathogen recognition-receptors leads to the proteolytic maturation of Spaetzle, which binds to and activates Toll (dotted arrows). Activated Toll recruits adapter proteins MyD88, Tube and Pelle, which targets Cactus for proteasomal degradation via phosphorylation. Cactus degradation releases the transcription factor Dorsal (Rel1 in mosquitoes) or Dif (Dorsal-related immune factor) when activated in response to bacterial infection. These translocate to the nucleus and activates the transcription of Toll pathway-regulated genes (e.g., cecropin, defensin and drosomycin). **IMD pathway**: Gram-negative PAMPs (e.g. peptidoglycan) bind to peptidoglycan recognition protein, PGRP-LC (or PGRP-LE) and signal through the adapter molecules IMD (Immune Deficiency) and dFADD (Drosophila Fas-associated death domain). This stimulates the caspase Dredd (Death-related ced-3/Nedd2-like protein), dTAK1 (Drosophila transforming growth factor ß-activated kinase 1), and dTAK1 adapter protein dTAB2 (TAK1-binding protein 2). These proteins signal through the JNK pathway, and activate the IκB kinases kenny and ird-5, which phosphorylate the C-terminal tail of the transcription factor Relish (Rel2 in mosquitoes), leading to its subsequent activation via proteolytic cleavage by Dredd. Activated Relish translocates to the nucleus and drives the expression of genes regulated by the IMD-pathway (e.g. diptericin, attacin and metchnikowin). **JAK-STAT pathway**: Virus infection, possibly through induction of stress or cellular damage, triggers the activation of the JAK (Janus kinase)-STAT (signal transducers and activators of transcription) pathway, which begins with the binding of a cytokine of the unpaired (upd) family to the dimeric receptor, domeless. Subsequently, the receptor-associated JAK-tyrosine kinase hopscotch phosphorylates the cytoplasmic tail of domeless, leading to the recruitment of Stat92E. After JAK-mediated phosphorylation, Stat92E proteins dimerize and shuttle to the nucleus to activate the transcription of genes such as vir-1, TotM, DVRF1 and DVRF2. **RNAi pathway**: Viral double-stranded RNA are recognized and processed by Dicer-2 (Dcr2) into 21 nt small interfering RNAs (siRNAs), which are then loaded onto Argonaute-2 (Ago2). Ago2 degrades one of the two RNA strands and uses the other strand as a guide RNA to target complementary viral sequences. Dcr2 can also activate the expression of the cytokine Vago through an unknown pathway (visualized as '?' in the figure). **RNA decay pathways**: Single-stranded viral mRNA can be targeted in the 3'–5' direction through the RNA exosome degradation pathway. 5'–3' degradation occurs through decapping enzymes Dcp1 and Dcp2 and the RNA exonuclease Xrn1. **Autophagy**: Some viruses can bind to the transmembrane receptor Toll-7, resulting in the induction of autophagy. This is most likely in an indirect manner by negatively regulating the PI3K (phosphatidylinositol 3-kinase)-Akt pathway. (Adapted from [94])*

1.11. RNA interference in mosquitoes

Most of the knowledge about RNA interference (RNAi) is derived from the fruit fly *D. melanogaster*, but the majority of the findings can be transferred to mosquitoes as both belong to the dipterans and share many biological features and characteristics. Differences in the RNAi pathway between the two organisms are described hereafter.

The discovery of the RNAi mechanism began in the 90s in plants with the description of a cellular-based, sequence-specific RNA degradation system acting antiviral against Tobacco etch virus and was first referred to as ‚post-transcriptional gene silencing' [113]. More reports were published on RNAi discovered in plants and fungi [114] until it was also discovered in animals. The model organism *Caenorhabditis elegans* was the first animal in which RNAi was described and secondly double-stranded RNA (dsRNA) was identified as the inducer molecule for the whole mechanism in 1998 [115]. In the same year, the existence and gene silencing capability of RNAi was shown for a variety of other organisms like *Drosophila*, yeast (*Saccharomyces*) or trypanosomes [116] proving effectiveness of RNAi for a wide range of invertebrates and additionally providing evidence for an ancient origin for the RNAi mechanism.

Shortly after this, in 2001, 21 nucleotide (nt) long siRNAs were shown to be the effector molecules of RNAi, capable of silencing heterologous but also endogenous genes in mammalian cells [117, 118]. Until then, the use of RNAi for experiments was limited to flies, plants and worms as the introduction of long dsRNAs into mammalian cells provoked the induction of the interferon response suspending RNAi. The finding that in both dsRNAs and 21 nt long siRNAs are able to silence genes also in mammalian cells was a breakthrough [119].

Further research then revealed the main components and effector proteins of the siRNA pathway: the dsRNA endonuclease Dicer 2 (Dcr2), which cleaves dsRNA substrates into 21 nt long siRNAs, the effector complex called ‚RNA-induced silencing complex' (RISC) [120] in which siRNAs are subsequently loaded and the protein Argonaute 2 (Ago2), which exhibits the slicer activity for the target RNA as part of the RISC [121]. This data provided the general understanding of RNA-mediated silencing with mainly long dsRNAs that are processed by Dcr2 into 21 nt siRNAs which are then incorporated into the RISC complex. While one strand of the siRNA duplex is dismissed, the other one is used as a guide strand by Ago2 to cleave complementary target RNAs.

Nowadays, RNAi is known to be active in many eukaryotes leading to inhibition of gene expression, post-transcriptional silencing, but also for providing an antiviral defense mechanism. These functionalities differ fundamentally between vertebrates and invertebrates. Invertebrates not only lack the genes for type I interferons or protein kinase R and other antiviral effector molecules and pathways, they also do not possess the adaptive immune system present in vertebrates. [122, 123]. Whether RNAi is also active as an antiviral defense mechanism in mammals is still under discussion, although RNAi has been shown to be active at least in infected, undifferentiated mouse embryonic cells [124, 125].

Knowledge about the RNAi mechanism has strongly expanded throughout the last 20 years. Today three different pathways based on different classes of small RNAs are associated with RNAi: the microRNA (miRNA), small-interfering RNA (siRNA) and PIWI-interacting RNA (piRNA) pathway (Figure 10).

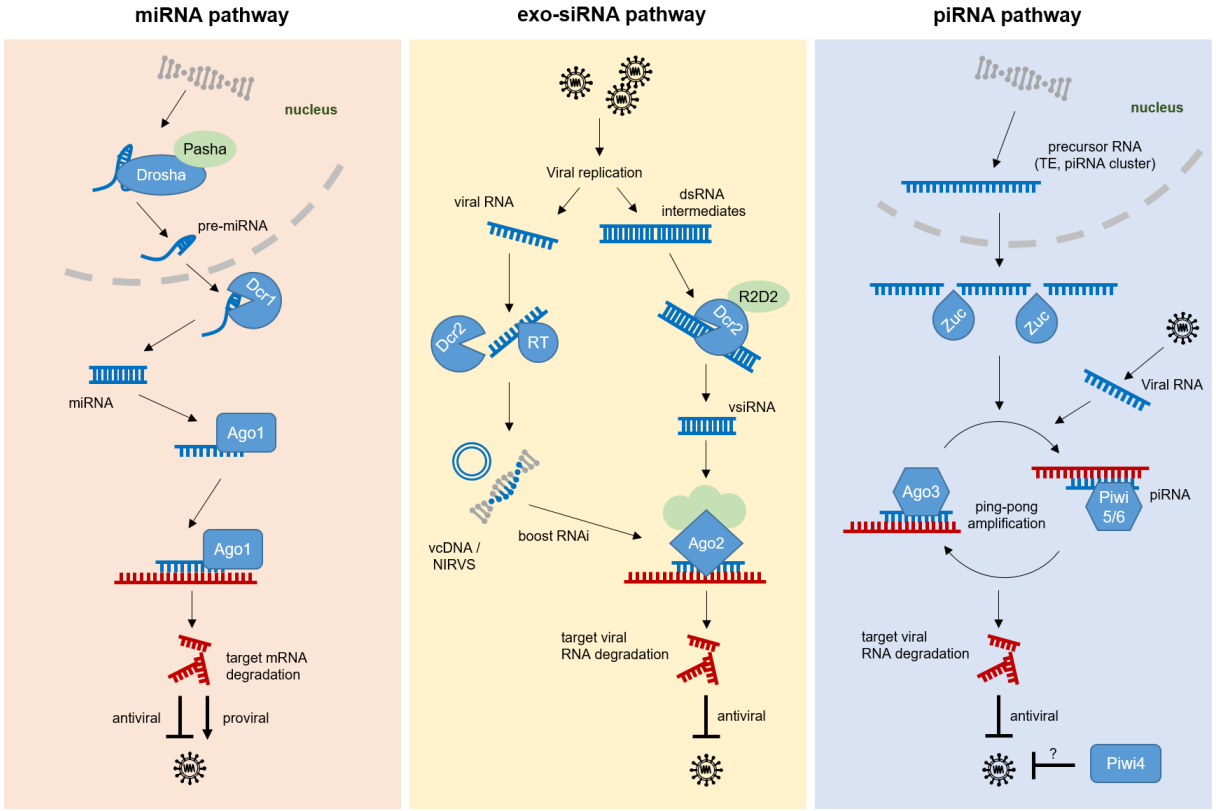

Figure 10: Schematic representation of small RNA pathways associated with RNAi.
miRNA pathway: *primary single-stranded miRNAs (pri-miRNAs) are transcribed from DNA sequences. They are further processed into precursor miRNAs (pre-miRNAs) by the enzyme Drosha and Pasha and exported from the nucleus. Upon slicing by Dicer1 (Dcr1) the pre-miRNA is processed into a mature miRNA duplex. miRNAs are loaded into Argonaute1 (Ago1) forming the miRISC enzyme complex which uses one strand of the mature miRNA to degrade target mRNA and thereby inhibits translation. Host-derived miRNAs can act antiviral or proviral.* ***Exogenous siRNA pathway:*** *Long dsRNA intermediates of viral replication are recognized by RNAse III endoribonuclease Dicer2 (Dcr2) under participation of dsRNA binding protein R2D2 and are cleaved into the characteristic 21 nt long vsiRNAs. The resulting double-stranded siRNAs are then incorporated into the RNA-induced silencing complex (RISC) and are further processed by Argonaute2 (Ago2). Ago2 uses one of the vsiRNA strands as a guide strand to recognize complementary viral target sequences resulting in sequence-specific target degradation. Dcr2 was lately suggested to participate in the formation of viral cDNA from defective viral genomes or replication intermediates, facilitated by endogenous reverse transcriptases.* ***piRNA pathway:*** *Precursor RNAs are generated from transposable elements (TEs) or piRNA clusters and are exported from the nucleus. Endonuclease Zucchini (Zuc) is slicing the precursor RNA into shorter transcripts in a phased manner. Resulting pre-piRNAs are fed into the ping-pong amplification cycle. During viral infection, virus-derived piRNAs (vpiRNAs) are derived from viral RNA that is cleaved by Zuc-mediated phased piRNA biogenesis and further fed into the ping-pong amplification cycle. Ago3 and Piwi5 give rise to new piRNA molecules conferring antiviral immunity. The antiviral role of Piwi4 has been documented, but the underlying mechanism is unknown [126, 127].*

1.11.1. The miRNA pathway

miRNAs are small non-coding RNAs with a typical length of 21-23 nts. They play an important role in the regulation of gene expression and have also been suggested to act antiviral in mosquitoes [126, 128-130].

The majority of miRNAs is transcribed as primary single-stranded RNAs (pri-miRNAs) with stem-loop structures forming regions of paired bases (Figure 10). The pri-miRNAs are then further processed into precursor miRNAs (pre-miRNAs) by the ribonuclease III enzyme Drosha. Subsequently, the pre-miRNA duplex is exported from the nucleus into the cytoplasm where it is sliced by another ribonuclease III enzyme called Dicer-1 with the help of co-factor Loquacious and is thereby processed into a mature miRNA duplex. The mature miRNA can then be loaded into an Argonaute protein (Ago1 in *Drosophila),* forming the miRNA-induced silencing complex (miRISC) in an ATP-dependent manner to degrade target mRNA [131-134] (Figure 10). Target recognition is based on pairing of nucleotides 2-7 of the miRNA called the seed region while mismatches of the following nucleotides are tolerated up to a certain degree [135].

This class of small RNAs has been shown to be involved in post-transcriptional gene regulation, but they are also involved in controlling mRNA stability, translation and transcription, using RNAi as a basic principle to convey their function. miRNAs also have been shown to be involved in viral replication either by regulating host factors crucial for virus production or by complementarity of miRNAs with viral RNA. The down-regulation of the metalloprotease expression in *Ae. albopictus* in response to WNV infection has been shown to limit viral replication [136]. The endosymbiont *Wolbachia* was suggested to use a host miRNA to regulate a methyltransferase to inhibit DENV replication in *Ae. aegypti* [137]. Synthetic miRNAs complementary to the viral genome of CHIKV, DENV and ZIKV have been shown to successfully reduce the transmission of these viruses in *Ae. albopictus* [134, 138]. Besides host miRNAs, some viruses have been shown to express their own miRNAs, playing a role in the viral lifecycle and facilitating successful infection. It was shown, that DENV is able to encode at least one miRNA which is important for virus autoregulation by targeting the viral non-structural protein 1 gene [139]. Viral miRNAs were documented to target different host miRNAs including the Kaposi sarcoma associated herpesvirus that inhibits viral lytic replication by upregulating the NF-κB pathway [140].

1.11.2. The siRNA pathway

The siRNA pathway can be divided into two different branches depending on the source of the dsRNAs as its inducer molecule. The endogenous siRNA pathway is induced by RNA transcripts with stem loop structures or sense/antisense transcripts derived from genomic loci or transposon sequences which form dsRNA (Figure 10). Its function is associated with somatic gene regulation, germline protection from transposable elements and heterochromatin formation in *Drosophila* [141-143]. The biogenesis and various functions of endogenous siRNAs have been shown to differ widely between species and remain enigmatic [144].

The exogenous siRNA (exo-siRNA) pathway is in turn induced by long double-stranded RNA transcripts and recognized by the cell as a pathogen-associated molecular pattern (PAMP). During viral replication of RNA viruses, double-stranded RNA intermediates of viral sequences can occur. This can be caused by pairing of single-stranded replication intermediates as well as formation of secondary structures like stem-loops. Also, transcripts from ambisense genomes which align, self-complementary regions or transcripts from tandem-repeat coding sequences can lead to the formation of dsRNA [145-147].

Recognition and cleavage of these dsRNAs is initiated by the RNaseIII enzyme Dcr2. The helicase domain of this enzyme is similar to that of RIG-I, a mammalian sensor responsible for the induction of the type-1 interferon response upon recognition of virus-infected cells [148, 149]. Dcr2 then cleaves the

long dsRNA into shorter 21 nt long siRNAs with 2 nt-long overhangs at the 3' end of the duplex and a phosphorylated 5' end [118, 120].

Subsequent to cleavage, the siRNA is loaded onto the RNase H family endonuclease Ago2 under participation of the dsRNA-binding protein R2D2. Ago2 is an active component of the RNA-induced silencing complex (RISC), which is a multiprotein complex functioning as a gene silencer [150]. RISC assembly of miRNAs and siRNAs occurs similarly. One strand of the RNA duplex is retained in the RISC as the 'guide strand' while the other 'passenger strand' is discarded [117, 151]. The choice of which strand is going to be discarded is not random but a matter of polarity and thermostability of the duplex loading [151-155]. The PAZ domain of Ago2 binds the 3' end of the guide strand while the 5' end is anchored by a pocket between the MID and PIWI domain. Loading of the guide strand leads to maturation and activation of the RISC. Bases 2 - 6 of the guide strand, the so called 'seed region' is fully exposed to the outside of the complex, guiding it to matching target RNAs by Watson-Crick base pairing and acting as an initial probe for viral RNA targeting [145, 146, 156-158]. Thereby RISC is a highly efficient enzyme with kinetics 10 times faster compared to annealing of guide and target strand in free solution [156, 159]. The PIWI domain of Ago2 then catalyzes slicing of the target RNA between bases 10 and 11 that match the guide strand. RISC can perform multiple rounds of target cleavage before the guide strand is released [145, 157, 159, 160]. In contrast to miRNAs, siRNA targeting requires base-pairing of the entire small RNA for further processing by Ago2 [161]. Biogenesis of small RNAs in mosquitoes requires a methylation step to gain biological activity and stabilize small RNAs. Similar to *D. melanogaster*, the methylation involves Ago2 as part of the RISC. A methyl group (-CH3) is introduced onto the 2' OH of the 3' terminal nucleotide on each strand of the duplex by methyltransferase Hen1, creating an active RISC [162-165]. The methylation status of small RNAs can be assessed by β-elimination assays [166].

Virus-derived siRNAs and their antiviral function

Virus-derived small RNAs were first discovered in plants infected with a positive-sense RNA virus [167]. Further research revealed that these small RNAs originate from viral replication intermediates or hairpin structures of single-stranded RNA precursors [168]. In addition, it was shown that Dicer proteins are involved in the production of those 21 nt long virus-derived siRNAs (vsiRNAs) targeting RNA as well as DNA viruses [145, 169]. Later, production of vsiRNAs was also confirmed for fungi, silkworms, nematodes, mosquitoes and the fruit fly upon infection with RNA viruses and revealed the antiviral function of vsiRNAs and the exo-siRNA pathway [170-173]. To date, vsiRNA production has also been confirmed for vertebrates including humans [161].

First demonstrated in the model insect *D. melanogaster*, it has been shown that the exo-siRNA pathway is crucial to control viral infection of various *Drosophila*-specific and other metazoonotic viruses that the fruit fly is susceptible to, like *Drosophila* C virus (DCV), Flock House virus (FHV), WNV, SINV and DENV [157, 160, 174-176]. Moreover, survival experiments have shown that the exo-siRNA-mediated control of arbovirus replication is important for the survival of *Drosophila* [176-178]. As the full genome sequences of *Ae. aegypti* and other vector mosquitoes like *Culex quinquefasciatus* and *Anopheles gambiae* became available, orthologues of the siRNA pathway key proteins Dcr2 and Ago2 were identified and described also in mosquitoes [51, 56, 179-181].

Ongoing research later confirmed the production of vsiRNAs also in *Aedes, Culex* and *Anopheles* mosquitoes demonstrating antiviral activity of the exo-siRNA pathway as a response to viral infection and the role of Dcr2 to produce siRNAs [54, 60, 123, 147, 177, 182-186]. Silencing of Dcr2 or Ago2 as the main pathway components of the exo-siRNA pathway led to increased viral replication in mosquitoes especially in *Ae. aegypti* for most arboviruses tested so far [59, 123, 172, 186-190]. Nevertheless, the importance of this pathway as antiviral defense can be tissue-, vector- and virus-specific as the

abundance of vsiRNAs is closely related to the efficiency of the siRNA pathway in targeting viral transcripts [191].

Although abundance of vsiRNAs is shown for all tested arboviruses, their distribution over the genome shows distinct patterns. vsiRNAs derived from alphaviruses like SFV, SINV and CHIKV and flaviviruses such as ZIKV or DENV serotype 2 (DENV2) were shown to map to both strands of the positive-sense genome equally and over the whole genome [59, 171, 181, 182, 189, 192-196]. However, compared to infections with alphaviruses, numbers of vsiRNAs mapping to DENV2 were very low. *Ae. aegypti* mosquitoes infected with ZIKV showed a clear vsiRNA production and RNAi response at 7 and 14 days post infection.

21 nt siRNA distribution of BUNV was shown to map to the whole length of every genome segment, but mappings to the particular strands differed. While L- and S-segment-derived vsiRNAs were mapping to both genome strands, M-segment-associated vsiRNAs had a mapping bias towards the anti-genomic strand [188]. Moreover, vsiRNAs derived from BUNV were shown to concentrate also to hotspots regions in the genome. In cells infected with RVFV, vsiRNAs derived from the whole length of every genome segment and vsiRNAs were mapped to both strands in equal ratios. A hotspot was detected for the ambisense S-segment of the intergenic region between N and NSs genes [177].

Overall, vsiRNAs are produced from all kinds of viruses while some exhibit specific hotspots or strand preference for the biogenesis of vsiRNAs. Nevertheless, the exogenous siRNA pathway is suggested to be the main antiviral response in arthropods including mosquitoes and has been shown to be linked to vector competence [191, 197, 198].

1.12. The piRNA pathway

Discovered more recently, the piRNA pathway is a highly conserved RNAi mechanism, which is found in a variety of organisms like plants and animals. This pathway was initially described in *D. melanogaster,* where it represses transposons and modulates gene expression, thereby maintaining genome stability in germline cells and somatic support cells [199, 200]. Additionally, piRNAs have regulatory functions for stem cell and germ cell differentiation as well as heterochromatin formation [201-204]. Heterochromatic regions of the genome are often rich in transposable elements (TEs) including DNA (retro)transposons. These TEs are selfish genetic elements with the ability to randomly integrate into the host genome thereby driving evolutionary processes, genome expansion and gene regulation [205]. Moreover, they can integrate into protein-coding regions or regulatory elements, mutating them and thereby impairing genome stability in the cells. The piRNA pathway provides repression of TEs as disruption led to infertility in male and female *Drosophila* as well as in mice as a result of DNA damage-induced impairment of stem cell differentiation [200-204, 206, 207].

The effector molecules of this pathway are piRNAs, which are single-stranded small RNAs that have a varying size of 24 - 30 nt and are 3‘-terminal 2-*O*-methylated in general [165, 208-210]. piRNAs act as guides for P-element induced wimpy testis (PIWI) proteins forming effector complexes (piRISC) similar to the RISCs of the miRNA and siRNA pathway. Akin to miRNA and siRNA RISCs, piRNA associated RISCs are able to cleave complementary target sequences and induce silencing using the RNAi mechanism. Whereas the miRNA and siRNA pathway involve Dicer proteins to fulfil their function, the piRNA pathway was shown to act independently of Dicer [211].

In *Drosophila*, single-stranded long antisense precursor RNAs are transcribed from genomic TE-rich clusters, exported into the cytoplasm where they are cleaved in a phased manner by the endonuclease Zucchini (Zuc) resulting in pre-piRNAs with a bias for uridine at the first position (U_1) [212, 213]. pre-piRNAs are further trimmed and loaded onto PIWI proteins like Aubergine (Aub) or Piwi. piRNAs are methylated by the Hen1 methyltransferase [164] and Piwi-associated piRNAs relocate to the nucleus

after forming a mature piRISC to guide installation of repressive histone marks at transposon loci. piRNAs associated with either Aub or Argonaute-3 (Ago3) remain in the cytoplasm to target cognate transposon mRNA sequences by slicing and thereby repressing transposable elements at the post-transcriptional level [200, 214].

In nuage-like structures in the nurse cells of the ovary, Zuc-mediated processing of primary piRNAs is combined with further processing by Ago3 and Aub proteins in the so called ping-pong amplification loop [215]. In this amplification loop, mature piRNAs with either U_1 and A_{10} bias (adenine at the 10^{th} position) and a 10 nt sequence overlap are created [215, 216]. This cycle leads to repeated rounds, producing new piRNAs and thereby consuming available target sequences [212-214, 217-219].

Protecting the germline from transposable elements (TEs) is a crucial function of the piRNA pathway in animals and plants. But lately, piRNA production was also observed in somatic tissues of mosquitoes in contrast to *Drosophila* where piRNA production is limited to the germline [193, 220]. Along with extended spatial expression of piRNAs also an expansion of the PIWI protein clade in some of the most important vector mosquitoes [181] was detected. In *Ae. aegypti* one Ago3 and seven PIWI proteins (Piwi1-7) have been identified without a direct orthologue of Aub or Piwi proteins [181, 221]. Two Ago3 and nine Piwi proteins were found in *Ae. albopictus* [222] and only one Ago3 and two Piwi proteins are present in some anopheline species [221].

1.12.1. The Argonaute protein family

The Argonaute protein family is well conserved in both the animal and plant kingdoms and was divided into two subfamilies based on phylogenetic analysis: the Argonaute (AGO) and the PIWI subfamily. The AGO family is closer related to the *Arabidopsis thaliana* Ago1 and the PIWI-like proteins are related to the P-element induced wimpy testis (PIWI) proteins of *D. melanogaster*. While AGO proteins are ubiquitously expressed in all tissues, the PIWI subfamily proteins are mainly expressed in the germline and supporting cells with a few exceptions in mosquitoes [223].

The number of AGO and PIWI proteins differ to a high degree, ranging from two AGO proteins in *D. melanogaster* (Ago1 and Ago2) and *Ae. aegypti* (Ago1-3) and four in humans (Ago1-4). But also the number of PIWI proteins differ from three in flies (Aub, Ago3, Piwi) and in mice (Miwi, Miwi2, Mili), to four in humans (Piwil1-4) to eight in *Ae. aegypti* (Piwi1-7, Ago3) [181, 221, 224, 225]. AGO and PIWI proteins share characteristic features regarding their domains, identifying them as highly specialized small RNA binding molecules. They possess an N-terminal domain, a PAZ domain, a MID domain and a PIWI domain [223, 226, 227] (Figure 11).

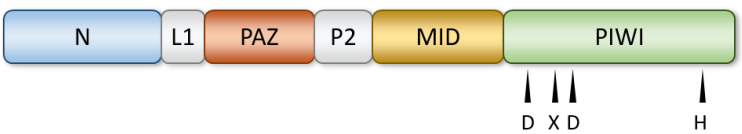

Figure 11: Schematic illustration of the primary structure of AGO proteins.
Black arrows indicate active residues of the slicer motif. Illustration is not drawn to scale.

The N-terminal domain is suggested to regulate target binding and unwinding of the small RNA duplex and protection of the 3‘ end of the guide RNA as shown for *D. melanogaster* recently [228]. The PAZ (PIWI-ARGONAUTE-ZWILLE) domain seems to be responsible for anchoring the 3‘ end of the guiding RNA strand in a hydrophilic cleft of the domain. The MID domain is suggested to be responsible for the

recognition and binding of the 5‘ phosphate of small RNAs by a nucleotide-specific loop structure. Cleavage of the target RNA is performed by the PIWI domain, which is structurally similar to RNase H containing a catalytic structure termed DXD H/D at the active site of the domain [223, 224, 229, 230]. Although AGO proteins were found to act catalytically for many species like *Schizosaccharomyces pombe* or *D. melanogaster*, not all Argonaute proteins possess a slicer activity as shown for the four human AGO proteins Ago1-4 of which only Ago2 is catalytically active [223, 231, 232]. In *Ae. aegypti* all AGO and PIWI proteins encode for a catalytic slicer motif, suggesting slicing activity for all of them [233] (Table 3).

Table 3: Catalytic slicer motif of AGO and PIWI proteins expressed in the vector mosquito Ae. aegypti [233].

Protein	Active residues
Ago1, Ago2	DTDH
Ago3	DYDH
Piwi1	DSDH
Piwi2-7	DCDH

1.12.2. Genomic origin of piRNAs

piRNAs were first discovered in 2001 in *Drosophila* deriving from the *Suppressor of Stellate* locus in *Drosophila* testes and were termed rasiRNAs [234, 235]. Later it was also discovered that the *flamenco* locus in *Drosophila* produces piRNAs that repress *gypsy* family transposons thereby revealing the concept of so called piRNA clusters [236, 237]. Most *Drosophila* piRNAs match repetitive elements and can therefore be mapped all over the *Drosophila* genome, but distinct sets of hotspot loci give rise to a major fraction of piRNAs and are designated ‚piRNA cluster‘.

These piRNA clusters harbours transposon content in the form of nested, truncated or damaged transcripts of TEs and can be several to hundreds of kb long [199, 217]. TEs by chance jump into these piRNA clusters and become trapped, producing corresponding piRNAs to regulate homologous elements expressed from different genomic loci [217]. Next to *D. melanogaster*, piRNA cluster have also been described in mosquito and mammalian genomes [199, 219, 238-241]. *Drosophila* piRNAs are mainly derived from transposon sequences and to a lesser extent from other genomic loci like the 3‘ untranslated region (UTR) [242, 243].

Although the *Ae. aegypti* genome harbours a lot of transposable elements (47%), only 19% of the produced piRNAs match TE sequences implying additional sources of piRNAs in mosquitoes [181, 193, 239]. piRNAs in *Aedes* mosquitoes were also suggested to originate from protein-coding genes like the histone family [243]. Besides transposon transcripts and protein-coding regions, piRNAs in *Ae. aegypti* were also described to originate from viral sequences of incoming virus, which were integrated into the vector genome. The proportion of these piRNAs derived from either viral genomes or integrated sequences was noted to be much higher in *Ae. aegypti* and *Ae. albopictus* than in other *Culex* or *Anopheles* vector mosquitoes [244-246].

1.12.3. The piRNA pathway and piRNA biogenesis in mosquitoes

The current model of piRNA biogenesis is based on knowledge about transposon control in the fruit fly *D. melanogaster* and is commonly accepted, although knowledge gaps exist. Nevertheless, evolutionary expansion of the PIWI protein clade and their expression also in somatic tissues together with viral sequences as an additional source of piRNAs, have shown, that knowledge about the *Drosophila* piRNA pathway and piRNA biogenesis can not be directly applied to *Aedes spp.* mosquitoes. An increasing number of studies have tried to characterize the piRNA pathway in mosquitoes in detail and the current state of research is summarized in Figure 12.

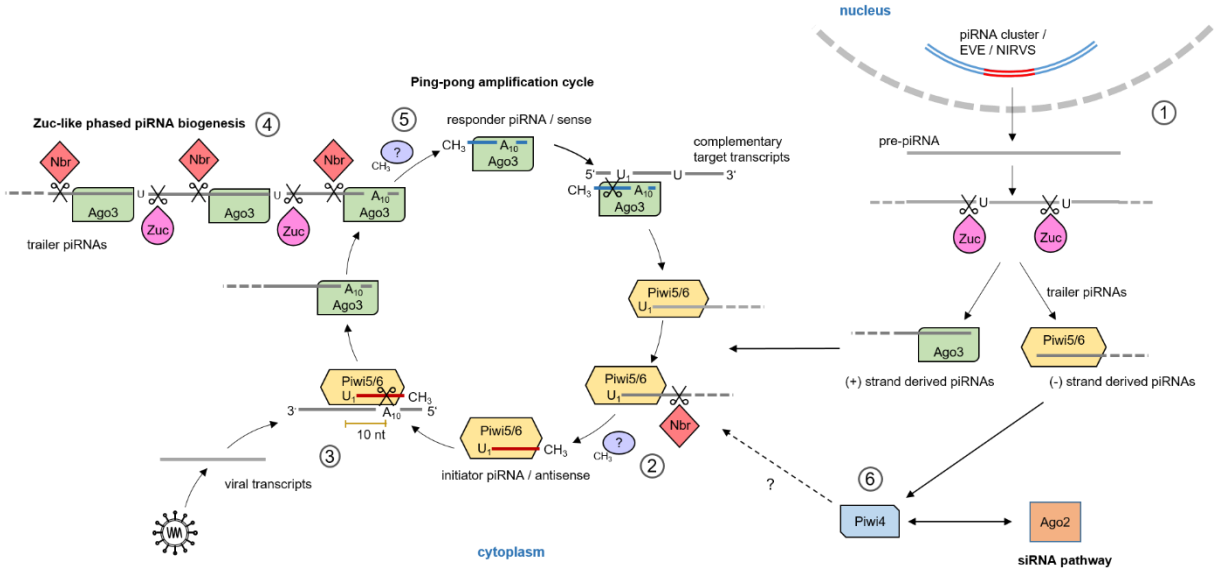

Figure 12: Working model of the piRNA pathway and piRNA biogenesis in mosquitoes.
Similar to piRNA biogenesis in Drosophila, long precursor transcripts are derived from either piRNA clusters, protein-coding genes, non-retroviral integrated RNA virus sequences (NIRVS) or viral transcripts (1). These pre-piRNAs are suggested to be cleaved by a Zucchini-like protein (Zuc) in a phased piRNA biogenesis process and are loaded onto Ago3, Piwi5 or Piwi6 with either positive-strand or negative-strand polarity respectively. It is suggested that besides further Zuc-mediated phased cleavage, these pre-mature complexes are also fed into the ping-pong amplification cycle for further amplification of piRNAs (2). Here, piRNAs are trimmed by the exonuclease Nibbler (Nbr) and methylated by a Hen1 homologue known from Drosophila. Piwi5 or Piwi6 form together with the mature piRNA a RISC complex, which is able to cleave complementary target sequences like viral or transposon transcripts (3). The cycle continues with a cleaved target RNA that is loaded onto Ago3. The overhanging target transcripts can either be further processed by Zuc-mediated phased piRNA biogenesis (4) while the Ago3-associated piRNA is trimmed and methylated again, closing the ping-pong amplification cycle by targeting new target transcripts which are again loaded onto Piwi5/6 (5). Cleavage and processing of transcripts results in a U_1/A_{10} bias of mature piRNAs and a 10 nt sequence overlap caused by ping-pong amplification similar to Drosophila processed piRNAs. Although an interplay between Piwi4 of the piRNA pathway and Ago2 as a key player of the exo-siRNA pathway have been suggested, the mode of interaction is currently unknown (6). It was recently suggested that Piwi4 associates with antisense vpiRNAs originating from endogenous viral elements (EVEs)/NIRVS [247]. Piwi5/6 is suggested to be loaded with antisense piRNAs with a U_1 bias, termed initiator piRNA, while Ago3 is loaded with sense piRNAs with an A_{10} bias, termed responder piRNA. piRNAs generated by Zuc-mediated processing are termed trailer piRNAs.

Initially, long precursor transcripts derived from piRNA clusters, endogenous viral elements (EVEs) or transposons are suggested to be cleaved in a phased biogenesis process by a Zucchini-like protein known from *D. melanogaster* [248] (Figure 12, step 1). Resulting premature piRNAs are loaded onto Ago3, Piwi5 or Piwi6, forming pre-piRISCS, where Ago3 is preferentially loaded with piRNAs derived from the sense strand and Piwi5 with anti-sense piRNAs respectively. It is suggested that these complexes also feed the ping-pong amplification cycle known from *Drosophila* for the amplification of

further piRNAs. In the ping-pong cycle, piRNAs are trimmed by the exonuclease Nibbler (Nbr) and methylated by a Hen1 homologue known from the fruit fly [164, 248] (Figure 12, step 2). After this processing step, Piwi5/6 together with the loaded piRNA form an active RISC which is able to cleave complementary target sequences like viral or transposon transcripts through Watson-Crick base pairing, akin to miRNA and siRNA pathways (Figure 12, step 3). Cleaved target RNAs are subsequently loaded onto Ago3. The overhanging transcripts are further processed by Zuc-mediated phased piRNA biogenesis again (Figure 12, step 4). The Ago3-associated piRNAs are then trimmed and methylated, closing the ping-pong amplification cycle by targeting another cognate target sequence which can be loaded onto Piwi5/6 again (Figure 12, step 5). Cleavage and processing of target RNAs in the ping-pong cycle results in a U_1/A_{10} bias and a 10 nt sequence overlap of mature piRNAs. The model proposes that the Piwi5-bound piRNA has a uracil at the first nucleotide position of the RNA (U_1) generated by Zuc-mediated cleavage. Piwi5 then prefers a target with a corresponding adenine at position 1 (A_1). When the resulting sequence is in turn loaded onto Ago3 after cleavage, the A_1 of the target strand becomes the adenine at the 10^{th} position (A_{10}), generating the characteristic nucleotide bias and 10 nt sequence overlap [238].

Although an interaction of Piwi4 with the exo-siRNA pathway has been suggested, the nature of this interaction is currently unknown [247, 249](Figure 12, step 6). Tassetto *et al.* proposed a maturation function of Piwi4 that was suggested to bind to antisense piRNAs derived from EVEs thereby providing antiviral immunity [247]. piRNAs produced by Zuc-mediated phased biogenesis are often called trailer piRNAs, whereas Piwi5/6 and Ago3 associated piRNAs are called initiator or responder piRNAs respectively [213, 248]. Although the RNAi mechanism is conserved, the biogenesis of piRNAs differs considerably from those of miRNAs or siRNAs. It was shown that this process is Dicer-independent and not induced by the presence of long dsRNAs [211, 250]. How the piRNA pathway is initiated in detail, still remains elusive. While miRNAs and siRNAs associate with AGO proteins, piRNAs are bound by PIWI clade proteins. Slicing of complementary target sequences by miRNA or siRNA-associated RISC complexes render these sequences susceptible to further degradation by cellular exonucleases. Cleavage products of piRISCs in contrast can also be processed into new piRNAs via phased biogenesis [251].

Although detailed knowledge about piRNA biogenesis in *Ae. aegypti* is still lacking, the proposed working model gives an idea about the suggested functions of AGO and PIWI proteins during piRNA biogenesis, indicating similarities, but also differences compared to piRNA production in *D. melanogaster*.

1.12.4. Virus-derived piRNAs and the antiviral function of PIWI proteins

The antiviral role of siRNAs as effector molecules of the exo-siRNA pathway is widely recognized. After the first report of virus-specific piRNAs (vpiRNAs) in addition to transposon piRNAs in *Drosophila* in 2010 [168], researchers also started looking for vpiRNAs in other species including *Aedes* and *Culex* mosquitoes [177, 242]. Until today, vpiRNAs derived from all major arbovirus families and orders have been detected in infected mosquitoes and cell lines like DENV, SINV, SFV and CHIKV, BUNV or insect-specific viruses (ISVs) [60, 177, 184, 188, 189, 193, 194, 242, 251-255] (Table 4). While research of the production of vpiRNAs upon infection in mosquitoes strongly increased for insect-specific as well as arboviruses, no extended antiviral function of the piRNA pathway in *Drosophila* was found [177, 256]. The widespread occurrence of vpiRNAs during infection and correlation with the expansion of the PIWI protein clade indicated the emergence of an additional antiviral function of the piRNA pathway in mosquitoes, targeting viral RNA instead of TEs.

Most arboviruses have a single-stranded RNA genome and the majority of them share a positive-sense orientation with the exception of the negative-sense genome of *Bunyavirales*. In contrast to vsiRNAs, which seem to derive equally from both strands of the whole virus genome [233, 257], vpiRNAs often seem to originate from specific hotspots. Moreover, vpiRNA production differs between different viruses and specifically between different virus families. It was suggested that specific markers trigger the vpiRNA biogenesis either by structural or sequence motifs thereby recruiting essential factors for vpiRNA production to specific sites of the viral genome [257].

For members of the *Alphavirus* genus like SFV, SINV and CHIKV, data showed that mainly the region directly downstream of the sub-genomic promoter is a target of vpiRNA biogenesis. This region encodes for the structural proteins including the capsid, which is essential for virion assembly and could be an important target for antiviral measures. In addition, also the higher abundance of the subgenomic RNA was proposed as a reason [189, 196, 233, 242, 251, 254, 255, 258]. vpiRNAs derived from *Flaviviridae* were mainly assigned to a few specific hotspot sites often located at the 3' end of the flaviviral genome. [59, 196, 242]. Conversely, *Bunyavirales*-derived vpiRNA distribution varies related to the genome segment. Although the whole BUNV genome seems to be covered, the main fraction of vpiRNAs is rather mapped to the anti-genome (sense) for the S- and M-segment, while vpiRNAs of the L-segment are hardly produced and rather map to the genomic strand [177, 184, 188].

Concerning the typical characteristics of vpiRNAs produced via ping-pong amplification, vpiRNAs derived from the *Togaviridae* and *Bunyavirales* have been shown to exhibit the expected U_1/A_{10} bias and 10 nt sequence overlap [242]. In contrast to this, it seems that *Flavivirus* infection (DENV2, ZIKV) of *Aedes* mosquitoes and cell lines leads to a decreased production of vpiRNAs compared to alpha- or bunyavirus infection with almost exclusively positive-sense (genomic) polarity and an A_{10} nucleotide bias [182, 196] (Table 4). Notably, anti-genomic vpiRNAs are carrying a U_1 bias whilst genomic vpiRNAs are generated with an A_{10} bias during ping pong amplification as shown for all tested viruses [184, 193, 233, 242, 251, 254] (Table 4). Methylation of the 3' end of mature vpiRNAs was also shown for DENV2 and SINV [247, 251].

In addition to arboviruses, ISVs that often persistently infect mosquitoes or mosquito derived cells have been reported over the years. Similar to arboviruses, persistent ISV infections have been shown to produce ISV-specific siRNAs and piRNAs in mosquitoes and derived cell lines. vsiRNAs had been reported for all investigated ISVs from different families, but vpiRNAs could only be found for some. For example, *Aedes aegypti*-derived Aag2 cells are known to be persistently infected with cell fusing agent virus (CFAV; family *Flaviviridae*, genus *Flavivirus*) and PCLV. Both viruses produce vsiRNAs, but only PCLV showed typical vpiRNA production [58, 259, 260]. About the biological function and possible antiviral activity of these ISV-specific small RNAs is nothing known.

Table 4: Arboviruses and insect-specific viruses shown to elicit biogenesis of vpiRNAs in Aedes mosquitoes and cell lines [233, 261].

Virus taxonomy	Name	Vector mosquito/ cell line	vpiRNA polarity/ nucleotide bias	vDNA demonstrated	Reference
Togaviridae/Alphavirus	SINV	Aag2, U4.4, C6/36	neg.-pos./U1-A10	Yes (Aag2)	[60] [193, 247, 251, 254]
	SFV	Aag2, U4.4	neg.-pos./U1-A10		[262]
	CHIKV	*Ae. aegypti, Ae. albopictus*, U4.4,C6/36, C7-10	neg.-pos./U1-A10	Yes	[192-194]
Flaviviridae/Flavivirus	DENV2	*Ae. aegypti, Ae. albopictus*, Aag2, C6/36	pos./A10 in *Ae. aegypti*; pos./A10 in C6/36; NF Aag2	Yes (Aag2, C6/36)	[182, 196, 222, 253, 263]
	ZIKV	*Ae. aegypti*, Aag2	pos./A10	Yes	[59, 195]
	WNV	Aag2, C6/36, U4.4, AP-61	pos./A10	Yes (C6/36, Aag2, CT)	[60, 263]
	CFAV	Aag2, C6/36	pos./A10	Yes	[71, 182, 247, 264]
Bunyavirales/Peribunyaviridae/ Orthobunyavirus	LACV	C6/36	neg.-pos./U1-A10	Yes (C6/36)	[60, 254, 263]
	SBV	Aag2	neg.-pos./ U1-A10		[262]
	BUNV	Aag2, U4.4	neg.-pos./U1-A10		[188, 265]
Bunyavirales/Phenuiviridae/ Phlebovirus	RVFV	*Ae. aegypti, Ae. vexans, Cx. quinquefasciatus*, Aag2, U4.4, C6/36	neg.-pos./U1-A10		[177, 184]
Bunyavirales/Phenuiviridae/ Phasivirus	PCLV	*Ae. aegypti*, Aag2	neg.-pos./U1-A10	No	[71, 252, 266]
Birnaviridae/Entomobirnavirus	CYV	Aag2, U4.4, C7-10	neg.-pos. (C7-10 only)	Yes (U4.4)	[267]

LACV: La Crosse orthobunyavirus; SBV: Schmallenberg orthobunyavirus; CYV: Culex Y virus; PCLV: Phasi Charoen-like phasivirus

Transient knockdowns and pull-down of PIWI family proteins (Ago3, Piwi1-7) were used to further determine similarities and differences of vpiRNA biogenesis with regard to specific viruses or virus families. Studies suggested that Ago3, Piwi5 and to a lesser extent Piwi6 are responsible for vpiRNA production in *Ae. aegypti* infected with SINV, SFV, CHIKV and DENV (Table 5).

In addition, knockdown of different proteins was used to investigate the antiviral activity of the piRNA pathway in mosquitoes. Slight effects - positive and negative - were reported for some piRNA-related proteins for certain viruses, but their biological relevance is uncertain, due to the small effect. Besides, the effects were strongly virus-specific. Silencing of Piwi4 was shown to act beneficial on viral infection in cell culture, for tested arboviruses from various families (Table 5) except from midge-borne Schmallenberg orthobunyavirus (SBV; order *Bunyavirales*, family *Peribunyaviridae*) where no antiviral effect was documented so far. Reports about the antiviral activity of ping-pong associated proteins Ago3, Piwi5 and Piwi6 were contradictory and specific for the viral species, whereby lack of these proteins is associated with the loss vpiRNA production (Table 5).

Table 5: Overview of PIWI proteins involved in the RNAi response in mosquitoes.
The table shows the effect of a lack of RNAi pathway protein during infection on either viral replication or vpiRNA biogenesis. Filled triangles indicate an increased (▲), decreased (▼) or unaltered (▶) viral replication.▽ indicates a decreased vpiRNA production (adapted from [257]).

Virus genus	Name	exo-siRNA pathway		piRNA pathway				
		Dcr2	Ago2	Ago3	Piwi4	Piwi5	Piwi6	Reference
Alphavirus	CHIKV		▲	▶▽	▲	▶▽	▽	[187, 247, 255]
	SFV	▲	▲	▶▽	▲	▶▽	▶▽	[59, 249]
	SINV	▲	▲	▽	▲▽	▽	▽	[123, 187, 247, 251]
Flavivirus	DENV2	▲	▲	▼▽	▲	▶▽	▶▽	[172, 196, 247]
	ZIKV	▲	▶	▼	▲	▶	▶	[59]
	CFAV	▲		▲▽	▲▽			[182, 247]
Orthobunyavirus	BUNV		▲	▼	▲	▲	▼	[188]
	SBV		▲	▶	▶	▼	▶	[188]
	RVFV		▲	▲	▲	▶	▶	[177]

1.12.5. vpiRNAs in non-Aedes mosquitoes

Besides *Aedes* mosquitoes, also *Anopheles gambiae* and *Culex* mosquitoes have been investigated to assess antiviral mechanisms based on the RNAi response (Table 6). During O'nyong nyong virus (ONNV, family *Togaviridae*, genus *Alphavirus*) infection in *An. gambiae*, vsiRNAs and vpiRNA-like small RNAs were produced. Although matching in nucleotide length, characteristic ping-pong properties found for *Alphaviruses* in *Aedes* mosquitoes were lacking in *Anopheles* mosquitoes [183, 233]. However, a slight increase of ONNV replication was observed in Ago3-silenced cells, hinting towards a possible antiviral activity [186].

Another vector for arboviruses are *Culex* mosquitoes. Induction of the siRNA response was reported for WNV *in vivo* and cell lines, but no vpiRNAs were detected [268] [269] (Table 6). *Culex tarsalis*-derived CT cell line showed a strong vsiRNA response upon Calbertado virus (CLBOV, family *Flaviviridae*, genus *Flavivirus*) infection but no vpiRNA production. CT cells infected with Phasi Charoen-like phasivirus (PCLV, order *Bunyavirales*, family *Phenuiviridae*) or RVFV induced the production of both, vsiRNAs and vpiRNAs [177, 267]. In contrast to findings for *Aedes* mosquitoes [60, 251, 254], SINV infection in *Cx. pipiens* did not result in the production of vpiRNAs [269].

Table 6: Arboviruses and insect-specific viruses for which biogenesis of vpiRNAs has been suggested in Culex spp. vector mosquitoes. Adapted from [261].

Virus taxonomy	Name	Vector mosquito/ cell line	vpiRNA polarity/ nucleotide bias	vDNA demonstrated	Reference
Flaviviridae/Flavivirus	WNV	*Cx. quinquefasciatus*, CT, Hsu	No	Yes (CT and Hsu only)	[170, 267, 269]
	CLBOV	CT	No		[267]
Togaviridae/Alphavirus	ONNV	*An. gambiae*	No		[183, 186, 233]
Bunyavirales/Phenuiviridae/ Phlebovirus	RVFV	*Cx. quinquefasciatus*	Yes, neg.-pos./ U1-A10		[177]
Bunyavirales/Phenuiviridae/ Phasivirus	PCLV	CT	Yes, neg.-pos./ U1-A10		
Rhabdoviridae	MERV	Hsu	Yes, neg.-pos./ U1-A10	Yes	[269]

CLBOV: Calbertado virus; MERV: Merida virus

1.13. RNA virus-derived cDNA

Most arboviruses investigated so far have a single-stranded RNA genome and do not encode for an RNA-dependent DNA polymerase (reverse transcriptase), which would make it possible for them to perform reverse transcription of their viral RNA genome into cDNA. Surprisingly, the production of viral cDNA (vcDNA) forms of non-retroviral FHV in *D. melanogaster* S2n cells was shown already 12 hours post infection (hpi). Recent research indicated that the proposed mechanism for reverse transcription of non-retroviral RNA viruses is dependent on reverse transcriptases encoded by endogenous retrotransposons or retroviruses. Presumably, vcDNA is generated by using viral RNA in a copy-choice recombination during reverse transcription [270-272].

Inspired by findings in *Drosophila*, vcDNA formation was also observed in *Aedes* mosquitoes and *Aedes*-derived cell lines upon WNV, DENV2, CHIKV or ZIKV infection as early as 24 hpi (Table 4) [192, 194, 244, 263, 273, 274]. Recently, viral DNA forms were also detected in *Cx. tarsalis* (CT) and *Cx. quinquefasciatus* (Hsu) cells upon infection with WNV and MERV (Table 6) [192, 269]. Although not well studied, involvement of Dcr2 and its DEX D/H helicase domain was suggested in the production of vcDNA from defective viral genomes [274].

Interestingly, the sequences of FHV and other viruses found in these episomal viral DNA molecules were highly reorganized, resembling non-homologous RNA recombination during negative-strand synthesis or defective particles serving as templates [270, 274]. Furthermore, it was demonstrated that generation of vcDNA forms is required for the production of small RNAs *in vivo* and that they are related to viral persistence and fitness of the infected host [194, 274]. To date, it is under discussion whether the vcDNA resides as episomes in the nucleus or is rather incorporated as endogenous viral elements in the host cell genome [246, 247].

In *Drosophila,* an inhibitory effect on FHV replication and increased cell death was observed in cells treated with the reverse transcriptase inhibitor AZT to prevent formation of vcDNA [270]. Similar to this, the administration of AZT caused a reduction of vpiRNAs in treated U4.4 cells (*Ae. albopictus*) but not of vsiRNAs. The infection of mosquitoes with CHIKV following AZT treatment, led to an earlier death of mosquitoes without a high increase in viral loads [194]. Mondotte *et al.* recently confirmed the formation of vcDNA molecules in CHIKV-infected *Ae. aegypti* mosquitoes and their progeny, conferring antiviral immunity in the offspring for several generations indepent of Dcr2 [275].

Overall, it is proposed that the formation of vcDNA is induced upon infection, although the trigger for this process is unknown. The existence of vcDNA and their rapid synthesis shortly after the onset of infection and production of small RNAs from these molecules is important to control tolerance to arbovirus infection rather than resistance. Additionally vcDNA formation might also generate some kind of inheritable immunity in mosquitoes.

1.14. Endogenous viral elements and non-retroviral integrated RNA virus sequences

In the last decade, owing to the better availability of new molecular techniques like Next Generation sequencing and the rise of bioinformatic tools, the whole genome sequences of several vector mosquitoes and newly discovered viruses including ISVs became available. This progress became the stepping stone which led to the discovery of virus-derived sequences that became integrated into the host genome, generally referred to as endogenous viral elements. These elements have been discovered in all kinds of organisms including fungi, plants, animals and humans [276-280]. In fact, around 5 - 8% of the human genome consist of EVEs [277, 278].

As previously described, viral RNA genomes are converted into vcDNA by reverse transcriptases and are suggested to be additionally integrated into the host genome by integrase enzymes also encoded by retroviruses or retrotransposons resulting in the formation of EVEs. Integrations can occur in both, somatic and germline cells, although the germline is generally better protected against invading genetic elements such as TEs by the piRNA pathway.

Besides the suggested episomal vcDNA, also viral sequences of non-retroviral viruses were found to be integrated into mosquito genomes. These integrations are referred to as ‚non-retroviral integrated RNA virus sequences' (NIRVS) to emphasize their unusual origin [281]. Often, these integrations consist of interrupted ORFs and resemble nucleo- or glycoproteins as well as polymerase coding regions of viral genomes [282]. Depending on the effect on the host fitness, EVEs or NIRVS can reach fixation and will be inherited by the offspring or will get lost throughout time by genetic drift, recombination or other selection mechanisms. EVE and NIRVS are usually unable to produce infectious viral particles due to mutations of the integrated sequence or insertions that might have destroyed the ORF. Nevertheless, they can express proteins or RNA that might act in a regulatory way as restriction factors or cellular co-factors impacting host immunity. Furthermore, NIRVS have also been shown to have acquired biological function, providing beneficial effects for the host [264, 282]. For example, human cells were transfected with the Endogenous Borna-like N element from the squirrel genome and were shown to interfere with Bornavirus polymerase activity [283]. In mice, the Gag protein Fv1 restricts murine leukemia virus after viral entry in the host cell [284]. Besides antiviral function, also regulatory functions of endogenous viral elements have been described [284]. Overall, the capacity of integrated viral sequences has been mostly linked to antiviral defense and the formation of heritable, adaptive immunity against incoming infections.

Recently, an increasing number of studies have shown the variety of genome integrations into somatic and germline cells from non-retroviral RNA viruses in *Aedes* mosquitoes including single- and double-stranded RNA viruses with either polarity. Especially the arbovirus vector *Ae. aegypti* seems to harbour a huge repertoire of NIRVS derived from all kinds of arboviral families but especially flavivirus-derived sequences [29, 246, 258, 285-293]. Furthermore, NIRVS are also present in a variety of other arbovirus vector genomes such as *Phlebotomus papatasi*, *Culicoides sonorensis*, *Rhipicephalus microplus* or *Ixodes scapularis* [246, 294].

The first discovery of NIRVS in *Ae. aegypti* and *Ae. albopictus* was published in 2004 by Crochu *et al.*, when four regions similar to the insect-specific viruses CFAV and Kamiti River virus (KRV) were described [286]. Additional viral integrations from ISVs were found in wild caught *Aedes spp.* mosquitoes

using flavivirus-specific primers [292, 295, 296]. Next Generation sequencing, metagenomic analyses and the availability of mosquito and virus genomes enabled further discoveries of NIRVS, adding to the knowledge provided about the origin and diversity of integrated viral sequences. Hundreds of individual NIRVS have been characterized deriving from genomes of flavi-, rhabdo-, reo-, bunya-, phlebo- and quaranjaviruses in *Aedes* spp. [29, 244, 246, 278, 282, 285, 289, 290, 293, 297]. Because of their recent discovery, little is known about the formation, function and control of these NIRVS.

Although mosquitoes like *Ae. aegypti* harbour a variety of NIRVS, specific and precise mapping to arboviral genome sequences is hardly documented. In contrast, integrations from vertically transmitted ISVs are highly abundant in the mosquito genome [246, 285]. To date, no NIRVS mapping to alphavirus genomes have been reported, but integrated sequences were found for Dengue virus serotype 1 (DENV1) in a population of *Ae. albopictus* in China [244]. Viral integrations of the insect-specific flavivirus CFAV have been documented in *Ae. aegypti* and derived cell lines [247, 258, 264]. This is not surprising, as the discovered NIRVS are the result of endogenization of viruses within the germline cells of host genomes and most ISVs are transmitted vertically from female mosquitoes to their offspring [298]. The character of NIRVS seems to be quite variable in the same mosquito species for different geographic locations, suggesting an acquisition of these integrations depending on the occasion of a viral encounter like the adaptive immunity in mammals [245, 246, 258, 285, 288].

Integration of viral sequences is not happening randomly all over the mosquito genome. It was found that especially piRNA cluster seem to facilitate incorporation of NIRVS, although the mechanism is unknown. NIRVS have been shown to be highly present in those clusters with 44 % (*Ae. aegypti*) and 12.5 % (*Ae. albopictus*) respectively of all NIRVS being part of these loci [246, 285]. NIRVS highly overlapping with piRNA clusters, indicate a strong drift towards integration of viral sequences into piRNA clusters and therefore piRNA production from these genomic loci [290].

In fact, production of vpiRNAs was reported in infected and uninfected cells but not for vsiRNAs, which were only produced in infected cells [60, 182, 239, 246, 282]. This indicates the production of NIRVS-derived vpiRNAs similar to TE-targeting piRNAs produced from piRNA clusters. Related to this, these vpiRNAs were characterized by an anti-sense orientation and a U_1 bias enabling them to directly target sense-strand viral RNAs.

Evidence for an antiviral role of NIRVS in combination with the piRNA pathway is rather scarce, but studies are increasing. Tassetto *et al.* showed the production of antisense vpiRNA originating from a CFAV-derived NIRVS. They suggested that these vpiRNAs associate with Piwi4 thereby providing an antiviral defense against CFAV infection [247]. Another study by Suzuki *et al.* could show that viral replication of CFAV in *Ae. aegypti* mosquitoes is controlled by a naturally occurring integrated CFAV sequence and the production of vpiRNAs derived from this NIRVS, targeting the incoming virus [264]. In addition, Marconcini *et al.* recently suggested that next to directly targeting the viral sequence through the exo-siRNA and piRNA pathway, NIRVS-derived vpiRNAs might also have a regulatory function on the expression of mosquito transcripts. In general, it is suggested that the combination of vpiRNA production from integrated viral sequences and the RNA genome of a cognate virus leads to an antiviral function of the piRNA pathway which decreases viral replication in addition to the production of secondary piRNAs by the ping-pong amplification cycle to target further replicated viral RNA (Figure 13).

The widespread occurrence and diversity of viral integrations and first reports on antiviral functionality of the piRNA pathway in connection with NIRVS *in vitro* and *in vivo*, strengthen the theory of an adaptive and heritable immune response in the mosquito host especially in *Aedes* mosquitoes. Moreover, production of vpiRNAs from NIRVS and their fixation in the genome harbour the potential to be vertically transmitted and establish an adaptive immunity analogous to the prokaryotic CRISPR/Cas9 system. Nevertheless, the piRNA pathway might not prevent or support clearance of the incoming virus but rather help to maintain persistence in the mosquito vector, thereby contributing to vector competence.

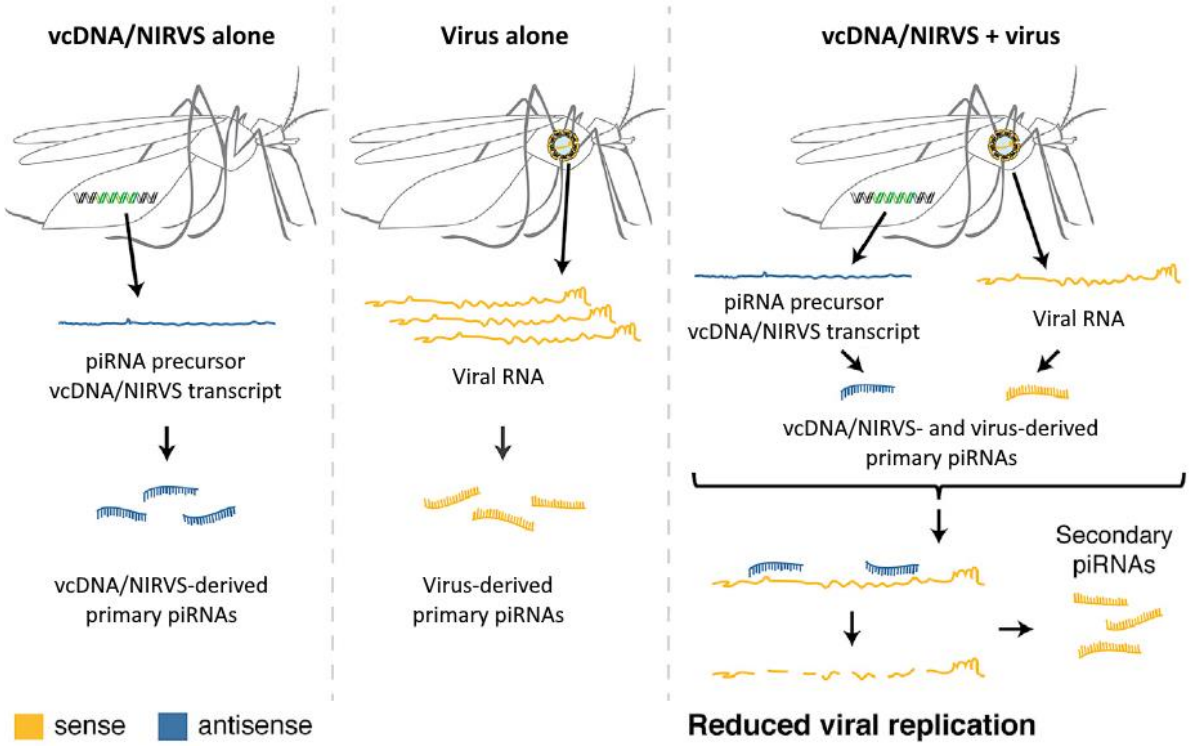

Figure 13: Proposed model for the antiviral function of NIRVS in mosquitoes.
Non-infected mosquitoes that harbor viral cDNA or NIRVS produce primary antisense piRNAs. In infected mosquitoes without vcDNA/NIRVS, primary piRNAs in sense orientation are produced. Only when vcDNA or NIRVS and cognate virus are present in the mosquito, primary piRNAs in sense and antisense orientation are produced that confer antiviral immunity through vcDNA/NIRVS-derived piRNAs that target the cognate viral RNA genome [264].

1.15. Objectives

Arbovirus infections have become a worldwide burden with a high impact on human health. Therefore, discerning vector competence and identifying determinants of virus-host interactions is of great medical and scientific importance. Deciphering the key components and functionality of RNAi pathways can provide mechanistic insights into the control of arboviral infection and identify new targets and strategies to reduce arbovirus transmission and infection. Characterizing the interplay of mosquito RNAi response and arboviruses in more detail should help to gain insights into how antiviral responses are initiated or regulated and their effect on the outcome of infection in their arthropod vector. Especially the piRNA pathway in mosquitoes has lately moved into the focus of researchers as it is suggested to constitute an additional line of defense against viruses in mosquitoes in terms of an immunological memory.

At the onset of this thesis, only limited knowledge about the antiviral role of the piRNA pathway in mosquitoes existed and evidence for an adaptive immune response in mosquitoes was lacking. Trying to confirm and to contribute to the current state of research, this study was designed to address knowledge gaps about the general interaction of arboviruses with the RNAi-related immune response. Moreover, it was planned to investigate the understudied effects related to the time aspect of the course of infection. Furthermore, the hypothesis that the piRNA pathway is able to confer adaptive immunity against arboviruses in mosquitoes, mediated by biologically active vpiRNAs, should be validated.

In order to prove the above-mentioned hypothesis and to provide further insights in virus-host interactions, the following objectives were formulated:

i. characterization of newly established Ago2 knockout cell lines for the use in downstream experiments, including silencing and methylation ability

ii. assess the impact of an impaired siRNA pathway on viral replication and methylation of virus-derived, transcriptomic and transposable element-derived small RNAs

iii. investigate differences between acute and persistent phase of SFV and BUNV infection with regard to the small RNA profile and characteristics

iv. determine biological activity of vpiRNAs produced during early and persistent stage of infection using reporter constructs for SFV and BUNV

v. assess characteristics of BUNV infection with regard to the antiviral activity of small RNAs with a special interest in the antiviral role of piRNA pathway proteins, their expression levels and impact on vpiRNA production during infection

vi. investigate the formation of vcDNA and/or NIRVS and the possible generation of an adaptive immunity affecting a recurring infection

The described experiments deliver new information and fundamental knowledge about the antiviral role of the piRNA pathway and its wide-ranging responsibilities, interactions and functions.

2. Materials and Methods

2.1. Materials

2.1.1. Cells

AF5, AF319, AF519, AF525 (Ae. aegypti)

Aag2-AF5 cells (AF5) (ECACC 19022601) [58] are a single cell clone of Aag2 cells, which derive from a pool of *Aedes aegypti* embryos [52, 299]. These cells have been generated to provide a more standardized and well-defined *Ae. aegypti* derived cell line than Aag2. Several properties of AF5 cell line were confirmed to ensure a similar behaviour like the parental Aag2 cell line in terms of infection and transfection efficiency and immune status among other factors. AF5 cells are immuno-competent allowing it to study the major antiviral defense mechanisms in mosquitoes. Parental Aag2 cells are known to be persistently infected with various ISVs such as CFAV and PCLV and so are AF5 cells as well [260, 300].

Aag2-AF319 cells (AF319) (ECACC 19022602) are a single cell clone of the parental AF5 cell line, containing a homozygous Dcr2 knockout mutation engineered using CRISPR/Cas9. The obtained single-cell colonies were screened for the loss of Dcr2 activity via reporter-based silencing assays [249].

Aag2-AF519 (AF519) is a single cell clone with a knockout mutation of Ago2 derived from AF5 cells by CRISPR/Cas9. A gRNA targeting exon 2 of the Ago2 gene was cloned into the pAF9 vector. One allele contains an early stop codon while the other allele is modified by an insertion in the Ago2 sequence. Overall AF519 cells are suggested to express low amounts of an altered version of Ago2.

Aag2-AF525 (AF525) is another single cell clone of the parental AF5 cell line, containing a homozygous Ago2 knockout mutation derived by CRISPR/Cas9. A gRNA targeting exon 2 of the Ago2 gene was cloned into the pAF9 vector.

C6/36 (Ae. albopictus)

C6/36 are derived from a pool of larvae of *Ae. albopictus* [53, 301]. C6/36 cells have a deficient siRNA pathway due to a mutation in the Dcr2 gene caused by a homozygous frameshift mutation.

All mosquito cell lines were kept at 28 °C in Leibovitz's L-15 medium supplemented with 10 % fetal calf serum (FCS), 1 % penicillin / streptomycin (P/S) and 10 % Tryptose phosphate broth (TPB) (all Gibco / Thermo Fisher Scientific Inc., Waltham, MA, USA).

Mammalian cell lines (BHK-21, A549-Npro)

Baby hamster kidney cells-21 (BHK-21) were derived from the parental cell line C-13 from baby hamster kidneys of five unsexed 1-day old hamsters [302]. Cells were maintained in Glasgow's Minimal Essential Medium (GMEM) supplemented with 5 % FCS, 1 % P/S and 10 % TPB.

A549-Npro cells, stably expressing the bovine viral diarrhea virus N pro protein [303] were maintained in Dulbecco's Modified Eagle Medium (DMEM) supplemented with 10 % or 5 % FCS respectively and 1 % P/S. All mammalian cell lines were kept at 37 °C with an atmosphere of 5 % CO_2 added.

2.1.2. Plasmids

The *Renilla* luciferase (pAcIE1-*Rluc*) expressing vector was already described elsewhere [304]. The plasmid was mainly used as an internal transfection control to correct for variations in transfection efficiency. Firefly luciferase (pIZ-FFluc) and Nano luciferase (pIZ-Nluc) expressing vectors were already described elsewhere [177, 304]. Briefly, the FFluc sequence was amplified from the pGL3 plasmid (Promega Corp., Fitchburg, WI, USA) and cloned into pIZ/V5 plasmid. The Nluc sequence was amplified from the pNL1.1 vector (Promega Corp., Fitchburg, WI, USA) and cloned into pIZ vector (Thermo Fisher Scientific Inc., Waltham, MA, USA). pPUb-myc-Ago2 (expressing *Ae. aegypti* Ago2) and pPUb-myc-eGFP vectors have already been described elsewhere [249, 305].
CHIKV replicase plasmid REP and control variant GAA, together with the template RNA SG-Nluc and SG-C-Nluc have already been described elsewhere [306]. Instead of a *Gaussia* luciferase reporter sequence, the used template RNAs encode for a Nluc reporter sequence plus an additional antibiotic cassette with the 2A autoproteolytic sequence, in tandem with a blasticidine resistance gene. In addition, the second part consists of an RNA template under the control of a Sp6 promoter for *in vitro* transcription.

2.1.3. Infectious agents

All pCMV-based SFV viruses were rescued and titrated as previously described [249, 307]. The plasmid pCMV-SFV4 [307] was used for the production of SFV4. The plasmid, pCMV-SFV6-2SG-Nluc containing reporter virus cDNA based on SFV strain 6 (L10R wt) [308] was used for reporter virus production. Expression is under control of a human cytomegalovirus promoter (CMV) in addition to a kanamycin resistance gene. The reporter virus contains a duplicated subgenomic promoter (spanning from position -37 to +17 in respect of subgenomic RNA start site) placed immediately downstream of the structural reading frame of the SFV genome and followed by the sequence expressing Nano luciferase (Nluc) reporter (Figure 14).

The plasmid pCMV-SFV4(3H)-FFluc [249] was used for the rescue of SFV4(3H)-FFluc reporter virus. SFV4(3H)-FFluc expresses Firefly luciferase (FFluc) as a part of its non-structural polyprotein with the reporter sequence inserted between nsP3 and nsP4 proteins and is flanked by duplicated nsP2 cleavage sites at the C terminus of nsP3. It is thereby released from the polyprotein by the protease activity of nsP2 [249, 255] (Figure 14).

BUNV-Nluc has been described elsewhere [188]. Briefly, to produce BUNV-Nluc plasmids, pTVT7RBUNM-NL, pT7riboBUNL(+) and pT7riboBUNS(+) encoding the BUNV antigenome, were used. In pTVT7RBUNM-NL, a part of the BUNV NSm cytoplasmic domain was replaced by the Nluc sequence resulting in a chimeric NSm-Nluc fusion protein (Figure 14).

The Brazilian ZIKV strain PE243 (ZIKV/H sapiens/Brazil/PE243/2015) has been already described elsewhere [309]. It was isolated in Recife (Brazil) in 2015 from positive serum samples of a patient.

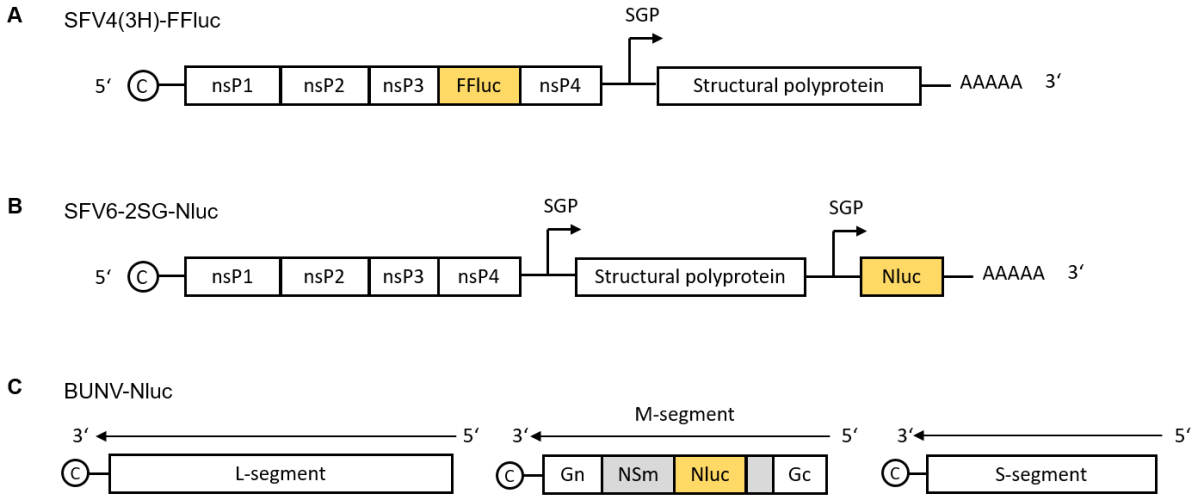

Figure 14: Structure of different reporter viruses.
(A) Firefly luciferase (FFluc) reporter sequence was inserted between non-structural protein 3 and 4 (nsP3 and nsP4) to create the SFV4(3H)-FFluc reporter virus. (B) To create SFV6-2SG-Nluc, the Nano luciferase (Nluc) encoding sequence was inserted behind a duplicated subgenomic promoter directly downstream of the structural polyprotein reading frame. (C) BUNV-Nluc was created by inserting the Nluc reporter sequence in the cytoplasmic domain of NSm resulting in a chimeric NSm-Nluc fusion protein.

2.1.4. Bacterial strains

Table 7: Ultracompetent E. coli used for transformation.

Bacteria	Manufacturer/Supplier	Genotype
Escherichia coli DH5α	Thermo Fisher Scientific Inc., Waltham, MA, USA	F⁻ Φ80*lac*ZΔM15 Δ(*lac*ZYA-*arg*F) U169 *rec*A1 *end*A1 *hsd*R17(r_k^-, m_k^+) *pho*A *sup*E44 *thi*-1 *gyr*A96 *rel*A1 λ⁻
Escherichia coli XL-10 Gold	Stratagene, La Jolla CA, USA	Tet^r Δ(*mcrA*)*183* Δ(*mcrCB-hsdSMR-mrr*)*173 endA1 supE44 thi-1 recA1 gyrA96 relA1 lac* Hte [F′ *proAB lacI*^{q} *ZΔM15* Tn*10* (Tet^r) Amy Cam^r]

2.1.5. Oligonucleotides

Primers

Table 8: Primers listed with identifier, description and sequence.

Identifier	Description	Sequence (5‘ - 3‘)	Reference
E167	SFV-piRNA-sensor1-SacII-FW	CCGCGGGGCAAAGCTAGCTTTCAAGAAATCG	
E168	SFV-piRNA-sensor1-SacII-RV	CCGCGGCAGTCGGCGCAGTACGCG	
E169	SFV-piRNA-sensor2-SacII-FW	CCGCGGCACTATGGAAAAGAGATCCCTTG	
E170	SFV-piRNA-sensor2-SacII-RV	CCGCGGCATAGTAGTACTGTACGATCTGATGCG	
E171	SFV-siRNA-sensor1-SacII-FW	CCGCGGGAACGGCGTATTGGATTGG	
E172	SFV-siRNA-sensor1-SacII-RV	CCGCGGCTTCCGTTCACAACTATCCTCTG	
E173	SFV-siRNA-sensor2-SacII-FW	CCGCGGGCAGAGGAGTGGAGCACC	
E174	SFV-siRNA-sensor2-SacII-RV	CCGCGGCGTAGCACCTATCGGCGC	
E322	BUNV M Segment qPCR RV	CCCACACACAGTCAGTAACAACA	
E327	BUNV M Segment qPCR FW	GGGGAAGATACAGGCAATGA	
E356	Aae-Piwi4-FW	CTTCTCCACCACAGCCAATG	
E357	Aae-Piwi4-RV	GTCCAATCTGCCTGTTCTCCA	

E358	Aae-Piwi5-FW	CAGTTTTGGAAGACAGAGTTGGA	
E359	Aae-Piwi5-RV	CCTGCCGTCACTTTGTAATTTTC	
E360	Aae-Piwi6-FW	TCCGACGTTTTCAAGTTTTGGA	
E361	Aae-Piwi6-RV	CACTTTACACTGATCCTGCTCG	
E362	Aae-Ago3-FW	TGCTCCAGACGACGGTTTTG	
E363	Aae-Ago3-RV	GGGTCAATATAACGGCTCCCAG	
E364	Aae-Ago2-FW	GGCTGCTCACCCAATGTATCAAGA	
E365	Aae-Ago2-RV	AACCGTTCGTTTTGGCGTTGAT	
E366	Aae-Ago1-FW	GTACGATGCGTCGTAAGTAC	
E367	Aae-Ago1-RV	GTACTTGTCGAGGAAGTATTTGG	
E368	Aae-S7 FW	CCAGGCTATCCTGGAGTTG	
E369	Aae-S7 RV	GACGTGCTTGCCGGAGAAC	
E396	BUNV S-seg SACII FW	CCGCGGCGGAACAACCCAGTTCCTGA	
E397	BUNV S-seg SACII RV	CCGCGGTGTACCTCTGCCGCATTGTT	
E398	BUNV M-seg SACII FW	CCGCGGTACGGCCGGTGGTAGTATAA	
E399	BUNV M-seg SACII RV	CCGCGGATTGCCATTGACCCTGGTAG	
E417	GL3-FFLuc-sequencing 1456nt FW	GTTTTGGAGCACGGAAAGAC	
E418	SP6_CH FW	TAAATTTAGGTGACACTATAGATGGCTGCGTGAGACACAC	
E419	Post_CH RV	GCCATGCCGACCCTTTTTTT	
E420	BUNV-S-Sensor-XbaI FW	CCTCTAGAGGCGGAACAACCCAGTTCCTGA	
E421	BUNV-S-Sensor-XbaI-RV	CCTCTAGAGGTGTACCTCTGCCGCATTGTT	
E422	BUNV-M-Sensor-XbaI-RV	CCTCTAGAGGATTGCCATTGACCCTGGTAG	
E423	Ae aegypti Actin FW	TTCGTAGATTGGGACTGTGTGCGA	
E424	Ae aegypti Actin RV	AACACCCAGTCCTGCTGACAGA	
E431	BUNV-M-sensor-XbaI FW	CCTCTAGAGGTACGGCCGGTGGTAGTATAA	
E444	pCMV-SFV6-2SG-NLuc sequencing FW	TATCCTGGTGCTGGTTGTGGTC	
E547	BUNV-S-SacII FW II	CCGCGGCTAACTTTAAGCGTGTCCACACC	
E548	BUNV-S XbaI FW II	CCTCTAGAGGCTAACTTTAAGCGTGTCCACACC	
E549	BUNV-S SacII RV II	CCGCGGGGTAAGACCATCGTCAGGAAC	
E550	BUNV-S XbaI RV II	CCTCTAGAGGGGTAAGACCATCGTCAGGAAC	
E551	pJET Seq FW	CGACTCACTATAGGGAGAGCGGC	
E556	ZIKV FW	GTTGTCGCTGCTGAAATGGA	
E557	ZIKV RV	GGGGACTCTGATTGGCTGTA	
E570	BUNV-S T7 FW	GTAATACGACTCACTATAGGGCTAACTTTAAGCGTGTCCACACC	
E571	BUNV-S T7 RV	GTAATACGACTCACTATAGGGGGTAAGACCATCGTCAGGAAC	
E592	BUNV-L-Segment T7 primer for dsRNA FW	GTAATACGACTCACTATAGGGGGACCCTATACTTTATCCAGC	
E593	BUNV-L-Segment T7 primer for dsRNA RV	GTAATACGACTCACTATAGGGCAGTCTCCGTCTAGTAACTTC	
E610	Dcr2 Ae ae SYBR FW	CGGGCAAACCCTGTTACATC	
E611	Dcr2 Ae ae SYBR RV	TGTTGGATCCTGCGCAAAC	
E352	*Ae. aegypti* dsRNA Ago1-T7 FW	GTAATACGACTCACTATAGGGACAGGTTTCACTGTTCAACCT	
E353	*Ae. aegypti* dsRNA Ago1-T7 RV	GTAATACGACTCACTATAGGGGGTTTGACCGTTTTCTAGCTGC	
E354	*Ae. aegypti* dsRNA Ago2-T7 FW	GTAATACGACTCACTATAGGGGCCCTCAACAAGAAACACC	
E355	*Ae. aegypti* dsRNA Ago2-T7 RV	GTAATACGACTCACTATAGGGGCGTTGATCTTGAGCCA	
E348	*Ae. aegypti* dsRNA Ago3-T7 FW	GTAATACGACTCACTATAGGGGAGTTACCTCATCAATGACGCG	[249]
E349	*Ae. aegypti* dsRNA Ago3-T7 RV	GTAATACGACTCACTATAGGGGGCACTTAAATCCTGTAGGTACCTT	[249]
E342	*Ae. aegypti* dsRNA Piwi4-T7 FW	GTAATACGACTCACTATAGGGCCGTATATCCGAAAAAGTGCTG	[189]
E343	*Ae. aegypti* dsRNA Piwi4-T7 RV	GTAATACGACTCACTATAGGGAGAGTCCACTCGATGTGTTTCA	[189]
E344	*Ae. aegypti* dsRNA Piwi5-T7 FW	GTAATACGACTCACTATAGGGCGTAATGTTGCTGTTTCGAATG	[249]
E345	*Ae. aegypti* dsRNA Piwi5-T7 RV	GTAATACGACTCACTATAGGGGATTTGGAACAATTAGAGGTG	[249]
E346	*Ae. aegypti* dsRNA Piwi6-T7 FW	GTAATACGACTCACTATAGGGACCAGAAATAGTGCAAACCCG	[249]

E347	*Ae. aegypti* dsRNA Piwi6-T7 RV	GTAATACGACTCACTATAGGGCATGTCGGTTGATAAGGTTGAA	[249]
E350	*Ae. aegypti* dsRNA eGFP-T7 FW	GTAATACGACTCACTATAGGGGGCGTGCAGTGCTTCAGCCGC	[310]
E351	*Ae. aegypti* dsRNA eGFP-T7 RV	GTAATACGACTCACTATAGGGGTGGTTGTCGGGCAGCAGCAC	[310]
E801	dsRNA SFV T7 FW	GTAATACGACTCACTATAGGGGAACGGCGTATTGGATTGG	
E802	dsRNA SFV T7 RV	GTAATACGACTCACTATAGGGCTTCCGTTCACAACTATCCTCTG	
E592	dsRNA BUNV L-segment T7 FW	GTAATACGACTCACTATAGGGGGACCCTATACTTTATCCAGC	
E593	dsRNA BUNV L-segment T7 RV	GTAATACGACTCACTATAGGGCAGTCTCCGTCTAGTAACTTC	
E373	dsRNA lacZ T7 FW	TAATACGACTCACTATAGGGGTCGCCAGCGGCACCGCGCCTTTC	[311]
E374	dsRNA lacZ T7 RV	TAATACGACTCACTATAGGGCCGGTAGCCAGCGCGGATCATCGG	[311]
E803	dsRNA FFluc T7 FW	GTAATACGACTCACTATAGGGACTTACGCTGAGTACTTC	[310]
E804	dsRNA FFluc T7 RV	GTAATACGACTCACTATAGGGGAAATCCCTGGTAATCCG	[310]
E805	dsRNA Rluc T7 FW	TAATACGACTCACTATAGGGATGACTTCGAAAGTTTATGATCCAG	[312]
E806	dsRNA Rluc T7 RV	TAATACGACTCACTATAGGGCTGCAAATTCTTCTGGT TCTAACTTTC	[312]

siRNAs

Table 9: siRNA listed with Description and sequence in sense orientation.

Description	sequence (5’ - 3’)
siFFluc	CUUACGCUGAGUACUUCGAdTdT

2.1.6. Enzymes

Table 10: List of enzymes used.

Enzyme	Manufacturer / Supplier
T4 DNA ligase	NEB, Ipswich, MA, USA
XbaI	NEB, Ipswich, MA, USA
SacII	NEB, Ipswich, MA, USA
FastAP	NEB, Ipswich, MA, USA
NotI	NEB, Ipswich, MA, USA

2.1.7. Antibodies / fluorescence dyes

Table 11: Primary and secondary antibodies conjugated to fluorescence dyes used for immunostaining.

Antibody	Dilution	Specificity	species	Reference / Manufacturer
nsP3-SFV	1:300	SFV nsP3	rabbit	[189]
BUNV-N rabbit anti BUNV N (#592)	1:300	BUNV N-protein	rabbit	[265]
3G1.1 dsRNA Hybridoma 3G1.1 supernatant	1:100	anti-dsRNA	mouse	[313]
DAPI	1:2000	DNA	rabbit	Thermo Fisher Scientific Inc., Waltham, MA, USA
Alexa Fluor™ 594 donkey anti-rabbit IgG (H+L) 2 mg/ml	1:1000		donkey	Invitrogen / Thermo Fisher Scientific Inc., Waltham, MA, USA
Alexa Fluor™ 488 goat anti-mouse IgG (H+L) 2 mg/ml	1:1000		goat	Invitrogen / Thermo Fisher Scientific Inc., Waltham, MA, USA

2.1.8. Chemicals and reagents

Table 12: Utilized chemicals for experiments.

Chemical	Manufacturer / Supplier
2x MEM	Gibco / Thermo Fisher Scientific Inc., Waltham, MA, USA
3M sodium acetate	Invitrogen / Thermo Fisher Scientific Inc., Waltham, MA, USA
5x PLB	Promega Corp., Fitchburg, WI, USA
Acetic acid	Carl Roth GmbH + Co. KG, Karlsruhe, Germany
Agarose	Carl Roth GmbH + Co. KG, Karlsruhe, Germany
Ampicillin	Gibco / Thermo Fisher Scientific Inc., Waltham, MA, USA
Avicel	FMC international, Ireland
Blasticidine S HCl	Gibco / Thermo Fisher Scientific Inc., Waltham, MA, USA
Borate buffer	Thermo Fisher Scientific Inc., Waltham, MA, USA
Cap Analog (m^7 G(5')ppp(5')G)	Invitrogen / Thermo Fisher Scientific Inc., Waltham, MA, USA
Chloroform (99 %)	Sigma-Aldrich / Merck KGaA, Darmstadt, Germany
Crystal violet	Carl Roth GmbH + Co. KG, Karlsruhe, Germany
CutSMart buffer	NEB, Ipswich, MA, USA
DharmaFECT2	Horizon Discovery Ltd., Cambridge, UK
Dimethyl sulfoxide (DMSO)	Sigma-Aldrich / Merck KGaA, Darmstadt, Germany
Dulbecco's Modified Eagle Medium (DMEM)	PAN-Biotech GmbH, Aidenbach, Germany
DNA gel loading dye	Thermo Fisher Scientific Inc., Waltham, MA, USA
dNTP Set	Thermo Fisher Scientific Inc., Waltham, MA, USA
DPBS	PAN-Biotech GmbH, Aidenbach, Germany
EDTA	Carl Roth GmbH + Co. KG, Karlsruhe, Germany
Ethanol (99 %)	Carl Roth GmbH + Co. KG, Karlsruhe, Germany
Ethidiumbromide	AppliChem GmbH, Darmstadt, Germany
FastAP alkaline phosphatase	Thermo Fisher Scientific Inc., Waltham, MA, USA
Fetal calf serum (FCS)	Biochrom AG, Berlin, Germany
Formaldehyde	Carl Roth GmbH + Co. KG, Karlsruhe, Germany
GeneRuler 1 kb Ladder	Thermo Fisher Scientific Inc., Waltham, MA, USA
GeneRuler 100 bp Ladder	Thermo Fisher Scientific Inc., Waltham, MA, USA
Glycerol	Carl Roth GmbH + Co. KG, Karlsruhe, Germany
Glycogen	Thermo Fisher Scientific Inc., Waltham, MA, USA

Glasgow's Minimal Essential Medium (GMEM)	Gibco / Thermo Fisher Scientific Inc., Waltham, MA, USA
Isopropanol	Carl Roth GmbH + Co. KG, Karlsruhe, Germany
Kanamycin	Gibco / Thermo Fisher Scientific Inc., Waltham, MA, USA
KCl	Carl Roth GmbH + Co. KG, Karlsruhe, Germany
KH_2 PO4	Carl Roth GmbH + Co. KG, Karlsruhe, Germany
LB-agar	Carl Roth GmbH + Co. KG, Karlsruhe, Germany
LB-medium	Carl Roth GmbH + Co. KG, Karlsruhe, Germany
Leibovitz's L-15 medium	Gibco / Thermo Fisher Scientific Inc., Waltham, MA, USA
Na_2 HPO_4-$7H_2O$	Carl Roth GmbH + Co. KG, Karlsruhe, Germany
NaCl	Carl Roth GmbH + Co. KG, Karlsruhe, Germany
Nuclease-free water	Ambion / Thermo Fisher Scientific Inc., Waltham, MA, USA
Oligo$(dT)_{18}$ primer	Thermo Fisher Scientific Inc., Waltham, MA, USA
Opti-MEM	Thermo Fisher Scientific Inc., Waltham, MA, USA
Phosphate buffered saline (PBS)	Carl Roth GmbH + Co. KG, Karlsruhe, Germany
Penicillin/streptomycin	Gibco / Thermo Fisher Scientific Inc., Waltham, MA, USA
Plasmid-Safe™ ATP-Dependant DNase (10 U/µl)	Lucigen, Middleton, WI, USA
Random hexamer primer	Thermo Fisher Scientific Inc., Waltham, MA, USA
RNase Away	Molecular Bio Products / Thermo Fisher Scientific Inc., Waltham, MA, USA
RNAse inhibitor	Promega Corp., Fitchburg, WI, USA
Sodium dodecyl sulfate (SDS)	Carl Roth GmbH + Co. KG, Karlsruhe, Germany
Sodium acetate	Carl Roth GmbH + Co. KG, Karlsruhe, Germany
Sodium periodate	Sigma-Aldrich / Merck KGaA, Darmstadt, Germany
T4 DNA ligase	NEB, Ipswich, MA, USA
Tragacanth	Sigma-Aldrich / Merck KGaA, Darmstadt, Germany
TRIS	Carl Roth GmbH + Co. KG, Karlsruhe, Germany
Triton X 100	Carl Roth GmbH + Co. KG, Karlsruhe, Germany
TRIzol Reagent	Invitrogen / Thermo Fisher Scientific Inc., Waltham, MA, USA
Trypsin / EDTA	PAN-Biotech GmbH, Aidenbach, Germany
Tryptose phosphate broth	Gibco / Thermo Fisher Scientific Inc., Waltham, MA, USA
Zeocine	Invitrogen / Thermo Fisher Scientific Inc., Waltham, MA, USA

2.1.9. Kits

Table 13: Used kits listed with manufacturer or supplier.

Kit	Manufacturer / Supplier
CloneJET PCR Cloning Kit	Thermo Fisher Scientific Inc., Waltham, MA, USA
GoTaq DNA polymerase	Promega Corp., Fitchburg, WI, USA
KOD DNA polymerase	Merck KGaA, Darmstadt, Germany
MEGAscript RNAi Kit	Invitrogen / Thermo Fisher, Waltham MA, USA
MEGAscript SP6	Invitrogen / Thermo Fisher Scientific Inc., Waltham, MA, USA
MEGAscript T7	Ambion / Thermo Fisher Scientific Inc., Waltham, MA, USA
M-MLV reverse transcriptase	Promega Corp., Fitchburg, WI, USA
Monarch RNA Cleanup Kit (50 µg)	NEB, Ipswich, MA, USA
NEXTflex Small RNA-Seq Kit v3	Perkin Elmer, Austin, TX, USA
NucleoBond Xtra Midi Kit	Macherey-Nagel, Düren, Germany
NucleoSpin Gel and PCR Clean-up	Macherey-Nagel, Düren, Germany
NucleoSpin Plasmid EasyPure	Macherey-Nagel, Düren, Germany
QIAamp DNA Mini Kit	Qiagen, Hilden, Germany

QIAGEN Plasmid Midi Kit	Qiagen, Hilden, Germany
QuantiTect SYBR Green PCR kit	Qiagen, Hilden, Germany
QuantiTect SYBR Green RT-PCR kit	Qiagen, Hilden, Germany
TURBO DNA-free Kit	Invitrogen / Thermo Fisher Scientific Inc., Waltham, MA, USA

2.1.10. Buffers and stock solutions

Table 14: Utilized buffers and stock solutions.

Buffer	Amount	Reagent
TAE (10x) buffer	242 g 57.1 ml 100 ml ad 1000 ml	TRIS 5.7 % acetic acid EDTA (pH 8.0) / 0.5 M stock solution dH_2O
Formaldehyde (8 %)	10 ml 40 ml	Formaldehyde (37 %) 1x PBS
PBS (10x)	8 g 0.2 g 1.44 g 0.24 g ad 1000 ml	NaCl KCl $Na_2 HPO_4$ $KH_2 PO_4$ dH_2O
PBS	80 ml 720 ml	10x PBS dH_2O
0.1 % SDS/PBS	0.1 ml 99.9 ml	SDS PBS
PBS-T	3 ml 597 ml	Triton X-100 PBS
Blocking solution	1 ml 9 ml	FCS PBT
Crystal violet (10x)	10 g 50 ml 100 ml ad 340 ml	Crystal violet Formaldehyde (37 %) Ethanol (96 %) dH_2O
Crystal violet (1x)	100 ml 100 ml ad 800 ml	Crystal violet (10x) stock solution Formaldehyde (37 %) dH_2O

2.1.11. Consumables

Table 15: Utilized consumption items.

Consumption items	Manufacturer / Supplier
25 ml pipetting reservoir	Argos Technologies / Cole-Parmer GmbH, Wertheim, Germany
96 well microplate, PS, F-bottom	Greiner Bio-One GmbH, Frickenhausen, Germany
Adhesive PCR seal	Roche, Basel, Switzerland
Biosphere Filter Tips (10 - 1000 µl)	Sarstedt AG & Co. KG, Nümbrecht, Germany
Cell culture flask (25 cm^2, 75 cm^2, filtered and non-filtered cap)	Greiner Bio-One GmbH, Frickenhausen, Germany
Cell scraper 25 cm	Sarstedt AG & Co. KG, Nümbrecht, Germany
Conical Centrifugation tube (15 ml, 25 ml)	Sarstedt AG & Co. KG, Nümbrecht, Germany
Cryo Tube vials	Thermo Fisher Scientific Inc., Waltham, MA, USA

Disposal bags	Carl Roth GmbH + Co. KG, Karlsruhe, Germany
Eppendorf tubes	Thermo Fisher Scientific Inc., Waltham, MA, USA
Inoculation loop, 10 µl	Greiner Bio-One GmbH, Frickenhausen Germany
LightCycler 480 Multiwell plate 96, white	Roche, Basel, Switzerland
Multiply-µStrip Pro 8-strip PCR tubes	Sarstedt AG & Co. KG, Nümbrecht, Germany
Parafilm	Bemis, Oshkosh, NE, USA
Serological pipets 5, 10, 25 ml	Corning Inc., Glendale, AZ, USA
Syringe (1, 2, 10 ml)	B. Braun Melsungen AG, Melsungen , Germany
TC plate (6, 12, 24 wells)	Sarstedt AG & Co. KG, Nümbrecht, Germany
Collection Tubes	Ambion / Invitrogen / Thermo Fisher Scientific Inc., Waltham, MA, USA
Filter Cartridges	Invitrogen / Thermo Fisher Scientific Inc., Waltham, MA, USA

2.1.12. Technical devices and equipment

Table 16: Technical devices and equipment used.

Devices	**Manufacturer / Supplier**
Agarose Casting stand MultiCast	PEQLAB / VWR, Darmstadt, Germany
Agarose gel chamber	PEQLAB / VWR, Darmstadt, Germany
Centrifuge 5415D	Eppendorf, Hamburg, Germany
Centrifuge ct15 himac	VWR, Darmstadt, Germany
Centrifuge Labofuge 400 R	Heraeus Holding GmbH, Hanau, Germany
Centrifuge Mini Star	VWR, Darmstadt, Germany
Centrifuge Pico 17	Thermo Fisher Scientific Inc., Waltham, MA, USA
Cleanbench Hera safe KS 12	Heraeus Holding GmbH, Hanau, Germany
Cleanbench Maxisafe 2020	Thermo Fisher Scientific Inc., Waltham, MA, USA
Erlenmeyer flask (1000 ml)	VWR, Darmstadt, Germany
Erlenmeyer flask (1000 ml)	VWR, Darmstadt, Germany
Evos FL Fluroeszenz Microcsope	Thermo Fisher Scientific Inc., Waltham, MA, USA
FlexCycler	Analytik Jena AG, Jena, Germany
Imaging System ChemiDoc Touch	Bio-Rad Laboratories GmbH, München, Germany
Incubator Function line	Heraeus Holding GmbH, Hanau, Germany
Incubator Heraeus 6000	Heraeus Holding GmbH, Hanau, Germany
Incubator innova co 170	Thermo Fisher Scientific Inc., Waltham, MA, USA
Luminometer GloMax Navigator	Promega Corporation, Mannheim, Germany
Metal Block Thermostat MBT 250	ETG, Ilmenau, Germany
Microscope AE2000	Motic, Wetzlar, Germany
Mini see-saw rocker SSM4	Stuart / Cole-Parmer, UK
Mr. Frosty Cryo Freezing Container	Thermo Fisher Scientific Inc., Waltham, MA, USA
Multipette 5 - 50 µl / 50 - 300 µl	PZ HTL S.A., Poland
NanoDrop 1000 Spectrophotometer	peqLab Biotechnologie GmbH, Erlangen, Germany
Neubauer counting-chamber	P. Marienfeld GmbH & Co. KG, Lauda Königshofen, Germany
Pipetus	Hirschmann Laborgeräte GmbH & Co. KG, Eberstadt, Germany
Portable tube luminometer Junior LB 9509	Berthold Technologies GmbH & Co KG, Bad Wildbad, Germany
PowerPac 300	Bio-Rad Laboratories GmbH, München, Germany
Research Plus Pipettes (10 µl, 100 µl, 1000 µl)	Eppendorf AG, Hamburg, Germany
Scale Scout Pro	OHAUS Europe GmbH, Switzerland
Thermomixer comfort	Eppendorf, Hamburg, Germany
Vortex Genie 1 & 2	Scientific Industries, Bohemia, USA
Watherbath WNB45	Memmert, Schwabach, Germany

2.1.13. Software and bioinformatic tools

Table 17: Software and tools used for analysis.

Software	Manufacturer
A plasmid Editor (ApE)	Open source (http://biologylabs.utah.edu/jorgensen/wayned/ape)
BLAST	https://blast.ncbi.nlm.nih.gov/Blast.cgi
ImageJ, v1.52e	Open source (http://imagej.nih.gov/ij)
Lightcycler 480 Software, v1.5.0	Roche Molecular Systems, Inc., 2021
SnapGene Viewer, v5.1.4.1	GSL Biotech LLC, 2017
Prism, v8.4.2	GraphPad Software LLC, 1992 - 2020
EVOS FL Auto Cell Imaging Software v1.7	Life Technologies Corporation, 2013

2.1.14. Nucleotide sequence accession numbers

Table 18: Accession numbers of various viruses.

Virus	Accession number
SFV4	KP699763.1
SFV6	KT009012.1
PCLV S-segment	KM001087.1
PCLV M-segment	KM001086.1
PCLV L-segment	KM001085.1
CFAV	NC_001564.1
BUNV S-segment	NC_001927.1
BUNV M-segment	NC_001926.1
BUNV L-segment	NC_001925.1

2.2. Methods

2.2.1. Molecular biology methods

2.2.1.1. Determination of concentration and purity of RNA and DNA samples

Concentration and purity of RNA and DNA samples was determined by measuring the absorbance of the samples at different wavelengths using a Nano Drop 2000 Spectrophotometer (Thermo Fisher Scientific Inc., Waltham, MA, USA) and associated software. Absorbance at 260 nm provides total nucleic acid content while absorbance at 280 nm measures the purity of the sample [314].

2.2.1.2. Agarose gel electrophoresis

To determine sizes of different DNA samples and separate DNA fragments according to their length in an electric field, agarose gel electrophoresis was performed. Gels had a varying concentration, which was ranging from 1 - 2 % w/v agarose dissolved in 1x TAE buffer containing 1 µg/ml ethidium bromide, which intercalates into the DNA and can be detected by UV-light illumination. Each sample was mixed with 6x DNA loading dye before loading them on the gel. For size determination, a 1 kb or 100 bp ladder (Thermo Fisher Scientific Inc., Waltham, MA, USA) was added into one pocket of the gel. Electrophoresis was performed in an electrophoresis chamber with 1x TAE buffer usually applying 10 volt/cm for 30 min approximately. Subsequently, gels were analyzed using UV light and a gel documentation system (ChemiDoc Touch Imaging System, Bio-Rad Laboratories GmbH, München, Germany) with the associated software.

2.2.1.3. DNA extraction from agarose gels

DNA fragments were extracted from agarose gels by cutting them out of the gel using a gel documentation table with UV light. The gel fragment was then purified with the NucleoSpin Gel and PCR Clean-up Kit (Macherey-Nagel, Düren, Germany) according to the manufacturer‘s protocol. DNA was eluted with 30 µl elution buffer.

2.2.1.4. Restriction digestion

Restriction digestion of purified plasmid was performed using different restriction enzymes for the experiments (SacII, XbaI, NotI) (New England Biolabs, Inc., Ipswich, MA, USA). Reagent mix and protocol for a single sample are listed below.

Table 19: Reaction mix for restriction digestion.

Amount	Reagent
4 µl	10x CutSmart buffer
4 µg	DNA / plasmid
4 µl	restriction enzyme
ad 40 µl	ddH_2O

Reaction mix was incubated for 1 h at 37 °C. For a double digestion, 4 µl of the second restriction enzyme was added and the mix was again incubated for 1 h at 37 °C and stored at -20 °C afterwards.

2.2.1.5. Plasmid preparation (Mini- and Midi preparation)

For plasmid amplification, single *E. coli* colonies were picked from agar plates with a pipette tip and transferred to either 2 ml Eppendorf tubes or conical flasks prepared with 1.8 ml or 100 ml LB-medium respectively with selected antibiotics. Solution was cultivated overnight at 37 °C and 250 rpm in a rotational shaker. Next day, plasmid DNA was extracted from bacterial cells by using the NucleoSpin Plasmid EasyPure Kit or the NucleoBond Midi Kit (both Macherey-Nagel, Düren, Germany) according to the manufacturer's protocol. Plasmid DNA was then either dissolved in 40 µl (Mini prep) or 150 µl (Midi prep) TE buffer.

2.2.1.6. Isolation of RNA

RNA from cells was isolated using TRIzol reagent (Invitrogen / Thermo Fisher Scientific Inc., Waltham, MA, USA). It contains a mixture of guanidine thiocyanate and phenol in one solution that effectively extracts DNA, RNA, and proteins from biological samples. Each well was lysed with TRIzol reagent (1 ml for a 6 well plate, 500 µl for a 24 well plate) and phases were separated with chloroform (100 µl / 1 ml TRIzol) by centrifugation for 15 min at 10,500 x g and 4 °C. Afterwards, the upper aqueous phase was transferred to a new tube adding 10 mg/ml glycogen as carrier and isopropanol (250 µl / 1ml TRIzol) to the sample for precipitation. After 10 min of incubation at room temperature, samples were again centrifuged for 15 min at 12,000 x g and 4°C. Supernatant was discarded and the remaining pellet was washed twice with 70 % ethanol, centrifuging for 10 min at 12,000 x g and 4 °C after each washing step. Pellet was air-dried and resuspended in 20 µl RNase-free water.

2.2.1.7. cDNA synthesis / reverse transription

cDNA synthesis from previously extracted RNA samples was performed using M-MLV reverse transcriptase (RT). Reagents and protocol for a single sample are listed below.

Table 20: Step 1 for cDNA synthesis with M-MLV reverse transcriptase.

Amount	Reagent
1.5 µg	RNA
1 µl	oligo dT / random hexamers
ad 15 µl	ddH_2O

Reaction mix was incubated for 5 min at 70 °C and placed for 1 min on ice aftwards. In a second step, M-MLV RT and further reagents were added.

Table 21: Step 2 for cDNA synthesis with M-MLV RT.

Amount	Reagent
5 µl	5x M-MLV buffer
1.25 µl	dNTPs (10 mM)
1 µl	RNase inhibitor
1 µl	M-MLV (200 U/µl)
1.75 µl	ddH_2O

Reaction mix was incubated for 1 hour at 42 °C (oligo dT) or 37 °C (random hexamers).

2.2.1.8. *In vitro RNA transcription*

CHIKV *trans*-replicase template RNA (SG-Nluc and SG-C-Nluc) was linearized by *NotI* digestion. RNA was synthesized from purified plasmid DNA using the MEGAscript SP6 kit (Invitrogen / Thermo Fisher Scientific Inc., Waltham, MA, USA). Reaction mix and protocol for a single sample is listed below.

Table 22: Reaction mix for in vitro transcription with MEGAScript SP6 kit.

Amount	Reagent
1 µg	linear DNA
2 µl	10x SP6 buffer
2 µl	of each rNTP (ATP, CTP, GTP (1:10), UTP)
2 µl	cap analog
2 µl	SP6 enzyme
ad 20 µl	ddH_2O

Reaction mix was incubated for 4 hours at 37 °C and was used directly for transfection of cells for CHIKV *trans*-replicase experiments.

2.2.1.9. *dsRNA production*

dsRNA targeting Ae. aegypti Ago1-3, Piwi4-6 [189, 249, 310-312] transcripts, SFV6-2SG-Nluc or BUNV-Nluc genome, Firefly luciferase (FFluc) [310], Renilla luciferase (Rluc) [312], lacZ [311] or eGFP [310] were produced with the Megascript T7 RNAi kit (Ambion / Thermo Fisher Scientific Inc., Waltham, MA, USA) as previously described [249] (for primers see Table 8). In short, sequence-specific PCR products flanked with a T7 RNA polymerase recognition sites were produced and used for in vitro transcription with T7 RNA polymerase. Reaction mix for a single sample is listed below (Table 23).

Table 23: Reaction mix for in vitro transcription with T7 polymerase.

Amount	Reagent
1 µg	linear DNA
2 µl	10x T7 buffer
2 µl	of each rNTP (ATP, CTP, GTP, UTP)
2 µl	T7 enzyme
ad 20 µl	ddH_2O

Reaction mix was incubated overnight at 37°C and heated to 70 °C for 5 min the next day. Mix was then slowly cooled down to room temperature to bind complementary sequences and thereby form dsRNA molecules. In a next step, nucleases were added to each reaction mix to remove template DNA and ssRNA (Table 24).

Table 24: Nuclease digestion on the transcription reaction.

Amount	Reagent
21 µl	ddH_2O
5 µl	10x digestion buffer
2 µl	RNase
2 µl	DNase I

The reaction mix was incubated for 1 hour at 37 °C. Afterwards, 50 µl of 10x binding buffer, 250 µl ethanol (99.8 %) and 150 µl ddH_2O was added to the mix and transferred to a filter cartridge (Ambion / Thermo Fisher Scientific Inc., Waltham, MA, USA) for centrifugation (2 min, 10,000 x g, room temperature). The filter cartridge was washed twice with 500 µl washing solution, centrifuging for 2 min at maximum speed. dsRNA was eluated with 104 µl elution buffer and stored at -20 °C until further use.

2.2.1.10. PCR

Polymerase chain reaction (PCR) is used for the amplification of specific DNA sequences. To amplify the target sequence, two primers are needed with a complementary sequence flanking the target region. GoTaq DNA polymerase (Promega, Madison, WI, USA) or KOD Hot Start DNA polymerase (Promega, Madison, WI, USA) with proof-reading ability were used for preparative PCRs for cloning, colony screens, sequence and integration checks and infection control according to manufacturer's protocol. Oligonucleotide primer were ordered at biomers.net (Ulm, Germany) (Table 8). Reagents for a single sample and protocol are listed below (GoTaq: Table 25, Table 27; KOD: Table 26,Table 28).

Table 25: GoTaq polymerase RT-PCR reaction mix.

Amount	Reagent
10 µl	5x GoTaq buffer
0.25 µl	Primer forward (100 pmol/µl)
0.25 µl	Primer reverse (100 pmol/µl)
1 µl	dNTPs (10 mM)
0.5 µl	GoTaq polymerase
xx µl	DNA (< 500 ng)
ad 50 µl	ddH_2O

Table 26: KOD polymerase RT-PCR reaction mix.

Amount	Reagent
5 µl	10x KOD buffer
1.5 µl	Primer forward (10 pmol/µl)
1.5 µl	Primer reverse (10 pmol/µl)
5 µl	dNTPs (2 mM)
1 µl	KOD polymerase
3 µl	$MgCl_2$
xx µl	DNA (1 pg - 10 ng)
ad 50 µl	ddH_2O

Table 27: GoTaq polymerase protocol for RT-PCR.

Temperature	Time	Repeat
95 °C	2 min	1x
95 °C	30 sec	30 - 35x
xx °C	30 sec	30 - 35x
72 °C	(60 sec for 1 kb)	30 - 35x
72 °C	7 min	1x
4 °C	∞	

Table 28: KOD polymerase protocol for RT-PCR.

Temperature	Time	Repeat
95 °C	2 min	1x
95 °C	20 sec	20 - 40x
xx °C	10 sec	20 - 40x
70 °C	(15 sec for 1 kb)	20 - 40x
70 °C	7 min	1x
4 °C	∞	

2.2.1.11. Quantitative Real-Time PCR (qPCR)

qPCR was used to determine expression levels of several transcripts and viral RNA levels. Either one-step quantitative RT-qPCR using total isolated RNA from samples (QuantiTect SYBR Green RT-PCR kit, Qiagen, Germany) or previously reverse transcribed cDNA was used (QuantiTect SYBR Green PCR kit, Qiagen, Germany). qPCR was performed using specific primers (Table 8) and a LightCycler 480 (Roche, Basel, Switzerland) according to manufacturer's instructions. Reaction mix for a single sample and protocol are listed below (RT-qPCR: Table 29, Table 31; qPCR: Table 30, Table 31).

Table 29: One-step SYBR Green RT-qPCR reaction mix.

Amount	Reagent
5 µl	2x QuantiTect Master Mix
0.4 µl	Primer forward (10 µM)
0.4 µl	Primer reverse (10 µM)
0.1 µl	QuantiTect RT Mix
3.1 µl	ddH_2O

Table 30: SYBR Green qPCR reaction mix.

Amount	Reagent
5 µl	2x QuantiTect Master Mix
0.3 µl	Primer forward (10 µM)
0.3 µl	Primer reverse (10 µM)
3.4 µl	ddH_2O

Table 31: (One-step) SYBR Green RT-qPCR LightCycler protocol.

Temperature	Time	Steps and repeats
50 °C	30 min	Reverse transcription (1x) (only one-step RT-qPCR)
95 °C	15 min	Initial activation
94 °C	15 sec	
60 °C	30 sec	Quantification (45x)
72 °C	45 sec	
95 °C	5 sec	
50 °C	15 sec	Melting curves
95 °C	continuous	

2.2.1.12. Sequencing

Sanger sequencing

Samples were sequenced at LGC Genomics GmbH (Berlin, Germany) with the Ready2Run setup. 4 µl of primer (5 µM) were added to 10 µl of DNA with a concentration of 80 - 100 ng/µl and submitted in a reaction tube.

Next Generation sequencing (NGS)

For small RNA sequencing at least 1 µg of total RNA was either sent to BGI Genomics (Shenzhen, China) for sequencing with an Illumina based system (BGISEQ-500, as 50SE) as previously described [315] or to IKMB (Kiel, Germany). For sequencing at BGI, total RNA was loaded on a PAGE gel and RNA molecules of 18-35 nts were isolated, followed by adaptor ligation, RT-PCR with SuperScriptII to produce and enrich for cDNA fragments. PCR products were PAGE gel purified, followed by circularization. The single strand circle DNA was used as final library and after validation on the bioanalyzer, DNA nanoballs were produced from the libraries with phi29 that in turn generated single end 50 base reads. At IKMB, 100 ng total RNA was used for library preparation with the NEXTflex Small RNA-Seq Kit v3 (PerkinElmer Inc., Waltham, MA, USA) according to manufacturer's protocol. Here, instead of isolating RNAs of 18-35 nts, total RNA was used to generate DNA libraries, followed by purification of PCR products of the corresponding length by PAGE gel. Following library sequencing on a NovaSeq6000 SP v1.0 (2x 50bp). For both companies at least 20 million clean reads per sample were received.

2.2.1.13. Expression analysis

Expression analysis was used to determine mRNA levels of different proteins to confirm knockdown efficiency of dsRNA or relative viral RNA levels of various viruses in infected cells. Either cDNA was produced from isolated total RNA of cells using M-MLV RT or one-step SYBR Green RT-qPCR was used with specific primers (Table 8). Ribosomal S7 RNA was used as a housekeeper for the $\Delta\Delta C_T$ method.

2.2.1.14. Cloning of Reporter sensor constructs based on pIZ-FFluc and pIZ-Nluc

In order to clone siRNA and piRNA reporter constructs, specific target sequences of the SFV or BUNV genome were first amplified from cDNA (2.2.1.7) in sense or antisense orientation using specific primers introducing SacII or XbaI restriction sites (Table 32).

To create a negative control for reporter constructs, eGFP DNA was amplified from pEGFP-C1 vector (Clontech / Takara Bio Inc., St-Germain-en-Laye, France) and also cloned into pIZ-FFluc and pIZ-Nluc vectors downstream of the luciferase reporter ORF to create pIZ-FFluc-eGFP and pIZ-Nluc-eGFP [177] control vectors. The amplification of inserts was controlled using agarose gel electrophoresis (chapter 2.2.1.2).

Table 32: SFV and BUNV reporter construct characteristics.
Name of the sensor construct, used primers, genomic location and length of the amplified fragment are shown.

Name	Identifier	Genome location (nt)	Length (nt)
pSFV-FFluc-1_s	E167/E168	7877 - 8486	609
pSFV-FFluc-1_{as}	E167/E168		
pSFV-FFluc-2_s	E169/E170	8857 - 9499	642
pSFV-FFluc-2_{as}	E169/E170		
pSFV-FFluc-1_s	E171/E172	600 - 1200	600
pSFV-FFluc-1_{as}	E171/E172		
pSFV-FFluc-2_s	E173/E174	3182 - 3695	513
pSFV-FFluc-2_{as}	E173/E174		
pBUNV-Nluc-$S1_s$	E420/E397	241 - 556 S-segment	315
pBUNV-Nluc-$S1_{as}$	E396/E421		
pBUNV-Nluc-$S2_s$	E548/E549	71 - 273 S-segment	202
pBUNV-Nluc-$S2_{as}$	E547/E550		
pBUNV-Nluc-M_s	E398/E422	314 - 649 M-segment	335
pBUNV-Nluc-M_{as}	E431/E399		

After successful amplification, inserts were blunt-end ligated into the pJET 1.2 cloning vector (CloneJET PCR Cloning kit, Thermo Fisher Scientific Inc., Waltham, MA, USA) according to manufacturer's protocols. Ligated product was transformed into *E. coli* and selected on ampicillin-LB-agar plates (100 µg/ml) (chapter 2.2.3.1). Plates were incubated overnight at 37 °C.

Next day, a colony-PCR was performed selecting for successful ligation products. Therefore, single colonies were picked with a pipet tip and transferred into 1.5 ml of LB-medium for an overnight culture and into 20 µl ddH_2O for subsequent colony PCR. Suspension was heated for 5 min at 95 °C to lyse the bacterial cells. Afterwards, 5 µl of heated sample was used for a PCR with GoTaq polymerase (chapter 2.2.1.10) and insert-specific primers (Table 8). PCR products were checked on an agarose gel and positive-tested colonies were incubated at 37 °C and 300 rpm overnight.

On the next day, amplified plasmid was extracted from bacterial cells using NucleoSpin Plasmid EasyPure kit (Macherey Nagel, Düren, Germany). Purified plasmid was digested with restriction enzymes *SacII* and *XbaI* to isolate the amplified insert sequence again for further ligation (chapter 2.2.1.4). Digested samples were checked for inserts using an agarose gel following clean up using NucleoSpin Gel and PCR Clean-up kit (Macherey-Nagel, Düren, Germany). In a next step, the backbone (SFV: pIZ-FFluc; BUNV: pIZ-Nluc) was prepared and digested with SacII and *XbaI* restriction enzymes (chapter 2.2.1.4). Linearized DNA was purified from an agarose gel and ligated with the insert sequence (Table 33).

Table 33: Reaction mix for ligation of backbone DNA and insert.

Amount	Reagent
2 µl	10x T4 DNA ligase buffer
1 µl	backbone DNA
3 µl	purified insert DNA
1 µl	T4 DNA ligase
13 µl	ddH_2O

The reaction mix was incubated at 16 °C overnight and incubated for 10 min at 65 °C to stop the reaction. Afterwards, 10 µl of the mix were used for transformation of *E. coli* on LB-agar plates containing zeocin (20 µg/ml) (chapter 2.2.3.1). Plates were incubated overnight at 37 °C. Next day, colony-PCR was performed on selected bacterial colonies. Positive-tested clones were cultivated overnight in LB-medium containing zeocin (20 µg/ml) at 37 °C and 300 rpm on a rotational shaker. The plasmid was isolated by mini-prep the next day according to manufacturer's protocol and samples were submitted to Sanger sequencing (LGC, Berlin, Germany) (chapter 2.2.1.12).

2.2.1.15. Luciferase assays

Relative luciferase activity was determined by using Dual-Luciferase Reporter Assay System, Firefly Luciferase Assay System, Renilla-Glo Luciferase Assay system and Nano-Glo Luciferase Assay System (all Promega Corp., Fitchburg, WI, USA) in a GloMax Navigator multi-luminometer with injectors following cell lysis in Passive Lysis buffer (Promega Corp., Fitchburg, WI, USA) according to manufacturer's protocols. 20 µl of lysed cell solution was used for the luciferase measurement.

2.2.2. Cellular biology and virology methods

2.2.2.1. Cell count determination

Cells counts per ml were determined using a Neubauer-improved counting chamber (Paul Marienfeld GmbH & Co. KG, Germany).

2.2.2.2. Infection of vertebrate and mosquito cells

The concept of multiplicity of infection (MOI) is used to determine the ratio of the number of infectious viral particles to the target cell number. Assuming that each infectious viral particle is able to infect a single cell, the amount of virus stock needed can be calculated as follows (V_{virus}: Volume of virus stock needed; c_{cells}: concentration of cells; c_{virus}: concentration of virus stock):

$$V_{virus}\ (ml) = \frac{C_{cells} \times MOI}{c_{virus}}$$

To inoculate cells, calculated stock was diluted with medium (ad 100 µl / per well).

2.2.2.3. Preparation of virus stocks and titration

SFV4, SFV4(3H)-FFluc, SFV6-2SG-Nluc, BUNV and BUNV-Nluc stocks were grown on BHK-21 cells, while ZIKV was grown on A549-Npro cells. Virus containing supernatant was harvested directly after onset of a visible CPE, cleared by centrifugation (10 min, 1000 xg, room temperature) and stored at -80 °C. Viral titers for SFV4, SFV4(3H)-FFluc, SFV6-2SG-Nluc and BUNV-Nluc were determined by plaque assays while ZIKV viral titres were determined by $TCID_{50}$ assays.

$TCID_{50}$ assays

For $TCID_{50}$ assays 2 x 10^4 BHK-21 or A549-Npro (ZIKV) cells in 180 µl GMEM or DMEM medium per well were seeded in a 96-well plate. 24 h later, cells were inoculated with 20 µl of virus stock solution of a serial dilution (1:10). After incubation and onset of CPE, cells were fixated with 4 % formaldehyde for 60 min. Afterwards, were stained with 100 µl crystal violet solution for 30 min. $TCID_{50}$ was calculated using Spearman & Kärber algorithm as described [316, 317].

Plaque Assay

For titration of virus stocks 2 x 10^5 BHK-21 cells in 1 ml complete GMEM medium per well were seeded in a 12-well plate. 24 h later, the medium was removed and cells were inoculated with 200 µl of a serial dilution (1:10) of virus stock and incubated for 1 h at 37 °C. Cells were then covered with 2 ml of a 1:1 solution of 1.2 % Avicel and 2x MEM with 4 % FCS solution. After the incubation period, the medium was removed and cells were fixated with 4 % formaldehyde for 60 min. Afterwards, plates were carefully washed with tap water and cells were stained with 500 µl crystal violet solution for 30 min. PFU/ml was calculated using the following formula ($n_{plaques}$: number of plaques counted; $V_{inoculum}$: inoculation volume of virus stock; dilution factor: dilution factor of the well of $n_{plaques}$):

$$\text{PFU/ml} = \frac{n_{plaques}}{V_{inoculum} \times \text{dilution factor}}$$

2.2.2.4. Immunostaining

Cell culture plates were fixated in 4 % formaldehyde for 60 min and plates were washed afterwards with tap water. Fixated cells were incubated with 0.1 % SDS in PBS-T for 10 min. After removing the SDS/PBS-T solution, cells were permeabilized in PBS-T for 30 min. Cells were incubated for 30 min in blocking solution (10 % FCS in PBS-T solution) and afterwards incubated with the primary antibody diluted in blocking solution for 2 h at room temperature or overnight at 4 °C. After the incubation period, the primary antibody solution was removed and cells were washed three times with PBS-T. The secondary antibody diluted in blocking solution was applied and either incubated for 2 h at room temperature or at 4 °C overnight. After incubation, the secondary antibody was removed and the cells were counter-stained with 1:1000 DAPI solution for 30 min. Cells were washed three times with PBS-T and finally covered in PBS. Directly afterwards, cells were analyzed using Evos FL fluorescence microscope and imaging system (Thermo Fisher Scientific Inc., Waltham, MA, USA).

2.2.3. Microbiological methods

2.2.3.1. Transformation

For transformation of competent *E. coli* XL-10 gold or DH5α, cells were thawed on ice. Afterwards 50 µl of the bacterial suspension was mixed with plasmid containing solution. The mixture was incubated on ice for 30 minutes. A heat shock was performed at 42 °C for 30 seconds in a thermoblock. After 2 minutes on ice, cells were resuspended in 500 µl of LB medium and incubated at 37 °C and 500 rpm for at least 60 minutes in a thermoblock. Cells were plated on antibiotic selective LB-agar plates and incubated overnight at 37 °C.

2.2.4. Statistical analysis

Results are expressed as mean ± standard error of the mean (SEM). Statistical significance between groups was determined using Student's *t*-test. Statistical analyses were carried out using GraphPad Prism 8.0 software (GraphPad, San Diego, CA, USA). p-values ≤ 0.05 were considered statistically significant.

2.2.5. Experiment design

2.2.5.1. Reporter-based silencing in knockout cells

For reporter-based silencing in knockout cells, AF519, AF525 and AF5 cells were seeded in a 24-well plate (1.5 x 10^5 cells/well) in triplicate. 24h later, cells were co-transfected using 2 µl of DharmaFECT2 (Horizon Discovery Ltd., Cambridge, UK) with 100 µl OptiMEM (Gibco / Thermo Fisher Scientific Inc., Waltham, MA, USA) per well. 60 ng of pIZ-FFluc or 10 ng pAcIE1-*Rluc* were co-transfected either with 1 ng siRNA (targeting FFluc or non-specific hygromycin B resistance gene as control [249]) or 10 ng dsRNA (targeting *Rluc* or eGFP (control)). For Ago2 reconstitution assays, cells were additionally co-transfected with 300 ng of plasmids expressing either myc-Ago2 (pUB-myc-Ago2) or myc-eGFP (pUB-myc-eGFP) (control). 48 hours post transfection (hpt), cells were lysed, and luciferase activity was measured using the Dual-Luciferase-Reporter Assay System (Promega Corp., Fitchburg, WI, USA).

2.2.5.2. Beta-elimination assays

Methylation status of small RNAs was determined using a β-elimination assay. AF5 and AF525 cells (1x10^6 cells/well) were seeded in 6-well plates, followed by infection with SFV4 (MOI 10) and harvested 24 hpi. Total RNA was isolated with TRIzol (Invitrogen / Thermo Fisher Scientific Inc., Waltham, MA, USA) according to the manufacturer's protocol, using glycogen as carrier prior to isopropanol addition. Isolated total RNA samples were equally divided into two portions. 5 µl of 20x borate buffer and 12.5 µl of sodium periodate (or water in case of control sample instead of sodium periodate) were added ad 100 µl RNase-free H_2O. After 15 min, 10 µl of glycerol was added and incubated for a further 15 min at room temperature. Afterwards, samples were treated with 1 µl glycogen, 1/10 V of 3M sodium acetate and 3X volume of 99.8% ethanol. Samples were transferred to a -20° C freezer overnight for precipitation.

Next day, samples were centrifuged for 15 min at 14,000 x g at 4°C. The supernatant was removed and again centrifuged for 5 min removing supernatant again afterwards. Subsequently, RNA was washed with 70 % ethanol and the dried pellets were resuspended in borate buffer followed by 90 min incubation

at 45° C. RNA was purified with Monarch RNA Cleanup kit (50 µg) (New England Biolabs, Inc., Ipswich, MA, USA) according to the manufacturer's protocol and sent for Illumina-based (Illumina, Inc., San Diego, CA, USA) small RNA sequencing. For the first repeat, at least 1 µg of total RNA was sent for small RNA sequencing at BGI as previously described [315]. For the second repeat, 100 ng total RNA was sent for small RNA sequencing at IKMB (chapter 2.2.1.12). Data was analyzed as previously described [318] by mapping small RNAs to the virus genome and antigenome of SFV4, CFAV, PCLV (accession numbers: Table 18). Besides, small RNAs were mapped to transposon elements using the TEfam transposon consensus sequence https://tefam.biochem.vt.edu/tefam, accessed 2014) and the transcriptome of *Aedes aegypti* (*Aedes aegypti* Liverpool AGWG, version AaegL5.2 accessed July 2020, https://vectorbase.org).

2.2.5.3. Viral replication assays in mosquito cells

AF5, AF319, AF519 and AF525 were seeded at a density of 1.5 x 10^5 cells/well in 24 well plates (SFV4(3H)-FFluc, SFV6-2SG-Nluc and BUNV-Nluc) or 3x10^5 cells/well (ZIKV). Cells were infected 24 hours after seeding at an MOI of 1 (SFV4(3H)-FFluc, SFV6-2SG-Nluc and BUNV-Nluc) or MOI 0.1 (ZIKV) and were left to incubate for 1 hour before additional L-15-supplemented medium was added (1 ml). At 48 hpi SFV- and BUNV-infected cells were lysed using Passive Lysis buffer and luciferase was measured by using Luciferase Assay System (FFluc) or Nano-Glo Luciferase Assay System (all Promega Corp., Fitchburg, WI, USA). For ZIKV, total RNA from cells was isolated at 72 hpi by TRIzol. ZIKV and ribosomal S7 RNA levels were determined by one-step quantitative RT-PCR (Qiagen, Germany).

2.2.5.4. Re-introduction of Ago2 in infected cells

AF525 cells were seeded in a 96-well plate (5x10^4 cells/well) and were transfected 24 h later with 500 ng of plasmid expressing myc-Ago2 (pUb-myc-Ago2) or myc-eGFP (pUB-myc-eGFP) (control) using 0.5 µl of DharmaFECT2 (Horizon Discovery, Cambridge, UK). 4 hpt, cells were infected with SFV6-2SG-Nluc (MOI 0.5). 48 hpi, SFV-infected cells were lysed using Passive Lysis Buffer and the luciferase activity was measured using the Nano-Glo Luciferase Assay System (Promega Corp., Fitchburg, WI, USA).

2.2.5.5. Small RNA sequencing of SFV4 or BUNV-infected cells

1 x 10^6 AF5 cells were seeded in a 6-well plate and infected with SFV4 or BUNV (MOI 1 or 10 respectively) or persistently infected cells were used. 24 hpi or seeding (persistent infection) total RNA of cells was isolated and submitted to Illumina-based NGS (chapter 2.2.1.12). Results were analysed and mapped to the SFV4 or BUNV genome (accession numbers: Table 18) and further normalized to the number of total clean reads.

2.2.5.6. Biological activity of small RNAs

In order to assess the biological activity of small RNAs during SFV4 or BUNV infection in mosquito cells, reporter constructs were used (chapter 2.2.1.14). SFV4 reporter constructs use FFluc as luciferase reporter, while BUNV reporter constructs express Nano luciferase (Nluc). AF5, AF319 and AF525 (1.5 x 10^5 cells per well) were seeded in duplicates in 24-well plates and were 24 h later either infected with SFV4 or BUNV (both MOI 1) or persistently infected cells were used. Non-infected cells were used as controls. 24 hpi or after seeding (persistently infected cells) the reporter construct were transfected using 1 µl DharmaFECT2 (Horizon Discovery Ltd., Cambridge, UK) with 100 µl OptiMEM (Gibco / Thermo

Fisher Scientific Inc., Waltham, MA, USA) per well according to manufacturer's protocol. 25 ng pAcIE1-*Rluc* (SFV) or pIZ-FFluc (BUNV) as internal transfection controls were co-transfected with 300 ng corresponding reporter construct. 24 hpt cells were lysed with Passive Lysis buffer (Promega Corp., Fitchburg, WI, USA) and luciferase activity of *Rluc*, FFluc or Nluc reporters was assessed (chapter 2.2.1.15). FFluc (SFV4) or Nluc (BUNV) results were normalized to their internal transfection controls. Afterwards results were further normalized to eGFP-expressing control reporter constructs and to results from non-infected cells.

2.2.5.7. Investigation on key RNAi transcripts during BUNV infection

To assess viral replication of BUNV wt and the expression of transcripts of various pathway proteins during infection, AF5, AF319 and AF525 cells were seeded (1 x 10^6 cells / well) in 6-well plates. Cells were either infected with BUNV (MOI 2) or persistently infected cells were used. Non-infected cells were used as control. After 48 h, 200 µl of supernatant was used to infect mammalian BHK-21 cells in $TCID_{50}$ assays to determine viral titers. Total RNA of infected cells was isolated and expression levels of Ago2, Dcr2, Ago3, Piwi4 and Piwi5 transcripts were determined by RT-qPCR (chapter 2.2.1.11) using specific primers (Table 8). Results were normalized to mRNA levels in non-infected AF5 cells with S7 RNA as housekeeper.

2.2.5.8. Altered BUNV replication in silenced AF5 cells

AF5 naive or cells persistently infected with BUNV were seeded (1 x 10^6 cells / well) in 6-well plates. 24 h later, cells were transfected with 400 ng of dsRNA targeting Ago2, Ago3, Piwi5, Ago3 and Piwi5 in combination (200 ng each) or dseGFP as control using 5 µl DharmaFECT2. 24 hpt, cells were infected with BUNV (MOI 5). Medium was exchanged 1.5 h after infection. 48 hpi or transfection (persistent infection) 200 µl of supernatant was used for $TCID_{50}$ assays with BHK-21 cells to determine viral titers. Besides, total RNA of cells was isolated and knockdown efficiency of dsRNA was determined by assessing mRNA levels of targeted proteins in infected and non-infected control cells by RT-qPCR using specific primers (Table 8). Results were normalized to mRNA levels in non-infected AF5 cells with S7 RNA as housekeeper. Total RNA was also used for small RNA analysis via Illumina-based NGS (chapter 2.2.1.12). Analysed results were normalized to total clean reads of the sequencing run and further to dseGFP-transfected controls.

2.2.5.9. Setup of the CHIKV trans-replicase system

1.5 x 10^5 AF5 or C6/36 cells were seeded in duplicates in 24-well plates. 24 h later, cells were co-transfected with 250 ng REP or GAA (control) plasmid and 250 ng of either SG-C-Nluc or SG-Nluc DNA template using 1 µl DharmaFECT2 per well. 48 hpt cells were lysed and relative FFluc and Nluc activity was determined using a GloMax luminometer (chapter 2.2.1.15). For the second experiment instead of DNA template, 3 µl *in vitro* transcribed and capped RNA of either SG-Nluc or SG-C-Nluc template were transfected together with 250 ng REP or GAA plasmid. Again, relative FFluc and Nluc activity was determined. Nluc activity in C6/36 cells was monitored over time using the NanoGlo luciferase assay kit (Promega Corp., Fitchburg, WI, USA) according to manufacturer's protocol.

2.2.5.10. Clearing persistently infected cells of SFV or BUNV infection

For the setup of this experiment, different prerequisites needed to be checked comprising the infectivity of persistently infected AF5 cells and the silencing ability of dsRNAs targeting the particular virus.

Infectivity of persistently infected AF5 cells

To verify the infection rate of cells persistently infected with either SFV6-2SG-Nluc or BUNV-Nluc using immunostaining, infected AF5 cells were seeded in a 24-well plate (2 x 10^5 cells/well) in duplicates. As a control, the same amount of naïve AF5 and C6/36 cells was seeded in a 24-well plate and 24 h later infected with either SFV6-2SG-Nluc or BUNV-Nluc (MOI 1).

24 h later, AF5 cells were fixed in formaldehyde followed by overnight incubation with SFV-nsP3-specific antibody (1:300) or BUNV N-protein antibody (1:300) respectively. After three washing steps with PBS, DAPI fluorescence dye (1:2000) was mixed with either a secondary anti-rabbit antibody conjugated with Alexa Fluor 594 (1:1000) and added to SFV-infected cells or it was mixed with a secondary anti-mouse antibody conjugated with Alexa Flour 488 (1:1000) and added to the BUNV-infected cells and left for incubation overnight (Table 11). Fluorescence was detected using fluorescence microscopy (chapters 2.2.2.4).

Silencing efficiency of dsRNAs

To control the efficiency of dsRNA-mediated silencing, AF5 cells (3x 10^5 cells/well) were seeded in 24-well plates in triplicates. 24 h later, cells were transfected with 200 ng of dsRNA targeting either SFV, BUNV or dseGFP (control) using 1 µl DharmaFECT2 per well. 24 hpt cells were infected with SFV6-2SG-Nluc or BUNV-Nluc respectively (both MOI 1). Relative Nluc activity was assessed 24 hpi after lyse of the cells by using the NanoGlo luciferase assay kit (Promega Corp., Fitchburg, WI, USA).

Clearing the persistent infection using dsRNA-mediated silencing

In order to clear the SFV6-2SG-Nluc or BUNV-Nluc infection from persistently infected cells, cells were repeatedly transfected with dsRNA targeting viral genome sequences. The production of infectious viral particles was monitored by assessing Nluc reporter activity and the development of CPE. Wells without apparent presence of infectious particles were used to generate cured single cell clones for further experiments.

AF5 cells persistently infected with SFV6-2SG-Nluc or BUNV-Nluc were seeded in 24-well plates in triplicates (3 x 10^5 cells/well). Next day, cells were transfected with 200 ng dsRNA targeting either SFV, BUNV or eGFP as a control using 1 µl DharmaFECT2 per well. 48 hpi, cells were passaged and relative Nluc activity was determined by lysing the remaining cells with Passive Lysis buffer and NanoGlo luciferase assay kit (Promega Corp., Fitchburg, WI, USA). 24 h after passaging, cells were again transfected with 200 ng of dsRNA. This cycle was repeated including passaging and dsRNA transfection twice a week while Nluc activity was assessed once a week. In addition, once a week 200 µl of cell culture supernatant of each well was applied on BHK-21 cells to assess the development of CPE and presence of infectious viral particles. Therefore, 4 x 10^5 BHK-21 cells were seeded in 24-well plates and infected the other day with the supernatant. CPE was monitored by light microscopy.

After 13 passages, wells without apparent CPE, were diluted and seeded in a 96-well plate to seed only 1 cell/well and left to grow. After three weeks, first colonies were transferred to a 24-well plate and again passaged and monitored for infectious virus production by CPE detection on BHK-21 cells. Total RNA of negative-tested cell colonies was isolated and cDNA produced to check for viral RNA present in the cells using SFV-, BUNV- and CFAV-specific primers by PCR (Table 8). Cells tested negative for SFV or BUNV were used for further experiments. Future steps will include whole genome and small RNA sequencing.

2.2.5.11. Re-infection of cured cells

AF5 cells previously cleared from SFV or BUNV persistent infection and non-infected AF5 cells (3×10^5 cells/well) were seeded in 24-well plates in triplicates. 24 h later, cells previously cured from SFV infection were re-infected again with SFV6-2SG-Nluc or BUNV-Nluc as a control while cells cured from BUNV-infection were re-infected again with BUNV-Nluc or SFV6-2SG-Nluc as a mutual control (both MOI 0.1). Additionally, naive AF5 cells were infected with either SFV6-2SG-Nluc or BUNV-Nluc (both MOI 0.1) as an additional control group. 48 hpi, cells were lysed and relative Nluc activity was measured using the NanoGlo luciferase assay kit (Promega Corp., Fitchburg, WI, USA). Results for luciferase activity normalized to naive AF5 cells infected for the first time with SFV6-2SG-Nluc or BUNV-Nluc and to cells infected with the mutual control virus.

3. Results

The role of RNAi mechanisms in the antiviral defense against arboviruses is under constant discussion and subject to fundamental research. So far, the exo-siRNA pathway with its key proteins Dcr2 and Ago2 has been confirmed as the major antiviral response against most tested arboviruses in mosquitoes [190]. Conversely, the role of the piRNA pathway and a suggested antiviral function is mainly unexplored with a growing body of evidence [241, 247]. Aggravated by the fact, that each arbovirus family exhibits diverse characteristics of the piRNA pathway response during infection in mosquitoes, further research is imperative to extend knowledge on this topic.

Previous studies on the impact of exo-siRNA key proteins in combination with arbovirus infection were based on transient silencing approaches in mosquito-derived cell lines. Results obtained were often marked with a considerable uncertainty regarding side effects caused by an incomplete knockdown of target proteins. To counter this issue, a CRISPR/Cas9 gene knockout approach was pursued by collaborators creating two *Ae. aegypti*-derived Ago2 knockout cell lines. Together with a similar, already characterized Dcr2 knockout cell line [59], the stable knockout enables a more thorough approach investigating the diverse roles and functions of RNAi pathways and their contribution to antiviral measures in the mosquito host.

Although reports about the antiviral role of piRNAs as mediators of an adaptive antiviral immunity are increasing, the working model still has significant gaps. This study aimed to frame a broader picture of arbovirus infection and virus-host interactions mainly in the vector mosquito *Ae. aegypti* and to comprehend the role of integrated viral sequences in the host genome during viral infection. Over the course of the study the aspects of acute and persistent infection relating to exo-siRNA and piRNA pathway were investigated as well as biological activity of piRNAs. Deducing from these results the roles of Argonaute proteins in piRNA biogenesis and antiviral activity were closer examined. Trying to re-enact the mechanisms for virus sequence integrations with different approaches to provide further evidence for the common hypothesis of an adaptive antiviral immunity in mosquitoes complemented the research.

3.1. Characterization of Ae. aegypti-derived Ago2 knockout cell lines Aag2-AF519 and Aag2-AF525

[Parts of this section have been submitted to the journal Viruses as Scherer et al.]

The exo-siRNA pathway relies on the function of the Ago2 protein, which is responsible for slicing complementary RNAs, using the guide strand of the 21 nt long siRNA duplex provided by Dcr2 in a previous step. In this model, antiviral activity is achieved by the interplay of Dcr2 and Ago2. Knockout cell lines open up the possibility to study their role in the host cell antiviral defense during infection. They also eliminate considerable uncertainty about side effects caused by an incomplete knockdown of target proteins or transfection. Moreover, the question whether the piRNA pathway takes over antiviral functions in cells with a dysfunctional siRNA response or the existence of interactions between pathways can be addressed.

A CRISPR/Cas9 gene knockout approach was pursued that has been successful in the past to create the *Ae. aegypti*-derived Dcr2 knockout cell line Aag2-AF319 (AF319) [59]. The resulting Ago2 knockout cell lines were called Aag2-AF519 (AF519) and Aag2-AF525 (AF525).

3.1.1. Reporter-based silencing in knockout cells

Following engineering of AF519 and AF525 cells, functionality of the Ago2 knockout was assessed by using reporter-based silencing assays. To check for impaired silencing efficiency in those cells, dsRNAs and siRNAs were used as silencing inducers. dsRNAs are considered to be the main substrate for Dcr2, which cleaves aforementioned dsRNAs into 21 nt long siRNAs, which are in turn the main substrate for Ago2.

For the silencing assays, AF5 (control), AF519 and AF525 cells were transfected with luciferase reporter plasmids expressing FFluc, or *Rluc* (internal control). For silencing induction either, dsRNA targeting FFluc or control (eGFP-specific; dsControl), or siRNA targeting FFluc or control (hygromycin B-specific; siControl) were co-transfected. Reporter-based silencing was assessed by determining luciferase activities at 48 hpt (Figure 15 A, B).

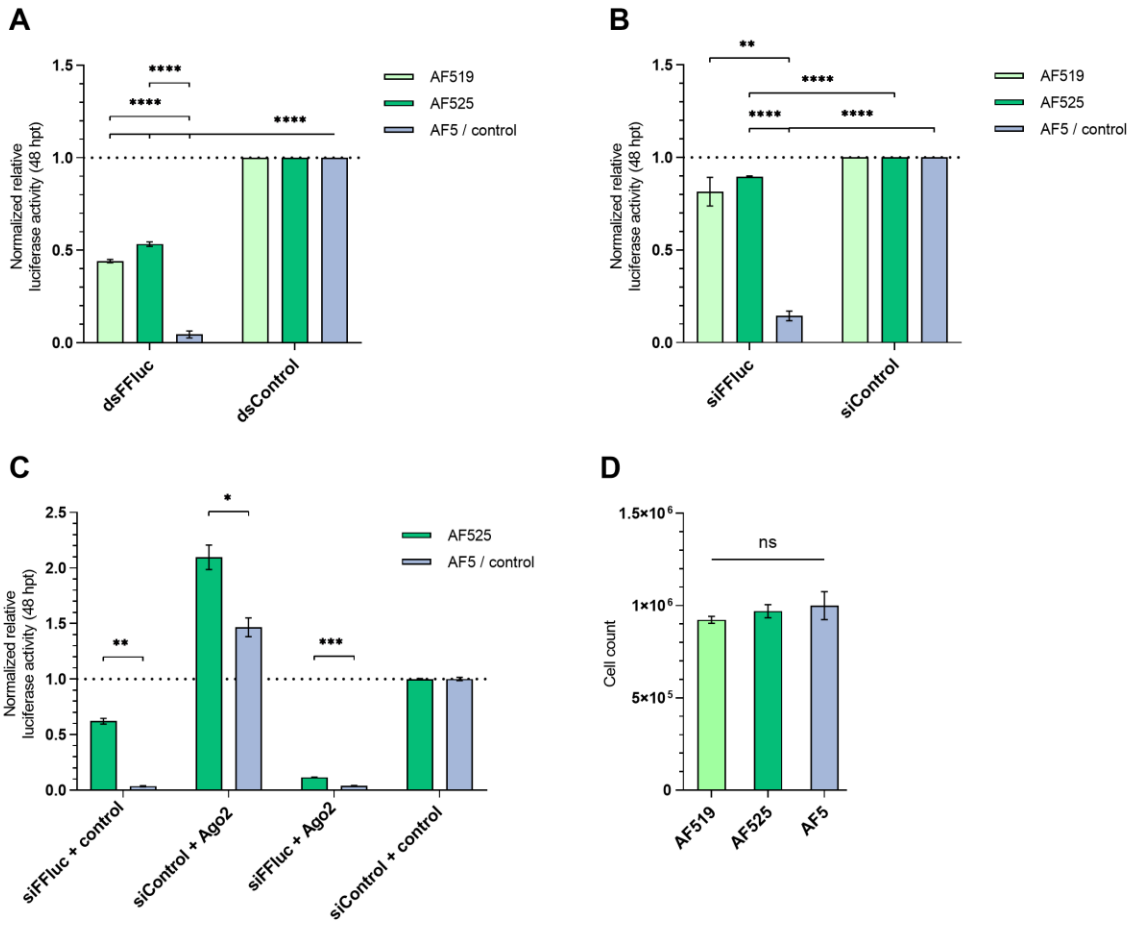

Figure 15: Characterization of AF519 and AF525 Ago2 knockout cells.

*Control cells AF5 and Ago2 knockout cells AF519 and AF525 were co-transfected with Rluc (internal transfection control) and FFluc luciferase reporter plasmids together with dsRNA (A) or siRNA (B) targeting FFluc or corresponding controls (dsRNA eGFP-specific or siRNA hygromycin B-specific; dsControl or siControl, respectively). At 48 hpt, relative luciferase activity (FFluc/Rluc) was determined and normalized to control cells. C: the experiment in panel B was repeated, but additionally either Ago2 or eGFP (control) expression constructs were co-transfected and results were normalized to definite controls (siControl + control). D: AF5, AF519 and AF525 cell numbers were determined 72 h after seeding. Means with standard error of the mean (SEM) are shown for three independent experiments performed in triplicate. * indicate significance by Student t-test (**** $p \leq 0.0001$, ** $p \leq 0.01$, * $p \leq 0.05$, ns = not significant).*

As shown in Figure 15 A and B, luciferase activity was strongly reduced in AF5 cells transfected with luciferase-specific dsRNA or siRNA compared to control. In contrast, significantly less reduction in luciferase was observed in Ago2 knockout cells (AF519/ AF525) (Fig. 1A and B). This reporter-based silencing assay indicates that the Ago2 knockout in either AF519 or AF525 cells leads to a consistently decreased silencing ability. This effect is more pronounced when siRNAs as the sole substrate for Ago2 are introduced in the cells.

To monitor the reporter-based silencing for side effects, the previous experiment using siRNAs was repeated for AF525 and AF5 cells (Figure 15 B), but this time Ago2 was re-introduced in the cells (Figure 15 C). In addition to the previous experiment already described for Figure 15 B, cells were transfected 24 h after the first transfection with Ago2 or eGFP (control) expression constructs. 48 h after the second transfection, cells were lysed and luciferase activity was assessed (Figure 15 C). As previously seen, less silencing of luciferase was observed in siFFluc transfected AF525 cells without additional Ago2 expression compared to AF5 cells (Figure 15C, siFFluc + control). Re-introducing Ago2 in AF525 cells leads to an increase in luciferase silencing (Figure 15 C).

3.1.2. Small RNA production in ϐ-eliminated Ago2 knockout cells

Biogenesis and maturation of small RNAs in mosquito cells requires a critical methylation step to gain biological activity and stabilize them. In *D. melanogaster*, methylation is carried out in the RISC by the methyltransferase Hen1. After dsRNA has been processed by Dcr2, the resulting siRNAs are bound by Ago2 as part of the RISC. A methyl group (-CH_3) is introduced onto the 2‘ OH of the 3‘ terminal nucleotide on each strand of the duplex by Hen1, creating an active RISC [162-165].

The methylation status of small RNAs can be determined by treating them with sodium periodate, which oxidates the 3‘ terminus of those RNAs, and subsequent β-elimination [166]. RNAs with free 3‘ OH are sensitive to further modification reactions through β-elimination reagents resulting in elimination of the last nucleotide by cleavage of the terminal ribose [319]. This prevents the successful ligation of linkers to these small RNAs during the NGS library preparation and therefore inability of detection during small RNA sequencing analysis [319]. In contrast, methylated small RNAs are successfully ligated and sequenced. To further verify the loss of Ago2 expression in AF525 and AF519 cells and the effect on siRNA methylation, β-elimination assays were performed on total RNA, followed by small RNA sequencing. Total RNA from AF525, AF519 or AF5 (control) cells infected with SFV4 (MOI 10, 24 hpi) was treated with sodium periodate, while control samples remained unprocessed. All samples were further treated with β-elimination reagents. Small RNAs from all samples were then analyzed by Illumina-based Next Generation sequencing (NGS). As both Ago2 knockout cell lines behave similarly in the above experiments and as the NGS data looks the same, follow-up experiments are conducted using mainly AF525 cells only.

Sequencing data shows that SFV4 infection results in the production of SFV4-specific 21 nt vsiRNAs and 24-30 nt vpiRNAs (Table 34, Figure 16) with the expected “ping-pong amplification” specific characteristic composition: U_1/A_{10} bias and 10 nts overlap in AF5 and AF525 control cells (Figure 17-18 A, D, E, F, I, J; suppl. data Figure S2, S3 A, D, E, F, I, J). Similar to previous reports of AF5 cells [249], SFV4-specific siRNAs in AF525 and AF5 cells derive from the genomic and antigenomic RNA and map across the whole genome / anti-genome. SFV4-specific piRNAs in AF525 and AF5 cells, were mainly derived from the genomic RNA and were mapped mostly to an area at 2/3s of the viral genome, where the subgenomic promoter is located, and at the 5’ end of the capsid coding region (Figure 17-18 B, C, G, H; suppl. data Figure S2, S3 B, C, G, H). In general, no difference in small RNAs mapping along the genome between treated or untreated AF5 cells was observed. In contrast, an increase of vsiRNAs in treated AF525 cells was observed mapping to the similar region than vpiRNAs.

Table 34: Analysis of clean reads for SFV4-infected AF5 and AF525 samples treated with ß-elimination reagents.
The total number of clean reads is listed for each sample as well as percentage of miRNAs detected in the sample. Furthermore, the percentage of total reads of 21 nt (% 21 nt) and 28 nt long RNAs (% 28 nt) and the share of those RNAs mapping to SFV4 referred to as % 21 nt (SFV) and % 28 nt (SFV) respectively. 21 nt as representative for siRNAs and 28 nt long reads as representative for piRNAs. Data of two independent sequencing runs is shown.

Sample	Clean reads	% miRNAs	% 21 nt	% 28 nt	% 21 nt (SFV)	% 28 nt (SFV)
AF5 β-eliminated I	28154509	0,13	2,56	20,97	0,25	0,05
AF5 β-eliminated II	22173319	1,89	0,59	1,62	0,68	0,01
AF5 control I	27608736	9,54	7,86	16,76	0,73	0,04
AF5 control II	47416333	17,11	0,50	1,09	0,36	0,01
AF525 β-eliminated I	27801658	0,03	1,6	18,08	0,10	1,20
AF525 β-eliminated II	27191855	1,27	0,86	2,36	0,14	0,14
AF525 control I	27053952	5,77	32,43	10,3	17,15	0,61
AF525 control II	40043576	12,41	0,43	1,01	13,79	0,05

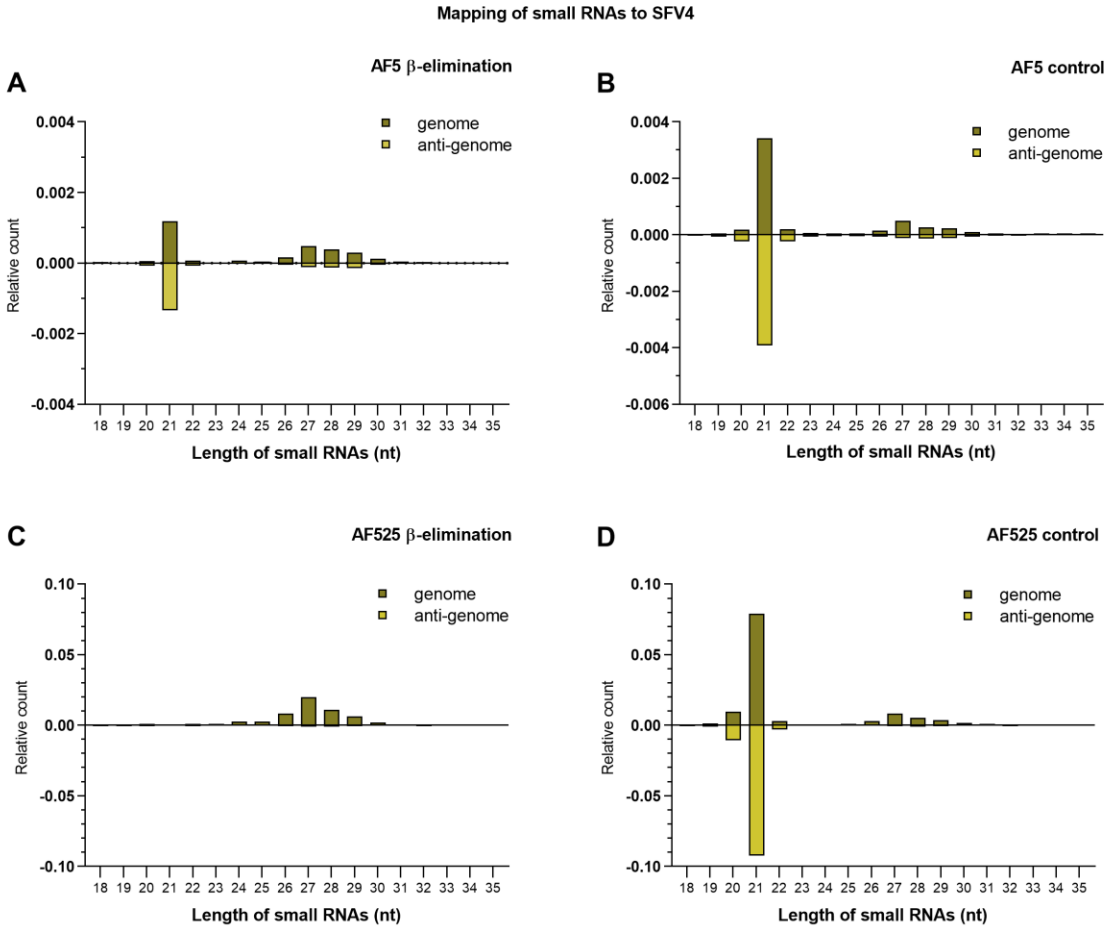

Figure 16: Length distribution of small RNAs in AF525 and AF5 cells treated with ß-elimination reagents (sequencing run I).
Small RNAs of SFV4-infected AF525 and AF5 cells was mapped to the SFV4 genome and antigenome. Positive numbers are RNAs mapping to the genomic strand of SFV4 (dark yellow) while negative numbers indicate RNAs mapping to the anti-genomic strand of SFV4 (light yellow). Y-axis: relative count of small RNAs normalized to clean reads. A: AF5 cells treated with complete ß-elimination reagents. B: AF5 ß-elimination control. C: AF525 cells treated with complete ß-elimination protocol. D: AF525 control. Two independent experiments were carried out and the results of one representative experiment are shown here.

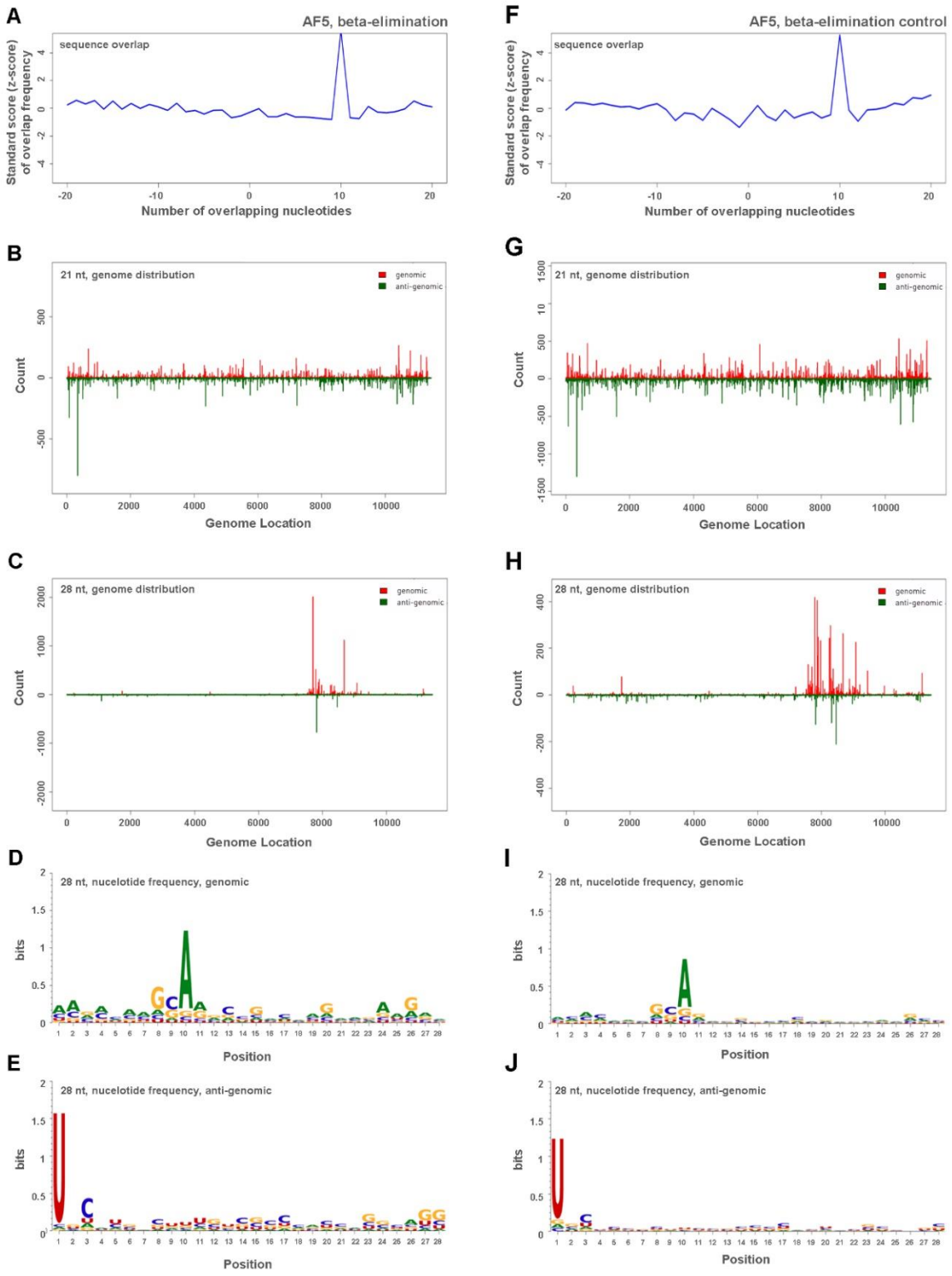

Figure 17: Characteristics of β-eliminated small RNAs of AF5 cells (sequencing run I).
SFV4-specific small RNAs of SFV4-infected AF5 cells treated with β elimination reagents (A-E) and control (F-J). A, F: sense and anti-sense sequence overlap of vpiRNAs (25-29 nt). Length distribution along the SFV4 genome for 21 nt siRNAs (B, G) or 28 nt piRNAs (C, H) (red, mapped to the genome; green, mapped to the antigenome). D, E, I, J: Relative nucleotide frequency and conservation per position of the 28 nt long vpiRNAs mapping to the SFV4 genome (D, I) or antigenome (E, J). Two independent experiments were carried out and the results of one representative experiment are shown here.

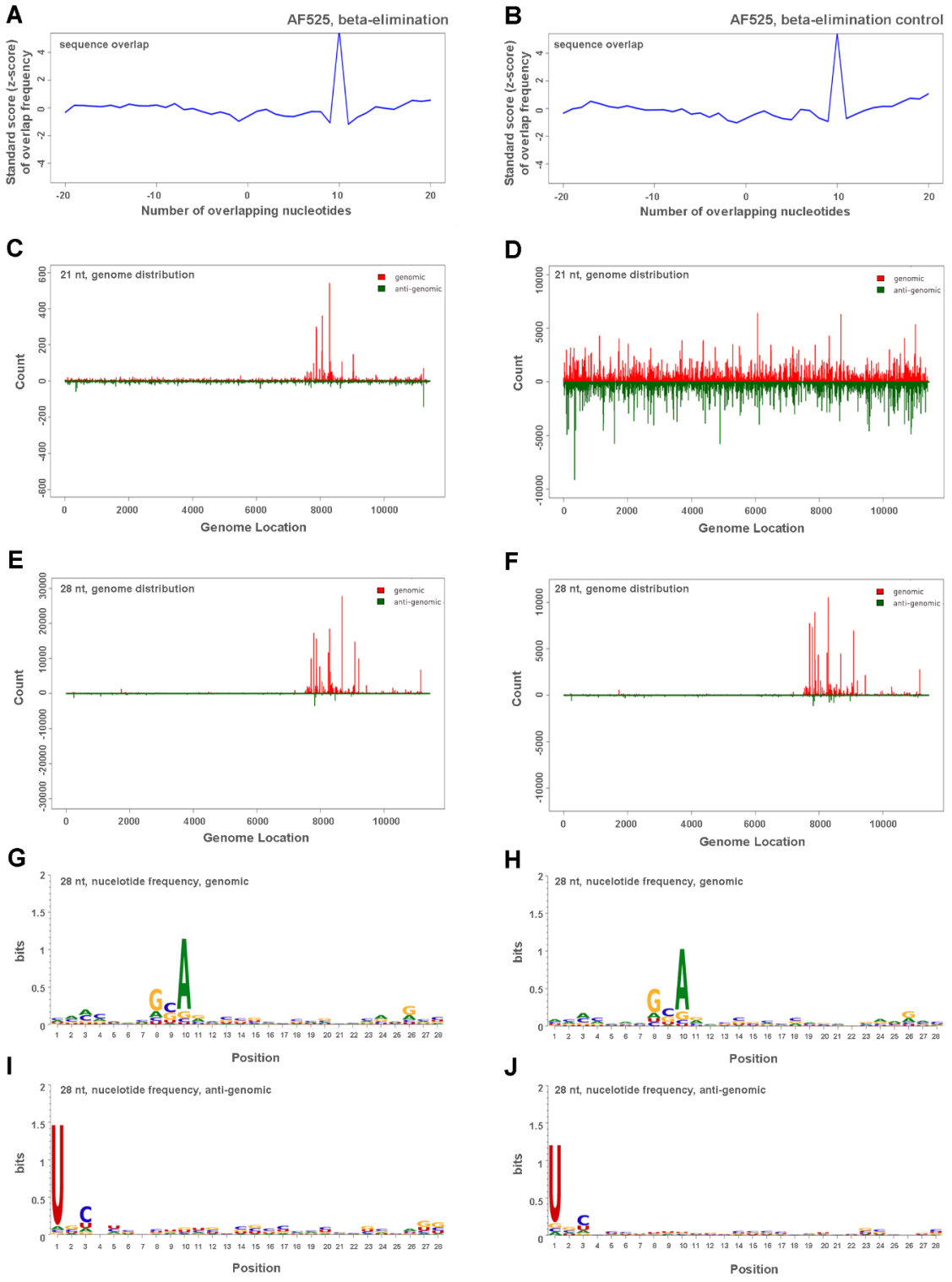

Figure 18: Characteristics of β-eliminated small RNAs of AF525 cells (sequencing run I).
SFV4-specific small RNAs of SFV4-infected AF525 cells treated with β-elimination reagents (A-E) and control (F-J). A, F: sense and anti-sense sequence overlap of virus-derived vpiRNAs (25-29 nt). Length distribution along the SFV4 genome for 21 nt siRNAs (B, G) or 28 nt piRNAs (C, H) (red, mapped to the genome; green, mapped to the antigenome). D, E, I, J: Relative nucleotide frequency and conservation per position of the 28 nt long vpiRNAs mapping to the SFV4 genome (D, I) or antigenome (E, J). Two independent experiments were carried out, and the results of one representative experiment are shown here.

Intriguingly, a large increase in SFV4-specific vsiRNAs and vpiRNAs is detectable for control samples in AF525 compared to AF5 cells (% 21 nt (SFV): 23.5 - 38.0-fold, % 28 nt (SFV): 5.0 - 15.3-fold, Table 34). This effect could be due to an increased viral replication in AF525 cells, as the antiviral pathway is non-functional and can no longer limit SFV4 replication. Another explanation might be the accumulation of small RNAs in the cell, as they are no longer processed by the RNAi response. To further examine this, the amount of SFV4 RNA in those samples was quantified. In AF525 cells, a 28-fold increase in viral RNA was detected compared to AF5 cells; supporting the hypothesis that higher viral infection and replication was the main driver of the increased SFV4-specific small RNA production in AF525 cells (Figure 19).

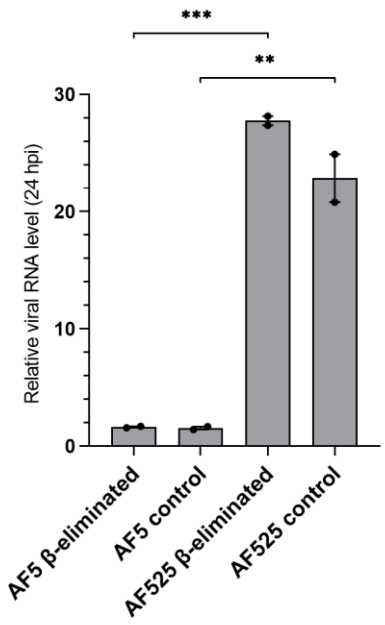

Figure 19: Relative viral RNA levels of SFV4-infected AF5 and AF525 cells treated with β-elimination reagents.
*Total RNA of SFV4-infected AF5 and AF525 cells was analyzed by RT-qPCR to determine viral RNA levels. Means with SEM are shown for two independent experiments. Ribosomal S7 RNA was used as a housekeeper for the $\Delta\Delta C_T$ method and non-treated cells as control. * indicate significance by Student t-test (*** $p \leq 0.001$, ** $p \leq 0.01$, * $p \leq 0.05$).*

To understand the involvement of Ago2 in the methylation of the different (viral) small RNAs in *Ae. aegypti*-derived cells, β-eliminated and controls of AF5 and AF525 cells were compared. miRNAs are known to be sensitive to β-elimination independent of Ago2 [320] and were therefore used as control to verify successful treatment. The number of miRNAs in β-eliminated samples (AF5 and AF525 cells) compared to controls was strongly reduced, supporting a successful β-elimination treatment. Read numbers of the total 21 nt long small RNAs (overall and SFV4-specific) in AF525 cells showed a strong decrease in β-eliminated samples (Table 34, Figure 16, suppl. data Figure S1). In contrast, only a slight reduction was observed for AF5 control cells, confirming the knockout of Ago2 in AF525 cells and the importance of Ago2 for 21 nt small RNA methylation in *Ae. aegypti*-derived cells. In addition to this, no reduction in piRNAs, including SFV4-specific ones, was observed in β-eliminated samples (neither in AF5 nor AF525 cells) (Table 34). This confirms that piRNA methylation happens independently of Ago2 in *Ae. aegypti* which renders piRNAs resistant to β-elimination [196].

As Aag2 cells are known to be persistently infected with insect-specific CFAV and PCLV [58, 259, 260], it was expected that these viruses are also present in the AF525 cells. This was confirmed, using the small RNA sequencing data in combination with the previously established virus discovery pipeline [315]. Mapping of reads to the CFAV genome revealed that vsiRNAs and a small amount of vpiRNAs are produced in AF5 and AF525 control cells in equal share, mapping to the viral genome and anti-genome (Table 35, suppl. data Figure S4, S5). Results revealed that also CFAV-derived vsiRNAs are Ago2-dependent methylated as the fraction of 21 nt long small RNAs disappears in AF525 cells treated with β-elimination reagents, compared to AF525 control (Table 35, suppl. data Figure S5, S6). Comparing the control cells, more CFAV-specific siRNAs were observed in AF525 than AF5 cells.

Table 35: Analysis of clean reads in AF5 and AF525 cells persistently infected with CFAV and PCLV and treated with β-elimination reagents.

Percentage of total reads of 21 nt and 28 nt long RNAs mapping to CFAV or PCLV S-, M- and L-segment. 21 nt as representative for siRNAs and 28 nt long reads for piRNAs. Data of two independent sequencing runs is shown.

Sample	% 21 nt (CFAV)	% 28 nt (CFAV)	% 21 nt (PCLV-S)	% 28 nt (PCLV-S)	% 21 nt (PCLV-M)	% 28 nt (PCLV-M)	% 21 nt (PCLV-L)	% 28 nt (PCLV-L)
AF5 β-eliminated I	0.07	0.02	0.07	0.84	0.01	0.21	0.01	0.01
AF5 β-eliminated II	0.37	0.01	0.53	2.04	0.06	0.23	0.04	0.02
AF5 control I	0.17	0.01	0.05	0.56	0.02	0.14	0.01	0.01
AF5 control II	0.12	0.01	0.18	0.55	0.02	0.08	0.01	0.01
AF525 β-eliminated I	0.05	0.11	0.03	0.28	0.02	0.15	0.00	0.01
AF525 β-eliminated II	0.12	0.11	0.83	4.61	0.06	0.50	0.01	0.04
AF525 control I	1.34	0.05	0.11	0.16	0.05	0.07	0.05	0.01
AF525 control II	1.96	0.03	0.84	0.95	0.17	0.12	0.15	0.01

Results for PCLV show that vsiRNAs and vpiRNAs are also produced in AF5 and AF525 cells, mapping to the genome or anti-genome in a variable manner when comparing first and second sequencing run (Table 35, suppl. data Figure S6-S11). It is noticeable, that the amount of vpiRNAs was higher or almost equal to the amounts of vsiRNAs produced at least for the S- and M-segments of PCLV; especially in β-eliminated samples. Additionally, the amount of vpiRNAs seemed to increase in β-eliminated samples for all three segments. For the L-segment a strong decrease of 21 nt vsiRNAs was observed in β-eliminated AF525, compared to AF525 control samples. Similar to SFV4 and CFAV, more PCLV-specific vsiRNAs were detected in AF525 than AF5 cells.

siRNAs and piRNAs from endogenous sources (e.g. transcripts or transposable elements) are known to be produced and important for mosquito cells. Therefore, the effect of Ago2 loss on the methylation of small RNAs, originating from transposable elements (TE) or the *Aedes aegypti* transcriptome was analysed. Sequencing analysis showed (Table 36, Figure 20, suppl. data Figure S12) that siRNAs (21 nt) and piRNAs (24 - 30 nt) were produced from the AF5 or AF525 genome and a clear reduction of siRNAs mapping to TEs was observed in β-eliminated RNA from AF525 cells, hinting towards a dependency on Ago2 for siRNA methylation also of TE-targeting 21 nt siRNAs. Conversely, the amount of piRNAs mapping to transposable elements in AF5 and AF525 cells, rather increased in treated cells. The effect is even stronger in AF525 cells, as a higher amount of piRNAs was detectable compared to AF5 controls (Table 34).

Overall, the data suggested that methylation of piRNAs targeting TEs, which are natural targets of piRNAs, was not heavily affected by the lack of Ago2, but rather, the methylation of endogenous siRNAs targeting TEs, which are also dependent on Ago2.

Table 36: Analysis of β-eliminated small RNA samples mapping to transposable elements of the AF5/AF525 genome and the Ae. aegypti transcriptome (Aedes aegypti Liverpool AGWG, version AaegL5.2).

Total number of clean reads is listed for each sample as well as percentage of total reads of 21 nt (% 21 nt) and 28 nt long RNAs (% 28 nt) mapping to TEs and the share of those RNAs mapping to the transcriptome of the cell. 21 nt as representative for siRNAs and 28 nt long reads as representative for piRNAs. Data of two independent sequencing runs is shown.

	TEs		Transcriptome	
Sample	**% 21 nt**	**% 28 nt**	**% 21 nt**	**% 28 nt**
AF5 β-eliminated I	1,24	3,47	4,80	11,18
AF5 β-eliminated II	4,20	4,17	14,10	13,80
AF5 control I	2,01	2,90	9,19	10,65
AF5 control II	1,58	1,41	8,64	5,14
AF525 β-eliminated I	1,09	2,93	2,82	11,45
AF525 β-eliminated II	1,48	4,33	6,44	13,94
AF525 control I	4,80	1,74	15,44	8,08
AF525 control II	8,36	1,26	22,93	4,49

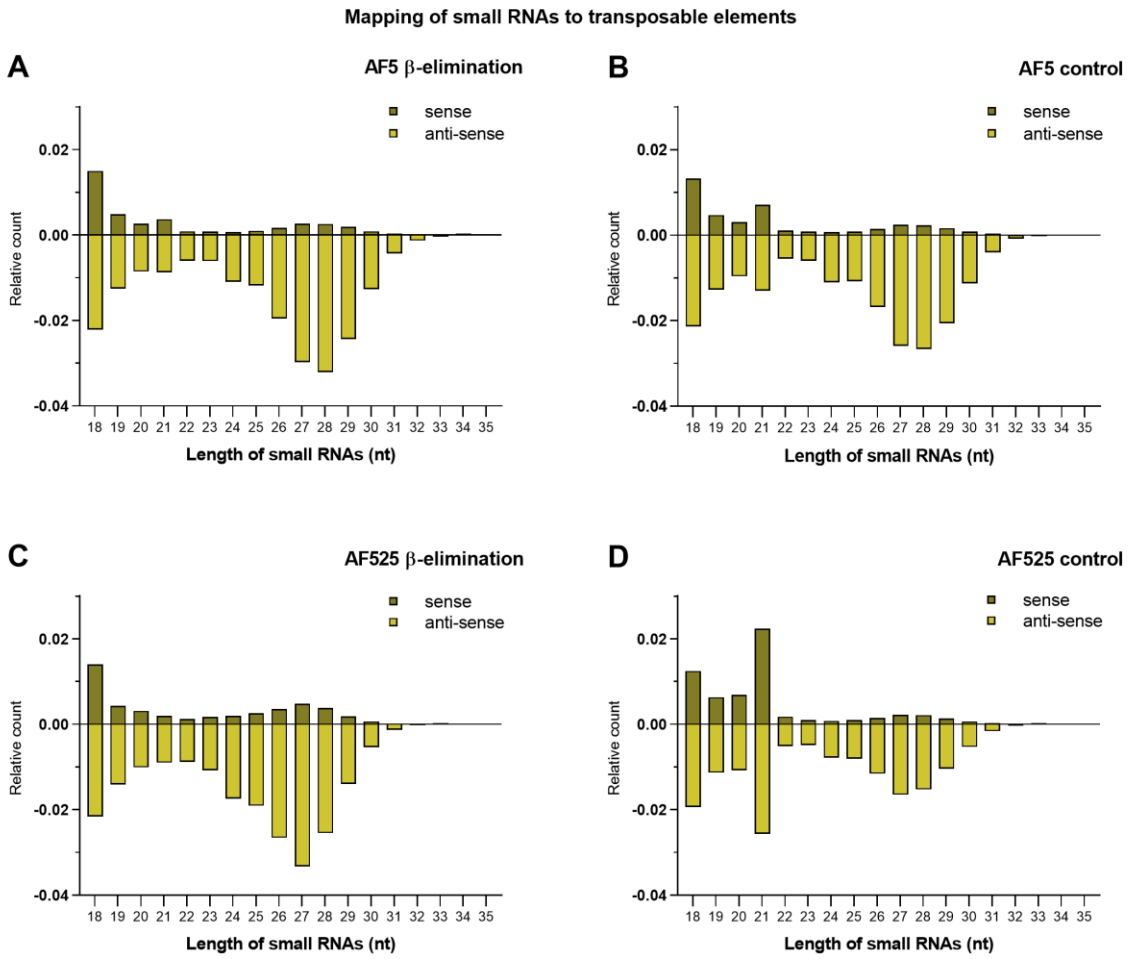

Figure 20: Length distribution of small RNAs from AF5 and AF525 cells mapping to TEs (sequencing run I).

The left panel side (A, C) shows treated samples of AF5 and AF525 cells, right panel side shows the results for untreated controls (B, D). Y-axis displays the relative amount of small RNAs normalized to clean reads. Positive numbers are RNAs mapping to the sense strand of TEs (dark yellow) while negative numbers indicate RNAs mapping to the anti-sense strand of TEs (light yellow). Two independent experiments were carried out and the results of one representative experiment are shown here.

Mapping small RNAs of AF5 and AF525 cells to the transcriptome revealed that small RNAs with a very diverse length distribution were produced, mapping to the sense and anti-sense transcriptome of AF5/AF525 cells (Figure 21, suppl. data Figure S13). Overall, read counts of 21 nt siRNAs decreased in β-eliminated AF525 cells hinting towards a general effect of β-elimination treatment and the involvement of Ago2 in the methylation status of transcriptome-derived siRNAs (Figure 21 C, suppl. data Figure S13 C). Similar to TE-derived piRNAs an increase in transcriptome-targeting piRNAs was observed in treated cells, especially for AF525 cells.

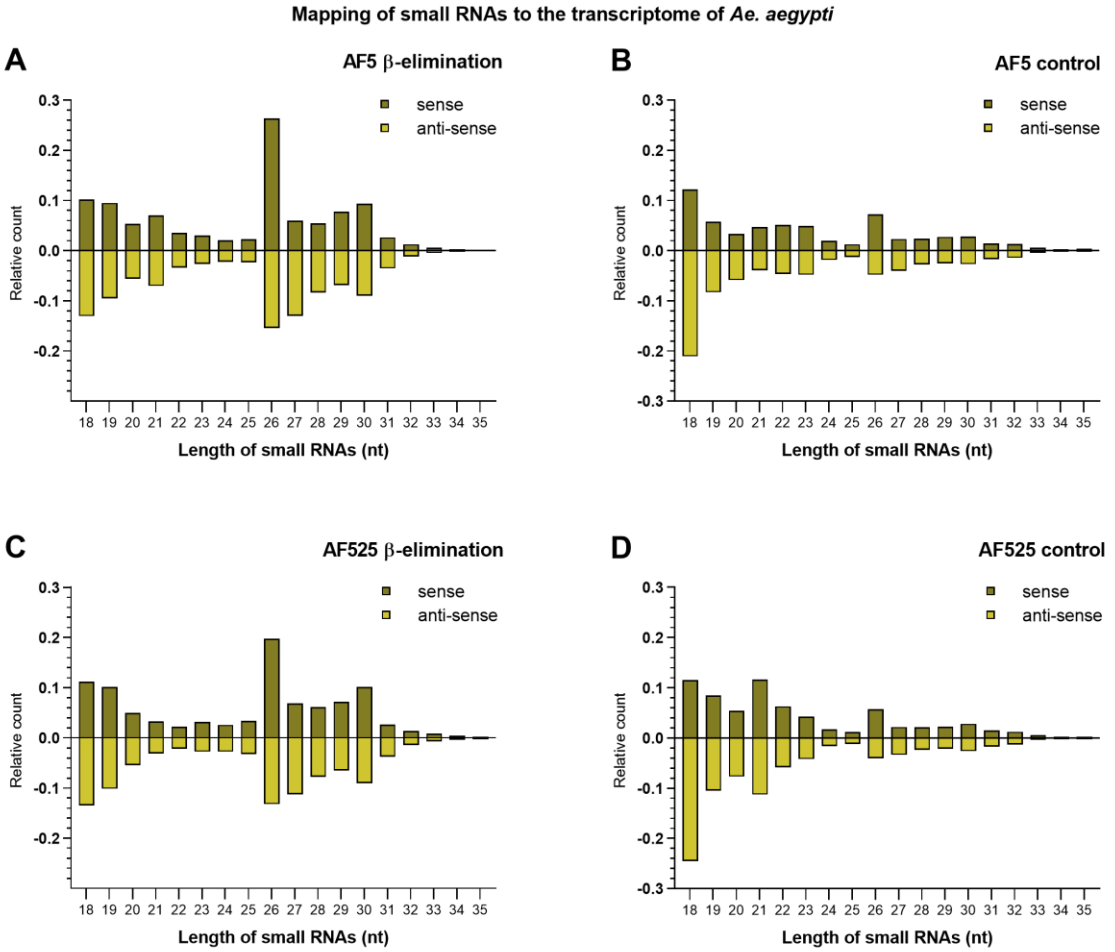

Figure 21: Length distribution of small RNAs from AF5 and AF525 cells mapping to the transcriptome of Aedes aegypti Liverpool AGWG, version AaegL5.2. (sequencing run II).
The left panel side (A, C) shows treated samples of AF5 and AF525 cells, right panel side shows the results for untreated controls (B, D). Y-axis displays the amount of small RNAs normalized to clean reads. Positive numbers are RNAs mapping to sense RNAs (dark yellow) while negative numbers map to anti-sense RNAs (light yellow). Two independent experiments were carried out and the results of one representative experiment are shown here.

Taken together, analysis of small RNA sequencing data suggested that Ago2 is strongly involved in the methylation not only of virus-derived exogenous siRNAs, but also in methylating endogenous derived siRNAs targeting transposable elements or gene transcripts.

3.2. Effect of Dcr2 and Ago2 knockout on viral replication

[Parts of this section has been submitted to the journal Viruses as Scherer et al.]

In order to investigate the antiviral roles of effectors Dcr2 and Ago2 in the exo-siRNA pathway in more detail using knockout cell lines, viral replication levels for various arboviruses were determined. This also includes ZIKV for which it was previously shown that its replication remains unaffected by Ago2 silencing. The impact of silencing or knocking out key players of the RNAi response has already been characterized for a variety of viruses in different vector mosquitoes [126]. It was shown that except from ZIKV, all tested arboviruses benefit from the shutdown of siRNA pathway proteins Dcr2 or Ago2 documented by increased viral replication.

Previously described Dcr2 knockout cells AF319 [249], AF519, AF525 and parental AF5 control cells were infected with luciferase-expressing SFV4(3H)-FFluc [249], SFV6-2SG-Nluc [249], BUNV-Nluc [188] (all three MOI 1) and ZIKV [59] (MOI 0.1). At 48 hpi, SFV4(3H)-FFluc, SFV6-2SG-Nluc- and BUNV-Nluc-infected cells were lysed and relative luciferase activities were determined. Total RNA of ZIKV-infected cells was isolated at 72 hpi and viral RNA concentration was determined by RT-qPCR.

Luciferase expression was significantly increased in AF525, AF519 and AF319 cells infected with SFV4(3H)-FFluc, SFV6-2SG-Nluc or BUNV-Nluc, compared to AF5 control cells (Figure 22 A, B, D). Although variation between single experiments was observed for SFV4(3H)-FFluc, no significant difference in viral replication levels was observed between Dcr2 and Ago2 KO cells for SFV4(3H)-FFluc, SFV6-2SG-Nluc or BUNV-Nluc infected cells, indicating that absence of both, Dcr2 or Ago2, similarly contributes to an improved viral replication.

Re-introducing Ago2 in the AF525 cells by transfection of a myc-Ago2 expression construct prior to SFV6-2SG-Nluc (MOI 0.5) infection (Figure 22 C), resulted in a decrease of luciferase activity compared to control cells (transfection of myc-eGFP construct). These results confirm that the increase in virus infection in AF525 cells is linked to the absence of Ago2 and thereby the antiviral activity of Ago2, at least for SFV.

For AF525 cells infected with ZIKV, cells accumulated 1.6-fold more viral RNA during the course of infection than AF5 control cells, although this was not statistically significant. Surprisingly, ZIKV replication was significantly increased in knockout cells AF519 compared to AF5 cells. The beneficial effect of a partial lack of Ago2 in AF519 cells questions the role of this protein in counteracting ZIKV. It has to be noted, that due to an insertion in one allele of the Ago2 gene in AF519 cells, it is possible that an altered version of Ago2 is expressed.

Overall, these data confirm the antiviral role of Dcr2 and Ago2 during arbovirus infection with the partial exception of ZIKV. To ensure that differences in virus infection is not due to an altered growth rate of the used cells, the cellular growth rate of knockout cell lines in comparison to AF5 control cells was determined (Figure 15 D). AF5, AF519 and AF525 cells were seeded in 24-well plates and cell numbers were assessed 72 hours later. As shown in Figure 15 D, the growth rate remains comparable to parental control cells AF5 for both knockout cell lines.

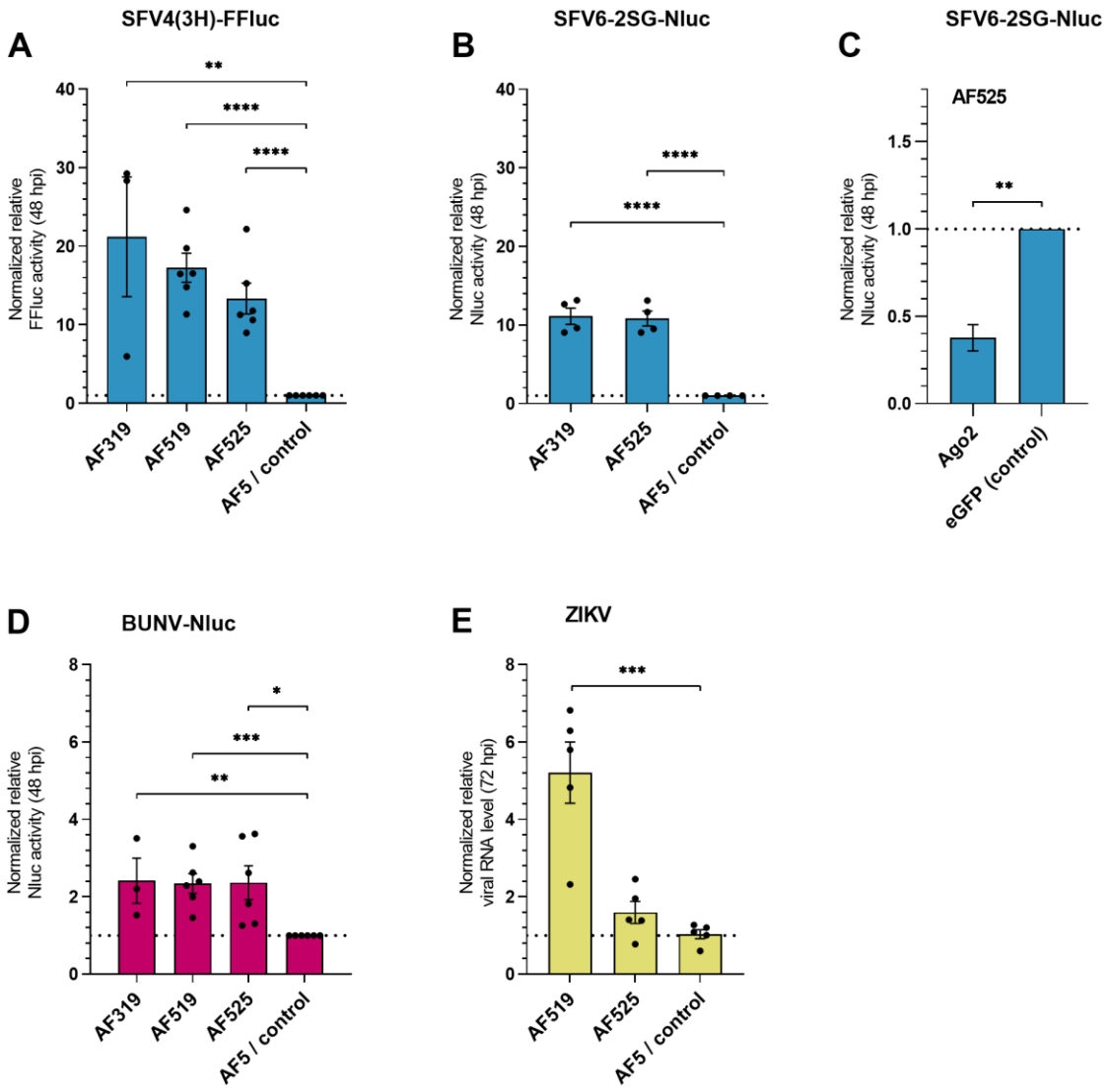

Figure 22: Viral replication in Ago2 and Dcr2 knockout cells.

*(A, B, D) AF5 (control), AF319, AF525 and/or AF519 cells were infected with SFV4(3H)-FFluc, SFV6-2SG-Nluc or BUNV-Nluc (all MOI 1). After 48 h, cells were lysed to determine the relative luciferase activity, normalized to the AF5 control cells. The means with SEM from at least three independent experiments performed in triplicates are shown. C: Re-introduction of Ago2 in infected cells. AF525 cells were transfected with myc-Ago2 or myc-eGFP (control) expression plasmids. 4 hpt, cells were infected with SFV6-2SG-Nluc (MOI=0.5). 48 hpi, cells were lysed to measure luciferase activity. The relative mean luciferase amounts of Nluc, normalized to eGFP transfected cells with SEM from three independent experiments conducted in triplicates are shown. (D) The mean relative ZIKV genomic RNA levels with SEM from five independent experiments in AF519, AF525 and AF5 cells infected with an MOI of 0.1 and total RNA isolation at 72 hpi are shown. Ribosomal S7 RNA was used as a housekeeper for the $\Delta\Delta C_T$ method with AF5 cells as a control. * indicate significance by Student t-test (**** $p \leq 0.0001$, *** $p \leq 0.001$, ** $p \leq 0.01$, * $p \leq 0.05$).*

3.2.1. Expression levels of Dcr2 and Ago2 in infection

In a next step, expression levels of the siRNA pathway proteins in AF5 cells were determined to check for possible alterations during acute infection (Figure 23).

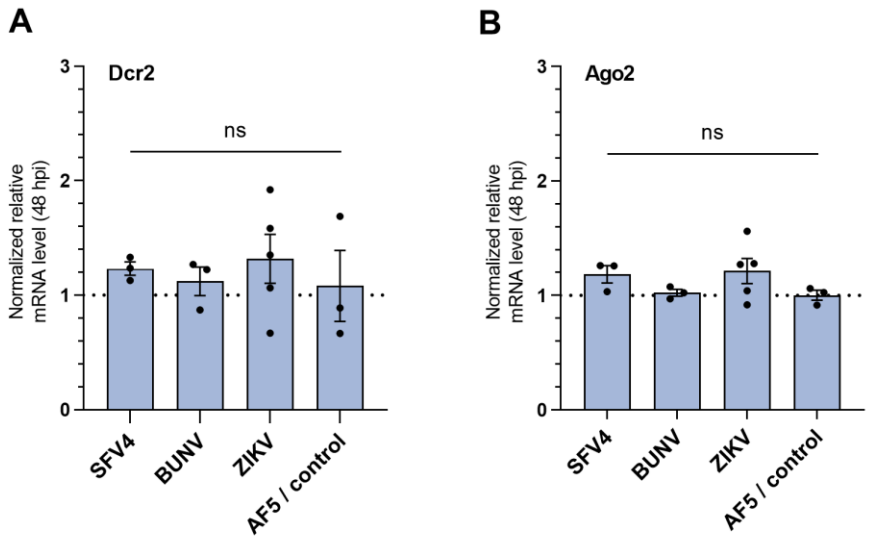

Figure 23: Expression levels of Dcr2 and Ago2 transcripts in AF5 cells in acute arbovirus infection.
AF5 cells were infected with SFV4, BUNV (both MOI 1) or ZIKV (MOI 0.1). 48 hpi total RNA of infected cells was isolated and submitted to RT-qPCR for determination of Dcr2 (A) and Ago2 (B) mRNA levels by using Dcr2 and Ago2-specific primers. Non-infected AF5 cells were used as a control. Ribosomal S7 RNA was used as a housekeeper for the $\Delta\Delta C_T$ method with AF5 cells as a control. Means with SEM are shown for at least three independent experiments. Significance indicated by Student t-test (ns = not significant).

No significant increase of Dcr2 (Figure 23 A) or Ago2 (Figure 23 B) expression levels was observed for either SFV4, BUNV or ZIKV infected cells compared to non-infected control cells. If any, RNA levels only showed a trend towards a slightly increased expression in infected cells.

3.3. Characterization of the RNAi response in acute versus persistent infection

Besides the exo-siRNA pathway, also the piRNA pathway is suggested to play an antiviral role during infection. More and more attention is brought to this topic, but findings are highly variable related to both, the host and virus species [147, 233, 321]. Moreover, differences seem to exist also in the time course of infection. For example Léger *et al.* showed that during acute infection of mosquito cells with RVFV, vsiRNAs were more prominent in the cells at an early stage of infection but the population of vpiRNAs increased progressively and outnumbered vsiRNAs in the later stage. This might indicate a different regulation of siRNA and piRNA pathway over time.

Furthermore, a direct comparison related to the RNAi response and small RNA characterization between a single-stranded positive sense RNA virus virus like SFV and a single-stranded negative sense RNA virus like BUNV was never done before including the time aspect. Moving the focus of this study to the details of biological activity of vpiRNAs, the involved proteins and their function during early and persistent stage of infection should bring new insights about the complex interaction of RNAi and arboviruses.

3.3.1. Small RNA sequencing profile of infected cells during acute and persistent infection phase

SFV is a representative of the *Togaviridae* family with a single-stranded positive sense RNA genome and has been used in the past regularly as model alphavirus to investigate the mosquito vector-virus interaction, specifically the antiviral RNAi response. The production of vsiRNA and vpiRNAs as well as the antiviral activity of the exo-siRNA pathway during acute infection was already shown [123, 249]. On the contrary, BUNV has a single-stranded negative sense RNA genome and is used as a model organism for other highly pathogenic arboviruses of the *Bunyavirales* order. BUNV is also known to induce the production of vsiRNA and vpiRNAs in mosquito cells upon infection [188], but little is known about the details of the antiviral response against negative-sense RNA viruses in mosquitoes.

Acute viral infections are characterized by a high rate of viral replication and the production of a large number of virions. In contrast to acute infections, where the virus is eventually cleared from the cells, persistent infections lead to an equilibrium at which viral infection is controlled but not eliminated [322]. To establish a persistent infection, the virus must avoid clearance by the host immune response and secondly avoid to destroy the host cell or kill the entire vector. If a virus exploits the host cell to synthesize high levels of viral proteins over a long time, the cell will probably die as a consequence, which entails a rather low level of virus production to maintain persistence [322]. This enables the virus to persist in the host cell for long periods of time, facilitating virus transmission to a vertebrate host. It is known that most mosquitoes are unable to completely abolish an arbovirus infection, thereby establishing a persistent infection at low levels of virus production [323]. SFV and BUNV are replicating well in insect cells reaching the peak of virus production as early as 10 hpi or 3 days post infection respectively [188, 324]. Persistent infection of SFV and BUNV in *Ae. aegypti*-derived cell lines was achieved by initially infecting the cells and passaging them several times for at least 2 weeks for SFV and at least 3 weeks for BUNV. Persistence was assayed by immunofluorescence assays and RT-qPCR.

SFV4

Small RNAs of AF5 cells infected with SFV4 (MOI 10, 24 hpi) in the acute or persistent phase of infection (3 weeks post infection) was isolated and total RNA was submitted to Illumina-based NGS and analyzed.

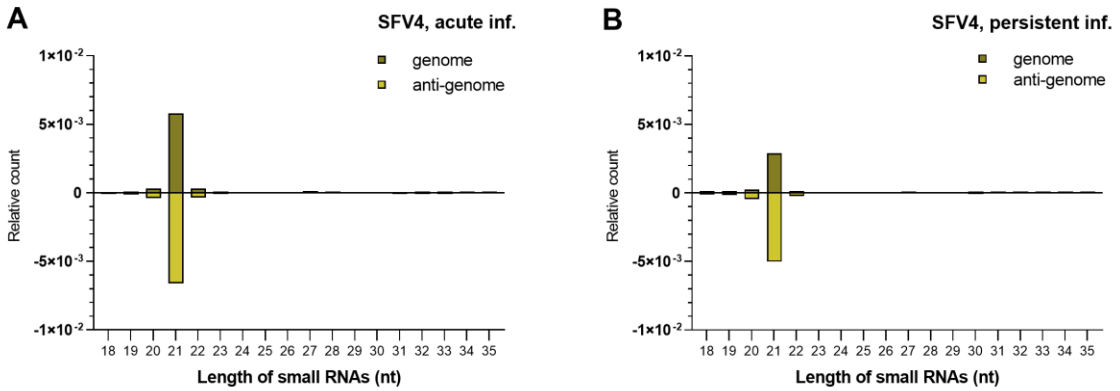

Figure 24: Length distribution of small RNAs in AF5 cells in SFV4 acute and persistent infection.
The total RNA of AF5 cells with either acute infection (MOI 10, 24 hpi) or persistent infection (3 weeks post infection) of SFV4 was isolated and submitted to NGS. Analyzed NGS data of small RNA sequencing was mapped to the SFV4 genome and presented in their size distribution. Dark yellow bars indicate sequences mapping to the genome of SFV4 while light yellow ones map to the anti-genome of the virus. The number of sequenced and SFV4-mapped reads presented on the y-axis was normalized to total reads. A: AF5 cells acutely infected with SFV4 (MOI 1). B: AF5 cells persistently infected with SFV4.

Analysis revealed the production of vsiRNAs but only small amounts of vpiRNAs (24 - 30 nt) mapping to SFV4 during acute and persistent infection of AF5.

vsiRNAs originated from both, genomic and anti-genomic strands, during acute and persistent infection, although less vsiRNAs were produced during the persistent infection with SFV4. Remarkably, while distribution of these vsiRNAs was spanning throughout the whole SFV4 genome or anti-genome during the acute phase as previously reported [249], production was highly concentrated at the 5' end of the genome during the persistent phase with a distinct peak for vsiRNAs produced from the anti-genome of SFV4 (Figure 24, suppl. data Figure S14 B, G).

vpiRNAs distribution looked similar during both stages of infection and comparable to previous reports [189]. With an accumulation of sense vpiRNAs mapping to the subgenomic region where the capsid coding region is located (suppl. data Figure S14 C, H). vpiRNAs show the characteristic 10 nt sequence overlap (suppl. data Figure S14 A, F) and U_1/A_{10} bias caused by ping-pong amplification of piRNAs in acute and persistent infection (suppl. data Figure S14 D, E, I, J).

Overall, results show the production of SFV-derived vsiRNAs and vpiRNAs with an excess of vsiRNAs in early and late stage of infection compared to vpiRNAs. During the persistent phase, the biogenesis of vsiRNAs is reduced and seems to concentrate on hotspots of the SFV genome. vpiRNAs are generated, but their distribution across the genome does not seem to be altered much in acute or persistent phase of SFV4 infection.

BUNV

It was already shown that single-stranded, negative-sense RNA viruses from the *Bunyaviridae* familiy like RVFV and BUNV produce vsiRNAs and vpiRNAs. Especially for RVFV, earlier results point towards an increased production and possible antiviral activity of vpiRNAs at a later stage of infection [177, 184, 188]. Therefore, *Ae. aegypti*-derived AF5, AF319 and AF525 cells were acutely infected with BUNV (MOI 1) or persistently infected cells (4 weeks post infection) were used to isolate small RNAs, which were sequenced and mapped to the virus genome and anti-genome.

Cumulated results in Figure 25 show the amount of vsiRNAs (21 nt) and vpiRNAs with a length of 28 nt as representative for vpiRNAs. Small RNAs were normalized to total clean reads and mapped individually to the three segments of the BUNV genome. vpiRNAs are identified by the typical 10 nt sequence overlap and the U_1/A_{10} bias characteristics of the ping-pong biogenesis of vpiRNAs (suppl. data, Figure S14 A, F, D, E, I, J).

Similar to cells infected with SFV4, also BUNV infection triggers the production of virus-derived siRNAs and piRNAs. vsiRNAs seem to derive almost equally from both strands of the genome in all three cell lines and for all three segments. Dietrich *et al.* showed that vsiRNAs map rather equally to both strands of the S- and L-segment at the onset of infection, while vsiRNAs maping to the M-segment are derived from the anti-genomic strand of the BUNV genome in Aag2 cells [188].

vpiRNAs are mapped rather to the anti-genome of the S- and M-segment of the virus while L-segment derived vpiRNAs are more equally mapped in all cell lines (Figure 25). This is in line with earlier findings for BUNV in the acute phase of infection, with the expception of the L-segment, where vpiRNAs were documented to mainly map to the genomic strand of BUNV [188].

In AF5 cells, the vast majority of small RNAs are vpiRNAs with a strong increase towards the persistent stage of infection. Especially vpiRNAs derived from the S-segment are present in high numbers (Figure 25B). Although only a small amount of vsiRNAs is produced in AF5 cells a slight increase was observed in the persistent phase (Figure 25 A). The small RNA distribution strongly varies in Dcr2 knockout cells AF319 compared to AF5 cells. vsiRNA still stay considerably low compared to vpiRNAs and similar

compared to amounts observed in AF5 cells (Figure 25 C). This is not surprising as Dcr2 would be responsible for the slicing and production of vsiRNAs. Amounts of vpiRNAs are still increasing for S- and L-segment towards persistent infection. Hardly any vpiRNAs are produced in AF319 cells from the M-segment anymore compared to AF5 cells (Figure 25 D).

The picture again changes looking at the small RNA distribution in Ago2 knockout cells AF525. Compared to AF5 cells, vsiRNA production is suddenly increased with a trend towards lower amounts produced during persistent infection for all three segments (Figure 25 E). Accumulation and increase of viral replication in those exo-siRNA pathway-deficient cells is the most probable reason for the strong increase of vsiRNAs as previously seen in β-elimination assays. Also vpiRNA production is increased compared to AF5 cells during the early phase of infection similar to the increase of vsiRNAs and possibly due to the same reasons of higher viral replication in knockout cells. Compared to AF5 cells, the amount of vpiRNAs seems to decrease during the persistent phase but compared to the acute phase, they are increasing (Figure 25 F).

Analysis of small RNAs show a similar shift towards increased vpiRNA production in AF5 cells during persistent infection like it was already shown for RVFV, another (-)ssRNA virus. In addition, also the anti-genomic mapping of vpiRNAs is similar to that found for RVFV [188]. Most vpiRNAs are mapping to the S-segment of BUNV which harbors the nucleocapsid protein N and the NSs protein. Whether this is due to the higher replication rate of that segment, remains to be investigated.

Taken together, results show that during SFV4 infection the amounts of vsiRNAs and vpiRNAs do not change significantly when the infection shifts from an acute state into the persistent phase. Unlike with BUNV where a shift from vsiRNA production to vpiRNA production is visible suggesting an increasing importance of vpiRNAs during the persistent phase of infection.

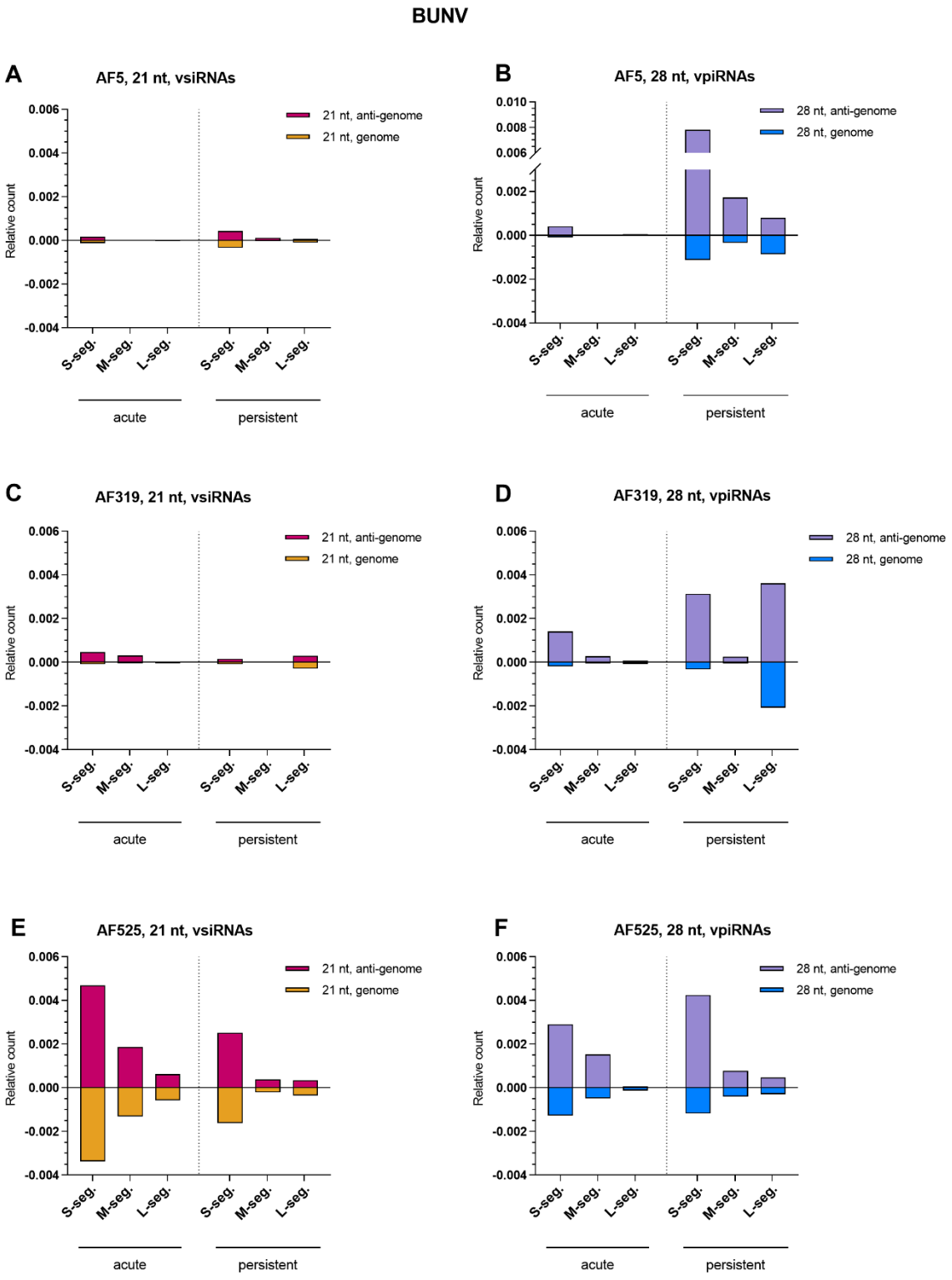

Figure 25: Production of vsiRNAs and 28 nt vpiRNAs of BUNV-infected AF5, AF319 and AF525 cells (acute and persistent infection).

Total RNA of AF5, AF319 and AF525 cells with either acute infection (MOI 1) or persistent infection of BUNV was isolated and submitted to NGS. X-axis: 21 nt and 28 nt sequencing data of the actual genome segment of BUNV (S-seg., M-seg., L-seg.) for acute and persistent stage of infection. Y-axis: relative count of small RNAs normalized to total clean reads of the sequencing run. Relative count of 21 nt vsiRNAs of the anti-genome (red) or genome (red); 28 nt vpiRNAs of the anti-genome (purple) or genome (blue) are shown. Figure shows the vsiRNA profile (A) and vpiRNA profile (B) in AF5 cells, in AF319 cells (C, D) and in AF525 cells (E, F).

3.4. Biological activity of small RNAs

Previous experiments demonstrated the production of virus-derived small RNAs during infection in mosquito cell lines, but also revealed differences related to the stage of infection, the specific virus that was investigated and deficiency of the exo-siRNA pathway.

In order to answer the remaining question whether the produced virus-specific small RNAs are biologically active and play an antiviral role, sensor expression constructs were designed. These constructs express short sequences of genomic loci, which were determined by sequencing analysis to be the main source of small RNAs during acute and persistent stage of infection. In short, downstream of an OpIE2 insect promoter, a luciferase reporter sequence is fused either to the sense or anti-sense sequence of the viral target sequence or parts of eGFP as a control (Figure 26, Figure 27).

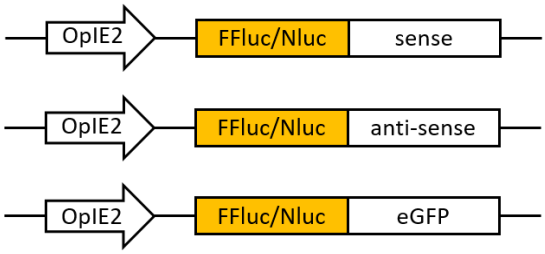

Figure 26: Schematic overview of the reporter constructs used to assess biological activity of small RNAs.
Downstream of the OpIE2 insect promoter, a luciferase coding sequence is fused to the selected sense or anti-sense sequence of SFV4 or BUNV, targeting genomic regions where high amounts of small RNAs originate from.

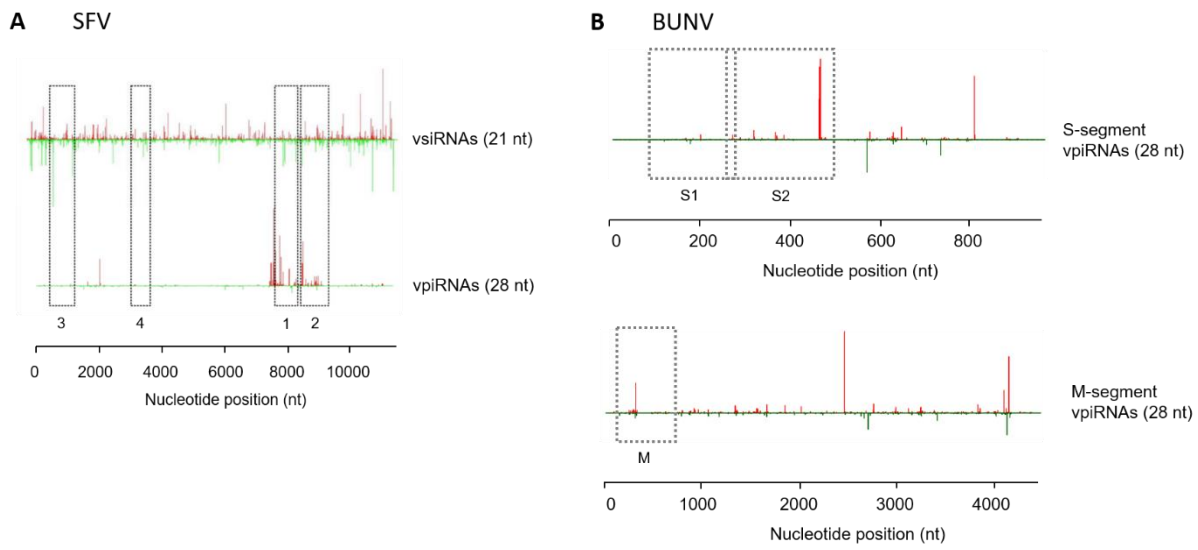

Figure 27: Schematic overview of the SFV and BUNV sensor reporter constructs.
A: Upper element shows the SFV genome with mappings of vsiRNAs and vpiRNAs. Numbers and dotted lines indicate the viral target sequences for the corresponding sensor constructs (pSFV-FFluc-$X_{s/as}$). B: S- and M-segment of the BUNV genome are shown with mappings to vpiRNAs. Characters and dotted lines indicate the viral target sequences for the corresponding sensor constructs (pBUNV-Nluc-$X_{s/as}$).

The method to detect biological activity of small RNAs is based on the RNAi mechanism which will degrade reporter transcripts and therefore luciferase activity upon matching of a virus-derived small RNA and its target sequence fused to a reporter mRNA. Reduction of luciferase activity is thereby used as an indirect measurement of the biological activity of a matching small RNA. Moreover, the exo-siRNA pathway-deficient cell lines AF319 and AF525 were used to examine the biological activity especially of vpiRNAs.

SFV4

AF5, AF319 and AF525 cells were infected with SFV4 (MOI 1) or persistently infected cells (3 weeks post infection) were used. 24 hpi or seeding (persistent infection), cells were transfected with the sensor construct and an internal control; following lysis of cells at 24 hpt to determine luciferase activity. For SFV4 sensor constructs a FFluc sequence was fused to the target sequences.

Trying to target vsiRNA and vpiRNA hotspots of the SFV4 genome, reporter sequences were specifically designed to match these regions. pSFV-FFluc-1-2 reporter constructs were designed to target vpiRNA hotspots while pSFV-FFluc-3-4 constructs were designed to target possible vsiRNA hotspots of the SFV4 genome previously defined by sequencing analysis (suppl. data Figure S14).

Compared to the control cells, no significant decrease of the relative luciferase activity was detected in AF5 cells during the early stage of SFV4 infection compared to cells transfected with the reporter control construct (control) (Figure 28 A). During the persistent phase relative luciferase activity of sensor constructs designed to target vpiRNA hotspots was rather increased (pSFV-FFluc-1-$2_{s/as}$) while a decreased relative luciferase activity was observed for vsiRNA targeting sensor constructs (Figure 28 B, pSFV-FFluc-3-$4_{s/as}$) indicating the successful targeting of small RNAs and degradation of cognate viral sequences.

Lacking Dcr2 and exo-siRNA functionality in AF319 cells, the relative luciferase activity of the second reporter construct was slightly decreased (Figure 28 C, pSFV-FFluc-$2_{s/as}$). In contrast to this, no significant change of relative luciferase activity was observed during persistent stage of infection (Figure 28 D). Unexpectedly, the luciferase activity increased for some sensor constructs especially in Ago2 knockout cells AF525 (Figure 28 E, pSFV-FFluc-2_{as}, -$4_{s/as}$) which was also the case for persistently infected cells (Figure 28 F, pSFV-FFluc-3_{s}). In addition no significant decrease of relative luciferase activity was observed for any sensor construct in AF525 cells during both stages of infection.

Taken together, the decreased luciferase activity observed for some of the sensor constructs in fully functional AF5 cells show that small RNAs are biologically active in AF5 and Dcr2-deficient cells during acute and persistent infection with SFV4. This hints towards a biological activity of vpiRNAs and a possible involvement of these small RNAs in antiviral immunity against SFV4 in mosquitoes. As only suspected parts of the SFV4 genome were targeted it might be possible that vpiRNAs derived from different genomic regions might display higher biological activity. It must also be noted that results from single experiments are highly variable which can be attributed on the one hand to the employed measuring method but also to variations of viral replication during infection. Why the luciferase activity increased in some samples remains elusive.

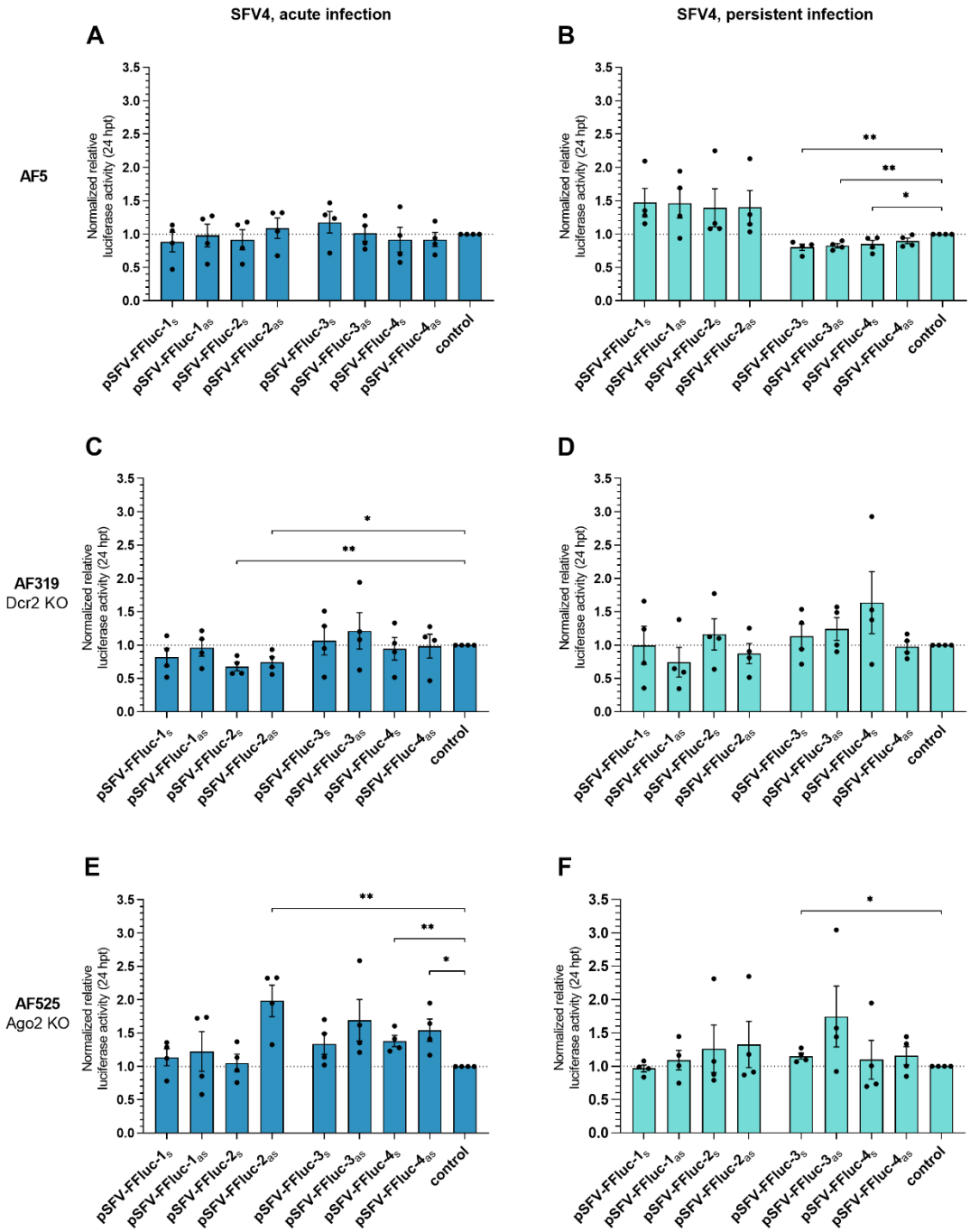

Figure 28: Biological activity of virus-derived small RNAs during acute and persistent SFV4 infection.
*AF5, AF319 and AF525 cells were either infected with SFV4 (MOI 1) (A, C, E) or persistently infected cells were used (B, D, F). 24 hpi or seeding (persistent infection), infected and non-infected cells as a control were co-transfected with Rluc expressing plasmid (internal transfection control) together with sensor constructs expressing either a SFV4-based target sequence or eGFP (control) and the FFluc reporter. pSFV-FFluc-1-2 constructs were designed to target vpiRNA hotspots in the SFV4 genome, while pSFV-FFluc-3-4 reporter constructs target vsiRNA hotspots in the genome. Subscripts stand for sense (s) and anti-sense (as) orientation of the inserted sequence. 24 hpt cells were lysed to determine relative luciferase activity. Results were normalized to Rluc activity, reporter eGFP control and non-infected cells. The mean relative luciferase activity with SEM from four independent experiments performed in duplicates is shown. * indicate significance by Student t-test (** $p \leq 0.01$, * $p \leq 0.05$).*

BUNV

AF5, AF319 and AF525 cells were infected with BUNV (MOI 1) or persistently infected cells (3 weeks post infection) were used. 24 hpi or seeding (persistent infection), cells were transfected with the reporter constructs and 24 hpt cells were lysed to determine luciferase activity. For BUNV reporter constructs a Nluc sequence was fused to the target sequence. The naming of the sensors includes the segment of the tripartite BUNV genome indicating where the target sequence is located (S1, S2: S-segment, M: M-segment).

Reporters were designed to target vpiRNA hotspot regions of the BUNV genome from which considerable amounts of vpiRNA originate, but it can not be excluded that also other small RNAs like vsiRNAs might originate from this region. See materials and method section for detailed information of the expressed target sequences.

In AF5 cells a decreased relative luciferase activity was observed for several candidates (Figure 29 A) indicating a biological activity of small RNAs matching the sequence of each target site. During persistent phase of infection the effects grew even stronger (Figure 29 B) and except for pBUNV-Nluc-$S1_{as}$, luciferase activity declined compared to control cells. In AF319 cells lacking Dcr2 thereby impairing the exo-siRNA pathway, no significant loss of luciferase activity was observed in the acute phase (Figure 29 C). In turn, a significant decrease of luciferase activity was observed for all reporter constructs during the persistent phase (Figure 29 D). No significant loss of luciferase activity was observed in Ago2 knockout cells AF525, similar to the observations made for AF319 cells during acute infection (Figure 29 E). Again, this changes in the persistent stage where decreased luciferase activity of vpiRNAs was observed for the majority of reporter sensor constructs compared to eGFP controls (Figure 29 F).

Overall, a remarkable trend towards a higher biological activity of small RNAs in persistently infected cells compared to acutely infected cells is visible. This is also in line with the analyzed sequencing data of this study that revealed the shift towards an increased production of vpiRNAs during the persistent phase while vsiRNAs were produced only to small amounts. Compared to SFV4, an overall higher biological activity of small RNAs and probably vpiRNAs was observed in cells persistently infected with BUNV. This is indicated by results obtained from knockout cell lines where the exo-siRNA pathway is non-functional.

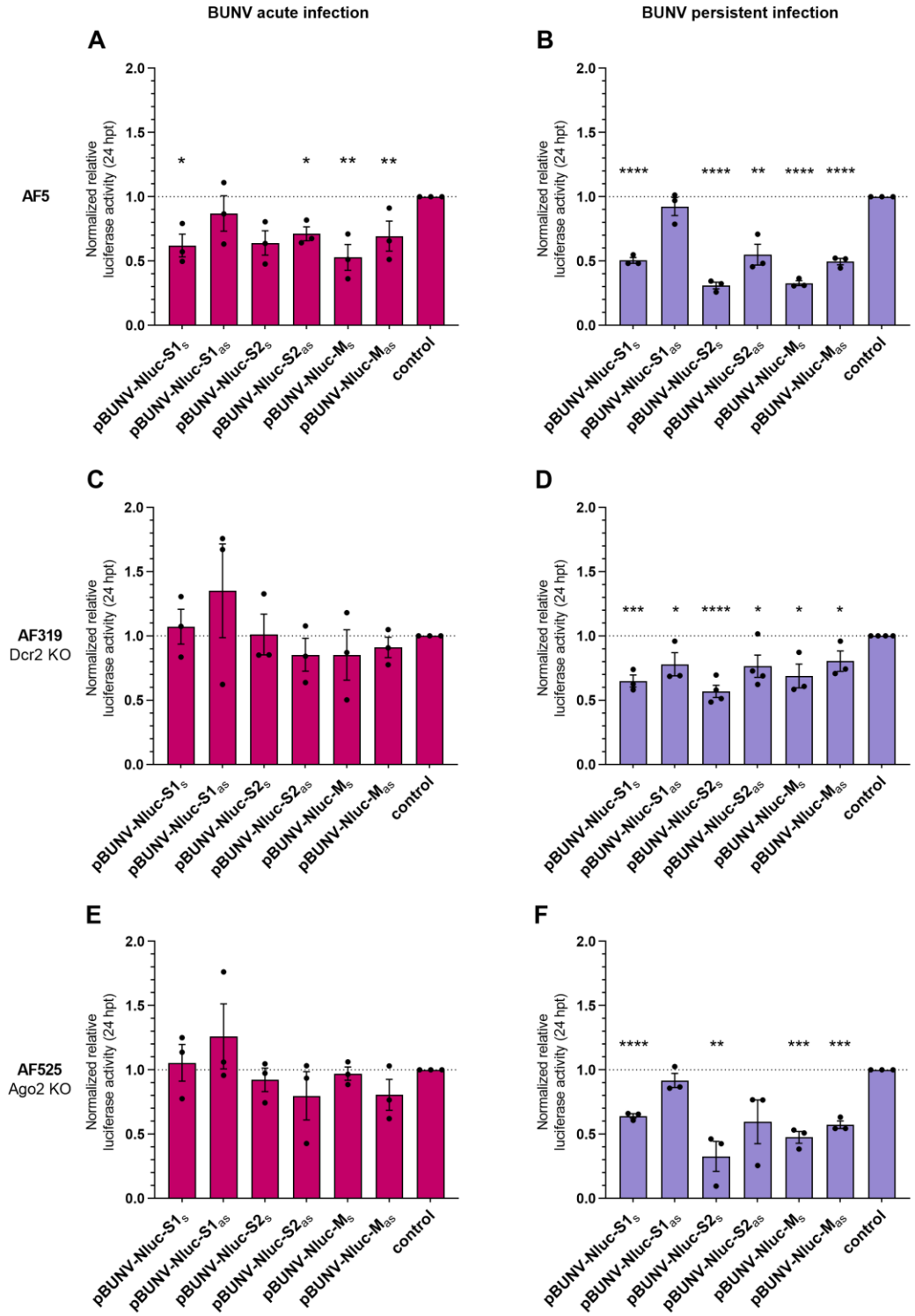

Figure 29: Biological activity of virus-derived small RNAs during acute and persistent BUNV infection.
*AF5, AF319 and AF525 cells were either infected with BUNV (MOI 1) (A, C, E) or BUNV persistently infected cells were used (B, D, F). 24 hpi or seeding (persistent infection), infected and non-infected cells as a control were co-transfected with FFluc expressing plasmid (internal transfection control) together with Nluc sensor constructs expressing either a BUNV-based targeted sequence or eGFP (control). pBUNV-Nluc constructs were designed to target vpiRNA hotspots in the BUNV. Subscripts stand for anti-genomic/sense (s) and genomic/anti-sense (as) orientation of the inserted sequence. 24 hpt cells were lysed to determine relative luciferase activity. Results were normalized to FFluc activity, reporter control and non-infected cells. The mean relative luciferase activity with SEM from four independent experiments performed in duplicates is shown. * indicates significance by Student t-test (**** p ≤ 0.0001, *** p ≤ 0.001, ** p ≤ 0.01, * p ≤ 0.05).*

3.5. Acute and persistent BUNV infection in knockout cell lines

Especially for BUNV an increase of vpiRNAs during the persistent phase of infection was shown and also the biological activity of vpiRNAs. As BUNV seemed to be a promising candidate for investigation of the antiviral role of vpiRNAs, the involved piRNA pathway proteins and their possible function during infection was moved into focus.

Therefore, AF5, AF319 and AF525 cells were infected with BUNV (MOI 2) or persistently infected cells (5 weeks post infection) were used. 48 hpi or seeding in case of BUNV persistently infected cells, mammalian BHK-21 cells were infected with the supernatant of infected cells to determine viral titers by $TCID_{50}$ assays. Results were normalized to the actual cell count of each well and virus production in parental AF5 cells.

Viral titers are increased in Dcr2 and Ago2 knockout cells in both infection stages (Figure 30 A, B). The titers in AF319 cells are overall higher during a persistent infection, but are also highly variable, which is likely due to the natural high variability of virus production in the persistent phase of infection. On the other hand, viral titers are increased in Ago2 knockout cells AF525 but are somewhat similar comparing acute to persistent phase. Findings are in line with earlier research using a BUNV reporter virus and a silencing approach for Dcr2, which also resulted in an increased viral replication during acute phase of infection [188].

Taken together, the exo-siRNA pathway is acting antiviral throughout early and late stage of BUNV infection, but viral replication benefits more from the lack of Dcr2 especially during persistent BUNV infection.

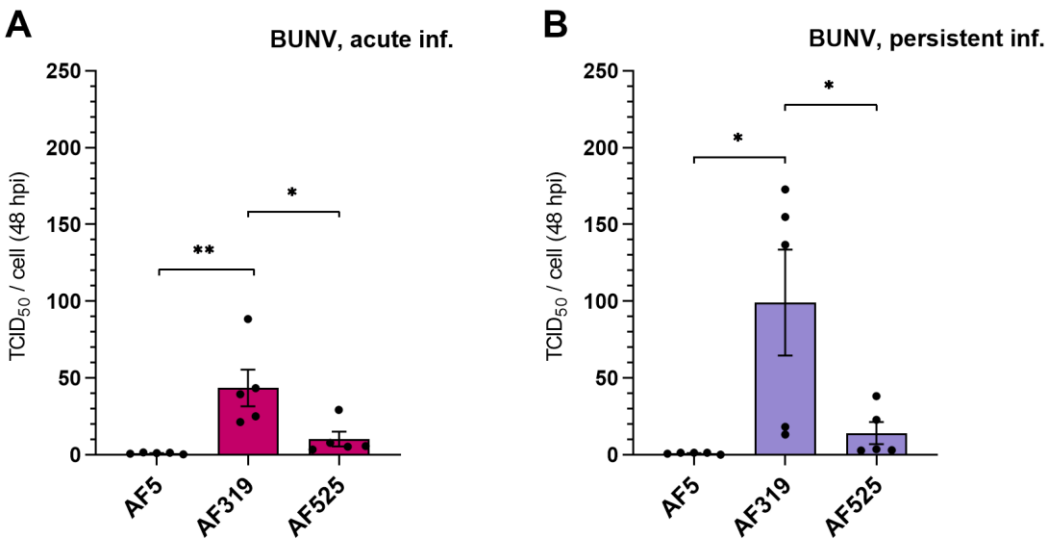

Figure 30: Viral titers of BUNV during acute and persistent infection assessed by $TCID_{50}$ assays.
*AF5, AF319 and AF525 cells were seeded and either infected with BUNV (MOI 2) or BUNV persistently infected cells were used. After 48 h supernatants were used to infect BHK-21 cells for a $TCID_{50}$ titration and cell numbers of each well were determined. A: Virus production during acute phase of infection. B: Virus production in AF5, AF319 and AF525 cells in persistent infection. Mean with SEM is shown for five independent experiments. Results were normalized to cell numbers and viral titer of AF5 cells. * indicates significance by Student t-test (** $p \leq 0.01$, * $p \leq 0.05$).*

3.5.1. Expression of RNAi key pathway proteins in BUNV acute and persistent infection

Using the same samples from the previous experiment, expression levels of relevant pathway proteins were assessed to analyze alterations during infection. Therefore, total RNA from acute and persistently infected AF5 cells as well as from uninfected cells was isolated and mRNA levels of different Argonaute and PIWI proteins were determined using sequence-specific primers in an RT-qPCR (Figure 31).

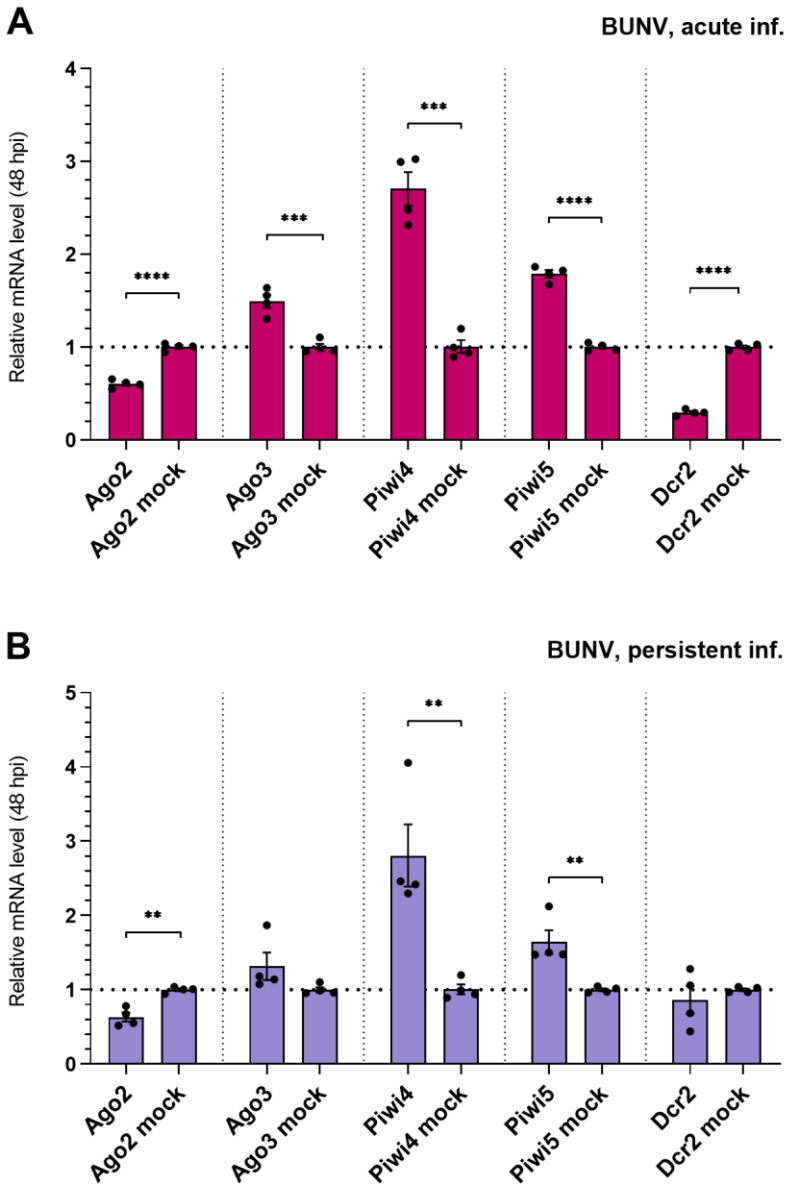

Figure 31: Expression levels of RNAi pathway proteins in AF5 cells during acute (A) or persistent (B) infection with BUNV. *AF5 cells were infected with BUNV (MOI 2) or BUNV persistently infected cells were used while non-infected AF5 cells were used as control. Total RNA was isolated 48 hpi or seeding (persistent infection). RT-qPCR was performed using sequence-specific primers. Ribosomal S7 RNA was used as a housekeeper for the $\Delta\Delta C_T$ method with non-infected AF5 cells as a control. Means with SEM are shown for four independent experiments. * indicate significance by Student t-test (**** $p \leq 0.0001$, *** $p \leq 0.001$, ** $p \leq 0.01$, * $p \leq 0.05$).*

Results indicate an overall consistent regulation pattern, no matter if the cells are in the acute or persistent phase of BUNV infection (Figure 31 A, B). Remarkably, both exo-siRNA pathway proteins (Dcr2 and Ago2) seem to be down-regulated during BUNV infection, although the effect is more prominent for Dcr2 during the acute stage rather than during the persistent stage. Ago3 and Piwi5 as probable vpiRNA producers in the ping-pong amplification cycle were overall upregulated during infection whereas this effect also decreased during the persistent phase. Piwi4 was similarly upregulated during the acute and persistent phase of infection. Whether this contributes to antiviral activities or not needs to be further investigated. Until today, the function of Piwi4 is under discussion, but an upregulation of Piwi4 has been reported after blood meal as well as an antiviral function against arboviruses. Moreover, also the interaction with proteins of the exo-siRNA and piRNA pathway has been suggested [59, 177, 247, 249, 251]. Overall, an influence of BUNV infection on expression levels of important pathway proteins is observable and significant.

3.6. BUNV replication in Ago3/Piwi5 silenced cells

Silencing of RNAi pathway proteins and subsequent sequencing of the same samples was used to further reveal the involvement of piRNA pathway proteins in BUNV-specific vpiRNA biogenesis and viral replication. Next to the knockdown of Ago3 and Piwi5, Ago2 was silenced as an additional control.

At first, AF5 cells were transfected with dsRNA targeting various key proteins of the siRNA and piRNA pathway and 24 hpt cells were infected with BUNV (MOI 5) or BUNV persistently infected cells (5 weeks post infection) were used. 48 hpi or transfection (persistent infection) supernatants were used to infect mammalian BHK-21 cells to determine viral titers using $TCID_{50}$ assays.

Results of the $TCID_{50}$ assays indicate that silencing of Ago2 leads to increased BUNV replication in the acute stage of infection similar to experiments performed in Ago2 knockout cells (acute infection: ~45-fold increase of virus production). Compared to dseGFP-transfected control cells (dsControl), silencing Ago3 and Piwi5, either alone or in combination, also leads to an increase of viral replication (Figure 32 A). Successful silencing was controlled by assessing mRNA levels of the respective protein as shown in Figure 32 B.

During the persistent phase, virus production was enhanced in cells transfected with dsPiwi5 or the combination of dsPiwi5 and dsAgo3 and not in cells silenced for Ago3 alone (Figure 32 C). Silencing controls confirm a strong silencing effect for all dsRNAs except for cells transfected with dsAgo2 (Figure 32 D). Instead of a decreased level of Ago2, expression was rather increased. Therefore, viral titers assessed in the $TCID_{50}$ assay were not evaluated.

Taken together, these results suggest an antiviral role also for the piRNA pathway proteins Ago3 and Piwi5 in the acute stage of infection, while in the persistent phase, only Piwi5 seems to act antiviral. Additionally, Ago2 is shown to act antiviral on BUNV at least during the acute phase of infection.

While silencing of Ago2 was efficient in acutely infected cells (Figure 32 B), dsRNA targeting Ago2 was unable to silence Ago2 in the persistently infected cells (Figure 32 D). Although the same aliquot of dsRNA was used for both experiments, which were performed in parallel and no apparent differences in Ago2 expression between both phases of BUNV infection was shown (Figure 31), silencing was not successful. This makes it impossible to interpret viral replication in this special case. However, previous results suggest an icrease of viral replication in Ago2 knockout cells (Figure 30 B).

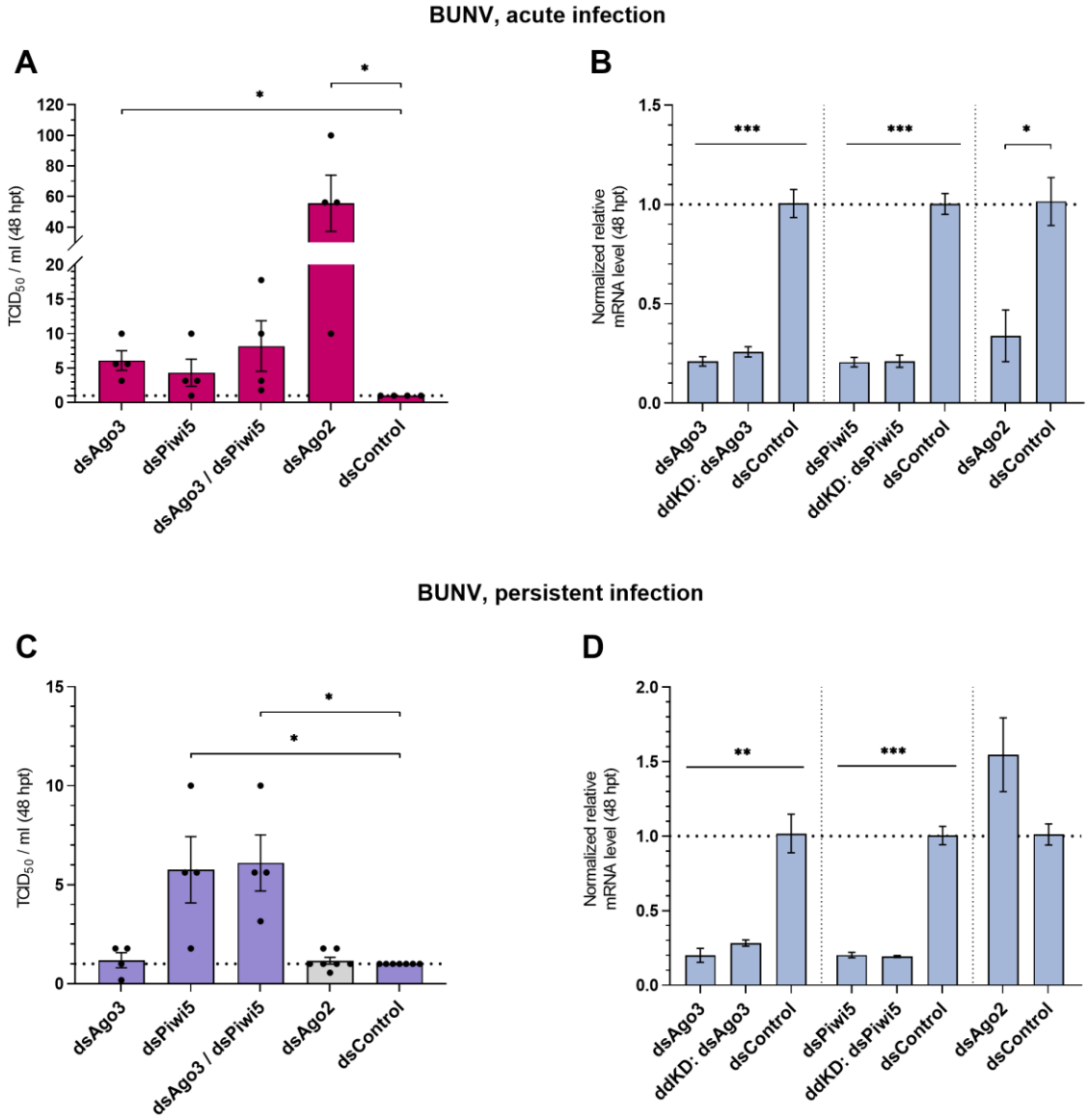

Figure 32: BUNV replication in silenced AF5 cells.

*Either naive or BUNV persistently infected AF5 cells were transfected with dsRNA targeting transcripts of various RNAi proteins (Ago2, Ago3, Piwi5 or Ago3 and Piwi5 in combination) or eGFP (dsControl). Naive AF5 cells were infected 24 h later with BUNV (MOI 5). Supernatants were taken 48 hpi or after transfection (persistent infection) and virus titer was determined by $TCID_{50}$ assays. A, C: Viral titers of AF5 cells either with acute BUNV (A) or persistent (C) infection transfected with corresponding dsRNA. B, D: Knockdown efficiency of dsRNA in acute (B) and persistent infection (D). ddKD: expression level of single protein in double knockdowns combining dsAgo3 and dsPiwi5. Total RNA from cells used in experiment (A) or (C) was isolated and submitted to RT-qPCR using sequence-specific primers to determine expression levels in acute infection (B) or persistent infection (D). Ribosomal S7 RNA was used as a housekeeper for the $\Delta\Delta C_T$ method with dseGFP-transfected cells as a control. Grey bars: Knockdown with dsAgo2 not sufficient. Means with SEM are shown for at least four independent experiments. * indicate significance by Student t-test (*** $p \leq 0.001$, ** $p \leq 0.01$, * $p \leq 0.05$).*

3.6.1. Small RNA production in Ago3/Piwi5 silenced cells infected with BUNV

To assess in a second step, whether antiviral effects in Ago3 and Piwi5 knockdowns were associated with a reduced vpiRNA biogenesis during ping-pong amplification, total RNA of the previous experiment was isolated and submitted to Illumina-based NGS.

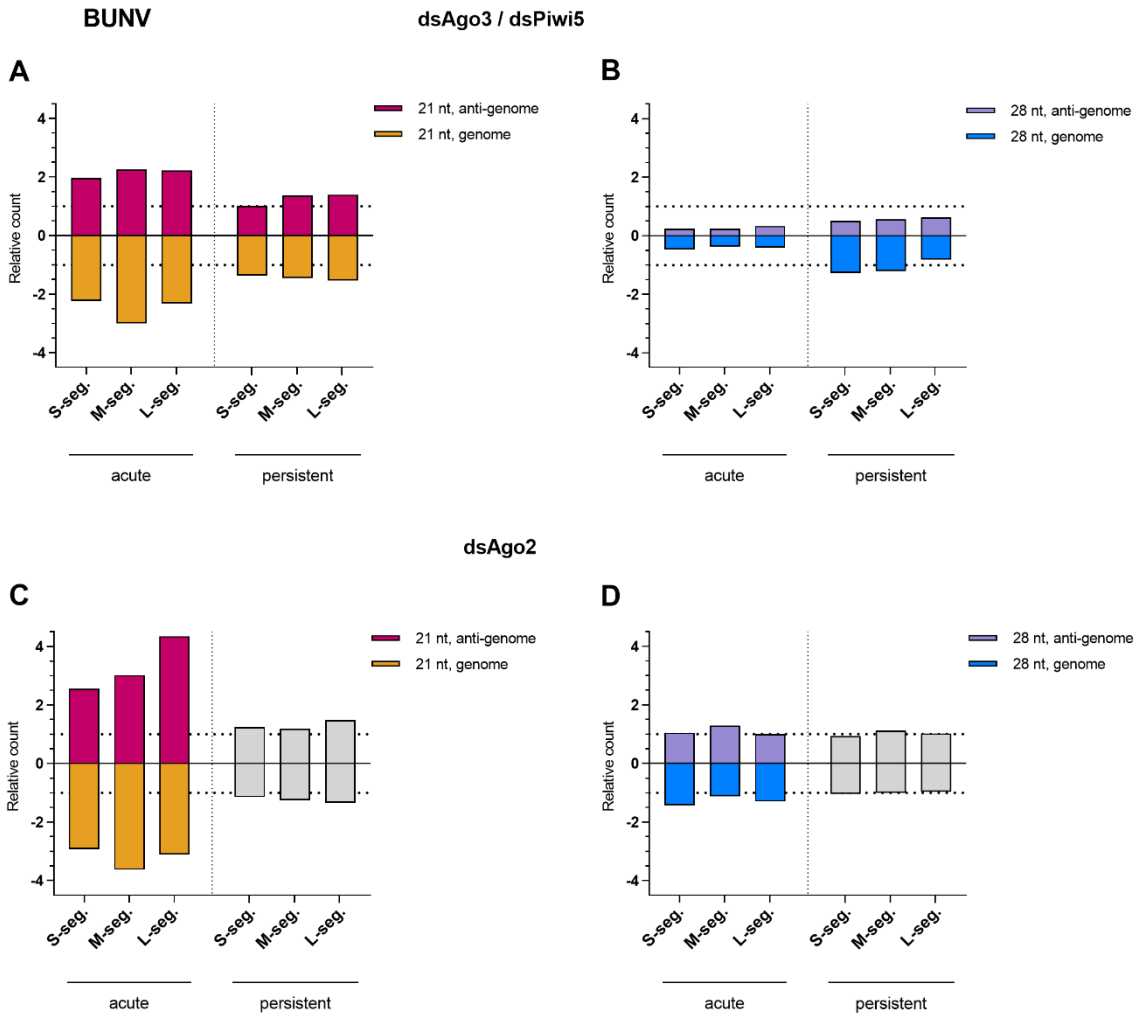

Figure 33: Distribution of 21 nt vsiRNAs and 28 nt vpiRNAs of BUNV infected AF5 cells transfected with dsRNA targeting RNAi pathway proteins.

Small RNA distribution determined by analysis of sequencing results of AF5 cells with either acute (MOI 5) or persistent BUNV infection, transfected with either dsAgo2 (A, B) or a combination of dsAgo3 and dsPiwi5 (C, D). X-axis: sequencing data of BUNV S, M and L segment for acute and persistent infection, y-axis: relative count of small RNAs normalized to total clean reads of the sequencing run and control cells transfected with dseGFP (dotted lines represent normalization levels). Relative count of 21 nt long vsiRNAs of the anti-genome (red) or genome (orange) or 28 nt long vpiRNAs of the anti-genome (purple) or genome (blue). Grey bars: Knockdown with dsAgo2 not sufficient, see associated data in Figure 32D.

Production of vsiRNAs was increased during the acute infection in Ago3 and Piwi5 silenced cells and normalizes during the later stage of infection (Figure 33 A). Production of 28 nt long vpiRNAs is strongly decreased in Ago3 and Piwi5 silenced cells compared to controls indicated by the dotted line (Figure 33 B). This effect is more prominent in the acute infection and decreases in the persistent stage of infection, but is still visible. Especially anti-genomic vpiRNAs are still decreased, while vpiRNAs derived from the genomic strand reach almost the level of control cells.

Silencing of Ago2 during acute BUNV infection, leads to a strong increase of vsiRNAs from both, the genomic and anti-genomic viral strands. This could be due to (i) the accumulation of Dcr2-generated vsiRNAs, which are not processed further anymore, (ii) an increase in virus replication (Figure 32 A) or a combination of both (Figure 33 C). Production of anti-genomic vsiRNAs from the L-segment seems to be increased compared to the other segments. Unexpectedly, silencing of Ago2 in the persistent stage was unsuccessful and the data is not further analyzed.

Compared to control cells, vpiRNA production in Ago2-silenced cells remained on a normal level during the acute phase and did not decrease as seen for Ago3 and Piwi5 knockdowns. Therefore, sequencing data indicates that Ago2 is not involved in BUNV-specific piRNA production in this experimental setup. In contrast, an increase of vpiRNAs is observed for the S- and M-segment of BUNV in sequencing data of acutely infected Ago2 knockout cells (Figure 25). Such effects might be related to the incomplete silencing of Ago2 in these previous experiments, different MOIs or general variation of the whole experiment.

vsiRNAs are produced in equal shares from both genome strands while production of vpiRNAs was highly biased towards the production of anti-genomic vpiRNAs for the S- and M-segment, similar to previously reported BUNV-specific small RNAs. Numbers of vpiRNAs originating from the L-segment were rather low and seem to be produced from both strands in an equal way (suppl. data, Figure S15).

Overall, results indicate that indeed Ago3 and Piwi5 are important proteins for BUNV-specific piRNA biogenesis during acute and persistent stage of infection. How vsiRNA biogenesis is influenced by a combined Ago3/Piwi5 knockdown remains enigmatic, although the interaction between the siRNA and piRNA pathway were already suggested [247, 249].

3.7. Integration of viral sequences into the mosquito genome

Viral sequences were found to be integrated into the host genome for all eukaryotes and for all virus families [29, 281, 286, 288, 325]. Especially the genomes of the important vectors *Ae. aegypti* and *Ae. albopictus* harbour the highest amount of integrated viral sequences enriched in piRNA clusters (*Ae. aegypti*: 44 %, *Ae. albopictus*: 12.5 %) [246, 285].

It was reported that upon arboviral infection in mosquito cells, viral RNA is in some cases converted into cDNA by reverse-transcriptases derived from endogenous retrotransposons, leading to the formation of vcDNA molecules. These vcDNA forms were suggested to support the antiviral RNAi response and are crucial to establish persistent infections [263, 270, 326]. To date it is not known, whether vcDNA remains in the host cell in the form of an episomal molecule or is rather integrated into the genome. However, the production of vpiRNAs from NIRVS and vcDNA had already been documented and suggested to confer an adaptive antiviral immunity [29, 246, 247, 264, 285]. Thus, if the mosquito is re-infected with the same (homologous) or a different (heterologous) virus, the immune response is able to act faster and more accurate. Both, homologous and heterologous viral interference, has been observed in mosquito cells. Cells persistently infected with SINV can not be super-infected with other SINV strains or alphaviruses, but can still be infected with bunya- or flaviviruses [327-329]. Mondotte *et al.* showed for *Ae. aegypti* that infection with CHIKV leads to the formation of vcDNA in females which is detectable in their offspring as well and confers an antiviral immunological memory to their progeny, lasting for several generations. Additionally, they suggested that this mechanism is Dcr2-independent in *D. melanogaster* [275]. Leger *et al.* showed that superinfection of Dcr2-incompetent C6/36 cells with a homologous strain of RVFV led to a drastically decreased viral replication of the super-infecting virus confirming a Dcr2-independent effect [184]. Subsequent infection with arboviruses of different families was shown to rather result in a co-infection (reviewed in [328])[330-332].

To further investigate this interesting hypothesis, different experimental approaches were started but not all of them succeeded. The initial difficulty lies in distinguishing the small RNAs derived from the ongoing infection and viral replication from the ones that originate from vcDNA forms or even viral integrations in the host genome. Secondly, cells need to be cleared of the viral infection to determine whether a follow-up infection with the same or another virus species affects viral replication in any way.

3.7.1.CHIKV trans-replicase system

At first, it was tried to generate a transient infection in mosquito cells and investigate if vcDNA forms and/or small RNAs are produced from these vcDNA forms similar to episomes or even from finally integrated sequences.

The previously published base for the experiment was a CHIKV *trans*-replicase system [306]. The idea is that the viral ORFs of CHIKV are divided, uncoupling the expression of the replicase nsPs from structural RNA expression controlled by the subgenomic promoter (SGP) resulting in two plasmids (Figure 34 A). One DNA plasmid encodes the nsPs and thereby the replicase of CHIKV (REP, Figure 34 B), while the second plasmid consists of an RNA template under a Sp6 promoter for *in vitro* transcription. In explanation, 77 N-terminal amino acid residues of nsP1 are followed by the FFluc reporter sequence instead of the nsPs followed by a Nluc reporter sequence plus an additional antibiotics cassette (blasticidine) with the 2A autoproteolytic sequence, in tandem with a blasticidine resistance gene under the control of the subgenomic promoter (SG-Nluc, Figure 34 C). As a variant of the RNA template, the SG-C-Nluc template additionally contains the CHIKV capsid sequence as previous results showed the predominant production of vpiRNAs from this region suggesting these vpiRNAs might also derive from vcDNA molecules.

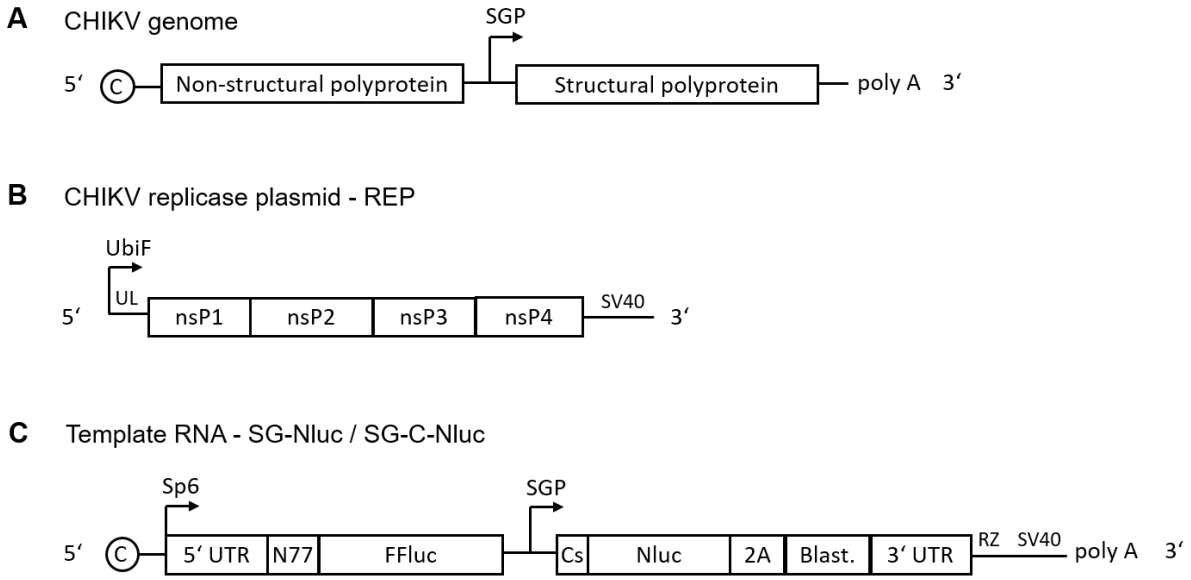

Figure 34: Schematic overview of the CHIKV wt genome, trans-replicase plasmid and RNA template.
A: Genome of CHIKV wt as a simplified representation. B: Expression construct for CHIKV ns-polyprotein with an UbiF, full length polyubiquitin promoter (Ae. aegypti), UL, transcribed leader of polyubiquitin gene containing naturally occurring intron, SV40, late polyadenylation region. C: RNA template expression constructs under Sp6 promoter with 5‘ and 3‘ UTRs derived from CHIKV. FFluc reporter, N77, encoding the 77 N-terminal amino acid residues of nsP1; FFluc reporter instead of nsPs; SGP, CHIKV subgenomic promoter, Cs, CHIKV capsid protein (only in SG-C-Nluc template variant), Nluc reporter; 2A-Blast., antibiotics cassette consisting of 2A autoproteolytic sequence in tandem with blasticidine resistance gene and followed by the 3‘ UTR, RZ, antisense-strand ribozyme of HDV. The drawings are not to scale and a simplified representation. Adapted from [306].

The general protocol intended to co-transfect mosquito cells with the replicase expressing plasmid (REP) or a non-functional replicase variant (GAA) together with the *in vitro* transcribed and capped RNA template (SG-Nluc or SG-C-Nluc). To select for successfully transfected cells and to ensure that the RNA template is not degraded ahead of time, cells would be treated with blasticidine. Several times of passaging with blasticidine should give the cells sufficient time to form viral cDNA and also for possible integrations into the genome. It was shown that those viral cDNA forms were already found for arboviruses such as DENV2, CHIKV, ZIKV or WNV 24 hpi in mosquitoes [194, 263, 273]. Subsequent to blasticidine selection, cells would be passaged several times without blasticidine to make sure the RNA template is degraded over time. This process is monitored by determining relative Nluc activity in the cells originating from the actively translated RNA template. Upon disappearance of the RNA template, produced small RNAs can be clearly assigned to *de novo* production from other sources than the initially transfected template. Whole genome sequencing and small RNA sequencing of those cells were assigned to provide evidence for viral integrations and small RNA production from integrated sequences or vcDNA forms.

To set up the whole experiment, several cell lines and combinations of the *trans*-replicase system were tested but are not shown here. Dcr2 active cell lines like AF5 and Aag2 (*Ae. aegypti*) were tested as well as Dcr2-deficient cell lines AF319 or C6/36 (*Ae. albopictus*). Cells were transfected with different combinations of the modified CHIKV *trans*-replicase system using also original [306] and modified plasmids of the RNA template as well as *in vitro* transcribed RNA.

One attempt was to first test the system only with original plasmid DNA instead of the *in vitro* transcribed RNA. Results of this experiment are shown in Figure 35 A and B. AF5 and C6/36 cells were co-transfected with the replicase construct (REP) or control (GAA) together with the plasmid expressing the SG-Nluc or the SG-C-Nluc construct. 48 hpt, cells were lysed to determine relative luciferase activity.

FFluc protein is produced from the nsP-region upstream of the subgenomic promoter of the template, while Nluc protein is expressed from the region downstream of the subgenomic promoter (Figure 34 C).

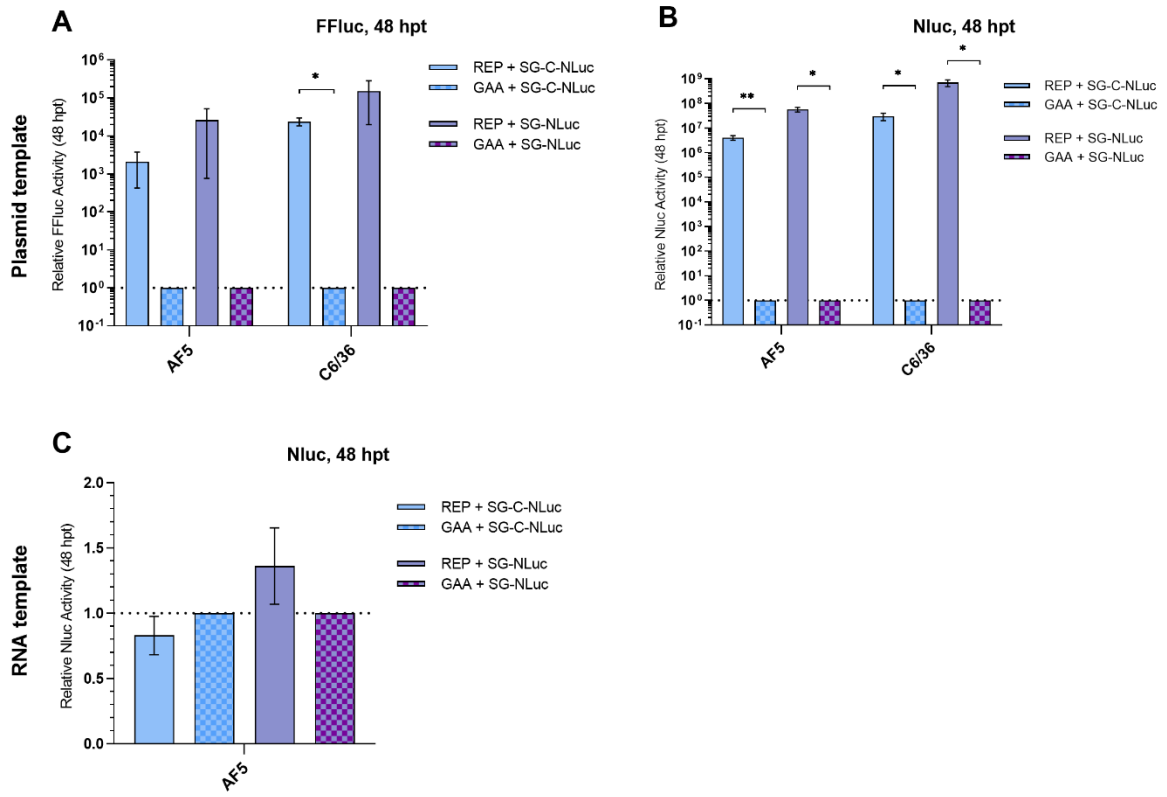

Figure 35: Selected experiments showing functionality of plasmids and template RNA of the CHIKV trans-replicase system.

*A: AF5 and C6/36 cells were co-transfected with functional replicase plasmid (REP) or non-functional variant (GAA) and plasmid expressing either the sequence template with the additional capsid sequence (SG-C-Nluc) or without (SG-Nluc). 48 hpt cells were lysed and relative FFluc (A) or Nluc (B) activity was determined. C: AF5 cells were co-transfected with functional replicase plasmid (REP) or non-functional variant (GAA) and capped in vitro transcribed template RNA encoding either the template sequence with additional capsid sequence (SG-C-Nluc) or without (SG-Nluc). Mean with SEM is shown for three independent experiments performed in duplicates. * indicates significance by Student t-test (** $p \leq 0.01$, * $p \leq 0.05$).*

Results show that relative FFluc (Figure 35 A) and Nluc activity (B) are both highly increased in either AF5 or C6/36 cells transfected with the functional replicase plasmid (REP) and one of the template plasmids compared to controls (GAA + SG-(C)-Nluc). The effect seems to be even slightly stronger for the SG-Nluc template plasmid. Results indicate that the whole *trans*-replicase system of two separated units of the CHIKV genome is functional and that in this case the complete DNA template including the region behind the subgenomic promoter is being expressed.

In a next step the previous experiment was repeated but this time instead of the DNA template construct, the capped *in vitro* transcribed RNA template was transfected into AF5 cells together with the REP or GAA replicase plasmids (Figure 35 C). Unfortunately, using the capped *in vitro* transcribed RNA, no increased Nluc activity compared to controls (GAA) was observed (Figure 35 C). In addition to this, FFluc activity was rendered undetectable. It was decided to use C6/36 cells and the SG-Nluc template RNA as these showed at least the most promising starting points during preliminary experiments.

C6/36 cells were transfected with a combination of replicase plasmid and capped *in vitro* transcribed template RNA. Relative Nluc activity was monitored every second passage to check for the time point when the template RNA is cleared from the cells after omitting the blasticidine additive. FFluc still remained undetectable in C6/36 cells, similar as observed in AF5 cells. At passage 4, 6 and 10, blasticidine (100 µg/ml) was added to the cell medium to select for transfected cells. However, Nluc activity was still present in the cells even after 36 passages (Figure 36). At this point, the experiment was cancelled as promising results were missing and reproducibility was not given.

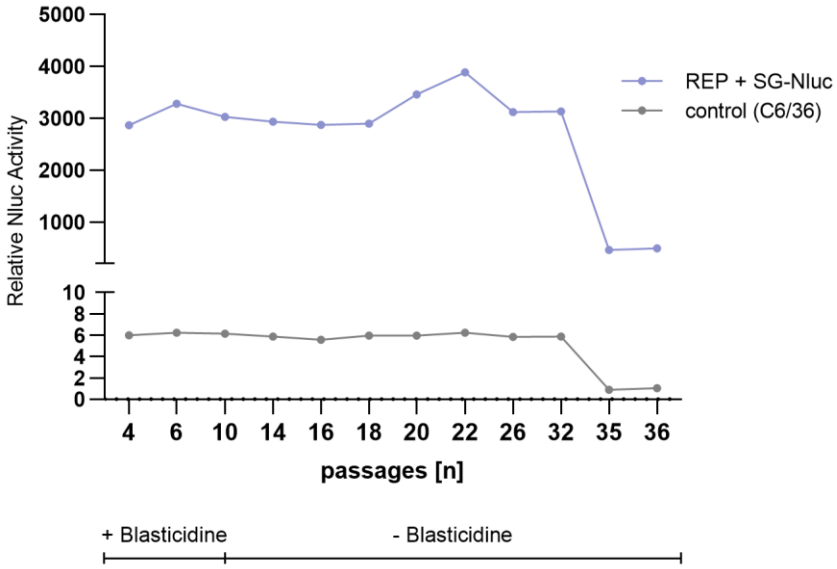

Figure 36: Monitoring of Nluc expression from the CHIKV template RNA during passaging of transfected and selected C6/36 cells.

Cells transfected with CHIKV trans-replicase template RNA were passaged twice a week adding blasticidine every second time to the medium (100 µg/ml) to select for actually transfected cells. After 10 passages blasticidine was omitted and cells were passaged until passage 36. During every second passage, a part of the cells was lysed to determine relative Nluc activity of the in vitro transcribed RNA and therefore to monitor the time point when the template RNA would be cleared of the cells by natural degradation. The graph displays the number of passages on the x-axis as well as the passage until blasticidine was added to the cell to select for transfected cells. Y-axis shows the relative Nluc activity.

3.7.2. Effects of a recurring arbovirus infection

Since it was shown for various insect-specific- and arboviruses that integrations of viral sequences can be found in the genome of several mosquito vector species and production of piRNAs from these sequences [29, 246, 285-289, 333], a new approach was pursued to assess the probability of such an integration for SFV6-2SG-Nluc and BUNV-Nluc infection in *Ae. aegypti*-derived AF5 cells. Preceding results indicated the production of small RNAs during acute and persistent infection of both viruses, which is suggested to be a main source and trigger of integrations into certain genomic cluster, especially into piRNA clusters.

The general aim of this experiment was to generate AF5 cells that had encountered a persistent SFV or BUNV infection once. Subsequent to clearing of this viral infection, cells can be used to determine effects on a second, recurring infection with the same virus, to assess the production of vcDNA or possible viral integrations into the host genome and virus-specific small RNA production even in the absence of the virus.

To achieve clearance of persistent infection regular transfections with dsRNA targeting the virus through RNAi were determined. Luciferase activity of reporter viruses and regular checks for cytopathic effects (CPE) caused by infectious particles in the supernatant of cultured cells were used to monitor the course of infection. Furthermore, whole genome and small RNA sequencing were planned after the successful recovery of treated cells from viral infection (Figure 37).

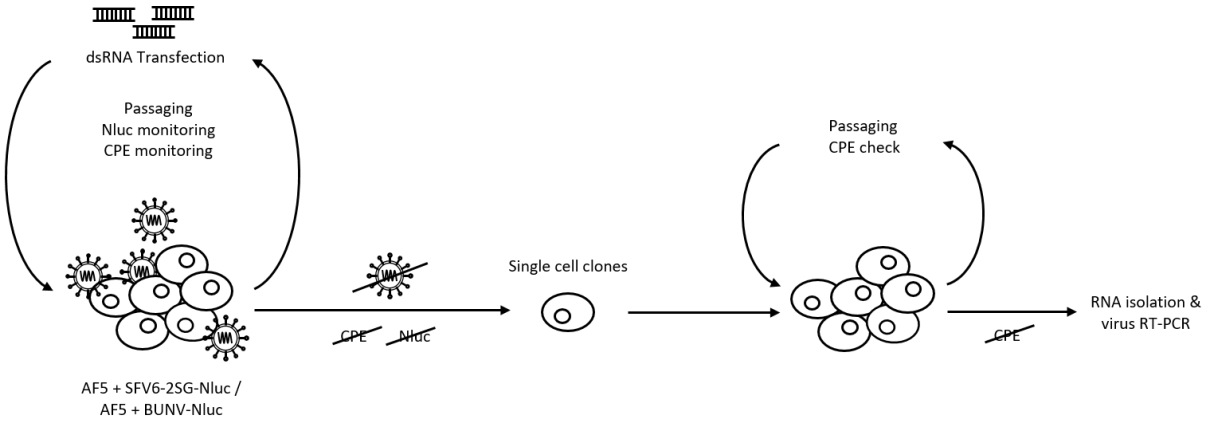

Figure 37: Schematic representation of experiments for clearing persistent arbovirus infection in AF5 cells.
AF5 cells persistently infected with SFV6-2SG-Nluc or BUNV-Nluc were seeded in 24-well plates and passaged. Twice a week, cells were transfected with dsRNA targeting either SFV6-2SG-Nluc or BUNV-Nluc. Infection was monitored by measuring Nluc activity once a week and additional testing for cytopathic effects (CPE) of collected supernatants on BHK-21 cells. Shortly after reporter Nluc signal disappeared and no signs of CPE were visible anymore, cells were separated and single cell clones were seeded in 96-well plates, followed again by passaging and the check for CPE. Total RNA of colonies without apparent CPE was isolated and submitted to RT-PCR testing for active arboviral infection. Negatively tested cultures were used for further experiments.

3.7.2.1. Infectivity of persistently infected cells

As a prerequisite for the experiment, infectivity of SFV6-2SG-Nluc and BUNV-Nluc was assessed by immunostaining of persistently infected AF5 cells. After fixation with formaldehyde and further preparation, SFV6-2SG-Nluc-infected cells were stained with primary antibodies against the SFV-nsP3 protein and against double-stranded RNA, while BUNV-Nluc infected cells were stained with antibodies against the BUNV N-protein (Figure 38). After the incubation period, cells were co-stained with the appropriate secondary antibody and DAPI. Fluorescence signals were checked using a fluorescence microscope. dsRNA was detected using a secondary antibody conjugated with Alexa 594 red-fluorescent dye, while SFV-nsP3 was detected using a secondary antibody conjugated with Alexa 488 green-fluorescent dye.

Evaluation of infectivity in persistently infected AF5 cells resulted in a 100 % infection rate for SFV6-2SG-Nluc infected cells while 94 % of the cells infected with BUNV-Nluc were analyzed as positive. Results indicate that both, SFV6-2SG-Nluc and BUNV-Nluc are able to induce a persistent infection in almost all cells of the AF5 cell culture ensuring reliable results and allowing for the possible formation of NIRVS in all cells.

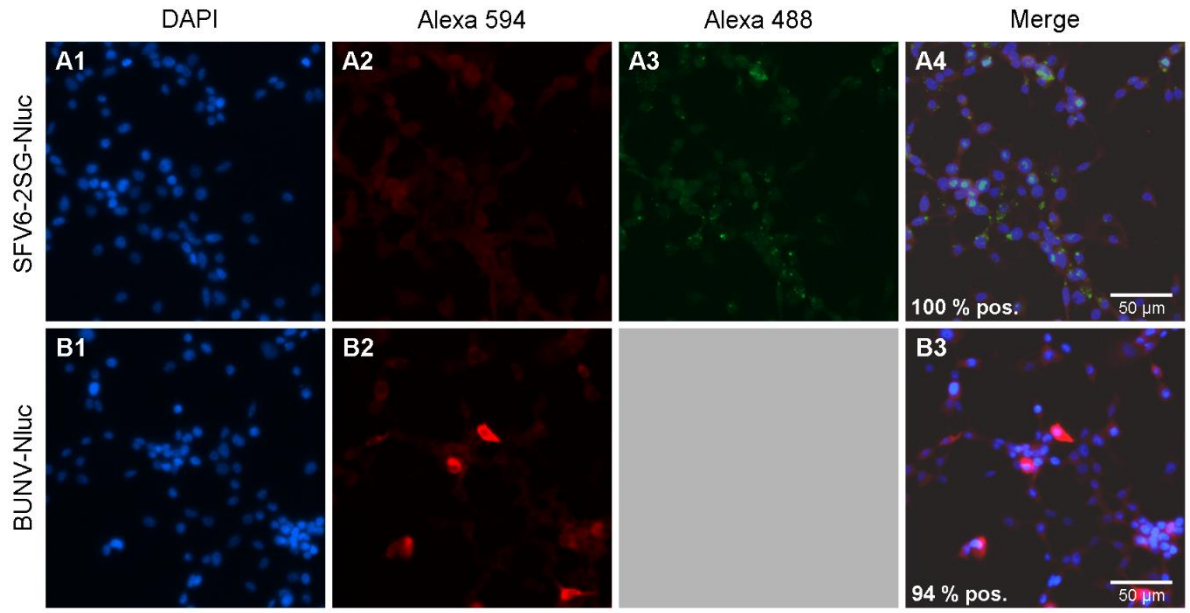

Figure 38: Infection rate in cells persistently infected with SFV6-2SG-Nluc and BUNV-Nluc.
AF5 cells persistently infected with SFV6-2SG-Nluc (A1-A4) or BUNV-Nluc (B1-B3) were seeded in 24-well plates. 24 h later, cells were stained and examined for presence of either SFV-nsP3 (A2, red), double-stranded RNA (A3, green) or BUNV N-protein (B2, red); DAPI signals show the nuclei (A1/B1, blue). Scale bar: 50 µm. Three independent sections of each well were analyzed. One representative section is shown here.

3.7.2.2. Efficiency of dsRNA targeting SFV and BUNV genome sequences

Following the assessment of infectivity, the ability to inhibit viral replication of the selected dsRNA targeting either SFV6-2SG-Nluc or BUNV-Nluc was determined. AF5 cells were infected with the respective virus and 24 hpi transfected with dsRNAs targeting either SFV or BUNV. 48 hpt cells were lysed and viral replication was assessed by measuring relative Nluc activity (Figure 39).

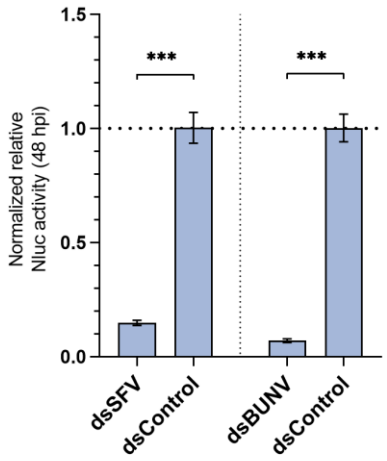

Figure 39: Inhibition of viral replication by sequence-specific dsRNA targeting either SFV6-2SG-Nluc or BUNV-Nluc.
*AF5 cells were infected with SFV6-2SG-Nluc or BUNV-Nluc (both MOI 1). 24 hpi cells were transfected with dsSFV targeting SFV6-2SG-Nluc or dsBUNV targeting BUNV-Nluc or with dseGFP (dsControl). 48 hpt cells were lysed and relative Nluc activity was determined and normalized to control cells. Means with SEM are shown for three independent experiments performed in triplicate. * indicate significance by Student t-test (*** $p \leq 0.001$).*

The results indicate a strong decrease in virus production suggesting the general ability to sequence-specific targeting of the corresponding viruses and thereby supporting the ability to clear persistent viral infection in AF5 cells (Figure 39).

3.7.2.3. Clearance of SFV and BUNV infection using dsRNA

After checking the infectivity of both viruses and efficiency of dsRNA, the main experiment was initiated. Therefore, AF5 cells with a recently established persistent infection (4 weeks post infection) with reporter viruses SFV6-2SG-Nluc and BUNV-Nluc, were seeded into 24-well plates. Cells were continuously passaged and transfected twice a week with sequence-specific dsRNA targeting the respective virus. Nluc activity in the cells was monitored (Figure 40) as well as the occurrence of cytopathic effects in mammalian BHK-21 cells incubated with supernatant of treated AF5 cells.

The timeline in Figure 40 shows that initial Nluc activity in SFV-infected cells decreased over time and is hardly detectable after five passages, while Nluc activity of BUNV reporter virus decreased more slowly. Accompanying tests for CPE indicated no infective particles in the supernatant after 13 passages any more of both experimental lines.

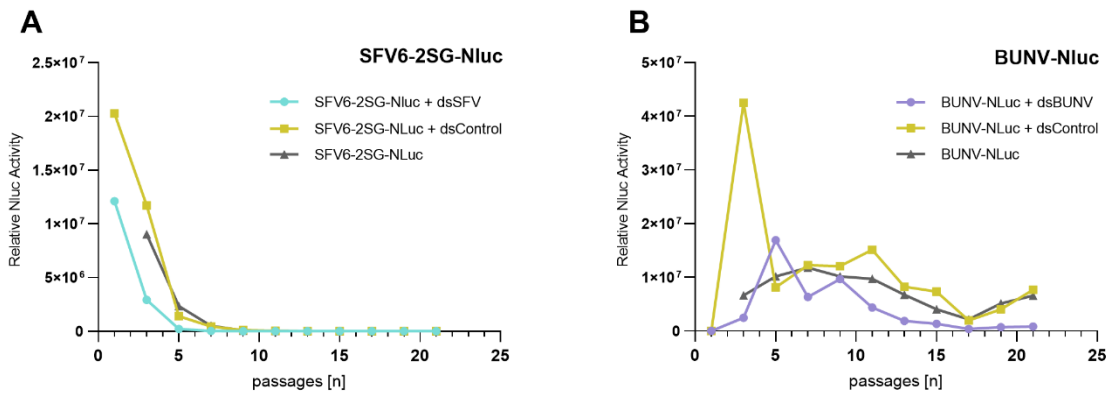

Figure 40: Monitoring of Nluc activity in AF5 cells persistently infected with two arboviral reporter viruses.
Cell culture suspensions were monitored every second passage during treatment with sequence-specific dsRNAs targeting either SFV or BUNV. A: Nluc activity in AF5 cells infected with SFV6-2SG-Nluc and treated with dsSFV (blue) or with dsRNA targeting eGFP as control (dsControl) (yellow) and non-transfected cells (grey). B: Nluc activity in AF5 cells infected with BUNV-Nluc and treated with dsBUNV (purple) or with dsRNA targeting eGFP as control (dsControl) (yellow) and AF5 cells solely infected with BUNV-Nluc as background (grey) measurement. X-axis: number of cell culture passage.

Shortly after reporter signal was not detectable anymore, single cells were seeded in a new 96-well plate and left to grow. Single cell colonies were again monitored for CPE and tested via RT-PCR for any signs of arboviral infection (Figure 41). Actin was used as control for housekeeper RNA. Furthermore, the presence of CFAV was also determined, as AF5 cells are known to be persistently infected with CFAV previously determined by sequencing analysis of β-eliminated samples [58].

RT-PCR results in Figure 41 show, that with an expected band size of 0.2 kb, all samples were tested positive for the presence of actin indicating successful isolation, reverse trancription and RT-PCR of all samples. Furthermore, expected bands of 0.2 kb for SFV and 0.6 kb for BUNV, were not detectable in any samples compared to positive controls (lane AF5 + SFV and AF5 + BUNV respectively). This indicates that treatment with dsRNA against the cognate viral sequence was successful to generate cured AF5 cell cultures, which can be used for further experiments. Surprisingly, also some cured cell

cultures were cleared from CFAV although the original AF5 cells used for the experiment were tested positive for CFAV (Figure 41, AF5 + CFAV). Bands detected in the BUNV samples at <100 bp are attributed to superfluous primers.

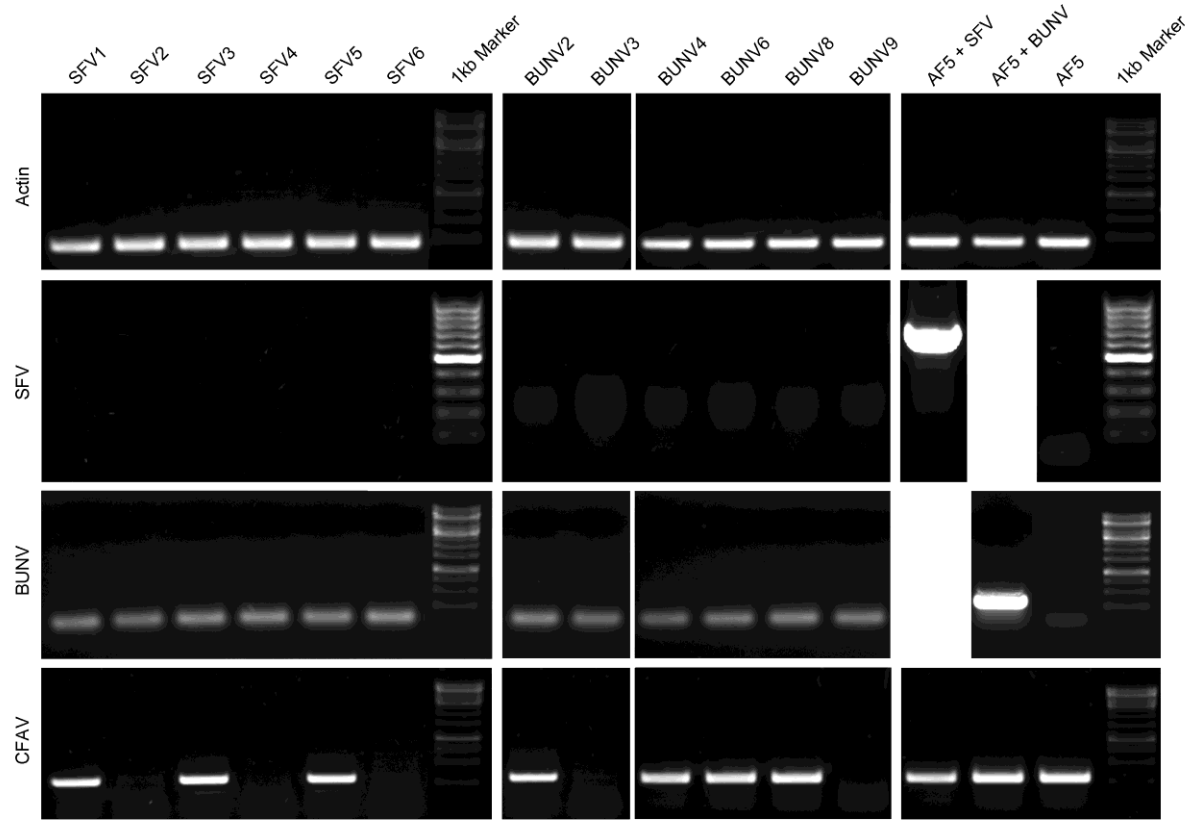

Figure 41: RT-PCR results of previously infected and cured AF5 cell cultures.
Total RNA of cells cleared from SFV6-2SG-Nluc and BUNV-Nluc infection was isolated and reverse transcribed into cDNA, which was used for RT-PCR. Virus-specific primers were used to confirm clearance of each virus and actin-specific primers were used as housekeeper. In addition, cells were also checked for an infection with CFAV which persistently infects AF5 cells. SFV1-6: colonies derived from single cell clones of AF5 infected with SFV6-2SG-Nluc treated with dsSFV. BUNV2-9: colonies derived from single cell clones of AF5 infected with BUNV-Nluc and treated with dsBUNV. 1 kb DNA Ladder used as a marker. Actin RNA was used as housekeeper.

3.7.2.4. The effect of re-infection in cells cleared from persistent infection

Cured cells were used for re-infection experiments to check whether preceding infection with those viruses has any impact on viral replication. For the re-infection experiment, previously SFV6-2SG-Nluc-cured cells were re-infected again with SFV6-2SG-Nluc or BUNV-Nluc as a control while cells cured of BUNV-Nluc-infection were re-infected again with BUNV-Nluc or SFV6-2SG-Nluc as a mutual control (both MOI 0.1). Additionally, naive AF5 cells were infected with either SFV6-2SG-Nluc or BUNV-Nluc as a control group. The whole setup is depicted in Figure 42. 48 hpi cells were lysed and relative Nluc activity was measured reflecting viral replication and infection in the cells.

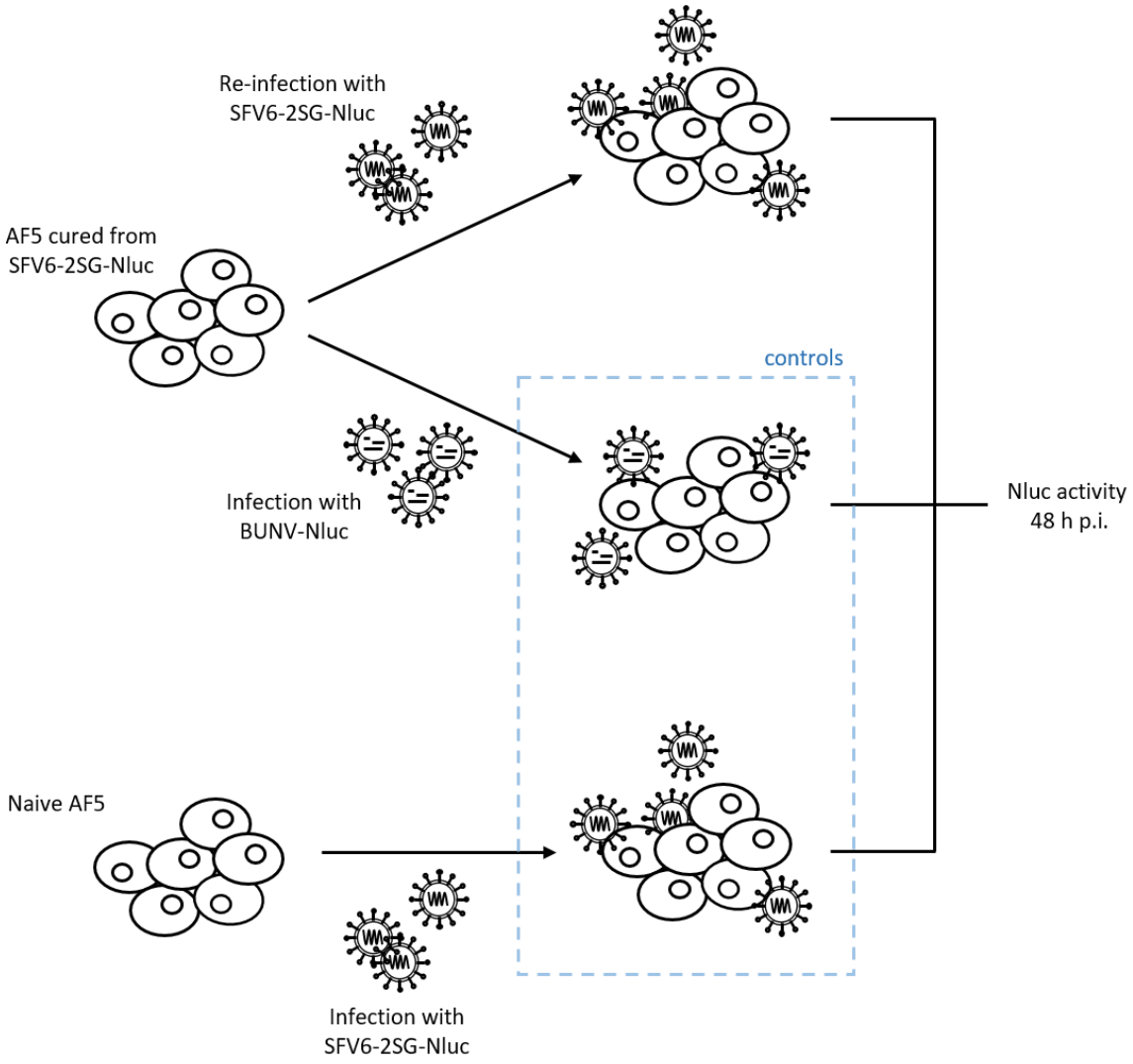

Figure 42: Exemplary presentation of re-infection experiment for AF5 cells cleared from SFV6-2SG-Nluc infection.
AF5 cells previously cured of persistent SFV6-2SG-Nluc infection and naive AF5 cells (control) were either re-infected with SFV6-2SG-Nluc or infected for the first time with BUNV-Nluc as a control. Naive AF5 cells were infected with SFV6-2SG-Nluc as a negative control to assess viral replication in comparison to re-infected cells. 48 hpi, viral infection in all cells was determined by assessing Nluc activity. The experiment was carried out vice versa for BUNV-Nluc: cells previously cured of BUNV infection were re-infected with BUNV-Nluc or SFV6-2SG-Nluc as a control. In addition, also naive AF5 cells were infected with BUNV-Nluc.

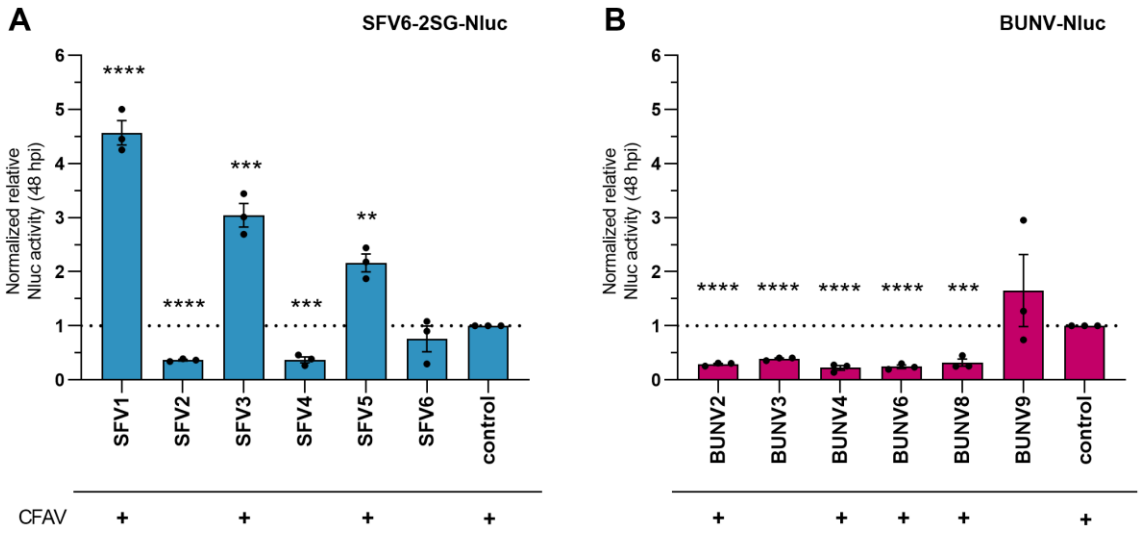

Figure 43: Arboviral replication in re-infected AF5 cells.

*Each cell clone of AF5 cells cleared from persistent infection (A: SFV1-6; B: BUNV2-4,6,8,9) was re-infected with SFV6-2SG-Nluc (A) or BUNV-Nluc (B) (both MOI 0.1). As control, previously SFV6-infected cells were also infected with BUNV-Nluc and vice versa. Furthermore, naive AF5 cells were infected with SFV6-2SG-Nluc or BUNV-Nluc as a second control. 24 hpi cells were lysed and relative Nluc luciferase activity was determined. Results were normalized to naive AF5 cells infected for the first time with SFV6-2SG-Nluc or BUNV-Nluc and to cells infected with the mutual control virus (control). Below the graph, results of RT-PCR for CFAV infection are added. Positive-tested samples are indicated with ‚+'. Means with SEM from three independent experiments conducted in triplicates are shown. * indicate significance by Student t-test (**** p ≤ 0.0001, *** p ≤ 0.001, ** p ≤ 0.01).*

A significant increase in viral replication was observed for some cell clones cured of SFV6-2SG-Nluc infection, namely SFV1, SFV3 and SFV5, while for samples SFV2, SFV4 a significant decrease in Nluc activity was detected. For SFV6 a slight reduction in viral replication was noted, which however was not significant (Figure 43 A).

For samples formerly infected, cured and re-infected with BUNV-Nluc, a strong decrease in Nluc activity was detected for samples BUNV2, 3, 4, 6 and BUNV8 suggesting an impaired viral replication in those cells. BUNV9 showed a slightly increased Nluc activity compared to control (Figure 43 B).

Strinkingly, in the samples where SFV6-2SG-Nluc replication was decreased after re-infection (SFV2, 4 or slightly 6) no CFAV infection could be detected. In contrast, cells with CFAV showed an increased luciferase activity after re-infection with SFV6-2SG-Nluc (Figure 43 A). For BUNV cell clones, this is reversed, although the increase of BUNV-Nluc in the absence of CFAV is rather small compared to SFV (Figure 43 B). It has to be noted that SFV has a positive-sense genome while BUNV is characterized by a negative-sense genome. Whether this hints towards a relation between arboviral replication and CFAV in infected cells remains to be investigated.

These results indicate, that for some cell cultures cleared from their persistent arboviral infection with SFV6-2SG-Nluc or BUNV-Nluc infection, a negative effect on a recurring virus infection is observable. This suggests some kind of acquired memory effect caused by the previous encounter with the same virus. Overall, the observed positive effect on virus replication seems to be stronger for replication of SFV6-2SG-Nluc rather than BUNV-Nluc, while negative effects are more pronounced in BUNV-Nluc infected cells.

4. Discussion

The exo-siRNA pathway is the main antiviral defense pathway in mosquitoes with Dcr2 and Ago2 having key roles [60, 123, 174, 249, 334, 335]. Although well characterized, similarities and differences among the different arboviruses related to the exo-siRNA pathway and infection characteristics still have to be revealed. Besides the exo-siRNA pathway, the piRNA pathway is intensively studied as a defense of germline cells against transposable elements in insects [215, 238, 336]. The discovery that the pathway is (i) also active in mosquito somatic tissues, (ii) has undergone an expansion in proteins and (iii) processes also viral RNA sources, has led to the suggestion that the mosquito piRNA pathway might have additional biological functions [220, 242]. Ongoing research has led to the implication of various processes involving the piRNA pathway in antiviral defense, especially in the vector mosquito *Ae. aegypti* [189, 193, 251, 254, 270]. The discovery of viral cDNA and non-retroviral integrations of RNA viruses in the host genome and vpiRNA production from these sites acting in an antiviral manner [194, 247, 258, 264], indicated that the pathway might confer adaptive and heritable immunity in mosquitoes as well. Nevertheless, also gene regulation and embryonic development were assigned as piRNA pathway functionalities, demonstrating the great versatility of this pathway [243, 249, 337-341]. Therefore, understanding the antiviral potential of the RNAi pathways is crucial, given that many human and animal pathogens such as DENV, ZIKV and RVFV are transmitted by vector mosquitoes.

4.1. Establishing Ago2 knockout cell lines: Aag2-AF525 and Aag2-AF519

Dcr2 and Ago2 are known proteins that facilitate the antiviral function of the exo-siRNA pathway. Silencing one of these key proteins during infection leads to an increase in viral replication for most tested arboviruses, including CHIKV, DENV and RVFV [190]. However, on occasion an increase in virus replication could only be reported following Dcr2, but not Ago2 knockdown, especially for flaviviruses like ZIKV [59]. Whether this was due to residual Ago2 activity following incomplete transient silencing of Ago2, or a lack of antiviral activity by the exo-siRNA pathway was unclear at this point.

To further assess the interplay of the exo-siRNA pathway and arboviral replication, a CRISPR/Cas9 based gene knockout approach was pursued leading to two Ago2 knockout cell lines, AF525 and AF519. Reporter-based silencing assays showed that both cell lines were not capable of gene silencing through the exo-siRNA pathway, independent of the inducer molecule.

Methylation is an important step during biogenesis of siRNAs. It establishes biological activity and stability of RNAs which originate from dicing by Dcr2 of viral double-stranded transcripts or endogenous sources, such as structured transcripts or transposons [163]. In *D. melanogaster*, siRNA methylation occurs in an Ago2-dependent manner [164]. Similar, Ago2 knockout in *Ae. aegypti*-derived cells, revealed a broad effect on the methylation of viral small RNAs. In Ago2 knockout cells, vsiRNAs and endo-siRNAs were no longer methylated, while vpiRNAs were hardly affected by the lack of Ago2. These results indicate that in *Ae. aegypti*-derived cell lines methylation of vsiRNAs as well as endo-siRNAs is dependent on Ago2.

Similar to SFV, more PCLV and CFAV specific small RNAs were detected in the Ago2 knockout cells compared to untreated controls. This suggests an antiviral activity of Ago2 not only for the acute infection of SFV, but also the persistent infection of CFAV and PCLV. However, vsiRNAs of persistently infecting viruses (CFAV, PCLV) showed an increase in treated AF5 cells, suggesting methylation and biological activity of the vast majority of vsiRNAs of PCLV and CFAV.

In contrast, the decrease of SFV-specific vsiRNAs in the same samples suggests for this acute virus infection, a lower percentage of SFV specific vsiRNAs being methylated and thereby biological active. Overall, more PCLV-specific vsiRNAs were detected in AF525 than AF5 cells. Whether this points towards Ago2-independent methylation of 21 nt long vsiRNAs of the S- and M-segment whilst vsiRNAs derived from the L-segment are methylated in an Ago2 dependent manner, remains elusive (suppl. data

Figure S6-S11). Additionally, the lower expression rate of the L-segment could have attributed to less dsRNA substrate. The amount of vpiRNAs mapping to CFAV and PCLV increased in treated AF525 cells and might be attributed to an increased viral replication of both viruses in the knockout cells.

4.2. Impairment of siRNA pathway key proteins benefits all tested arboviruses except ZIKV

Knocking out Ago2 or Dcr2 in *Ae. aegypti*-derived cell lines resulted in a strong enhancement of SFV replication for both reporter viruses, which is in accordance with knockdown studies [189, 249] (Figure 22). Thus, both key players of the siRNA pathway are clearly required to perform its antiviral function. Re-introducing Ago2 in the knockout cells led to a significant decrease of luciferase compared to control cells, showing that the positive effect on SFV infection was due to the lack of Ago2 in AF525 cells, similar to what was previously shown for Dcr2 in AF319 cells [249].

BUNV-Nluc infection, determined by expression of luciferase reporters, did benefit to similar extents from the lack of Dcr2 and Ago2, although the overall increase of luciferase was lower than for SFV. In contrast, viral titer of BUNV wild type (wt), revealed an increase for both knockout cell lines, but with a significantly higher viral titer in Dcr2 knockout cells especially throughout the persistent stage (~ 100-fold, passage 10 post infection). Of course, results are hardly comparable, as different parameters like the relative luciferase activity of the Nluc reporter virus and end point dilution assay for virus titers of BUNV wt virus were used. The production of Nluc reporter proteins indirectly reflects the virus replication and protein production, while a $TCID_{50}$ assay reflects the production of infectious particles, which can be differently regulated. The insertion of the Nluc reporter sequence, partly replacing the NSm coding sequence in the BUNV genome, might have led to effects impairing viral replication. The NSm protein was suggested to play a role in assembly and morphogenesis of BUNV, but it seems that NSm functionality is diverse related to different bunyaviruses [342-347]. Nevertheless, the different approaches demonstrate the antiviral role of Ago2 and Dcr2 during BUNV infection and indicate the importance of Dcr2 and its antiviral properties.

Compared to SFV and BUNV, results for ZIKV infection in Ago2 knockout cells are contradictory. Varjak *et al.* already confirmed a beneficial effect on ZIKV replication in Dcr2 knockout cells AF319, while viral titers were shown to be unaffected by a transient knockdown of Ago2 [59]. In addition to these findings, experiments in AF525 knockout cells used in this study, revealed no increase of ZIKV replication either and suggest no antiviral activity of Ago2 against ZIKV. Surprisingly, knockout in AF519 cells acts beneficial on ZIKV replication. It has to be noted, that AF519 cells were engineered with an early stop in one allele and an insertion in the other allele, most likely resulting in an altered version of Ago2.

As shown by others, replication increases for most mosquito-borne flaviviruses in *Ae. aegypti* or *D. melanogaster*, *in vitro* as well as *in vivo*, in the absence of an exo-siRNA response [172, 175, 334]. Moreover, previous studies observed the production of ZIKV-specific siRNAs in infected mosquito cells and increased ZIKV infection in the Dcr2 knockout cell line, supporting an antiviral activity of the exo-siRNA pathway [59, 195]. Possible explanations for the lack of an effect of Ago2 knockout in AF525 cells could be the inaccessibility of ZIKV RNA, the expression of an RNAi silencing suppressor by ZIKV or the compensation of Ago2 activity by another Argonaute protein. It is not known if another Argonaute protein, e.g., Ago1 of the miRNA pathway, in *Ae. aegypti* is able to compensate for Ago2 antiviral activity, although the results obtained from preceding Ago2 rescue experiments would suggest this is unlikely. As knockdown and knockout of Ago2 normally results in an increase of virus infection, this would be rather specific for ZIKV infection.

Various studies indicate a combination of separated replication sites to protect viral RNA intermediates passively from host cell antiviral mechanisms and active protection by suppressor functions of viral proteins [348-352] as even protected replication sites need to be connected to the cytosol. The fact that ZIKV-specific siRNAs are produced in infected cells and mosquitoes proves the accessibility of ZIKV

dsRNA at least for dicing by Dcr2. If the same is true for the accessibility of the active RISC is not known but can be expected. Dcr2 might act antiviral itself through the exo-siRNA pathway and might additionally induce other antiviral pathways, but either the transfer of siRNAs to the Ago2-RISC machinery or targeting and degradation by Ago2 is impaired or target of viral suppressors of RNAi (VSRs). For several medically important flaviviruses, the capsid protein has been reported to be a VSR, including DENV, yellow fever virus and ZIKV [349]. However, other studies of ZIKV capsid protein showed that the VSR activity is independent of the exo-siRNA pathway [59]; supporting the observed lack of Ago2 antiviral activity for ZIKV. In contrast to ZIKV, knockdown of Ago2 led to an increase in DENV (also a member of the *Flavivirus* genus) [172, 196], although the NS2A protein and capsid protein have recently been suggested to act as VSR [353], supporting the hypothesis that DENV2 is still susceptible to an antiviral RNAi response [172, 182].

In contrast to the findings in AF525 cells, it remains elusive how the incomplete Ago2 knockout in AF519 cells leads to an increase in viral RNA levels of ZIKV. Initial experiments to assess the silencing efficiency in both knockout cell lines revealed hardly any differences despite the incomplete knockout of Ago2, indicating that already lower amounts of Ago2 are sufficient for silencing activity. Whether the engineered insertion in one of the alleles might have caused unknown side effects needs further research. One should also consider, whether some functions of Ago2 are regulated via certain thresholds of the protein. Overall, the discrepancy of the two key siRNA pathway proteins Dcr2 and Ago2 and their ability to act antiviral on ZIKV therefore remains to be further investigated.

Taken together, SFV and BUNV replication both benefitted from the lack of exo-siRNA pathway proteins Dcr2 or Ago2 in both knockout cell lines. In contrast, ZIKV replication showed no significant increase upon Ago2 knockout in AF525 cells in contrast to Ago2 knockout cells AF519. The magnitude of the observed increase during Ago2 knockdown for different viruses can be very variable, which is most likely due to different experimental conditions, including the chosen MOI and methods used to assess the viral replication as well as differences in virus replication characteristics. Nevertheless, these findings are in accordance with previous publications, as variations in the importance of Ago2 antiviral activity between viruses have been suggested [59, 188, 249, 255, 334]. Increased replication in Dcr2 and Ago2 knockout cell lines is a main indicator for an antiviral role of the exo-siRNA pathway and its key proteins. Intriguingly, Dcr2 is able to recognize and cleave virus-derived dsRNA or to induce an alternative antiviral response, like the Vago protein, hence acting antiviral independently of Ago2, although the induction of Vago was recently doubted [103, 111, 112]. In turn, Ago2 has always been linked to the siRNA pathway and the incorporation of siRNAs, which are used as guide to cleave complementary viral RNA, with the exception of ZIKV.

4.3. Small RNA characteristics of SFV and BUNV infection reveal essential differences with regard to the RNAi response

A strong antiviral response against SFV and BUNV infection mediated by the key siRNA pathway proteins Dcr2 and Ago2 has already been described [188, 189, 249] and was confirmed by previous experiments. Besides the exo-siRNA pathway, also the piRNA pathway has moved into focus, after vpiRNA production was also reported in mosquitoes upon arboviral infection [60, 177, 184, 188, 189, 193, 242, 253-255, 257]. Although knowledge is constantly increasing, it becomes clearer that each arbovirus seems to own specific characteristics related to infection and the induction of the RNAi response. In order to identify similarities and differences, small RNA sequencing data of cells with an acute or persistent SFV or BUNV infection was evaluated with regard to changes in small RNA composition or RNAi protein function. In order to confirm the biological activity of the observed virus-derived small RNAs, RNAi sensor assays were used.

4.3.1. SFV

Sequencing of small RNAs in SFV-infected AF5 cells revealed that the overall number of vsiRNAs was high compared to vpiRNAs and slightly decreased towards the persistent phase of infection. This decline of vsiRNA production is most likely linked to a general reduction of viral replication during the later stages of infection for SFV [354] (Figure 24).

Regarding the distribution of vsiRNAs, an almost consistent mapping along the whole genome / anti-genome was observed at the onset of infection, but this pattern changed towards the persistent phase. Instead, an accumulation of vsiRNAs generated from a hotspot located around the 400 bp region close to the 5' end of the genome with a strong bias of vsiRNAs mapping to the anti-genomic strand was observed. It has to be noted that this hotspot region was already producing high numbers of vsiRNAs during the acute infection phase, but at the persistent stage, vsiRNA production is concentrated and highly increased mapping to this single region, which encodes for the nsP1 protein of SFV. nsP1 is a major component of the SFV replicase complex and involved in mRNA capping [355].

A similar hotspot for vsiRNA production at the acute stage of infection has been observed previously for SFV and SINV in Aag2 cells [243, 247, 255], but not for the alphavirus CHIKV [192]. Two independent reports were documenting a similar accumulation during both the acute and persistent FHV infection phase in *D. melanogaster* cells [145, 146]. Proposed reasons for such a vsiRNA accumulation were manifold, ranging from an inefficient replication initiation that causes an accumulation of dsRNA targets from this genome region for cleavage [170] or the expression of VSRs as a countermeasure that limits access of Dcr2 only to this hotspot [356]. In line with this, the B2 protein expressed by FHV was shown to prevent dsRNA from being cleaved by Dcr2 and sequesters vsiRNAs to protect it from further processing by Ago2 [357]. The same mechanism was lately discovered for the capsid protein of SFV and SINV [358]. This suggests, that SFV is able to protect replication intermediates from degradation by Dcr2 by actively sequestering dsRNA and vsiRNAs by the capsid protein, thus preventing the antiviral activity of the exo-siRNA pathway and possibly limiting vsiRNA production to a small sequence of the SFV genome.

Instead of blocking accessibility of Dcr2, it is likewise conceivable, that regulatory factors of the host cell or structural characteristics increase targeting by Dcr2 of this specific region in an unknown way or a combination of both mechanisms. As this region is still coding for the non-structural proteins it is rather unlikely that it is assigned as a decoy similar to what was proposed for the generation of subgenomic flaviviral RNA [359]. On the other hand, it was shown that vsiRNAs derived from hotspot regions were found to act poorly antiviral compared to vsiRNAs derived from other (cold-spot) regions [54]. Siu *et al.* suggested a nucleic acid-mediated RNAi decoy mechanism for these hotspots. However, another reason might be that the necessity to target the whole genome might become less critical during the persistent stage and targeting of this specific region might be sufficient to control the persistent infection.

In addition to the formation of a hotspot region during persistent SFV infection, the bias of vsiRNAs for the anti-genomic strand could indicate a preference for secondary structures forming dsRNA from the anti-genomic (antisense) strand. dsRNA replication intermediates as substrates for Dcr2 cleavage would rather result in a more evenly distribution of vsiRNAs from both strands of the genome. However, it was suggested by Siu *et al.* that generation of SFV-derived vsiRNAs during the acute infection phase is rather linked to dsRNA replication intermediates than secondary structures of the virus [54]. In addition to this, only a small amount of secondary RNA structures was predicted for the specific hotspot region [54], indicating that vsiRNAs derived from this region originate from dsRNA intermediates rather than secondary structures, leaving the reasons for the observed bias unclear.

Compared to vsiRNAs, the number of vpiRNAs stayed comparatively low, but possessed the typical U_1/A_{10} bias and 10 nt sequence overlap, characteristic for the ping-pong produced piRNAs. vpiRNAs were distributed along the whole genome of SFV to equal shares deriving from genomic and anti-genomic strands in early and persistent stage of infection. However, distinct hotspot regions for vpiRNA production were observed mapping to the region shortly downstream of the subgenomic promoter where

the capsid coding region is located. This is in line with previous findings for SFV and other alphaviruses [189, 193, 254]. Concluding, the overall pattern of vpiRNA distribution did not differ much and vpiRNA production was rather low compared to vsiRNAs.

In order to investigate, whether SFV-derived small RNAs were biologically active, sensor constructs were transfected in different cell lines (Figure 28). These sensor constructs were engineered to express viral sequences matching hot- or cold-spot regions of the viral genome. Experiments revealed hardly any biological activity of small RNAs either during acute or persistent phase of infection. A slight activity was observed for some reporter constructs in AF5 cells during the persistent infection phase. Although significant, it can not be ruled out if the observed effect can be attributed to the biological activity of vsiRNAs or vpiRNAs respectively, as AF5 cells are fully functional with regard to the exo-siRNA pathway. In AF319 cells with a dysfunctional Dcr2, one sensor construct revealed a slightly decreased luciferase activity for both target sequences in either sense or antisense orientation at the onset of infection, indicating the activity of vpiRNAs from the targeted region. Preceding experiments, characterizing AF525 as an Ago2-deficient knockout cell line, also provided the evidence by β-elimination assays, that the methylation of SFV-derived vsiRNAs strongly depends on Ago2 functionality to further facilitate an antiviral activity. Furthermore, vpiRNA production was shown to be independent from Ago2, which confirms that biological activity observed in AF319 or AF525 cells can only be attributed to the biological activity of vpiRNAs.

Taken together, these experiments and results document the importance of the exo-siRNA pathway as an antiviral defense against SFV infection. SFV-derived small RNAs were shown to exhibit biological activity to a low extent, although the exo-siRNA response is rather strong in SFV-infected mosquito cells. This correlates well with findings by Siu *et al.* that vsiRNAs derived from hotspot regions of the SFV genome have a poor biological activity and are less capable of targeting viral RNA in contrast to cold-spot vsiRNAs [54]. The concentration of vsiRNAs that are being produced mainly from a single hotspot region during the persistent stage, indicates a different regulation of SFV in this phase of infection and needs further investigation. Moreover, it was shown that although vpiRNA production is induced during SFV infection, these vpiRNAs only displayed a low biological activity during the acute phase of infection. Beyond these observations, several other studies already characterized the role of the piRNA pathway during SFV infection in more detail. Varjak *et al.* demonstrated the antiviral function of Piwi4 during SFV infection, but its knockdown had no effect on vpiRNA production [249]. In turn, silencing of Ago3 and Piwi5 did not enhance SFV replication either in AF319 or in Aag2 cells, but did impair vpiRNA production [189, 249, 251]. Together with the results obtained from this study it can be suggested that the exo-siRNA plays the major role in the antiviral defense against SFV, but that it is supported by the piRNA pathway, although the whole picture of the antiviral function of the piRNA pathway remains incomplete.

4.3.2. BUNV

In contrast to SFV, only little is known about the RNAi response against BUNV and other bunyaviruses. In order to characterize the early and persistent phase of BUNV infection in more detail, the virus production of BUNV wt was initially assessed together with the expression levels of different RNAi pathway proteins (Figure 30, 31). Determination of viral titers for BUNV wt infection in AF5, Dcr2 and Ago2 knockout cell lines revealed an overall increase of virus production in cells with an impaired siRNA pathway. Interestingly, lack of Dcr2 benefitted the production of infectious viral particles more than the lack of Ago2. This effect was even more pronounced during persistent infection and would indicate an increasing importance of Dcr2 towards the persistent phase, although results were highly variable, reflecting natural variations of BUNV infection. Dcr2 might act antiviral itself by dicing viral RNA and induce other antiviral pathways like JAK-STAT via Vago [111, 112], although this possibility was lately disproven for Aag2 cells [103]. Moreover, the involvement of Dcr2 in the formation of vcDNA has been

suggested and the antiviral function of these molecules by producing small RNAs [194, 274]. It is conceivable that this mechanism contributes to the observed effect, strengthening the antiviral role of Dcr2.
Shielding the replication complex from the access of siRNA pathway proteins might be another reason for the observed effect. BUNV replication was shown to take place in tubular structures associated with the Golgi in mammalian cells, protecting viral RNA intermediates passively from the host cell antiviral response [343]. The fact that BUNV-specific vsiRNAs are produced in infected cells proves the accessibility of BUNV dsRNA at least for dicing by Dcr2. Whether the produced vsiRNAs can be loaded onto Ago2 as part of the RISC is not known. However, the initial results suggest the antiviral role of the exo-siRNA pathway and functionality of its key proteins in both, acute and persistent infection of BUNV and indicate an extended role of Dcr2 for the antiviral defense in the persistent infection phase.

During infection, viruses not only seize the host cell metabolism or alter host cell structures to set up their replication factories for the production of new virions, they also influence the expression of a wide range of genes including those that are involved in the antiviral defense. In turn, the host cell regulates various factors and proteins in response to the infection likewise. To assess, how RNAi key proteins are regulated during the course of BUNV infection, their expression levels were determined via qPCR.

The expression pattern of siRNA and piRNA pathway proteins was very similar with regard to acute or persistent infection phase. While Dcr2 and Ago2 were downregulated during acute infection and to a lesser extent in persistent infection, Ago3, Piwi4 and Piwi5 as piRNA pathway proteins were upregulated with the strongest effect observed for Piwi4 in both infection stages. Most likely, VSRs are responsible for the repression of Dcr2 and Ago2 expression trying to suppress their antiviral function as shown for the SFV capsid protein in mammalian cells [358]. Upregulation of PIWI proteins, might be linked to the antiviral function of the piRNA pathway and in particular Piwi4, documented for BUNV and other viruses [59, 177, 188, 189, 249, 255]. Elevated expression levels for Piwi4, Ago2 and Ago3 as well as decreased levels for Piwi5 were documented for SINV infection in Aag2 cells [247], demonstrating the differential regulation of RNAi proteins at the transcriptional level upon arbovirus infection. Although effects on the transcriptional level are visible during BUNV infection, they do not provide an explanation for the observed differences in virus production in Dcr2 and Ago2 knockout cells.

In order to assess whether the small RNAs predominantly produced from the S- and M-segments during BUNV infection are biologically active, sensor construct assays were performed (Figure 29). Results showed that a biological activity of small RNAs was detected in AF5 cells already at the onset of infection, whereas no significant activity was observed either in Dcr2 or in Ago2 knockout cells at 24 hpt, suggesting that mainly vsiRNAs are responsible for the observed effect. In contrast, reporter activity was significantly decreased for almost all reporter constructs in all cell lines in the persistent infection, indicating an increased biological activity of both, vsiRNAs and vpiRNAs. Taken together, with the observed increase of vpiRNA production during the persistent phase of BUNV infection, it seems that vpiRNAs are becoming highly active during the later stages of infection and are loaded into piRISCs, enabling them to target and degrade the cognate sequences cloned into the sensor constructs, thereby confirming their biological activity.

Additionally, it seems that sensor constructs with a sense (anti-genomic) sequence of the viral RNA exhibit a stronger degradation effect on target viral RNA sequences. Preceding experiments with BUNV-infected cells showed a clear bias towards the production of anti-genomic (sense) vpiRNAs. Therefore, it is conceivable, that although present in high amounts, these anti-genomic vpiRNAs might be less biologically active than genomic ones. Why a biological activity was not detected for the other SFV and BUNV sensor constructs of either sense or antisense orientation might be due to choosing the wrong target sequence or a low production of virus-derived small RNAs that fail to trigger a visible effect on luciferase activity. Moreover, it has to be considered, that transfection efficiency is rather low in mosquito cells, which can conceal a weak luciferase signal. For some of the transfected constructs even an increase of luciferase activity was observed compared to controls encoding for eGFP. Whether this is due to some unknown regulation of expressed sequences or elevated translation of the reporter protein

remains elusive. In summary, it was shown that BUNV-derived vpiRNAs and vsiRNAs are able to target homologous RNA sequences and are incorporated into their specific RISC, thus demonstrating their biological functionality especially during the persistent stage of infection.

Small RNA sequencing of silenced cells reveals differences between acute and persistent BUNV infection

To shed more light on the characteristics of BUNV infection with regard to small RNA composition and the role of RNAi proteins in their biogenesis during the course of infection, small RNA sequencing was performed for various samples. Small RNAs from either fully functional AF5 cells infected with BUNV, but also from infected Dcr2 and Ago2 knockout cell lines were analysed (Figure 25). In addition, small RNA characteristics from AF5 cells transfected with dsRNA targeting Ago3 and Piwi5 in combination were determined (Figure 33). Overall, sequencing of BUNV small RNAs revealed the production of vsiRNAs and vpiRNAs in all functional and knockout cell lines and throughout both stages of infection for all three genomic segments of BUNV. Throughout onset and persistent infection phase, vpiRNAs displayed the characteristic U_1/A_{10} bias and 10 nt sequence overlap.

The profile of vsiRNAs showed a large degree of similarity between early and persistent infection phase with regard to genome distribution. vsiRNAs covered the whole genome, mapping in equal shares to each strand in all tested cell lines. The amount of BUNV vsiRNAs was small in AF319 cells in both stages of infection, most likely caused by the lack of Dcr2. Compared to the amount of BUNV vsiRNAs in AF5 and AF319 cells, vsiRNA amount highly increased in Ago2 knockout cells as well as in Ago2-silenced cells compared to controls. This effect is most likely caused by the increased viral replication that was already shown for BUNV wt in this study and the accumulation of vsiRNAs that are not further processed by the siRISC. Results indicate, that Dcr2-dependent dicing accounts for the majority of generated 21 nt vsiRNAs, which is in line with earlier findings for BUNV [188] and RVFV in Aag2 cells [177, 184]. No major changes in vsiRNA production were observed comparing acute and persistent phase of infection, indicating that BUNV infection is not regulated differently with regard to vsiRNA production.

During SFV infection the predominant species of small RNAs were vsiRNAs, clearly outnumbering vpiRNAs. In the case of BUNV, vsiRNAs and vpiRNAs are produced to rather equal amounts during the acute infection phase in AF5 cells with slightly increased levels observed for vpiRNAs in AF319 cells. It is conceivable that the vpiRNA production benefits from increased viral RNA levels, producing more vpiRNAs. Contributing to this, it has been shown for various viruses from different families that vpiRNA production is Dcr2-independent [189, 196, 247, 249, 251, 255].

Lacking Ago2 in either knockout or silenced cells, has contradictory effects on the small RNA composition. While the amount of vpiRNAs increases in the Ago2 knockout cells in the acute infection phase, vpiRNA production remains unchanged in dsAgo2-transfected knockdown cells. An increase of vpiRNAs in response to a higher availability of viral RNA caused by the increased viral replication due to the Ago2 knockdown seems most likely. It has to be noted, that both small RNA sequencing results are based on single runs, which increases the possibility of natural variation at the time point of RNA isolation in the cells. Moreover, the experiments differ in the used methods as one was performed in knockout cells and the other in transiently silenced cells. Probably, biological variations are the cause of the varying results and further sequencing runs are needed to confirm the observed effects. In the persistent infection, silencing of Ago2 was not successful, although the same dsRNA aliquot was used for both, acutely or persistently infected cells.

Looking at the persistent infection, small RNA distribution is changing. In contrast to the acute stage of BUNV infection, vpiRNAs become the prominent small RNA species in the persistent stage, clearly outnumbering the production of vsiRNAs. Especially vpiRNAs mapping to the S-segment of BUNV are highly increased in AF5 cells, but decrease in AF319 and AF525 cells, although virus production was

shown to be increased. These findings correlate well with the observed higher biological activity of BUNV sensor constructs discussed earlier and indicate an increasing importance for the piRNA pathway during the persistent infection stage. For RVFV the same shifting effect was observed towards an increased vpiRNA production in the persistent infection phase and linked to the establishment of a combined antiviral response mediated by both the siRNA and the piRNA pathway in Aag2 cells [184]. Nevertheless, previous experiments have shown, that both Dcr2 and Ago2 are highly efficient in restricting SFV or BUNV virus growth. Furthermore, experiments showed that the piRNA pathway alone was not able to compensate and to establish an effective antiviral response upon SFV or BUNV infection. However, the suspicion is increasing, that siRNA and piRNA pathway are differentially controlled during the course of BUNV infection and that a shift from a siRNA-mediated antiviral response during early infection, is followed by a piRNA-mediated response being dominant throughout the persistent phase. Hence, the piRNA pathway might be responsible for the establishment of a persistent state of infection in mosquitoes rather than fighting an acute infection thereby shaping vector competence.

A clear favouring of the S-segment was observed for BUNV small RNAs in the acute phase for all cell lines tested, independent of the mode of silencing. This is in accordance with previous findings for BUNV [188]. For RVFV it was shown that the S-segment is the most abundant segment with a ratio of 1:3:13 (L-, M-, S-segment) during infection, at least in mammalian cells [360]. In contrast, Dietrich *et al.* observed an overrepresentation of the M-segment in RVFV-infected mosquitoes and derived cell lines [177]. Preponderance of vsiRNAs and vpiRNAs mapping to the S-segment indicates an important target region that might be easily accessible for Dcr2 as well as for several piRNA pathway proteins like Ago3 and Piwi5 or Piwi6, suggesting them to be involved in vpiRNA biogenesis. As the N and NSs protein are encoded by overlapping reading frames in the S-segment [361], the occurrence of dsRNA replication intermediates is suggested to be rather high next to the occurrence of panhandle structures formed by 3’ and 5’ non-coding regions of each BUNV segment [362]. The N protein is a multifunctional protein that encapsidates the negative-sense genome segments to form ribonucleoprotein complexes but also interacts with the RdRp, while the NSs protein is suggested to contribute to viral pathogenesis [362-364]. Therefore, it is facilitating various functions and might be an attractive target for antiviral responses in order to control viral replication.

Besides, a preference for the production of vpiRNAs mapping to the anti-genome of BUNV is observed in contrast to vsiRNAs, which derive mainly from both strands equally. This is especially noticeable for the highly abundant S-segment. Reports on the different quantities of genome strands occurring during infection of BUNV are currently lacking, but for RVFV it was shown that more genome (antisense) RNA is present during replication than anti-genome RNA [365]. However, a preference for the production of anti-genome derived vpiRNAs was also observed by other researchers: for the BUNV S- and M-segment in infected Aag2 cells, for all three segments of LACV (*Bunyaviridae*) in C6/36 cells (*Ae. albopictus*, Dcr2-deficient) and for the S-segment of RVFV in different mosquito cells [60, 177, 184, 188, 254]. It can be expected that anti-genomic (sense) viral mRNAs are more accessible to RNAi pathway proteins in the cytoplasm rather than encapsidated ribonucleoparticles suggesting them as the main source for virus-derived small RNAs. However, this is in contrast to the observation that BUNV sensor constructs expressing sense (anti-genomic) sequences of BUNV have a slightly higher biological activity compared to antisense sensor constructs. Similar to SFV, it might be that a higher abundance is not indicative of the actual biological activity of the specific vpiRNAs.

Ago3 and Piwi5 are acting antiviral during BUNV infection and facilitate vpiRNA biogenesis

While the role of the exo-siRNA pathway as the major antiviral defense mechanism is well established, the role of PIWI proteins remains enigmatic and above all variable. Previous studies indicated the induction of the piRNA pathway upon infection with SFV and that knockdown of PIWI proteins enhances viral replication and impairs vpiRNA production. More specifically, it was shown that the production of SFV-specific vpiRNAs depends on Ago3 and Piwi5 and to a lesser extent on Piwi6 [189, 249, 255]. Still, some aspects of the functional scope of PIWI proteins seem to be highly virus-specific. Preceding experiments and results indicated the up-regulation of piRNA pathway protein expression in both stages of infection. Besides, vpiRNAs were shown to be produced in high amounts and to display a strong biological activity especially in the persistent infection stage. Taken together, this might be crucial for the control or establishment of a persistent BUNV infection. In order to investigate these aspects, the functionalities of Ago3 and Piwi5 were studied in more detail by silencing these proteins in AF5 cells (Figure 33, suppl. data Figure S15).

Knockdown of either single Ago3, Piwi5 or in combination resulted in an overall increased virus production during the acute infection phase, suggesting that both proteins contribute equally to the antiviral effect. Antiviral activity during the persistent phase was only seen for Piwi5 alone or in combination with Ago3, but not with Ago3 alone, indicating an antiviral role only for Piwi5. The results strengthen the idea of a differently regulated RNAi response during persistent BUNV infection. Reports of other researchers for different arboviruses present an ambiguous picture: positive effects on virus production were observed in Ago3-silenced cells infected with RVFV or CFAV and in Piwi5-silenced cells infected with BUNV at the onset of infection [177, 188, 247]. However, Dietrich *et al.* observed that upon Ago3 knockdown viral replication of BUNV was decreasing, suggesting a pro-viral effect for Ago3, which is in contrast to findings of this study. Nevertheless, it has to be noted that the experimental setup of their study highly differs related to chosen MOI and method for assessment of viral replication. Negative effects on ZIKV and SBV infection were documented upon knockdown of Ago3 and Piwi5 respectively, indicating a rather pro-viral function of these proteins for specific viruses [59]. In turn, no changes related to viral replication were observed for CHIKV and SFV (both alphaviruses) upon knockdown of both proteins [59, 255]. This is in line with the observations of this study that vpiRNA production is comparatively low during SFV infection and that mainly vsiRNAs are biologically active and presumably responsible for the antiviral activity of the RNAi response. These recent findings highlight the high variability in antiviral function of piRNA pathway proteins with regard to the specific virus species.

Analysis of BUNV small RNA composition showed that vsiRNA production benefitted from the lack of Ago3 and Piwi5 in the acute stage of infection but not during the persistent phase. The most obvious explanation for this increase is provided by the enhanced virus production in consequence of the lack of Ago3 and Piwi5. Still, it is remarkable, that vsiRNAs exhibit a ping-pong bias, usually characteristic for piRNAs. Several studies suggested an interplay of the exo-siRNA and piRNA pathway that might compensate for the loss of vpiRNAs in this case by increasing vsiRNA production. Recent studies by Tassetto *et al.* showed that knockdown of Piwi4 led to the loss of both, vsiRNAs and vpiRNAs in SINV-infected cells [247]. In addition, Varjak *et al.* showed that Ago2 and Piwi4 interact. Moreover, they could also show that Piwi4 also interacts with Ago3, Piwi5 and Piwi6 and that the knockout of Dcr2 leads to the increased production of vpiRNAs in SFV-infected AF319 cells [249]. It is conceivable, that the excess of vsiRNAs in Ago3/Piwi5 silenced cells and the noticeable U_1/A_{10} bias of 21 nt long vsiRNAs might be the result of an interplay between the siRNA and piRNA pathway, compensating for the loss of vpiRNA production. Further efforts are needed to determine whether these specific small RNAs are either shorter, 21 nt long vpiRNAs or if crosstalk between the two RNAi pathways causes this effect and produces vsiRNAs with a ping-pong signature.

Silencing of Ago3 and Piwi5 resulted in a decrease of vpiRNAs for both strands of the genome during the acute stage, demonstrating the involvement of these proteins in vpiRNA biogenesis. Notably, while the amount of vpiRNAs derived from the genomic (antisense) strand normalized in Ago3/Piwi5 silenced

cells to the level of dseGFP-transfected control cells during persistent stage, anti-genomic (sense) vpiRNAs did not recover and stayed low. In general, it was shown, that vpiRNAs deriving from the anti-genome are mainly associated with Piwi5 while Ago3-bound vpiRNAs often derive from the genomic strand as a consequence of being processed by the ping-pong amplification cycle [251, 337]. The observed preponderance of anti-genomic (sense) vpiRNAs might be a result of Zuc-mediated vpiRNA biogenesis that was lately proposed by Joosten *et al.* and others to be active in mosquitoes, similar to the model described for *Drosophila [212, 213, 248, 366]*. It was reported, that both strands of the positive-sense SINV were targets of Zuc-mediated cleavage and that in addition also negative-sense RNA viruses like PCLV are targeted by Zuc-like vpiRNA biogenesis [248]. In connection with these findings, a strong interaction between Zuc and Piwi5 in Aag2 cells and with the orthologue Aub in *D. melanogaster* has been described, while no interaction with Ago3 was observed [248]. Experiments and results indicate the antiviral role of Piwi5 and the need for Ago3 and Piwi5 for vpiRNA biogenesis during BUNV infection. Zuc-mediated processing might be an explanation for the accumulation of mainly anti-genomic vpiRNAs, while the ping-pong amplification loop, involving Ago3, contributes to the generation of vpiRNAs from both genome strands. To date, the formation of viral cDNA has not been assessed for BUNV infection, but it was shown that vcDNA molecules produce vsiRNAs and vpiRNAs [194, 274] that might as well contribute to the accumulation of vpiRNAs in BUNV infected cells.

Interestingly, the bias for anti-genomic vpiRNAs seems to increase depending on the overall amount of vpiRNAs produced from each genome segment of BUNV, while the amount of genomic vpiRNAs stayed comparably low throughout the whole course of infection. Numbers of vpiRNAs mapping to the S-segment were found to be very high with a strong bias for vpiRNAs deriving from the anti-genomic strand, while vpiRNAs mapping to the M- and L-segment were rather low with a less pronounced bias towards anti-genomic vpiRNAs. Possibly, the contribution of Zuc-mediated vpiRNA biogenesis correlates positively to the abundance of each genome segment of BUNV during infection. It is questionable, whether the high amounts of anti-genomic vpiRNAs produced are not loaded onto piRISCs and are just accumulating in the cells as a result of Zuc-mediated cleavage that might already be sufficient to control BUNV replication. Results for FHV have already shown that not all vsiRNAs are loaded onto Ago2 during the persistent phase of infection [146] and for SFV it was shown that vsiRNAs from hotspot regions are less biologically active compared to cold-spot vsiRNAs [54]. A similar effect might therefore be conceivable for BUNV vpiRNAs as well.

Besides the key RNAi proteins, other factors and proteins might contribute to the antiviral defense in mosquitoes and facilitate RNAi pathway functionality. The role of viral suppressors of RNAi, auxiliary factors and proteins and regulators of gene expression is poorly understood. In *D. melanogaster* and other model organisms, Tudor proteins containing a TUDOR-domain were shown to facilitate vpiRNA production [337]. Knockdown of several Tudor genes in *Ae. aegypti* resulted in a significant decrease of vpiRNA levels. One of the tested proteins called Veneno, directly interacts with Ago3. Other interaction partners of this protein were shown to interact with Piwi5 hinting towards a multi-protein complex that facilitates ping-pong amplification of vpiRNAs by guiding diverse RNA substrates into distinct piRISCs. Just recently, two newly disovered interactors of PIWI proteins, Atari and Pasilla, were discovered and linked to piRNA biogenesis, with Atari providing a scaffold for Ago3 during piRNA amplification [338]. The lack of Ago3 and Piwi5 as interaction partners for these protein complexes might have contributed to the observed effects on vpiRNA biogenesis and virus production. In addition to well-known immune pathways like JAK-STAT or the Toll and Imd pathways, other proteins were lately suggested to carry out antiviral functions, interacting with key proteins of the siRNA and piRNA pathway, but are sometimes acting independently, like the aBravo protein in *Aedes* [305]. Moreover, the knowledge about regulatory processes controlling siRNA or piRNA pathway effector proteins during infection is hardly investigated. Understanding the network and the interplay of small RNAs, pathway proteins and regulatory factors adds to functional insights into the antiviral response in mosquitoes. This was shown recently by McFarlane *et al.*, uncovering the regulatory and antiviral function of the *Drosophila* Domino orthologue p400, which was shown to regulate activity of the siRNA pathway and expression of Ago2 in *Ae. aegypti* mosquitoes *[367]*. Spellberg *et al.* showed that the transcription factor FOXO in *Drosophila* was found

to regulate the expression of core RNAi pathway proteins in response to viral infection, enhancing Ago2 and Dcr2 transcription [368]. This indicates the need for further studies on interaction partners and their regulatory and antiviral functions.

Comparing characteristics of SFV and BUNV infection, the recent findings suggest, that arbovirus infection is controlled in varying ways related to the RNAi response in mosquitoes. Moreover, the piRNA pathway contributes to the antiviral immunity in mosquitoes and plays a distinct role during BUNV infection. Unfortunately, reports about persistent arbovirus infections are scarce, although the findings of this study suggest that time is a factor that can not be ignored and further research is needed to better understand these matters.

4.4. Control of a recurring infection is enhanced in cells previously cleared of the virus

The recent discovery of vcDNA and NIRVS formation upon infection in *D. melanogaster* and vector mosquitoes has led to the hypothesis that these integrated viral sequences might confer an adaptive and heritable immunity in mosquitoes [194, 247, 297]. To date, the majority of NIRVS are related to ISVs and only little evidence of arbovirus integrations has been documented so far. Most of these viral sequences were found to be fragmented and resemble defective viral particles [297]. Nevertheless, the production of vpiRNAs from these elements was documented and newest findings support their role in an adaptive antiviral defense mechanism [194, 247, 264, 275].

Trying to reproduce a recurring viral encounter and to assess the potential availability of an adaptive immune response, cells persistently infected with SFV and BUNV were cleared from viral infection through the use of dsRNA targeting the particular virus genome. Prepared single cell clones from treated cells were then challenged again with the same virus and effects on viral replication were determined (Figure 43).

Results obtained from the re-infection experiment showed an either increased or decreased viral replication for cells encountering SFV6-2SG-Nluc for the second time, with a significant difference to the control cells. Suprisingly, as all cell clones were tested negative for SFV replication after treatment, the outcome of a second encounter with SFV is highly variable. In cells that were challenged with a BUNV infection for the second time, almost all cell clones were able to significantly reduce viral replication compared to the control cells that were infected only once with the virus.

Preceding experiments already demonstrated the mounting of an effective antiviral response in AF5 cells and the production of vsiRNAs and vpiRNAs during SFV or BUNV infection. Moreover, the antiviral role of the piRNA pathway was demonstrated for both viruses either in this study or reported by others [188, 249, 255]. According to the common hypothesis, the formation of virus-derived cDNA forms has been reported for a variety of arboviruses in *Aedes* mosquitoes and derived cell lines, but not for SFV or BUNV to date [233, 261]. Several reports exist, which suggest that these vcDNA forms confer an adaptive long-term immunity involving the piRNA pathway. In line with this, Mondotte *et al.* recently demonstrated the inheritance of vcDNA, conferring an adaptive immunity in the mosquito offspring and suggested that this mechanism is Dcr2-independent in *Drosophila* [275]. Related to the experiments of this study, Leger *et al.* super-infected several mosquito cell lines with a different strain of RVFV and observed a drastically inhibited replication of the super-infecting virus in Dcr2-deficient C6/36 cells [184]. In addition, abolishing vcDNA molecules using a reverse transcriptase inhibitor, led to decreased fitness of the infected host [194, 274]. To date, nothing is known about the induction and regulation of viral cDNA formation or the integration of viral sequences into the host genome and whether vcDNA is present as episomes in the host cell. vcDNA forms can be detected shortly after the onset of infection and were suggested to be a precursor of NIRVS. SINV-derived vcDNA forms were detected in fruit flies already 24 hpi and were maintained for up to 2 weeks post infection. In *Ae. albopictus*-derived cell lines,

CHIKV-derived vcDNA was detected already after 6 hpi and in *Ae. aegypti*-derived Aag2 cells after 12 hpi [194, 274]. The fast induction of the formation of vcDNA molecules in mosquito cells contributes to the hypothesis that the formation of vcDNA is an almost immediate response to arbovirus infection, possibly granting its functionality over a long time. However, it is conceivable, that the generation of vcDNA forms might be a reason for the observed effects in the different cell clones, possibly mediated by the piRNA pathway.

Several reports confirmed the antiviral activity of vpiRNAs derived from viral integrations in the mosquito genome related to ISVs [194, 247, 264, 275]. However, ISVs are suggested to be mainly transmitted vertically in contrast to horizontally transmitted arboviruses [298, 369]. Therefore, it remains uncertain whether an adaptive immunity associated with the piRNA pathway, that already protects the genome from invading transposable elements, is more reasonable for the protection against ISVs than against arboviruses. The discovery of at least several CFAV-related NIRVS in the *Aedes* genome, conferring antiviral immunity, further supports this theory [247, 264]. Nevertheless, orthobunyaviruses like LACV were reported to have a higher vertical transmission efficiency compared to alpha- and flaviviruses [369]. This increases the possibility of an antiviral defense based on NIRVS against BUNV and correlates well with the strong inhibition of a recurring BUNV infection demonstrated by the initial experiments.

Coincidently checking for the presence of persistently infecting CFAV in the treated cell clones, viral RNA was detected in some of the cell cultures, indicating an active replication of CFAV. It seems that while cell cultures were cleared from SFV or BUNV infection, in some cases they were also cleared of CFAV infection. Moreover, in cell cultures persistently infected with CFAV, SFV replication was found to be enhanced and seemed to correlate positively with CFAV presence. Conversely, in cell cultures cleared from BUNV infection, CFAV infection did not exhibit strong effects on the viral replication during the second encounter, but nevertheless also seemed to slightly correlate. In this case, slight effects seemed to be rather negatively correlated with regard to CFAV presence compared to cell cultures cleared of SFV infection. How a persistent CFAV infection might have affected the observed results in the end, remains to be determined. Recent studies suggested that ISVs can interfere with arbovirus replication, but this was not shown for *Ae. aegypti*-derived cell lines so far [370, 371].

However, there may be additional, as of yet unidentified, signalling components or host cell and viral factors that contribute to the JAK-STAT or RNAi pathways or are acting proviral during a recurring infection. Although formation of vcDNA or the integration of viral sequences has not been assessed for SFV or BUNV until today, it is a possible explanation for the acquired adaptive immunity of treated cells. It is reasonable that virus-derived cDNA forms enable the treated cells to control a second infection more efficiently. Possibly, the piRNA pathway is currently just evolving and expanding to other virus families as a concept of adaptive immunity in mosquitoes. Perhaps, the selection of single cell clones from the healed cell colonies might have accidently picked cells that are less susceptible to SFV or BUNV infection, inducing a poor infection rate. However, next steps would include the optimization of re-infection experiments with regard to persistent CFAV infection, investigation on the formation of vcDNA forms and integration of NIRVS and the production of small RNAs from these sequences using small RNA and whole genome sequencing of promising cell clones. It is also conceivable to repeat re-infection experiments in the available AF319 or AF525 knockout cell line to study observed effects without the siRNA pathway interfering.

4.5. Conclusion and outlook

The various interactions between arboviruses and vector mosquitoes are poorly understood until today. Although the siRNA pathway is under constant investigation, knowledge about the piRNA pathway is still lacking and rather scarce. This study provides exciting new knowledge and adds key insights into the RNAi response upon arbovirus infection related to the exo-siRNA and piRNA pathway. Characteristics of acute and persistent infection were described as well as the functionality of key proteins from both pathways. Moreover, the hypothesis that vpiRNAs are biologically active and the antiviral activity of the piRNA pathway in mosquitoes were confirmed for selected arboviruses. More research is needed on the adaptive immunity recently observed in the cured cell clones, but first results deliver promising hints and new insights.

Two Ago2-deficient *Ae. aegypti* cell lines were characterized and used together with an already established Dcr2 knockout cell line [59] to determine the importance of both proteins in the antiviral siRNA response against different arboviruses together with Ago2 dependency to siRNA methylation. Loss of Ago2 resulted in the lack of methylation of siRNA molecules of different origins, including exogenous virus, persistent viruses, TE-derived and transcriptome derived RNAs. SFV and BUNV replication both benefitted from the lack of exo-siRNA pathway proteins. In contrast, ZIKV replication showed contradictory results. While Ago2 knockout in AF525 cells did not benefit ZIKV replication, knockout in AF519 cells was rather beneficial and indicated the need for further studies on the RNAi response against ZIKV. Overall, Ago2 knockout cell lines thus provide a useful tool to study the impact of this protein on specific viruses and could also be used to investigate Ago2 functions further.

In additional experiments the antiviral response to SFV and BUNV infection with regard to the induction of the exo-siRNA and piRNA pathway and associated small RNA characteristics were assessed. Results reflect the differential RNAi response towards specific viruses. During SFV infection, the host cell relies merely on the exo-siRNA pathway as antiviral defense. Conversely, vpiRNAs produced during BUNV infection are biologically active especially during persistent infection and rely on Ago3 and Piwi5 for their biogenesis in the ping-pong amplification cycle. A remarkable shift from a balanced vsiRNA and vpiRNA production at the onset of infection towards a highly increased vpiRNA production in the persistent stage was observed for BUNV, indicating a growing significance of the piRNA pathway towards the later stages of infection. In addition, the expression of piRNA pathway proteins was found to be upregulated during the course of infection. The results document the joint antiviral activity of Ago3 and Piwi5 at the onset of infection, while Piwi5 alone is responsible for the control of a BUNV infection during the persistent infection phase. Finally investigating the effect of a recurring infection in cells cleared from either SFV or BUNV, hinted towards the acquisition of an adaptive antiviral immunity leading to a more efficient control of the repeated infection with an already known virus.

Overall, this study suggests that the piRNA pathway can be part of the antiviral countermeasures in mosquitoes next to the efficacious siRNA pathway. It provides new mechanistic insights into the antiviral defense in mosquitoes in response to various arbovirus infections and gives clues to how different RNAi proteins interact and control viral infection as well as their role in vpiRNA production. This study shows how highly variable the RNAi response is regulated regarding the acute and persistent phase of arbovirus infection. Moreover, the antiviral response to arboviruses does not only seem to vary between different arbovirus families, but already between single virus species of the same family. This work demonstrates the need for continuous research on the piRNA pathway and its antiviral function to provide new approaches to antiviral measures against arboviruses.

Nevertheless, regulatory factors within the piRNA pathway remain largely unclear as well as the prerequisites for the formation of viral cDNA and the ability to induce an adaptive immune memory. Perhaps, in depth analysis of RNAi protein interactions and determination of further regulatory mechanisms might elicit a more detailed picture on virus-host interactions and their determinants with regard to the piRNA pathway as an additional line of defense.

Multi-omics studies of viruses from different families could help to identify the interactome of arboviruses and their influence on the transcriptome or proteome of the vector host to investigate related mechanisms and similarities in response to infection. Especially the role of Piwi4 is still enigmatic. It was shown that knockdown of Piwi4 acts antiviral and interacts with the siRNA pathway [247, 249, 255], but how this function is facilitated remains unclear. Interactome studies using methods like cross-linking immunoprecipitation-high-throughput sequencing (CLIP-seq) might reveal aspects of the interplay between the siRNA and piRNA pathway as recently suggested [247, 249, 372]. In light of *Ae. aegypti* and *Ae. albopictus*, it would be interesting to assess the production of vpiRNAs in other vector mosquitoes as well and to determine the dependency of vpiRNA production on specific PIWI proteins in these vectors. So far, vpiRNA production in the important vector *Culex quinquefasciatus* has seldom been documented, although its PIWI proteins have undergone an evolutionary expansion as well [267, 269].

Cell culture systems faithfully represent essential aspects of virus-vector interactions and can provide preliminary evidence. Of course, results obtained from *in vitro* experiments of this study should be verified *in vivo* in a next step to confirm the recent findings.

Regarding the hypothesis of an adaptive immunity in mosquitoes, further experiments should be performed using the cell clones that were cured from either SFV or BUNV infection. The initial results raise many questions related to ISV-specific interactions with arbovirus infection and the details of the mechanism that facilitated the suggested acquisition of an adaptive immunity remain unclear. It should be determined whether the formation of viral cDNA can be observed in the treated cells that might produce antiviral vpiRNAs. Several re-infection experiments are conceivable with ISVs or arboviruses from different families, determining effects on infection. Moreover, it would be interesting to produce a new cell line using CRISPR/Cas9 that harbours a viral sequence originating from an arbovirus and to assess small RNA production from this integrated sequence and its impact on an incoming infection with the original virus. This could help determine the effects of superinfection as they were described previously for some arboviruses and ISVs [184, 298]. ISVs were suggested to be used as viral agents to control vectorial capacity of arboviruses resulting in decreased infections thereby reducing the public health burden, similar to the approaches using *Wolbachia* [67, 71, 96].

Different reports have documented a high variety related to the RNA-mediated antiviral response in different insects [257] and more insights are needed to ensure that virus- or host-specific side effects do not counteract efforts to control infection or vector populations. Engineering genetically modified mosquitoes has been an approach that was taken by different research groups and is already being successful in the control of vector populations as shown for the modified OX513A variant of *Ae. aegypti* that is used in Brazil currently [74]. Progress has also been made to engineer insects that are more resistant or less susceptible towards arbovirus infections [373-376]. Understanding the virus-host interactions and especially the RNAi response is crucial to ensure the success of such approaches. Determining similarities of the virus-host interactions could also lead to a broader approach in finding antiviral measures as a central point of action.

5. References

1. Bandea, C., *The Origin and Evolution of Viruses as Molecular Organisms.* Nature Precedings, 2009.
2. Mokili, J.L., F. Rohwer, and B.E. Dutilh, *Metagenomics and future perspectives in virus discovery.* Curr Opin Virol, 2012. **2**(1): p. 63-77.
3. Hendrix, R.W., et al., *Evolutionary relationships among diverse bacteriophages and prophages: All the world's a phage.* Proceedings of the National Academy of Sciences, 1999. **96**(5): p. 2192-2197.
4. Xu, P., et al., *Virus infection improves drought tolerance.* New Phytol, 2008. **180**(4): p. 911-21.
5. Bhattarai, N. and J.T. Stapleton, *GB virus C: the good boy virus?* Trends Microbiol, 2012. **20**(3): p. 124-30.
6. Virgin, H.W., *The virome in mammalian physiology and disease.* Cell, 2014. **157**(1): p. 142-50.
7. Gould, E., et al., *Emerging arboviruses: Why today?* One Health, 2017. **4**: p. 1-13.
8. García-Sastre, A. and T.P. Endy, *Arboviruses*, in *Encyclopedia of Microbiology (Third Edition)*, M. Schaechter, Editor. 2009, Academic Press: Oxford. p. 313-321.
9. Venter, M., *Assessing the zoonotic potential of arboviruses of African origin.* Current Opinion in Virology, 2018. **28**: p. 74-84.
10. Manson, P., *On the Development of Filaria sanguinis hominis, and on the Mosquito considered as a Nurse*.* Zoological Journal of the Linnean Society, 2008. **14**(75): p. 304-311.
11. Finlay, C., *The Mosquito Hypothetically Considered as an Agent in the Transmission of Yellow Fever Poison.* The Yale journal of biology and medicine, 1937. **9**(6): p. 589-604.
12. Reed, W. and A. Agramonte, *Landmark article. Feb 16, 1901: The etiology of yellow fever. An additional note. By Walter Reed, Jas. Carroll and Aristides Agramonte.* Jama, 1983. **250**(5): p. 649-58.
13. Posen, H.J., et al., *Epidemiology of Zika virus, 1947-2007.* BMJ Glob Health, 2016. **1**(2): p. e000087.
14. Petersen, L.R., et al., *Zika Virus.* N Engl J Med, 2016. **374**(16): p. 1552-63.
15. Succo, T., et al., *Autochthonous dengue outbreak in Nîmes, South of France, July to September 2015.* Euro Surveill, 2016. **21**(21).
16. Schmidt-Chanasit, J., et al., *Dengue virus infection in a traveller returning from Croatia to Germany*. 2010, Robert Koch-Institut, Infektionsepidemiologie.
17. Heitmann, A., et al., *Experimental risk assessment for chikungunya virus transmission based on vector competence, distribution and temperature suitability in Europe, 2018.* Eurosurveillance, 2018. **23**(29): p. 1800033.
18. Ziegler, U., et al., *West Nile Virus Epidemic in Germany Triggered by Epizootic Emergence, 2019.* Viruses, 2020. **12**(4).
19. Weaver, S.C. and W.K. Reisen, *Present and future arboviral threats.* Antiviral Res, 2010. **85**(2): p. 328-45.
20. Girard, M., et al., *Arboviruses: A global public health threat.* Vaccine, 2020. **38**(24): p. 3989-3994.
21. Dutuze, M.F., et al., *A Review of Bunyamwera, Batai, and Ngari Viruses: Understudied Orthobunyaviruses With Potential One Health Implications.* Front Vet Sci, 2018. **5**: p. 69.
22. Paupy, C., et al., *Aedes albopictus, an arbovirus vector: From the darkness to the light.* Microbes and Infection, 2009. **11**(14): p. 1177-1185.
23. Powell, J.R. and W.J. Tabachnick, *History of domestication and spread of Aedes aegypti--a review.* Memorias do Instituto Oswaldo Cruz, 2013. **108 Suppl 1**(Suppl 1): p. 11-17.
24. Bellone, R. and A.-B. Failloux, *The Role of Temperature in Shaping Mosquito-Borne Viruses Transmission.* Frontiers in Microbiology, 2020. **11**(2388).
25. Kraemer, M.U.G., et al., *The global compendium of Aedes aegypti and Ae. albopictus occurrence.* Scientific Data, 2015. **2**(1): p. 150035.
26. Huang, Y.S., S. Higgs, and D.L. Vanlandingham, *Arbovirus-Mosquito Vector-Host Interactions and the Impact on Transmission and Disease Pathogenesis of Arboviruses.* Front Microbiol, 2019. **10**: p. 22.
27. Authority, E.C.f.D.P.a.C.a.E.F.S., *Mosquito maps [Internet]*, in *Stockholm: ECDC*. 2018.
28. Agarwal, A., M. Parida, and P.K. Dash, *Impact of transmission cycles and vector competence on global expansion and emergence of arboviruses.* Rev Med Virol, 2017.
29. Houe, V., M. Bonizzoni, and A.B. Failloux, *Endogenous non-retroviral elements in genomes of Aedes mosquitoes and vector competence.* Emerg Microbes Infect, 2019. **8**(1): p. 542-555.

30. Bonizzoni, M., et al., *The invasive mosquito species Aedes albopictus: current knowledge and future perspectives.* Trends Parasitol, 2013. **29**(9): p. 460-8.
31. Chevillon, C., et al., *The Chikungunya threat: an ecological and evolutionary perspective.* Trends in Microbiology, 2008. **16**(2): p. 80-88.
32. Ruckert, C., et al., *Impact of simultaneous exposure to arboviruses on infection and transmission by Aedes aegypti mosquitoes.* Nat Commun, 2017. **8**: p. 15412.
33. Napp, S., D. Petrić, and N. Busquets, *West Nile virus and other mosquito-borne viruses present in Eastern Europe.* Pathog Glob Health, 2018. **112**(5): p. 233-248.
34. Lwande, O.W., et al., *Global emergence of Alphaviruses that cause arthritis in humans.* Infect Ecol Epidemiol, 2015. **5**: p. 29853.
35. Jupille, H., et al., *Arboviruses: variations on an ancient theme.* Future Virology, 2014. **9**(8): p. 733-751.
36. Nyaruaba, R., et al., *Arboviruses in the East African Community partner states: a review of medically important mosquito-borne Arboviruses.* Pathogens and Global Health, 2019. **113**(5): p. 209-228.
37. Wu, P., et al., *Arbovirus lifecycle in mosquito: acquisition, propagation and transmission.* Expert Rev Mol Med, 2019. **21**: p. e1.
38. Leta, S., et al., *Global risk mapping for major diseases transmitted by Aedes aegypti and Aedes albopictus.* Int J Infect Dis, 2018. **67**: p. 25-35.
39. Mansfield, K.L., et al., *Rift Valley fever virus: A review of diagnosis and vaccination, and implications for emergence in Europe.* Vaccine, 2015. **33**(42): p. 5520-5531.
40. Alexander, R.A., *Rift valley fever in the Union.* Journal of the South African Veterinary Association, 1951. **22**(3): p. 105-112.
41. Cunha, R.V.d. and K.S. Trinta, *Chikungunya virus: clinical aspects and treatment - A Review.* Memorias do Instituto Oswaldo Cruz, 2017. **112**(8): p. 523-531.
42. Zeller, H., W. Van Bortel, and B. Sudre, *Chikungunya: Its History in Africa and Asia and Its Spread to New Regions in 2013–2014.* The Journal of Infectious Diseases, 2016. **214**(suppl_5): p. S436-S440.
43. Gao, S., S. Song, and L. Zhang, *Recent Progress in Vaccine Development Against Chikungunya Virus.* Front Microbiol, 2019. **10**: p. 2881.
44. Dick, G.W., S.F. Kitchen, and A.J. Haddow, *Zika virus. I. Isolations and serological specificity.* Trans R Soc Trop Med Hyg, 1952. **46**(5): p. 509-20.
45. Masmejan, S., et al., *Zika virus, vaccines, and antiviral strategies.* Expert Review of Anti-infective Therapy, 2018. **16**(6): p. 471-483.
46. Musso, D., A.I. Ko, and D. Baud, *Zika Virus Infection — After the Pandemic.* New England Journal of Medicine, 2019. **381**(15): p. 1444-1457.
47. Poinar Jr, G.P., R, *Evidence of Vector-Borne Disease of Early Cretaceous Reptiles.* Vector-Borne and Zoonotic Diseases, 2004. **4**(4): p. 281-284.
48. response, W.H.O.W.G.v.c., *Global vector control response 2017–2030 [Internet].* 2018. Available from: http://www.who.int/vector-control/publications/global-control-response/en/.
49. Benelli, G., A.B.B. Wilke, and J.C. Beier, *Aedes albopictus (Asian Tiger Mosquito).* Trends Parasitol, 2020. **36**(11): p. 942-943.
50. Matthews, B.J., *Aedes aegypti.* Trends in Genetics, 2019. **35**(6): p. 470-471.
51. Matthews, B.J., et al., *Improved reference genome of Aedes aegypti informs arbovirus vector control.* Nature, 2018. **563**(7732): p. 501-507.
52. Peleg, J., *Growth of arboviruses in monolayers from subcultured mosquito embryo cells.* Virology, 1968. **35**(4): p. 617-9.
53. Singh, K., *Cell cultures derived from larvae of Aedes albopictus (Skuse) and Aedes aegypti (L.).* Current Science, 1967. **36**(19): p. 506-508.
54. Siu, R.W., et al., *Antiviral RNA interference responses induced by Semliki Forest virus infection of mosquito cells: characterization, origin, and frequency-dependent functions of virus-derived small interfering RNAs.* J Virol, 2011. **85**(6): p. 2907-17.
55. Barletta, A.B.F., M.C.L.N. Silva, and M.H.F. Sorgine, *Validation of Aedes aegypti Aag-2 cells as a model for insect immune studies.* Parasites & Vectors, 2012. **5**(1): p. 148.
56. Nene, V., et al., *Genome sequence of Aedes aegypti, a major arbovirus vector.* Science, 2007. **316**(5832): p. 1718-23.
57. Walker, T., et al., *Mosquito cell lines: history, isolation, availability and application to assess the threat of arboviral transmission in the United Kingdom.* Parasit Vectors, 2014. **7**: p. 382.

58. Fredericks, A.C., et al., *Aedes aegypti (Aag2)-derived clonal mosquito cell lines reveal the effects of pre-existing persistent infection with the insect-specific bunyavirus Phasi Charoen-like virus on arbovirus replication.* PLoS Negl Trop Dis, 2019. **13**(11): p. e0007346.
59. Varjak, M., et al., *Characterization of the Zika virus induced small RNA response in Aedes aegypti cells.* PLoS Negl Trop Dis, 2017. **11**(10): p. e0006010.
60. Brackney, D.E., et al., *C6/36 Aedes albopictus cells have a dysfunctional antiviral RNA interference response.* PLoS Negl Trop Dis, 2010. **4**(10): p. e856.
61. Kuno, G. and G.J. Chang, *Biological transmission of arboviruses: reexamination of and new insights into components, mechanisms, and unique traits as well as their evolutionary trends.* Clin Microbiol Rev, 2005. **18**(4): p. 608-37.
62. Mueller, C.G. and V.-M. Cao-Lormeau, *Chapter 8 - Insect-Borne Viruses and Host Skin Interface*, in *Skin and Arthropod Vectors*, N. Boulanger, Editor. 2018, Academic Press. p. 275-292.
63. Franz, A.W.E., et al., *Tissue Barriers to Arbovirus Infection in Mosquitoes.* Viruses, 2015. **7**(7): p. 3741-3767.
64. Rückert, C. and G.D. Ebel, *How Do Virus–Mosquito Interactions Lead to Viral Emergence?* Trends in Parasitology, 2018. **34**(4): p. 310-321.
65. Kean, J., et al., *Fighting Arbovirus Transmission: Natural and Engineered Control of Vector Competence in Aedes Mosquitoes.* Insects, 2015. **6**(1): p. 236-78.
66. Walker, T., et al., *The wMel Wolbachia strain blocks dengue and invades caged Aedes aegypti populations.* Nature, 2011. **476**(7361): p. 450-453.
67. MOUSSON, L., et al., *Wolbachia modulates Chikungunya replication in Aedes albopictus.* Molecular Ecology, 2010. **19**(9): p. 1953-1964.
68. Mousson, L., et al., *The Native Wolbachia Symbionts Limit Transmission of Dengue Virus in Aedes albopictus.* PLOS Neglected Tropical Diseases, 2012. **6**(12): p. e1989.
69. Nazni, W.A., et al., *Establishment of Wolbachia Strain wAlbB in Malaysian Populations of Aedes aegypti for Dengue Control.* Current Biology, 2019. **29**(24): p. 4241-4248.e5.
70. Xue, L., X. Fang, and J.M. Hyman, *Comparing the effectiveness of different strains of Wolbachia for controlling chikungunya, dengue fever, and zika.* PLOS Neglected Tropical Diseases, 2018. **12**(7): p. e0006666.
71. Schnettler, E., et al., *Wolbachia restricts insect-specific flavivirus infection in Aedes aegypti cells.* J Gen Virol, 2016. **97**(11): p. 3024-3029.
72. Johnson, K.N., *The Impact of Wolbachia on Virus Infection in Mosquitoes.* Viruses, 2015. **7**(11): p. 5705-5717.
73. Robinson, A.S., *Genetic Basis of the Sterile Insect Technique*, in *Sterile Insect Technique: Principles and Practice in Area-Wide Integrated Pest Management*, V.A. Dyck, J. Hendrichs, and A.S. Robinson, Editors. 2005, Springer Netherlands: Dordrecht. p. 95-114.
74. Evans, B.R., et al., *Transgenic Aedes aegypti Mosquitoes Transfer Genes into a Natural Population.* Scientific Reports, 2019. **9**(1): p. 13047.
75. Smithburn, K.C. and A.J. Haddow, *Semliki Forest Virus.* I. Isolation and Pathogenic Properties, 1944. **49**(3): p. 141-157.
76. Holmes, A.C., et al., *A molecular understanding of alphavirus entry.* PLoS Pathog, 2020. **16**(10): p. e1008876.
77. De Caluwe, L., K.K. Arien, and K. Bartholomeeusen, *Host Factors and Pathways Involved in the Entry of Mosquito-Borne Alphaviruses.* Trends Microbiol, 2020.
78. Jose, J., J.E. Snyder, and R.J. Kuhn, *A structural and functional perspective of alphavirus replication and assembly.* Future Microbiol, 2009. **4**(7): p. 837-56.
79. Pietilä, M.K., K. Hellström, and T. Ahola, *Alphavirus polymerase and RNA replication.* Virus Res, 2017. **234**: p. 44-57.
80. Brown, R.S., J.J. Wan, and M. Kielian, *The Alphavirus Exit Pathway: What We Know and What We Wish We Knew.* Viruses, 2018. **10**(2): p. 89.
81. Kokernot, R.H., et al., *Isolation of Bunyamwera virus from a naturally infected human being and further isolations from Aedes (Banksinella) circumluteolus theo.* Am J Trop Med Hyg, 1958. **7**(6): p. 579-84.
82. Smithburn, K.C., A.F. Mahaffy, and A.J. Haddow, *Semliki Forest Virus.* II. Immunological Studies with Specific Antiviral Sera and Sera from Humans and Wild Animals, 1944. **49**(3): p. 159-173.

83. Hu, C., et al., *The severe fever with thrombocytopenia syndrome bunyavirus (SFTSV) antibody in a highly endemic region from 2011 to 2013: a comparative serological study.* The American journal of tropical medicine and hygiene, 2015. **92**(3): p. 479-481.
84. Blakqori, G., A.C. Lowen, and R.M. Elliott, *The small genome segment of Bunyamwera orthobunyavirus harbours a single transcription-termination signal.* J Gen Virol, 2012. **93**(Pt 7): p. 1449-1455.
85. Shi, X., et al., *Visualizing the replication cycle of bunyamwera orthobunyavirus expressing fluorescent protein-tagged Gc glycoprotein.* J Virol, 2010. **84**(17): p. 8460-9.
86. Elliott, R.M., *Orthobunyaviruses: recent genetic and structural insights.* Nature Reviews Microbiology, 2014. **12**(10): p. 673-685.
87. Elliott, R.M., *Orthobunyaviruses: recent genetic and structural insights.* Nat Rev Microbiol, 2014. **12**(10): p. 673-85.
88. Lowe, R., et al., *The Zika Virus Epidemic in Brazil: From Discovery to Future Implications.* Int J Environ Res Public Health, 2018. **15**(1).
89. Sirohi, D. and R.J. Kuhn, *Zika Virus Structure, Maturation, and Receptors.* J Infect Dis, 2017. **216**(suppl_10): p. S935-s944.
90. Agrelli, A., et al., *ZIKA virus entry mechanisms in human cells.* Infect Genet Evol, 2019. **69**: p. 22-29.
91. Kuno, G. and G.J.J. Chang, *Full-length sequencing and genomic characterization of Bagaza, Kedougou, and Zika viruses.* Archives of Virology, 2007. **152**(4): p. 687-696.
92. Souza-Neto, J.A., J.R. Powell, and M. Bonizzoni, *Aedes aegypti vector competence studies: A review.* Infect Genet Evol, 2019. **67**: p. 191-209.
93. Tsetsarkin, K.A., et al., *A single mutation in chikungunya virus affects vector specificity and epidemic potential.* PLoS Pathog, 2007. **3**(12): p. e201.
94. Palmer, W.H., F.S. Varghese, and R.P. van Rij, *Natural Variation in Resistance to Virus Infection in Dipteran Insects.* Viruses, 2018. **10**(3).
95. Moreira, L.A., et al., *A Wolbachia Symbiont in Aedes aegypti Limits Infection with Dengue, Chikungunya, and Plasmodium.* Cell, 2009. **139**(7): p. 1268-1278.
96. Rainey, S.M., et al., *Wolbachia Blocks Viral Genome Replication Early in Infection without a Transcriptional Response by the Endosymbiont or Host Small RNA Pathways.* PLoS Pathog, 2016. **12**(4): p. e1005536.
97. Beerntsen, B.T., A.A. James, and B.M. Christensen, *Genetics of mosquito vector competence.* Microbiol Mol Biol Rev, 2000. **64**(1): p. 115-37.
98. Fujita, R., et al., *Persistent viruses in mosquito cultured cell line suppress multiplication of flaviviruses.* Heliyon, 2018. **4**(8): p. e00736.
99. Rosales, C. *Cellular and Molecular Mechanisms of Insect Immunity*. 2017.
100. Satyavathi, V.V., A. Minz, and J. Nagaraju, *Nodulation: An unexplored cellular defense mechanism in insects.* Cellular Signalling, 2014. **26**(8): p. 1753-1763.
101. Manniello, M.D., et al., *Insect antimicrobial peptides: potential weapons to counteract the antibiotic resistance.* Cellular and Molecular Life Sciences, 2021.
102. Yi, H.-Y., et al., *Insect antimicrobial peptides and their applications.* Applied microbiology and biotechnology, 2014. **98**(13): p. 5807-5822.
103. Russell, T.A., et al., *Imd pathway-specific immune assays reveal NF-κB stimulation by viral RNA PAMPs in Aedes aegypti Aag2 cells.* PLoS Negl Trop Dis, 2021. **15**(2): p. e0008524.
104. Luplertlop, N., et al., *Induction of a peptide with activity against a broad spectrum of pathogens in the Aedes aegypti salivary gland, following Infection with Dengue Virus.* PLoS Pathog, 2011. **7**(1): p. e1001252.
105. Jupatanakul, N., et al., *Engineered Aedes aegypti JAK/STAT Pathway-Mediated Immunity to Dengue Virus.* PLoS Negl Trop Dis, 2017. **11**(1): p. e0005187.
106. Arbouzova, N.I. and M.P. Zeidler, *JAK/STAT signalling in Drosophila: insights into conserved regulatory and cellular functions.* Development, 2006. **133**(14): p. 2605-2616.
107. Fragkoudis, R., et al., *Semliki Forest virus strongly reduces mosquito host defence signaling.* Insect Mol Biol, 2008. **17**(6): p. 647-56.
108. Xi, Z., J.L. Ramirez, and G. Dimopoulos, *The Aedes aegypti toll pathway controls dengue virus infection.* PLoS Pathog, 2008. **4**(7): p. e1000098.
109. Angleró-Rodríguez, Y.I., et al., *Aedes aegypti Molecular Responses to Zika Virus: Modulation of Infection by the Toll and Jak/Stat Immune Pathways and Virus Host Factors.* Front Microbiol, 2017. **8**: p. 2050.
110. Ahlers, L.R.H., et al., *Insulin Potentiates JAK/STAT Signaling to Broadly Inhibit Flavivirus Replication in Insect Vectors.* Cell Reports, 2019. **29**(7): p. 1946-1960.e5.

111. Paradkar, P.N., et al., *Secreted Vago restricts West Nile virus infection in Culex mosquito cells by activating the Jak-STAT pathway.* Proc Natl Acad Sci U S A, 2012. **109**(46): p. 18915-20.
112. Paradkar, P.N., et al., *Dicer-2-dependent activation of Culex Vago occurs via the TRAF-Rel2 signaling pathway.* PLoS Negl Trop Dis, 2014. **8**(4): p. e2823.
113. Lindbo, J.A. and W.G. Dougherty, *Plant Pathology and RNAi: A Brief History.* Annual Review of Phytopathology, 2005. **43**(1): p. 191-204.
114. Romano, N. and G. Macino, *Quelling: transient inactivation of gene expression in Neurospora crassa by transformation with homologous sequences.* Mol Microbiol, 1992. **6**(22): p. 3343-53.
115. Fire, A., et al., *Potent and specific genetic interference by double-stranded RNA in Caenorhabditis elegans.* Nature, 1998. **391**(6669): p. 806-11.
116. Sen, G.L. and H.M. Blau, *A brief history of RNAi: the silence of the genes.* FASEB J, 2006. **20**(9): p. 1293-9.
117. Elbashir, S.M., W. Lendeckel, and T. Tuschl, *RNA interference is mediated by 21- and 22-nucleotide RNAs.* Genes Dev, 2001. **15**(2): p. 188-200.
118. Elbashir, S.M., et al., *Duplexes of 21-nucleotide RNAs mediate RNA interference in cultured mammalian cells.* Nature, 2001. **411**(6836): p. 494-8.
119. Gantier, M.P. and B.R. Williams, *The response of mammalian cells to double-stranded RNA.* Cytokine Growth Factor Rev, 2007. **18**(5-6): p. 363-71.
120. Bernstein, E., et al., *Role for a bidentate ribonuclease in the initiation step of RNA interference.* Nature, 2001. **409**(6818): p. 363-6.
121. Liu, J., et al., *Argonaute2 is the catalytic engine of mammalian RNAi.* Science, 2004. **305**(5689): p. 1437-41.
122. Waterhouse, R.M., et al., *Evolutionary dynamics of immune-related genes and pathways in disease-vector mosquitoes.* Science, 2007. **316**(5832): p. 1738-43.
123. Campbell, C.L., et al., *Aedes aegypti uses RNA interference in defense against Sindbis virus infection.* BMC microbiology, 2008. **8**: p. 47-47.
124. Berkhout, B., *RNAi-mediated antiviral immunity in mammals.* Current Opinion in Virology, 2018. **32**: p. 9-14.
125. tenOever, B.R., *Questioning antiviral RNAi in mammals.* Nat Microbiol, 2017. **2**: p. 17052.
126. Donald, C.L., A. Kohl, and E. Schnettler, *New Insights into Control of Arbovirus Replication and Spread by Insect RNA Interference Pathways.* Insects, 2012. **3**(2): p. 511-31.
127. Tikhe, C.V. and G. Dimopoulos, *Mosquito antiviral immune pathways.* Dev Comp Immunol, 2021. **116**: p. 103964.
128. Vodovar, N. and M.-C. Saleh, *Chapter 1 - Of Insects and Viruses: The Role of Small RNAs in Insect Defence*, in *Advances in Insect Physiology*, E.L. Jockusch, Editor. 2012, Academic Press. p. 1-36.
129. Asgari, S., *MicroRNA functions in insects.* Insect Biochemistry and Molecular Biology, 2013. **43**(4): p. 388-397.
130. Asgari, S., *Role of microRNAs in arbovirus/vector interactions.* Viruses, 2014. **6**(9): p. 3514-34.
131. O'Brien, J., et al., *Overview of MicroRNA Biogenesis, Mechanisms of Actions, and Circulation.* Frontiers in Endocrinology, 2018. **9**(402).
132. Breving, K. and A. Esquela-Kerscher, *The complexities of microRNA regulation: mirandering around the rules.* Int J Biochem Cell Biol, 2010. **42**(8): p. 1316-29.
133. Soleimani, S., et al., *Small regulatory noncoding RNAs in Drosophila melanogaster: biogenesis and biological functions.* Brief Funct Genomics, 2020. **19**(4): p. 309-323.
134. Feng, X., et al., *microRNA profiles and functions in mosquitoes.* PLoS Negl Trop Dis, 2018. **12**(5): p. e0006463.
135. Chipman, L.B. and A.E. Pasquinelli, *miRNA Targeting: Growing beyond the Seed.* Trends in Genetics, 2019. **35**(3): p. 215-222.
136. Slonchak, A., et al., *Expression of mosquito microRNA Aae-miR-2940-5p is downregulated in response to West Nile virus infection to restrict viral replication.* J Virol, 2014. **88**(15): p. 8457-67.
137. Zhang, G., et al., *Wolbachia uses a host microRNA to regulate transcripts of a methyltransferase, contributing to dengue virus inhibition in Aedes aegypti.* Proc Natl Acad Sci U S A, 2013. **110**(25): p. 10276-81.
138. Yen, P.S., et al., *Assessing the Potential Interactions between Cellular miRNA and Arboviral Genomic RNA in the Yellow Fever Mosquito, Aedes aegypti.* Viruses, 2019. **11**(6).

139. Hussain, M. and S. Asgari, *MicroRNA-like viral small RNA from Dengue virus 2 autoregulates its replication in mosquito cells.* Proceedings of the National Academy of Sciences of the United States of America, 2014. **111**(7): p. 2746-2751.
140. Lei, X., et al., *Regulation of herpesvirus lifecycle by viral microRNAs.* Virulence, 2010. **1**(5): p. 433-5.
141. Czech, B., et al., *An endogenous small interfering RNA pathway in Drosophila.* Nature, 2008. **453**(7196): p. 798-802.
142. Fagegaltier, D., et al., *The endogenous siRNA pathway is involved in heterochromatin formation in Drosophila.* Proc Natl Acad Sci U S A, 2009. **106**(50): p. 21258-63.
143. Piatek, M.J. and A. Werner, *Endogenous siRNAs: regulators of internal affairs.* Biochem Soc Trans, 2014. **42**(4): p. 1174-9.
144. Ghildiyal, M. and P.D. Zamore, *Small silencing RNAs: an expanding universe.* Nat Rev Genet, 2009. **10**(2): p. 94-108.
145. Aliyari, R., et al., *Mechanism of induction and suppression of antiviral immunity directed by virus-derived small RNAs in Drosophila.* Cell Host Microbe, 2008. **4**(4): p. 387-97.
146. Flynt, A., et al., *Dicing of viral replication intermediates during silencing of latent Drosophila viruses.* Proc Natl Acad Sci U S A, 2009. **106**(13): p. 5270-5.
147. Blair, C.D. and K.E. Olson, *The role of RNA interference (RNAi) in arbovirus-vector interactions.* Viruses, 2015. **7**(2): p. 820-43.
148. Sinha, N.K., et al., *Dicer uses distinct modules for recognizing dsRNA termini.* Science, 2018. **359**(6373): p. 329-334.
149. Cenik, E.S., et al., *Phosphate and R2D2 restrict the substrate specificity of Dicer-2, an ATP-driven ribonuclease.* Mol Cell, 2011. **42**(2): p. 172-84.
150. Hammond, S.M., et al., *An RNA-directed nuclease mediates post-transcriptional gene silencing in Drosophila cells.* Nature, 2000. **404**(6775): p. 293-6.
151. Matranga, C., et al., *Passenger-strand cleavage facilitates assembly of siRNA into Ago2-containing RNAi enzyme complexes.* Cell, 2005. **123**(4): p. 607-20.
152. Khvorova, A., A. Reynolds, and S.D. Jayasena, *Functional siRNAs and miRNAs Exhibit Strand Bias.* Cell, 2003. **115**(2): p. 209-216.
153. Rand, T.A., et al., *Argonaute2 cleaves the anti-guide strand of siRNA during RISC activation.* Cell, 2005. **123**(4): p. 621-9.
154. Miyoshi, K., et al., *Slicer function of Drosophila Argonautes and its involvement in RISC formation.* Genes Dev, 2005. **19**(23): p. 2837-48.
155. Leuschner, P.J., et al., *Cleavage of the siRNA passenger strand during RISC assembly in human cells.* EMBO Rep, 2006. **7**(3): p. 314-20.
156. Pratt, A.J. and I.J. MacRae, *The RNA-induced silencing complex: a versatile gene-silencing machine.* J Biol Chem, 2009. **284**(27): p. 17897-901.
157. van Rij, R.P., et al., *The RNA silencing endonuclease Argonaute 2 mediates specific antiviral immunity in Drosophila melanogaster.* Genes Dev, 2006. **20**(21): p. 2985-95.
158. van Mierlo, J.T., et al., *Convergent evolution of argonaute-2 slicer antagonism in two distinct insect RNA viruses.* PLoS Pathog, 2012. **8**(8): p. e1002872.
159. Haley, B. and P.D. Zamore, *Kinetic analysis of the RNAi enzyme complex.* Nat Struct Mol Biol, 2004. **11**(7): p. 599-606.
160. Wang, X.H., et al., *RNA interference directs innate immunity against viruses in adult Drosophila.* Science, 2006. **312**(5772): p. 452-4.
161. Schuster, S., P. Miesen, and R.P. van Rij, *Antiviral RNAi in Insects and Mammals: Parallels and Differences.* Viruses, 2019. **11**(5).
162. Yang, Z., et al., *Approaches for Studying MicroRNA and Small Interfering RNA Methylation In Vitro and In Vivo*, in *Methods in Enzymology*. 2007, Academic Press. p. 139-154.
163. Ji, L. and X. Chen, *Regulation of small RNA stability: methylation and beyond.* Cell research, 2012. **22**(4): p. 624-636.
164. Horwich, M.D., et al., *The Drosophila RNA methyltransferase, DmHen1, modifies germline piRNAs and single-stranded siRNAs in RISC.* Curr Biol, 2007. **17**(14): p. 1265-72.
165. Saito, K., et al., *Pimet, the Drosophila homolog of HEN1, mediates 2'-O-methylation of Piwi-interacting RNAs at their 3' ends.* Genes Dev, 2007. **21**(13): p. 1603-8.
166. Alefelder, S., B.K. Patel, and F. Eckstein, *Incorporation of terminal phosphorothioates into oligonucleotides.* Nucleic Acids Res, 1998. **26**(21): p. 4983-8.
167. Hamilton, A.J. and D.C. Baulcombe, *A species of small antisense RNA in posttranscriptional gene silencing in plants.* Science, 1999. **286**(5441): p. 950-2.

168. Wu, Q., et al., *Virus discovery by deep sequencing and assembly of virus-derived small silencing RNAs.* Proc Natl Acad Sci U S A, 2010. **107**(4): p. 1606-11.
169. Mlotshwa, S., G.J. Pruss, and V. Vance, *Small RNAs in viral infection and host defense.* Trends Plant Sci, 2008. **13**(7): p. 375-82.
170. Brackney, D.E., J.E. Beane, and G.D. Ebel, *RNAi Targeting of West Nile Virus in Mosquito Midguts Promotes Virus Diversification.* PLOS Pathogens, 2009. **5**(7): p. e1000502.
171. Myles, K.M., et al., *Alphavirus-derived small RNAs modulate pathogenesis in disease vector mosquitoes.* Proceedings of the National Academy of Sciences, 2008. **105**(50): p. 19938-19943.
172. Sánchez-Vargas, I., et al., *Dengue virus type 2 infections of Aedes aegypti are modulated by the mosquito's RNA interference pathway.* PLoS Pathog, 2009. **5**(2): p. e1000299.
173. Segers, G.C., et al., *Evidence that RNA silencing functions as an antiviral defense mechanism in fungi.* Proc Natl Acad Sci U S A, 2007. **104**(31): p. 12902-6.
174. Galiana-Arnoux, D., et al., *Essential function in vivo for Dicer-2 in host defense against RNA viruses in drosophila.* Nat Immunol, 2006. **7**(6): p. 590-7.
175. Chotkowski, H.L., et al., *West Nile virus infection of Drosophila melanogaster induces a protective RNAi response.* Virology, 2008. **377**(1): p. 197-206.
176. Mukherjee, S. and K.A. Hanley, *RNA interference modulates replication of dengue virus in Drosophila melanogaster cells.* BMC Microbiology, 2010. **10**(1): p. 127.
177. Dietrich, I., et al., *RNA Interference Restricts Rift Valley Fever Virus in Multiple Insect Systems.* mSphere, 2017. **2**(3).
178. Kemp, C., et al., *Broad RNA Interference–Mediated Antiviral Immunity and Virus-Specific Inducible Responses in Drosophila.* The Journal of Immunology, 2013. **190**(2): p. 650-658.
179. Arensburger, P., et al., *Sequencing of Culex quinquefasciatus establishes a platform for mosquito comparative genomics.* Science, 2010. **330**(6000): p. 86-8.
180. Holt, R.A., et al., *The Genome Sequence of the Malaria Mosquito Anopheles gambiae.* Science, 2002. **298**(5591): p. 129-149.
181. Campbell, C.L., et al., *Comparative genomics of small RNA regulatory pathway components in vector mosquitoes.* BMC Genomics, 2008. **9**: p. 425.
182. Scott, J.C., et al., *Comparison of dengue virus type 2-specific small RNAs from RNA interference-competent and -incompetent mosquito cells.* PLoS Negl Trop Dis, 2010. **4**(10): p. e848.
183. Carissimo, G., et al., *Antiviral immunity of Anopheles gambiae is highly compartmentalized, with distinct roles for RNA interference and gut microbiota.* Proc Natl Acad Sci U S A, 2015. **112**(2): p. E176-85.
184. Leger, P., et al., *Dicer-2- and Piwi-mediated RNA interference in Rift Valley fever virus-infected mosquito cells.* J Virol, 2013. **87**(3): p. 1631-48.
185. Myles, K.M., E.M. Morazzani, and Z.N. Adelman, *Origins of alphavirus-derived small RNAs in mosquitoes.* RNA biology, 2009. **6**(4): p. 387-391.
186. Keene, K.M., et al., *RNA interference acts as a natural antiviral response to O'nyong-nyong virus (Alphavirus; Togaviridae) infection of Anopheles gambiae.* Proc Natl Acad Sci U S A, 2004. **101**(49): p. 17240-5.
187. McFarlane, M., et al., *Characterization of Aedes aegypti innate-immune pathways that limit Chikungunya virus replication.* PLoS Negl Trop Dis, 2014. **8**(7): p. e2994.
188. Dietrich, I., et al., *The Antiviral RNAi Response in Vector and Non-vector Cells against Orthobunyaviruses.* PLoS Negl Trop Dis, 2017. **11**(1): p. e0005272.
189. Schnettler, E., et al., *Knockdown of piRNA pathway proteins results in enhanced Semliki Forest virus production in mosquito cells.* J Gen Virol, 2013. **94**(Pt 7): p. 1680-9.
190. Samuel, G.H., Z.N. Adelman, and K.M. Myles, *Antiviral Immunity and Virus-Mediated Antagonism in Disease Vector Mosquitoes.* Trends Microbiol, 2018. **26**(5): p. 447-461.
191. Schulz, C. and S.C. Becker, *Mosquitoes as Arbovirus Vectors: From Species Identification to Vector Competence*, in *Mosquito-borne Diseases: Implications for Public Health*, G. Benelli and H. Mehlhorn, Editors. 2018, Springer International Publishing: Cham. p. 163-212.
192. Marconcini, M., et al., *Profile of Small RNAs, vDNA Forms and Viral Integrations in Late Chikungunya Virus Infection of Aedes albopictus Mosquitoes.* Viruses, 2021. **13**(4).
193. Morazzani, E.M., et al., *Production of virus-derived ping-pong-dependent piRNA-like small RNAs in the mosquito soma.* PLoS Pathog, 2012. **8**(1): p. e1002470.
194. Goic, B., et al., *Virus-derived DNA drives mosquito vector tolerance to arboviral infection.* Nat Commun, 2016. **7**: p. 12410.

195. Saldaña, M.A., et al., *Zika virus alters the microRNA expression profile and elicits an RNAi response in Aedes aegypti mosquitoes.* PLOS Neglected Tropical Diseases, 2017. **11**(7): p. e0005760.
196. Miesen, P., et al., *Small RNA Profiling in Dengue Virus 2-Infected Aedes Mosquito Cells Reveals Viral piRNAs and Novel Host miRNAs.* PLoS Negl Trop Dis, 2016. **10**(2): p. e0004452.
197. Olson, K.E. and C.D. Blair, *Arbovirus-mosquito interactions: RNAi pathway.* Curr Opin Virol, 2015. **15**: p. 119-26.
198. Airs, P.M. and L.C. Bartholomay, *RNA Interference for Mosquito and Mosquito-Borne Disease Control.* Insects, 2017. **8**(1): p. 4.
199. Brennecke, J., et al., *Discrete small RNA-generating loci as master regulators of transposon activity in Drosophila.* Cell, 2007. **128**(6): p. 1089-103.
200. Duc, C., et al., *Trapping a somatic endogenous retrovirus into a germline piRNA cluster immunizes the germline against further invasion.* Genome Biology, 2019. **20**(1): p. 127.
201. Thomson, T. and H. Lin, *The biogenesis and function of PIWI proteins and piRNAs: progress and prospect.* Annu Rev Cell Dev Biol, 2009. **25**: p. 355-76.
202. Cox, D.N., et al., *A novel class of evolutionarily conserved genes defined by piwi are essential for stem cell self-renewal.* Genes Dev, 1998. **12**(23): p. 3715-27.
203. Lin, H. and A.C. Spradling, *A novel group of pumilio mutations affects the asymmetric division of germline stem cells in the Drosophila ovary.* Development, 1997. **124**(12): p. 2463-76.
204. Banisch, T.U., M. Goudarzi, and E. Raz, *Small RNAs in germ cell development.* Curr Top Dev Biol, 2012. **99**: p. 79-113.
205. Bourque, G., et al., *Ten things you should know about transposable elements.* Genome Biology, 2018. **19**(1): p. 199.
206. Story, B., et al., *Defining the expression of piRNA and transposable elements in Drosophila ovarian germline stem cells and somatic support cells.* Life science alliance, 2019. **2**(5): p. e201800211.
207. Saito, K. and M.C. Siomi, *Small RNA-mediated quiescence of transposable elements in animals.* Dev Cell, 2010. **19**(5): p. 687-97.
208. Kurth, H.M. and K. Mochizuki, *2'-O-methylation stabilizes Piwi-associated small RNAs and ensures DNA elimination in Tetrahymena.* RNA, 2009. **15**(4): p. 675-85.
209. Simon, B., et al., *Recognition of 2'-O-methylated 3'-end of piRNA by the PAZ domain of a Piwi protein.* Structure, 2011. **19**(2): p. 172-80.
210. Tian, Y., et al., *Structural basis for piRNA 2'-O-methylated 3'-end recognition by Piwi PAZ (Piwi/Argonaute/Zwille) domains.* Proceedings of the National Academy of Sciences, 2011. **108**(3): p. 903-910.
211. Vagin, V.V., et al., *A distinct small RNA pathway silences selfish genetic elements in the germline.* Science, 2006. **313**(5785): p. 320-4.
212. Mohn, F., D. Handler, and J. Brennecke, *Noncoding RNA. piRNA-guided slicing specifies transcripts for Zucchini-dependent, phased piRNA biogenesis.* Science, 2015. **348**(6236): p. 812-817.
213. Han, B.W., et al., *Noncoding RNA. piRNA-guided transposon cleavage initiates Zucchini-dependent, phased piRNA production.* Science, 2015. **348**(6236): p. 817-21.
214. Gunawardane, L.S., et al., *A slicer-mediated mechanism for repeat-associated siRNA 5' end formation in Drosophila.* Science, 2007. **315**(5818): p. 1587-90.
215. Czech, B. and G.J. Hannon, *One Loop to Rule Them All: The Ping-Pong Cycle and piRNA-Guided Silencing.* Trends Biochem Sci, 2016. **41**(4): p. 324-337.
216. Huang, X., K. Fejes Toth, and A.A. Aravin, *piRNA Biogenesis in Drosophila melanogaster.* Trends Genet, 2017. **33**(11): p. 882-894.
217. Yamanaka, S., M.C. Siomi, and H. Siomi, *piRNA clusters and open chromatin structure.* Mob DNA, 2014. **5**: p. 22.
218. Senti, K.A. and J. Brennecke, *The piRNA pathway: a fly's perspective on the guardian of the genome.* Trends Genet, 2010. **26**(12): p. 499-509.
219. Aravin, A.A., G.J. Hannon, and J. Brennecke, *The Piwi-piRNA pathway provides an adaptive defense in the transposon arms race.* Science, 2007. **318**(5851): p. 761-4.
220. Lewis, S.H., et al., *Pan-arthropod analysis reveals somatic piRNAs as an ancestral defence against transposable elements.* Nat Ecol Evol, 2018. **2**(1): p. 174-181.
221. Lewis, S.H., H. Salmela, and D.J. Obbard, *Duplication and Diversification of Dipteran Argonaute Genes, and the Evolutionary Divergence of Piwi and Aubergine.* Genome Biol Evol, 2016. **8**(3): p. 507-18.

222. Wang, Y., et al., *piRNA Profiling of Dengue Virus Type 2-Infected Asian Tiger Mosquito and Midgut Tissues.* Viruses, 2018. **10**(4).
223. Müller, M., F. Fazi, and C. Ciaudo, *Argonaute Proteins: From Structure to Function in Development and Pathological Cell Fate Determination.* Frontiers in Cell and Developmental Biology, 2020. **7**(360).
224. Hutvagner, G. and M.J. Simard, *Argonaute proteins: key players in RNA silencing.* Nature Reviews Molecular Cell Biology, 2008. **9**(1): p. 22-32.
225. Zhou, X., et al., *Identification and characterization of Piwi subfamily in insects.* Biochem Biophys Res Commun, 2007. **362**(1): p. 126-131.
226. Ku, H.Y. and H. Lin, *PIWI proteins and their interactors in piRNA biogenesis, germline development and gene expression.* Natl Sci Rev, 2014. **1**(2): p. 205-218.
227. Wu, J., et al., *Argonaute proteins: Structural features, functions and emerging roles.* J Adv Res, 2020. **24**: p. 317-324.
228. Hur, J.K., et al., *Regulation of Argonaute slicer activity by guide RNA 3' end interactions with the N-terminal lobe.* J Biol Chem, 2013. **288**(11): p. 7829-40.
229. Song, J.-J., et al., *Crystal Structure of Argonaute and Its Implications for RISC Slicer Activity.* Science, 2004. **305**(5689): p. 1434-1437.
230. Singh, R.K., et al., *Molecular evolution and diversification of the Argonaute family of proteins in plants.* BMC Plant Biology, 2015. **15**(1): p. 23.
231. Jinek, M. and J.A. Doudna, *A three-dimensional view of the molecular machinery of RNA interference.* Nature, 2009. **457**(7228): p. 405-412.
232. Meister, G., *Argonaute proteins: functional insights and emerging roles.* Nature Reviews Genetics, 2013. **14**(7): p. 447-459.
233. Varjak, M., M. Leggewie, and E. Schnettler, *The antiviral piRNA response in mosquitoes?* J Gen Virol, 2018. **99**(12): p. 1551-1562.
234. Aravin, A.A., et al., *Double-stranded RNA-mediated silencing of genomic tandem repeats and transposable elements in the D. melanogaster germline.* Curr Biol, 2001. **11**(13): p. 1017-27.
235. Aravin, A.A., et al., *Dissection of a natural RNA silencing process in the Drosophila melanogaster germ line.* Mol Cell Biol, 2004. **24**(15): p. 6742-50.
236. Guida, V., et al., *Production of Small Noncoding RNAs from the flamenco Locus Is Regulated by the gypsy Retrotransposon of Drosophila melanogaster.* Genetics, 2016. **204**(2): p. 631-644.
237. Kotelnikov, R.N., et al., *Peculiarities of piRNA-mediated post-transcriptional silencing of Stellate repeats in testes of Drosophila melanogaster.* Nucleic Acids Res, 2009. **37**(10): p. 3254-63.
238. Ozata, D.M., et al., *PIWI-interacting RNAs: small RNAs with big functions.* Nat Rev Genet, 2019. **20**(2): p. 89-108.
239. Arensburger, P., et al., *The mosquito Aedes aegypti has a large genome size and high transposable element load but contains a low proportion of transposon-specific piRNAs.* BMC Genomics, 2011. **12**: p. 606.
240. Liu, P., et al., *Developmental piRNA profiles of the invasive vector mosquito Aedes albopictus.* Parasites & Vectors, 2016. **9**(1): p. 524.
241. Aguiar, E., et al., *A single unidirectional piRNA cluster similar to the flamenco locus is the major source of EVE-derived transcription and small RNAs in Aedes aegypti mosquitoes.* RNA, 2020.
242. Miesen, P., J. Joosten, and R.P. van Rij, *PIWIs Go Viral: Arbovirus-Derived piRNAs in Vector Mosquitoes.* PLoS Pathog, 2016. **12**(12): p. e1006017.
243. Girardi, E., et al., *Histone-derived piRNA biogenesis depends on the ping-pong partners Piwi5 and Ago3 in Aedes aegypti.* Nucleic Acids Res, 2017. **45**(8): p. 4881-4892.
244. Chen, X.G., et al., *Genome sequence of the Asian Tiger mosquito, Aedes albopictus, reveals insights into its biology, genetics, and evolution.* Proc Natl Acad Sci U S A, 2015. **112**(44): p. E5907-15.
245. Olson, K.E. and M. Bonizzoni, *Nonretroviral integrated RNA viruses in arthropod vectors: an occasional event or something more?* Curr Opin Insect Sci, 2017. **22**: p. 45-53.
246. Palatini, U., et al., *Comparative genomics shows that viral integrations are abundant and express piRNAs in the arboviral vectors Aedes aegypti and Aedes albopictus.* BMC Genomics, 2017. **18**(1): p. 512.
247. Tassetto, M., et al., *Control of RNA viruses in mosquito cells through the acquisition of vDNA and endogenous viral elements.* Elife, 2019. **8**.

248. Joosten, J., R.P. Van Rij, and P. Miesen, *Slicing of viral RNA guided by endogenous piRNAs triggers the production of responder and trailer piRNAs in Aedes mosquitoes.* bioRxiv, 2020: p. 2020.07.08.193029.
249. Varjak, M., et al., *Aedes aegypti Piwi4 Is a Noncanonical PIWI Protein Involved in Antiviral Responses.* mSphere, 2017. **2**(3).
250. Houwing, S., et al., *A Role for Piwi and piRNAs in Germ Cell Maintenance and Transposon Silencing in Zebrafish.* Cell, 2007. **129**(1): p. 69-82.
251. Miesen, P., E. Girardi, and R.P. van Rij, *Distinct sets of PIWI proteins produce arbovirus and transposon-derived piRNAs in Aedes aegypti mosquito cells.* Nucleic Acids Res, 2015. **43**(13): p. 6545-56.
252. Aguiar, E.R., et al., *Sequence-independent characterization of viruses based on the pattern of viral small RNAs produced by the host.* Nucleic Acids Res, 2015. **43**(13): p. 6191-206.
253. Hess, A.M., et al., *Small RNA profiling of Dengue virus-mosquito interactions implicates the PIWI RNA pathway in anti-viral defense.* BMC Microbiol, 2011. **11**: p. 45.
254. Vodovar, N., et al., *Arbovirus-derived piRNAs exhibit a ping-pong signature in mosquito cells.* PLoS One, 2012. **7**(1): p. e30861.
255. Varjak, M., et al., *Spindle-E Acts Antivirally Against Alphaviruses in Mosquito Cells.* Viruses, 2018. **10**(2).
256. Petit, M., et al., *piRNA pathway is not required for antiviral defense in Drosophila melanogaster.* Proc Natl Acad Sci U S A, 2016. **113**(29): p. E4218-27.
257. Kolliopoulou, A., et al., *PIWI pathway against viruses in insects.* Wiley Interdiscip Rev RNA, 2019. **10**(6): p. e1555.
258. Crava, C.M., et al., *Population genomics in the arboviral vector Aedes aegypti reveals the genomic architecture and evolution of endogenous viral elements.* Molecular ecology, 2021. **30**(7): p. 1594-1611.
259. Cook, S., et al., *Molecular evolution of the insect-specific flaviviruses.* Journal of General Virology, 2012. **93**(2): p. 223-234.
260. Maringer, K., et al., *Proteomics informed by transcriptomics for characterising active transposable elements and genome annotation in Aedes aegypti.* BMC Genomics, 2017. **18**(1): p. 101.
261. Blair, C.D., *Deducing the Role of Virus Genome-Derived PIWI-Associated RNAs in the Mosquito-Arbovirus Arms Race.* Front Genet, 2019. **10**: p. 1114.
262. Schnettler, E., et al., *RNA interference targets arbovirus replication in Culicoides cells.* J Virol, 2013. **87**(5): p. 2441-54.
263. Nag, D.K., M. Brecher, and L.D. Kramer, *DNA forms of arboviral RNA genomes are generated following infection in mosquito cell cultures.* Virology, 2016. **498**: p. 164-171.
264. Suzuki, Y., et al., *Non-retroviral endogenous viral element limits cognate virus replication in Aedes aegypti ovaries.* bioRxiv, 2020: p. 2020.03.28.013441.
265. Shi, X., et al., *Bunyamwera orthobunyavirus glycoprotein precursor is processed by cellular signal peptidase and signal peptide peptidase.* Proc Natl Acad Sci U S A, 2016. **113**(31): p. 8825-30.
266. Lee, M., et al., *Understanding the role of microRNAs in the interaction of Aedes aegypti mosquitoes with an insect-specific flavivirus.* Journal of General Virology, 2017. **98**(7): p. 1892-1903.
267. Goertz, G.P., et al., *Mosquito Small RNA Responses to West Nile and Insect-Specific Virus Infections in Aedes and Culex Mosquito Cells.* Viruses, 2019. **11**(3).
268. Fros, J.J., et al., *Comparative Usutu and West Nile virus transmission potential by local Culex pipiens mosquitoes in north-western Europe.* One Health, 2015. **1**: p. 31-36.
269. Ruckert, C., et al., *Small RNA responses of Culex mosquitoes and cell lines during acute and persistent virus infection.* Insect Biochem Mol Biol, 2019. **109**: p. 13-23.
270. Goic, B., et al., *RNA-mediated interference and reverse transcription control the persistence of RNA viruses in the insect model Drosophila.* Nat Immunol, 2013. **14**(4): p. 396-403.
271. Geuking, M.B., et al., *Recombination of retrotransposon and exogenous RNA virus results in nonretroviral cDNA integration.* Science, 2009. **323**(5912): p. 393-6.
272. Negroni, M. and H. Buc, *Copy-choice recombination by reverse transcriptases: reshuffling of genetic markers mediated by RNA chaperones.* Proceedings of the National Academy of Sciences of the United States of America, 2000. **97**(12): p. 6385-6390.
273. Nag, D.K. and L.D. Kramer, *Patchy DNA forms of the Zika virus RNA genome are generated following infection in mosquito cell cultures and in mosquitoes.* J Gen Virol, 2017. **98**(11): p. 2731-2737.

274. Poirier, E.Z., et al., *Dicer-2-Dependent Generation of Viral DNA from Defective Genomes of RNA Viruses Modulates Antiviral Immunity in Insects.* Cell Host Microbe, 2018. **23**(3): p. 353-365 e8.
275. Mondotte, J.A., et al., *Evidence For Long-Lasting Transgenerational Antiviral Immunity in Insects.* Cell Reports, 2020. **33**(11).
276. Taylor, D.J. and J. Bruenn, *The evolution of novel fungal genes from non-retroviral RNA viruses.* BMC Biol, 2009. **7**: p. 88.
277. Katzourakis, A. and M. Tristem, *Phylogeny of human endogenous and exogenous retroviruses.* Retroviruses and primate genome evolution, 2005. **186**: p. 203.
278. Katzourakis, A. and R.J. Gifford, *Endogenous viral elements in animal genomes.* PLoS Genet, 2010. **6**(11): p. e1001191.
279. Koonin, E.V., *Taming of the shrewd: novel eukaryotic genes from RNA viruses.* BMC Biol, 2010. **8**: p. 2.
280. Feschotte, C. and C. Gilbert, *Endogenous viruses: insights into viral evolution and impact on host biology.* Nat Rev Genet, 2012. **13**(4): p. 283-96.
281. Holmes, E.C., *The evolution of endogenous viral elements.* Cell Host Microbe, 2011. **10**(4): p. 368-77.
282. Blair, C.D., K.E. Olson, and M. Bonizzoni, *The Widespread Occurrence and Potential Biological Roles of Endogenous Viral Elements in Insect Genomes.* Curr Issues Mol Biol, 2020. **34**: p. 13-30.
283. Fujino, K., et al., *Inhibition of Borna disease virus replication by an endogenous bornavirus-like element in the ground squirrel genome.* Proceedings of the National Academy of Sciences, 2014. **111**(36): p. 13175-13180.
284. Frank, J.A. and C. Feschotte, *Co-option of endogenous viral sequences for host cell function.* Current Opinion in Virology, 2017. **25**: p. 81-89.
285. Whitfield, Z.J., et al., *The Diversity, Structure, and Function of Heritable Adaptive Immunity Sequences in the Aedes aegypti Genome.* Curr Biol, 2017. **27**(22): p. 3511-3519 e7.
286. Crochu, S., et al., *Sequences of flavivirus-related RNA viruses persist in DNA form integrated in the genome of Aedes spp. mosquitoes.* J Gen Virol, 2004. **85**(Pt 7): p. 1971-80.
287. Cook, S., et al., *Isolation of a new strain of the flavivirus cell fusing agent virus in a natural mosquito population from Puerto Rico.* J Gen Virol, 2006. **87**(Pt 4): p. 735-48.
288. Suzuki, Y., et al., *Uncovering the Repertoire of Endogenous Flaviviral Elements in Aedes Mosquito Genomes.* J Virol, 2017. **91**(15).
289. Fort, P., et al., *Fossil rhabdoviral sequences integrated into arthropod genomes: ontogeny, evolution, and potential functionality.* Mol Biol Evol, 2012. **29**(1): p. 381-90.
290. Palatini, U., et al., *Improved reference genome of the arboviral vector Aedes albopictus.* Genome Biology, 2020. **21**(1): p. 215.
291. Ma, Q., et al., *A mosquito small RNA genomics resource reveals dynamic evolution and host responses to viruses and transposons.* Genome Research, 2021.
292. Roiz, D., et al., *Detection of novel insect flavivirus sequences integrated in Aedes albopictus (Diptera: Culicidae) in Northern Italy.* Virol J, 2009. **6**: p. 93.
293. Pischedda, E., et al., *Insights Into an Unexplored Component of the Mosquito Repeatome: Distribution and Variability of Viral Sequences Integrated Into the Genome of the Arboviral Vector Aedes albopictus.* Front Genet, 2019. **10**: p. 93.
294. Russo, A.G., et al., *Novel insights into endogenous RNA viral elements in Ixodes scapularis and other arbovirus vector genomes.* Virus Evol, 2019. **5**(1): p. vez010.
295. Sánchez-Seco, M.P., et al., *Surveillance of arboviruses in Spanish wetlands: detection of new flavi- and phleboviruses.* Vector Borne Zoonotic Dis, 2010. **10**(2): p. 203-6.
296. Rizzo, F., et al., *Molecular characterization of flaviviruses from field-collected mosquitoes in northwestern Italy, 2011–2012.* Parasites & Vectors, 2014. **7**(1): p. 395.
297. Ter Horst, A.M., et al., *Endogenous Viral Elements Are Widespread in Arthropod Genomes and Commonly Give Rise to PIWI-Interacting RNAs.* J Virol, 2019. **93**(6).
298. Öhlund, P., H. Lundén, and A.-L. Blomström, *Insect-specific virus evolution and potential effects on vector competence.* Virus genes, 2019. **55**(2): p. 127-137.
299. Lan, Q. and A.M. Fallon, *Small Heat Shock Proteins Distinguish between two Mosquito Species and Confirm Identity of Their Cell Lines.* The American Journal of Tropical Medicine and Hygiene, 1990. **43**(6): p. 669-676.
300. Weger-Lucarelli, J., et al., *Adventitious viruses persistently infect three commonly used mosquito cell lines.* Virology, 2018. **521**: p. 175-180.

301. Igarashi, A., *Isolation of a Singh's Aedes albopictus cell clone sensitive to Dengue and Chikungunya viruses.* J Gen Virol, 1978. **40**(3): p. 531-44.
302. Macpherson, I. and M. Stoker, *Polyoma transformation of hamster cell clones—an investigation of genetic factors affecting cell competence.* Virology, 1962. **16**(2): p. 147-151.
303. Hilton, L., et al., *The NPro product of bovine viral diarrhea virus inhibits DNA binding by interferon regulatory factor 3 and targets it for proteasomal degradation.* J Virol, 2006. **80**(23): p. 11723-32.
304. Ongus, J.R., et al., *The 5' non-translated region of Varroa destructor virus 1 (genus Iflavirus): structure prediction and IRES activity in Lymantria dispar cells.* J Gen Virol, 2006. **87**(Pt 11): p. 3397-407.
305. Varjak, M., et al., *aBravo Is a Novel Aedes aegypti Antiviral Protein that Interacts with, but Acts Independently of, the Exogenous siRNA Pathway Effector Dicer 2.* Viruses, 2020. **12**(7).
306. Bartholomeeusen, K., et al., *A Chikungunya Virus trans-Replicase System Reveals the Importance of Delayed Nonstructural Polyprotein Processing for Efficient Replication Complex Formation in Mosquito Cells.* J Virol, 2018. **92**(14).
307. Ülper, L., et al., *Construction, properties, and potential application of infectious plasmids containing Semliki Forest virus full-length cDNA with an inserted intron.* Journal of Virological Methods, 2008. **148**(1): p. 265-270.
308. Saul, S., et al., *Differences in Processing Determinants of Nonstructural Polyprotein and in the Sequence of Nonstructural Protein 3 Affect Neurovirulence of Semliki Forest Virus.* J Virol, 2015. **89**(21): p. 11030-45.
309. Donald, C.L., et al., *Full Genome Sequence and sfRNA Interferon Antagonist Activity of Zika Virus from Recife, Brazil.* PLoS Negl Trop Dis, 2016. **10**(10): p. e0005048.
310. Donald, C.L., et al., *Antiviral RNA Interference Activity in Cells of the Predatory Mosquito, Toxorhynchites amboinensis.* Viruses, 2018. **10**(12): p. 694.
311. Stokes, S., et al., *The SUMOylation pathway suppresses arbovirus replication in Aedes aegypti cells.* PLoS Pathog, 2020. **16**(12): p. e1009134.
312. Attarzadeh-Yazdi, G., et al., *Cell-to-cell spread of the RNA interference response suppresses Semliki Forest virus (SFV) infection of mosquito cell cultures and cannot be antagonized by SFV.* J Virol, 2009. **83**(11): p. 5735-48.
313. O'Brien, C.A., et al., *Viral RNA intermediates as targets for detection and discovery of novel and emerging mosquito-borne viruses.* PLoS Negl Trop Dis, 2015. **9**(3): p. e0003629.
314. Warburg, O. and W. Christian, *Isolierung und Kristallisation des Gärungsferments Enolase.* Naturwissenschaften, 1941. **29**(39): p. 589-590.
315. Franzke, K., et al., *Detection, infection dynamics and small RNA response against Culex Y virus in mosquito-derived cells.* Journal of General Virology, 2018. **99**(12): p. 1739-1745.
316. Kärber, G., *Beitrag zur kollektiven Behandlung pharmakologischer Reihenversuche.* Naunyn-Schmiedebergs Archiv für experimentelle Pathologie und Pharmakologie, 1931. **162**(4): p. 480-483.
317. Hierholzer, J.C. and R.A. Killington, *2 - Virus isolation and quantitation*, in *Virology Methods Manual*, B.W.J. Mahy and H.O. Kangro, Editors. 1996, Academic Press: London. p. 25-46.
318. Watson, M., E. Schnettler, and A. Kohl, *viRome: an R package for the visualization and analysis of viral small RNA sequence datasets.* Bioinformatics, 2013. **29**(15): p. 1902-3.
319. Elmer, K., et al., *Analysis of endo-siRNAs in Drosophila.* Methods Mol Biol, 2014. **1173**: p. 33-49.
320. Okamura, K., N. Liu, and E.C. Lai, *Distinct mechanisms for microRNA strand selection by Drosophila Argonautes.* Mol Cell, 2009. **36**(3): p. 431-44.
321. Blair, C.D., *Mosquito RNAi is the major innate immune pathway controlling arbovirus infection and transmission.* Future Microbiol, 2011. **6**(3): p. 265-77.
322. Randall, R.E. and D.E. Griffin, *Within host RNA virus persistence: mechanisms and consequences.* Curr Opin Virol, 2017. **23**: p. 35-42.
323. Goic, B. and M.C. Saleh, *Living with the enemy: viral persistent infections from a friendly viewpoint.* Curr Opin Microbiol, 2012. **15**(4): p. 531-7.
324. Žusinaite, E., et al., *Mutations at the palmitoylation site of non-structural protein nsP1 of Semliki Forest virus attenuate virus replication and cause accumulation of compensatory mutations.* Journal of General Virology, 2007. **88**(7): p. 1977-1985.
325. Tassetto, M., et al., *Antiviral adaptive immunity and tolerance in the mosquito Aedes aegyti.* bioRxiv, 2018: p. 438911.
326. Tassetto, M., M. Kunitomi, and R. Andino, *Circulating Immune Cells Mediate a Systemic RNAi-Based Adaptive Antiviral Response in Drosophila.* Cell, 2017. **169**(2): p. 314-325 e13.

327. Stollar, V. and T.E. Shenk, *Homologous viral interference in Aedes albopictus cultures chronically infected with Sindbis virus.* J Virol, 1973. **11**(4): p. 592-5.
328. Laureti, M., et al., *Superinfection Exclusion in Mosquitoes and Its Potential as an Arbovirus Control Strategy.* Viruses, 2020. **12**(11).
329. Karpf, A.R., et al., *Superinfection exclusion of alphaviruses in three mosquito cell lines persistently infected with Sindbis virus.* Journal of Virology, 1997. **71**(9): p. 7119-7123.
330. Vazeille, M., et al., *Orally Co-Infected Aedes albopictus from La Reunion Island, Indian Ocean, Can Deliver Both Dengue and Chikungunya Infectious Viral Particles in Their Saliva.* PLOS Neglected Tropical Diseases, 2010. **4**(6): p. e706.
331. Goertz, G.P., et al., *Mosquito co-infection with Zika and chikungunya virus allows simultaneous transmission without affecting vector competence of Aedes aegypti.* PLoS Negl Trop Dis, 2017. **11**(6): p. e0005654.
332. Furuya-Kanamori, L., et al., *Co-distribution and co-infection of chikungunya and dengue viruses.* BMC Infect Dis, 2016. **16**: p. 84.
333. Tassetto, M., et al., *Control of RNA viruses in mosquito cells through the acquisition of vDNA and endogenous viral elements.* eLife, 2019. **8**: p. e41244.
334. Sasaki, T., et al., *Argonaute 2 Suppresses Japanese Encephalitis Virus Infection in Aedes aegypti.* Jpn J Infect Dis, 2017. **70**(1): p. 38-44.
335. Sanchez-Vargas, I., et al., *RNA interference, arthropod-borne viruses, and mosquitoes.* Virus Res, 2004. **102**(1): p. 65-74.
336. Czech, B., et al., *piRNA-Guided Genome Defense: From Biogenesis to Silencing.* Annu Rev Genet, 2018. **52**: p. 131-157.
337. Joosten, J., et al., *The Tudor protein Veneno assembles the ping-pong amplification complex that produces viral piRNAs in Aedes mosquitoes.* Nucleic Acids Res, 2019. **47**(5): p. 2546-2559.
338. Joosten, J., et al., *PIWI proteomics identifies Atari and Pasilla as piRNA biogenesis factors in Aedes mosquitoes.* Cell Reports, 2021. **35**(5).
339. Halbach, R., et al., *A satellite repeat-derived piRNA controls embryonic development of Aedes.* Nature, 2020. **580**(7802): p. 274-277.
340. Betting, V., et al., *A regulatory network of a piRNA and lncRNA initiates responder and trailer piRNA formation during embryonic development of Aedes mosquitoes.* bioRxiv, 2020: p. 2020.03.23.003038.
341. Betting, V. and R.P. Van Rij, *Countering Counter-Defense to Antiviral RNAi.* Trends Microbiol, 2020. **28**(8): p. 600-602.
342. Shi, X., et al., *Requirement of the N-Terminal Region of Orthobunyavirus Nonstructural Protein NSm for Virus Assembly and Morphogenesis.* Journal of Virology, 2006. **80**(16): p. 8089-8099.
343. Fontana, J., et al., *The unique architecture of Bunyamwera virus factories around the Golgi complex.* Cell Microbiol, 2008. **10**(10): p. 2012-28.
344. Leventhal, S.S., et al., *A Look into Bunyavirales Genomes: Functions of Non-Structural (NS) Proteins.* Viruses, 2021. **13**(2).
345. Kraatz, F., et al., *Schmallenberg virus non-structural protein NSm: Intracellular distribution and role of non-hydrophobic domains.* Virology, 2018. **516**: p. 46-54.
346. Tilston-Lunel, N.L., et al., *Generation of Recombinant Oropouche Viruses Lacking the Nonstructural Protein NSm or NSs.* J Virol, 2015. **90**(5): p. 2616-27.
347. Ishihara, Y., et al., *Akabane virus nonstructural protein NSm regulates viral growth and pathogenicity in a mouse model.* J Vet Med Sci, 2016. **78**(9): p. 1391-1397.
348. Seong, R.-K., J.K. Lee, and O.S. Shin, *Zika Virus-Induction of the Suppressor of Cytokine Signaling 1/3 Contributes to the Modulation of Viral Replication.* Pathogens (Basel, Switzerland), 2020. **9**(3): p. 163.
349. Samuel, G.H., et al., *Yellow fever virus capsid protein is a potent suppressor of RNA silencing that binds double-stranded RNA.* Proceedings of the National Academy of Sciences, 2016: p. 201600544.
350. Blanchard, E. and P. Roingeard, *The Hepatitis C Virus-Induced Membranous Web in Liver Tissue.* Cells, 2018. **7**(11).
351. Junjhon, J., et al., *Ultrastructural characterization and three-dimensional architecture of replication sites in dengue virus-infected mosquito cells.* J Virol, 2014. **88**(9): p. 4687-97.
352. Welsch, S., et al., *Composition and three-dimensional architecture of the dengue virus replication and assembly sites.* Cell Host Microbe, 2009. **5**(4): p. 365-75.

353. Qiu, Y., et al., *Flavivirus induces and antagonizes antiviral RNA interference in both mammals and mosquitoes.* Sci Adv, 2020. **6**(6): p. eaax7989.
354. Brown, D. *Alphavirus growth in cultured vertebrate and invertebrate cells*. in *Vectors in virus biology*. 1984.
355. Ahola, T., et al., *Semliki Forest virus mRNA capping enzyme requires association with anionic membrane phospholipids for activity.* The EMBO Journal, 1999. **18**(11): p. 3164-3172.
356. Guo, Z., Y. Li, and S.W. Ding, *Small RNA-based antimicrobial immunity.* Nat Rev Immunol, 2019. **19**(1): p. 31-44.
357. Chao, J.A., et al., *Dual modes of RNA-silencing suppression by Flock House virus protein B2.* Nat Struct Mol Biol, 2005. **12**(11): p. 952-7.
358. Qian, Q., et al., *The Capsid Protein of Semliki Forest Virus Antagonizes RNA Interference in Mammalian Cells.* J Virol, 2020. **94**(3).
359. Schnettler, E., et al., *Noncoding flavivirus RNA displays RNA interference suppressor activity in insect and Mammalian cells.* J Virol, 2012. **86**(24): p. 13486-500.
360. Gauliard, N., et al., *Rift Valley fever virus noncoding regions of L, M and S segments regulate RNA synthesis.* Virology, 2006. **351**(1): p. 170-179.
361. Fuller, F., A.S. Bhown, and D.H. Bishop, *Bunyavirus nucleoprotein, N, and a non-structural protein, NSS, are coded by overlapping reading frames in the S RNA.* J Gen Virol, 1983. **64 (Pt 8)**: p. 1705-14.
362. Kohl, A., et al., *Genetic elements regulating packaging of the Bunyamwera orthobunyavirus genome.* J Gen Virol, 2006. **87**(Pt 1): p. 177-87.
363. Eifan, S.A. and R.M. Elliott, *Mutational analysis of the Bunyamwera orthobunyavirus nucleocapsid protein gene.* Journal of virology, 2009. **83**(21): p. 11307-11317.
364. Eifan, S., et al., *Non-structural proteins of arthropod-borne bunyaviruses: roles and functions.* Viruses, 2013. **5**(10): p. 2447-68.
365. Brennan, B., S.R. Welch, and R.M. Elliott, *The Consequences of Reconfiguring the Ambisense S Genome Segment of Rift Valley Fever Virus on Viral Replication in Mammalian and Mosquito Cells and for Genome Packaging.* PLOS Pathogens, 2014. **10**(2): p. e1003922.
366. Gainetdinov, I., et al., *A Single Mechanism of Biogenesis, Initiated and Directed by PIWI Proteins, Explains piRNA Production in Most Animals.* Mol Cell, 2018. **71**(5): p. 775-790 e5.
367. McFarlane, M., et al., *The Aedes aegypti Domino Ortholog p400 Regulates Antiviral Exogenous Small Interfering RNA Pathway Activity and ago-2 Expression.* mSphere, 2020. **5**(2).
368. Spellberg, M.J. and M.T. Marr, *FOXO regulates RNA interference in Drosophila and protects from RNA virus infection.* Proceedings of the National Academy of Sciences, 2015. **112**(47): p. 14587-14592.
369. Lequime, S., R.E. Paul, and L. Lambrechts, *Determinants of Arbovirus Vertical Transmission in Mosquitoes.* PLOS Pathogens, 2016. **12**(5): p. e1005548.
370. Schultz, M.J., H.M. Frydman, and J.H. Connor, *Dual Insect specific virus infection limits Arbovirus replication in Aedes mosquito cells.* Virology, 2018. **518**: p. 406-413.
371. Bolling, B.G., et al., *Insect-Specific Virus Discovery: Significance for the Arbovirus Community.* Viruses, 2015. **7**(9): p. 4911-28.
372. Rozen-Gagnon, K., et al., *Argonaute-CLIP delineates versatile, functional RNAi networks in Aedes aegypti, a major vector of human viruses.* Cell Host Microbe, 2021. **29**(5): p. 834-848.e13.
373. Olson, K.E., et al., *Developing arbovirus resistance in mosquitoes.* Insect Biochem Mol Biol, 2002. **32**(10): p. 1333-43.
374. Lambrechts, L. and M.-C. Saleh, *Manipulating Mosquito Tolerance for Arbovirus Control.* Cell Host & Microbe, 2019. **26**(3): p. 309-313.
375. Flores, H.A. and S.L. O'Neill, *Controlling vector-borne diseases by releasing modified mosquitoes.* Nature Reviews Microbiology, 2018. **16**(8): p. 508-518.
376. Achee, N.L., et al., *Alternative strategies for mosquito-borne arbovirus control.* PLOS Neglected Tropical Diseases, 2019. **13**(1): p. e0006822.

Publications

Some results of this project were submitted to peer-reviewed journals:

Scherer, C.; Knowles, J.; Vattipally, B. S.; Fredericks, A. C, Fuss, J.; Maringer, K.; Fernandez-Sesma, A.; Merits, A.; Varjak, M.; Kohl, A.; Schnettler, E., 2021: *An Aedes aegypti-derived Ago2 knockout cell line to investigate arbovirus infections*, submitted to Viruses

Hofmann, S., Krajewski, M., **Scherer, C.**, Scholz, V., Mordhorst, V., Truschow, P., Schöbel, A., Reimer, R., Schwudke, D., Herker, E., 2018: *Complex lipid metabolic remodeling is required for efficient hepatitis C virus replication*, BBA - Molecular and Cell Biology of Lipids 1863, 1041–1056

Acknowledgements

Heureka! Despite a worldwide pandemic and a facade renovation, I am finally done. I would not have gotten that far without some people helping and supporting me.

First of all, I would like to thank Prof. Dr. Esther Schnettler for giving me the opportunity to work on my PhD in her lab. It has been a time full with trial and error, but your door was always open for a fruitful conversation. Thank you for your extensive advise and guidance and staying open-minded towards strange ideas and hypotheses. I would also like to thank our collaborators Alain Kohl, Kevin Maringer, Margus Varjak, Andres Merits and whoever I forgot now that provided me with reporter viruses, plasmids and first author papers. Thank you.

But all of this would have been nothing without a team and a really motivational, engaging and helpful atmosphere in the team. I would like to thank Mayke, Mine, András, Marlis, Marvin and 'the late' Bernhard for all their support, a sympathetic ear and teasing verbal exchanges.

I was lucky to get one of the best office seats in the whole building: at the reflectorium (* Harry Potter jingle playing). I got the chance to spend at least some of the time up there with so many great people. First of all, thank you, Jonny, for being my constant companion through the chaos of the PhD. You are a great discussion partner and supported me in so many ways. But there are so many more like Herr Heepmann, Caro, Nadine, Magda, Rashwita (always to the point) and Eric, thank you for a fantastic time up there. Unfortunately, the severe acute respiratory syndrome-related coronavirus type 2 (SARS-Cov2, family *Coronaviridae*, genus *Betacoronavirus*) has stolen much of our shared time.

Although my family stopped asking me what the hell I am investigating on shortly after starting my PhD (and ended up with "She is feeding mosquitoes. I really can't tell you what she does"), they always supported me from afar and I am very thankful for their understanding.

Talking about understanding and support I have to mention all the other friends outside the institute that helped me getting through my PhD. Thank you Maxi for reading this 'thing' and the time spent together. Thank you Marius not only for helping me to understand the whole administrative shit of the Studienbüro and the university of Hamburg, but being a constant companion throughout the whole time. And all the other people that distracted me while having a beer.

Till, I know you were close to establishing a support group for temporary life companions suffering from their PhD girlfriends, but thank you for your love. You were never doubting my decision and supported me not only with the best menus I ever had. #EinsNachDemAnderen #SchlefazenWirHeute

So, that's it.

"We've always defined ourselves by the ability to overcome the impossible. And we count these moments. These moments when we dare to aim higher, to break barriers, to reach for the stars, to make the unknown known. We count these moments as our proudest achievements."

Interstellar, Cooper

Eidesstattliche Versicherung

Hiermit erkläre ich an Eides statt, dass ich die vorliegende Dissertationsschrift selbst verfasst und keine anderen als die angegebenen Quellen und Hilfsmittel benutzt habe.

Hamburg, den 20.05.2021

Christina Scherer

6. Supplementary data

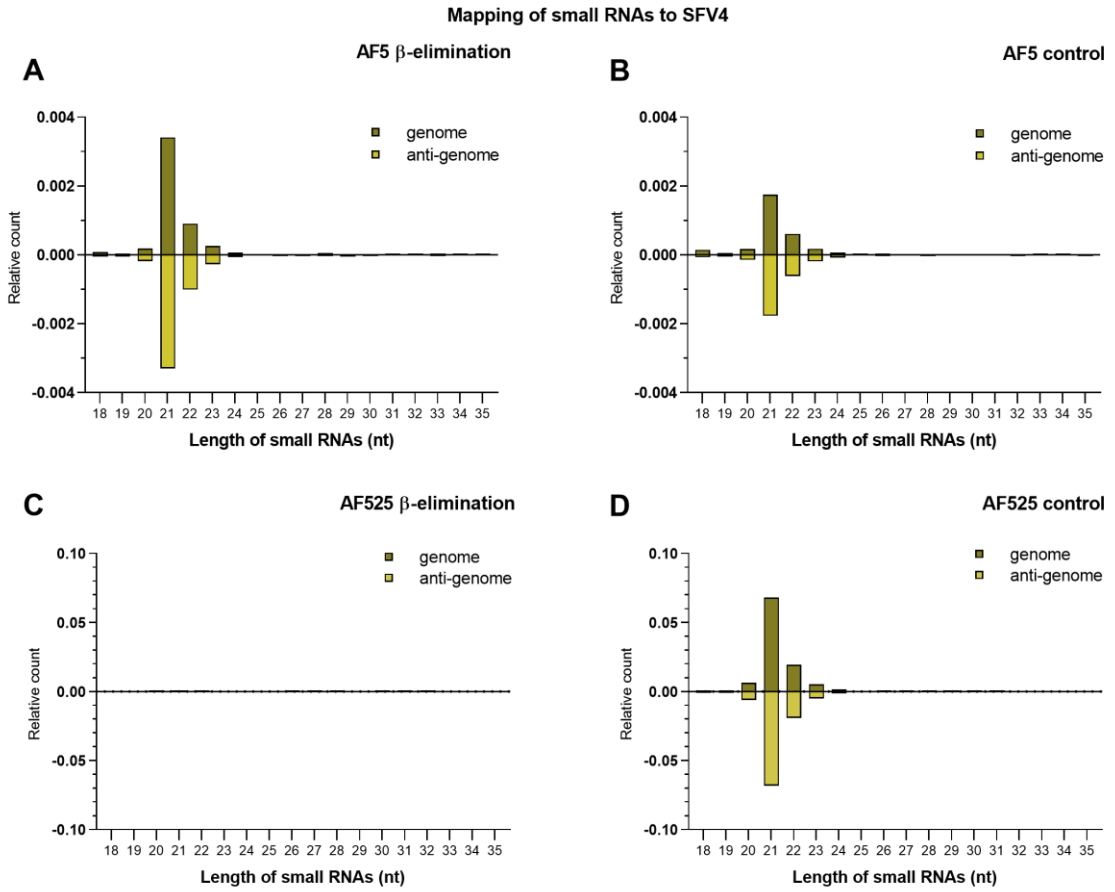

Figure S1: Length distribution of small RNAs in AF525 and AF5 cells, infected with SFV4 and treated with β-elimination reagents (sequencing run II).

NGS data of SFV4-infected AF525 and AF5 cells was mapped to the SFV4 genome and antigenome. Dark yellow bars indicate sequences mapping to the genome of SFV4 while light yellow ones map to the anti-genome of the virus. Positive numbers are RNAs mapping to the sense strand of SFV4 (dark yellow) while negative numbers indicate RNAs mapping to the anti-sense strand of SFV4 (light yellow). Y-axis: relative count of small RNAs normalized to clean reads. A: AF5 cells treated with complete β-elimination reagents. B: AF5 β-elimination control. C: AF525 cells treated with complete β-elimination protocol. D: AF525 control. Two independent experiments were carried out and the results of one representative experiment are shown here.

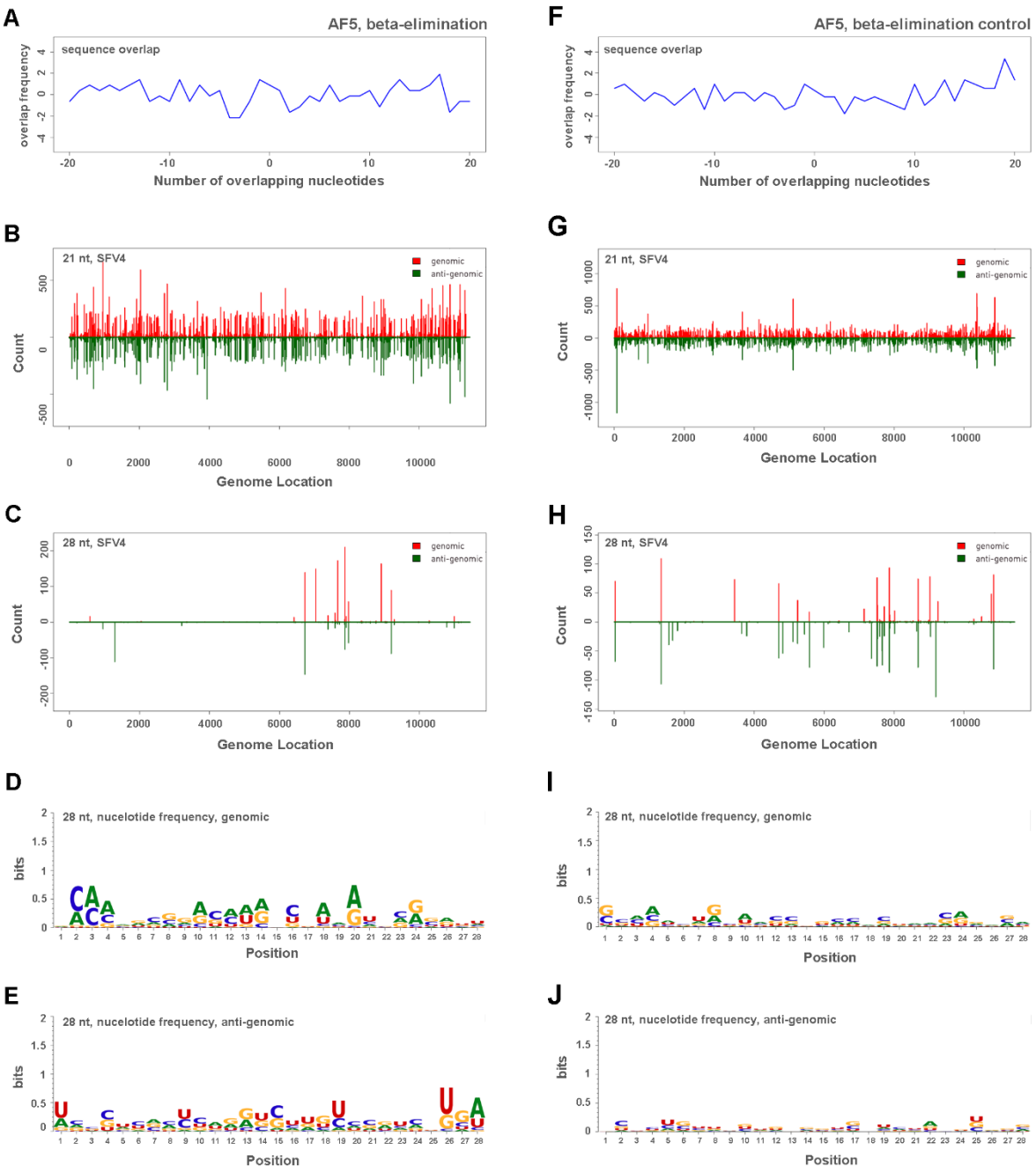

Figure S2: Characteristics of β-eliminated small RNAs of SFV4-infected AF5 cells (sequencing run II).
Small RNAs of AF5 cells treated with β elimination reagents (A-E) and control (F-J). A, F: sense and anti-sense sequence overlap of vpiRNAs (25-29 nt). B, G: siRNA (21 nt) length distribution along the SFV4 genome (red, mapped to the genome; green, mapped to the antigenome). C, H: vpiRNA (28 nt) length distribution over the SFV4 genome (red, mapped to the genome; green, mapped to the antigenome). D, E, I, J: Relative nucleotide frequency and conservation per position of the 28 nt long vpiRNAs mapping to the SFV4 genome (D, I) or antigenome (E, J). Two independent experiments were carried out and the results of one representative experiment are shown here.

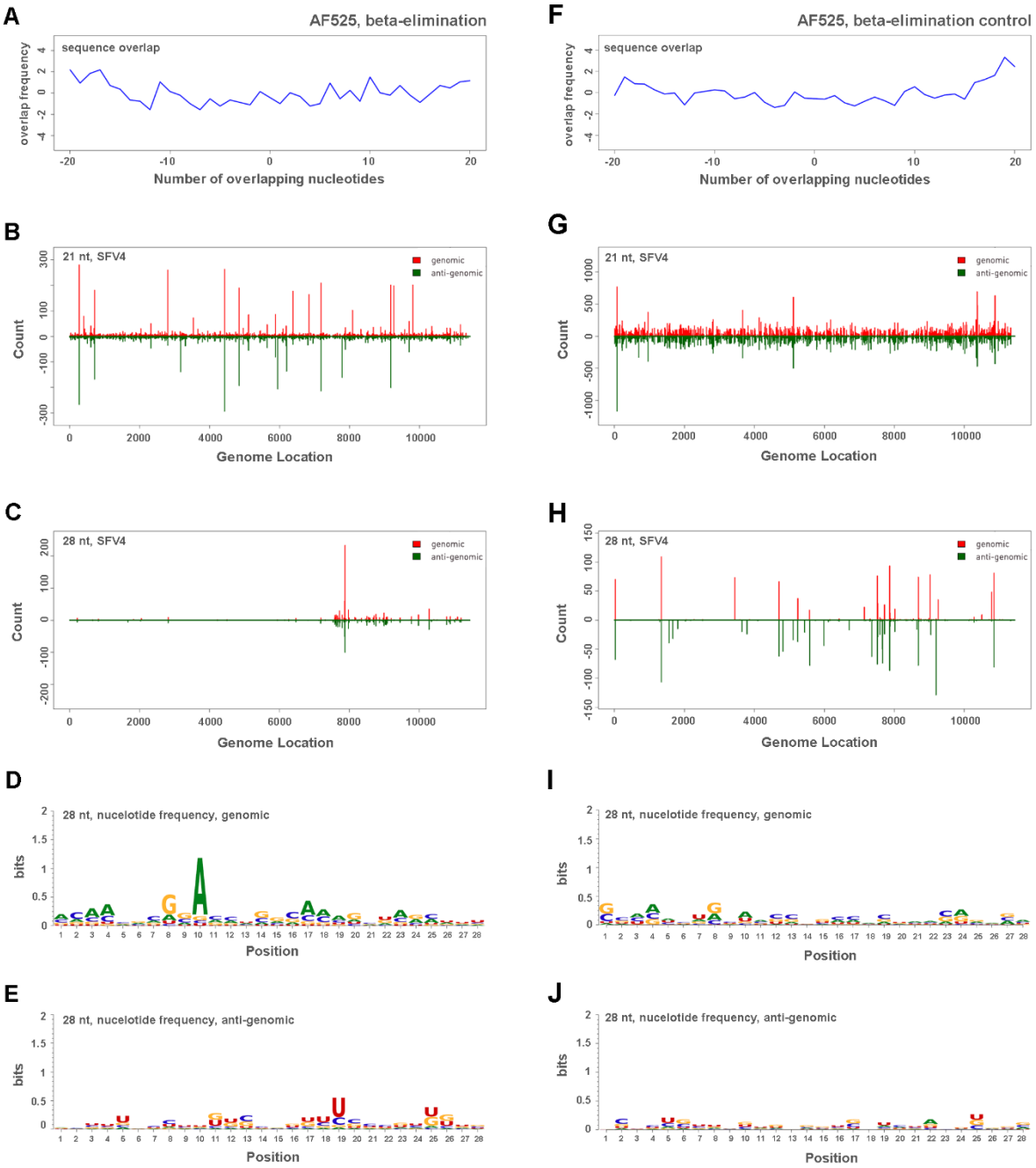

Figure S3: Characteristics of β-eliminated small RNAs of SFV4-infected AF525 cells (sequencing run II).
Small RNAs of SFV4-infected AF525 cells treated with β-elimination reagents (A-E) and control (F-J). A, F: sense and anti-sense sequence overlap of vpiRNAs (25-29 nt). B, G: siRNA (21 nt) length distribution along the SFV4 genome (red, mapped to the genome; green, mapped to the antigenome). C, H: vpiRNA (28 nt) length distribution over the SFV4 genome (red, mapped to the genome; green, mapped to the antigenome). D, E, I, J: Relative nucleotide frequency and conservation per position of the 28 nt long vpiRNAs mapping to the SFV4 genome (D, I) or antigenome (E, J). Two independent experiments were carried out, and the results of one representative experiment are shown here.

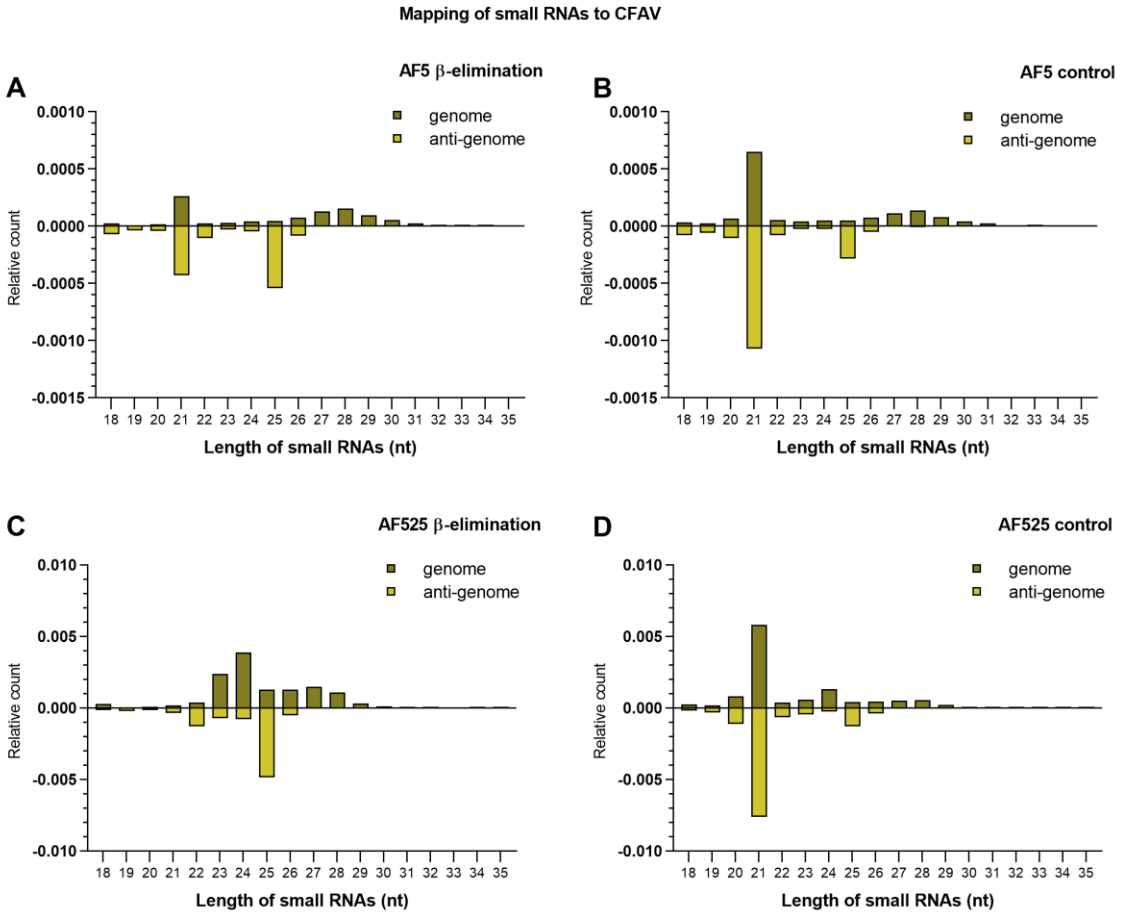

Figure S4: Length distribution of small RNAs in AF5 and AF525 cells treated with β-elimination reagents mapping to CFAV (sequencing run I).

NGS data of AF525 and AF5 cells was mapped to the genome and anti-genome of persistently infecting CFAV. Dark yellow bars indicate sequences mapping to the genome of CFAV while light yellow ones map to the anti-genome of the virus. X-axis: length of small RNAs, y-axis: relative count of small RNAs normalized to clean reads. A: AF5 cells treated with complete β-elimination reagents. B: AF5 β-elimination control. C: AF525 cells treated with complete β-elimination protocol. D: AF525 control.

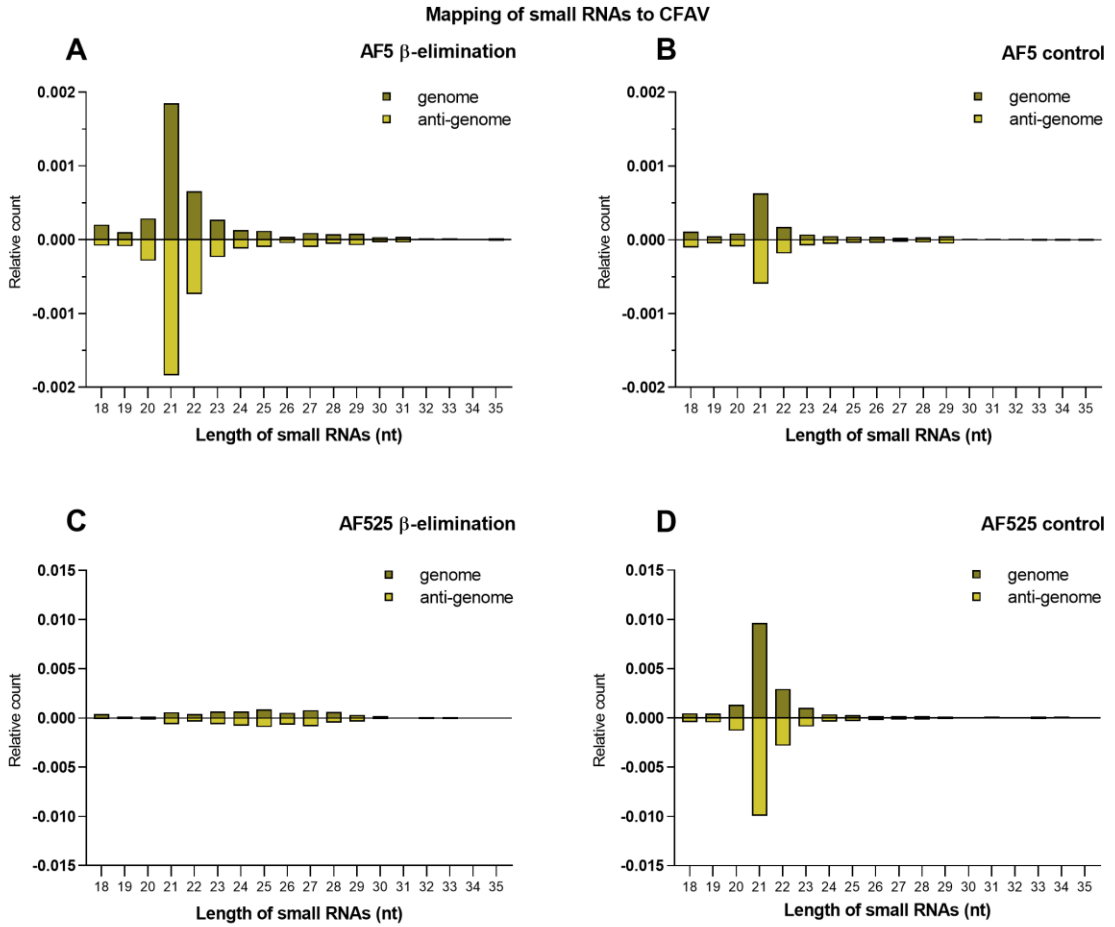

Figure S5: Length distribution of small RNAs in AF5 and AF525 cells treated with β-elimination reagents mapping to CFAV (sequencing run II).

NGS data of AF525 and AF5 cells was mapped to the genome and anti-genome of persistently infecting CFAV. Dark yellow bars indicate sequences mapping to the genome of CFAV while light yellow ones map to the anti-genome of the virus. X-axis: length of small RNAs, y-axis: relative count of small RNAs normalized to clean reads. A: AF5 cells treated with complete β-elimination reagents. B: AF5 β-elimination control. C: AF525 cells treated with complete β-elimination protocol. D: AF525 control.

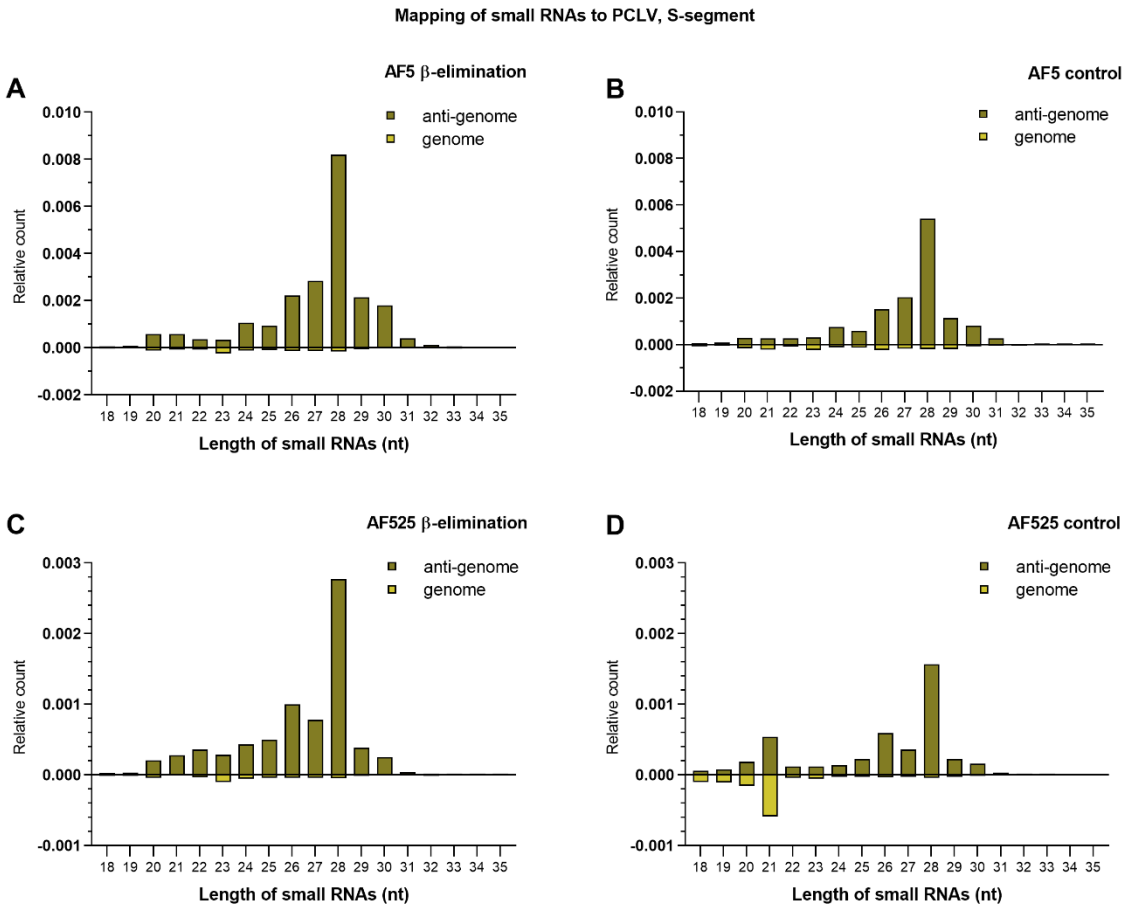

Figure S6: Length distribution of small RNAs in AF5 and AF525 cells treated with β-elimination reagents mapping to the S-segment of PCLV (sequencing run I).

NGS data of AF525 and AF5 cells was mapped to the genome and anti-genome of persistently infecting PCLV S-segment. Dark yellow bars indicate sequences mapping to the genome of PCLV while light yellow ones map to the anti-genome of the virus. X-axis: length of small RNAs, y-axis: relative count of small RNAs normalized to clean reads. A: AF5 cells treated with complete β-elimination reagents. B: AF5 β-elimination control. C: AF525 cells treated with complete β-elimination protocol. D: AF525 control.

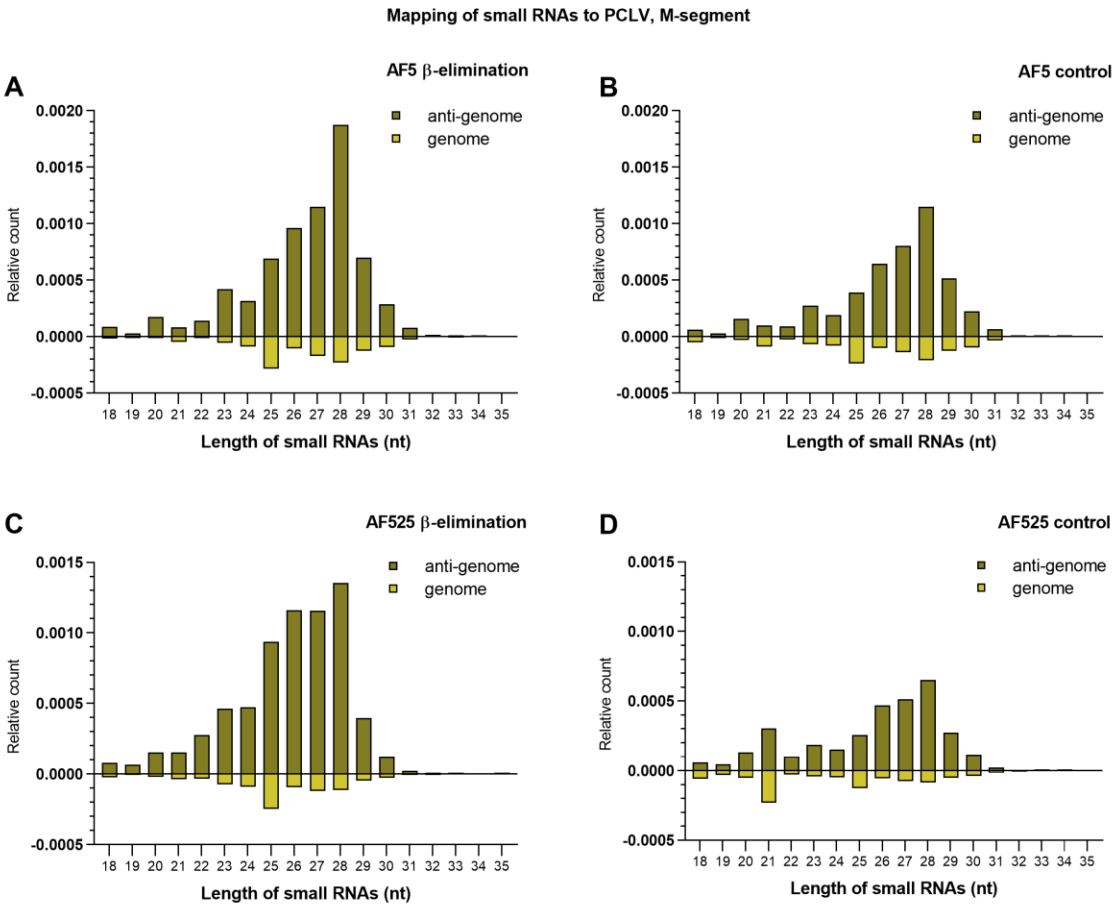

Figure S7: Length distribution of small RNAs in AF5 and AF525 cells treated with β-elimination reagents mapping to the M-segment of PCLV (sequencing run I).

NGS data of AF525 and AF5 cells was mapped to the genome and anti-genome of persistently infecting PCLV M-segment. Dark yellow bars indicate sequences mapping to the genome of PCLV while light yellow ones map to the anti-genome of the virus. X-axis: length of small RNAs, y-axis: relative count of small RNAs normalized to clean reads. A: AF5 cells treated with complete β-elimination reagents. B: AF5 β-elimination control. C: AF525 cells treated with complete β-elimination protocol. D: AF525 control.

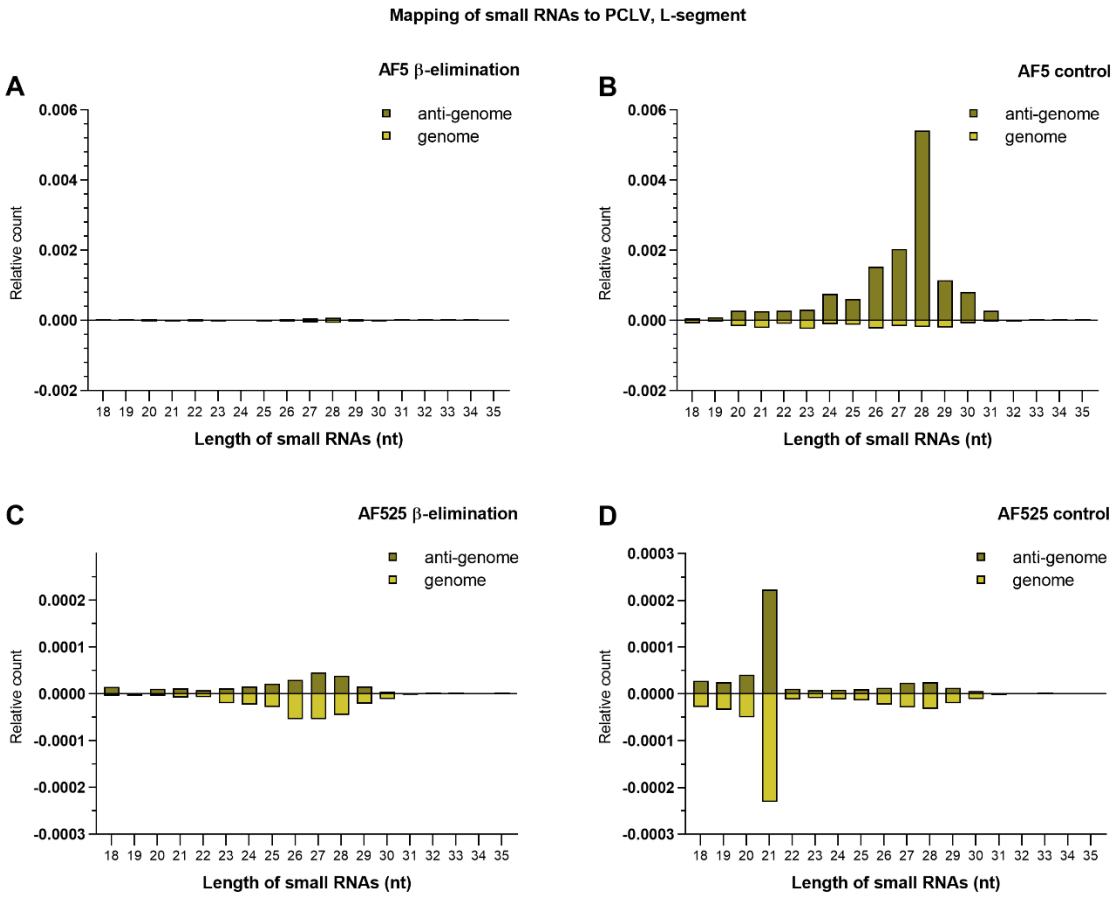

Figure S8: Length distribution of small RNAs in AF5 and AF525 cells treated with ß-elimination reagents mapping to the L-segment of PCLV (sequencing run I).

NGS data of AF525 and AF5 cells was mapped to the genome and anti-genome of persistently infecting PCLV L-segment. Dark yellow bars indicate sequences mapping to the genome of PCLV while light yellow ones map to the anti-genome of the virus. X-axis: length of small RNAs, y-axis: relative count of small RNAs normalized to clean reads. A: AF5 cells treated with complete ß-elimination reagents. B: AF5 ß-elimination control. C: AF525 cells treated with complete ß-elimination protocol. D: AF525 control.

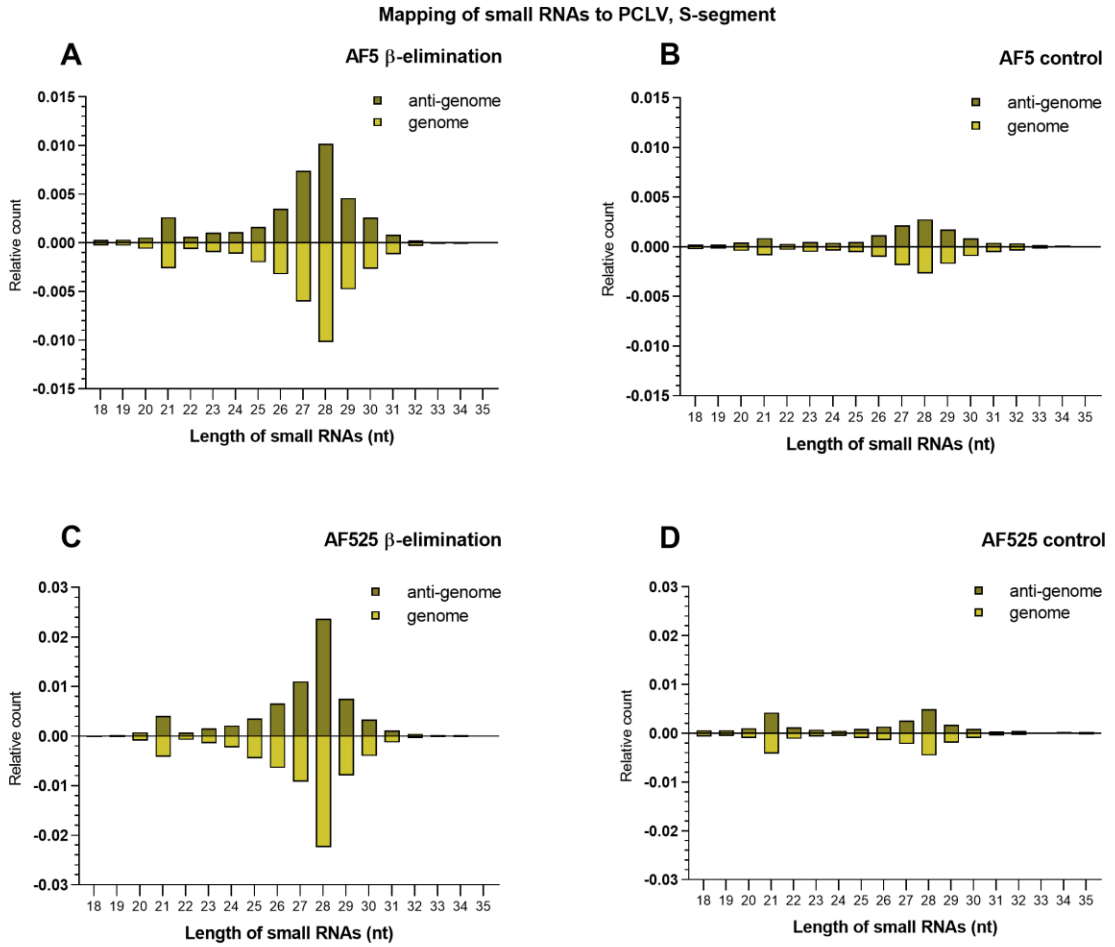

Figure S9: Length distribution of small RNAs in AF5 and AF525 cells treated with ß-elimination reagents mapping to the S-segment of PCLV (sequencing run II).

NGS data of AF525 and AF5 cells was mapped to the genome and anti-genome of persistently infecting PCLV S-segment. Dark yellow bars indicate sequences mapping to the genome of PCLV while light yellow ones map to the anti-genome of the virus. X-axis: length of small RNAs, y-axis: relative count of small RNAs normalized to clean reads. A: AF5 cells treated with complete ß-elimination reagents. B: AF5 ß-elimination control. C: AF525 cells treated with complete ß-elimination protocol. D: AF525 control.

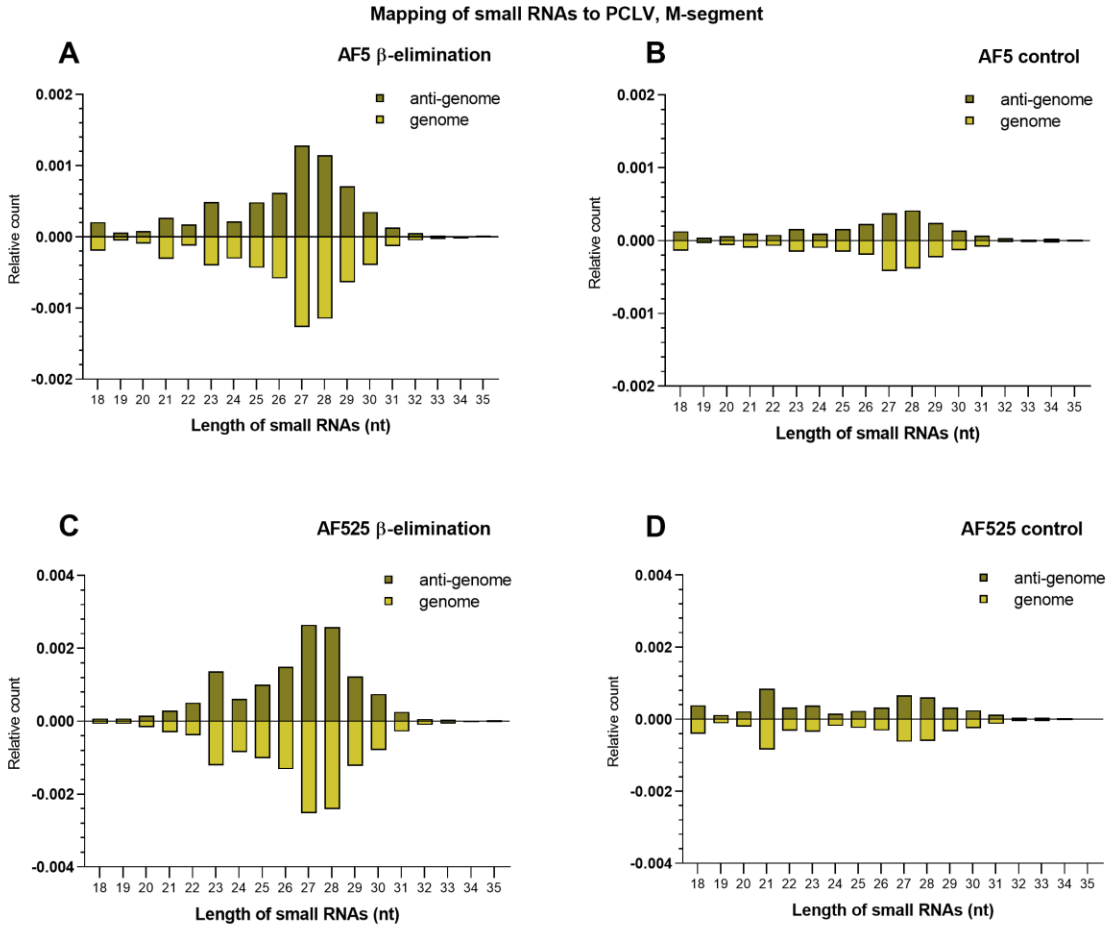

Figure S10: Length distribution of small RNAs in AF5 and AF525 cells treated with β-elimination reagents mapping to the M-segment of PCLV (sequencing run II).

NGS data of AF525 and AF5 cells was mapped to the genome and anti-genome of persistently infecting PCLV M-segment. Dark yellow bars indicate sequences mapping to the genome of PCLV while light yellow ones map to the anti-genome of the virus. X-axis: length of small RNAs, y-axis: relative count of small RNAs normalized to clean reads. A: AF5 cells treated with complete β-elimination reagents. B: AF5 β-elimination control. C: AF525 cells treated with complete β-elimination protocol. D: AF525 control.

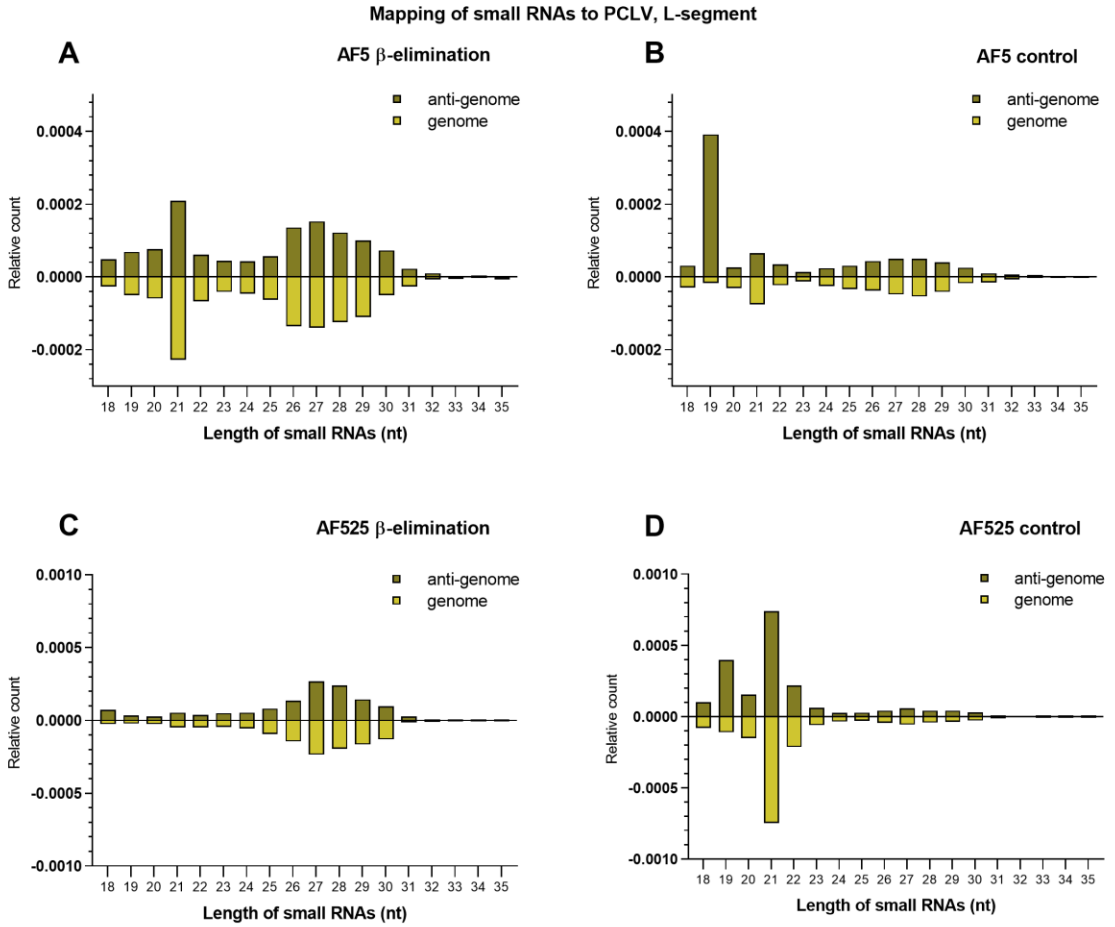

Figure S11: Length distribution of small RNAs in AF5 and AF525 cells treated with ß-elimination reagents mapping to the L-segment of PCLV (sequencing run II).

NGS data of AF525 and AF5 cells was mapped to the genome and anti-genome of persistently infecting PCLV L-segment. Dark yellow bars indicate sequences mapping to the genome of PCLV while light yellow ones map to the anti-genome of the virus. X-axis: length of small RNAs, y-axis: relative count of small RNAs normalized to clean reads. A: AF5 cells treated with complete ß-elimination reagents. B: AF5 ß-elimination control. C: AF525 cells treated with complete ß-elimination protocol. D: AF525 control.

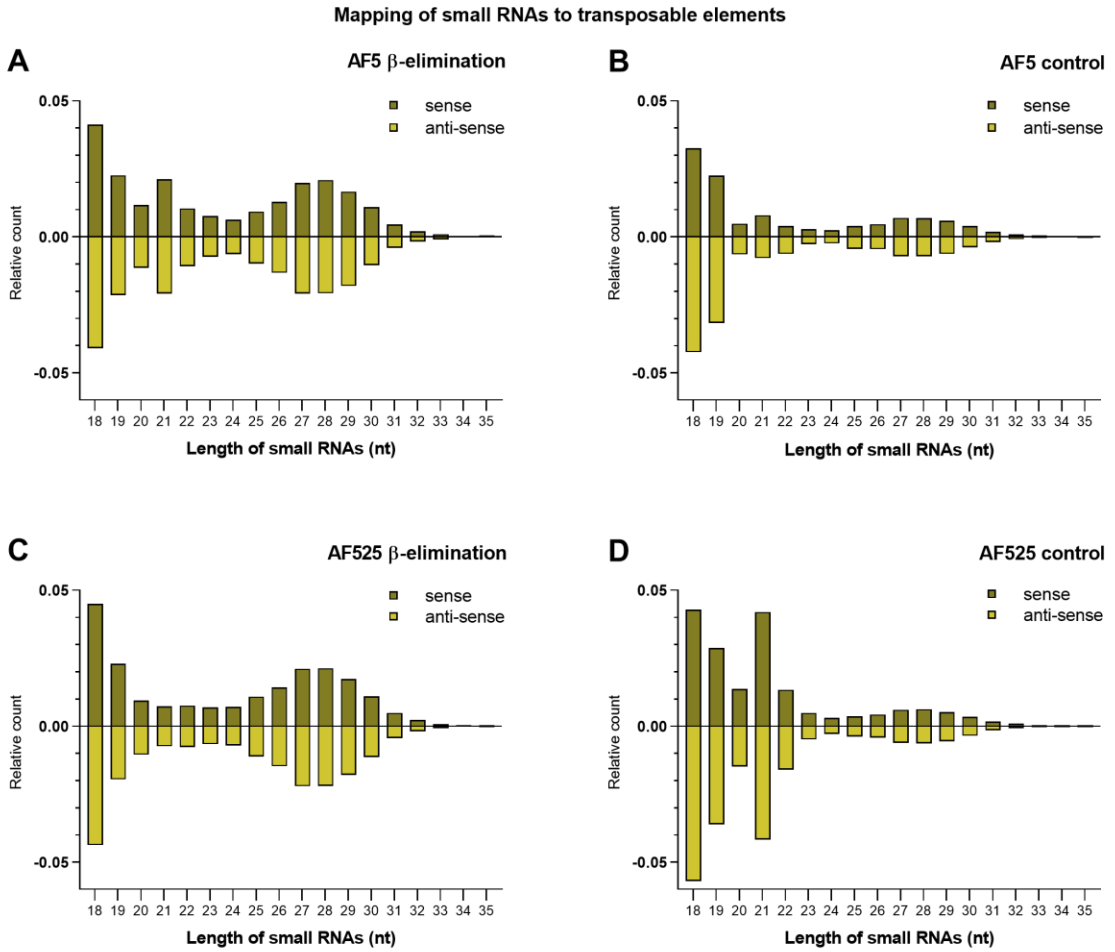

Figure S12: Length distribution of small RNAs from SFV4-infected AF5 and AF525 cells mapping to TEs (sequencing run II). *Left panel side (A, C) shows β-eliminated treated samples of SFV4-infected AF5 and AF525 cells, right panel side shows the results for untreated controls (B, D). X-axis displays the different lengths of small RNAs from 18 nt to 35 nt and y-axis displays the relative amount of small RNAs normalized to clean reads. Positive numbers are RNAs mapping to the sense strand of TEs (dark yellow) while negative numbers indicate RNAs mapping to the anti-sense strand of TEs (light yellow). Two independent experiments were carried out and the results of one representative experiment are shown here.*

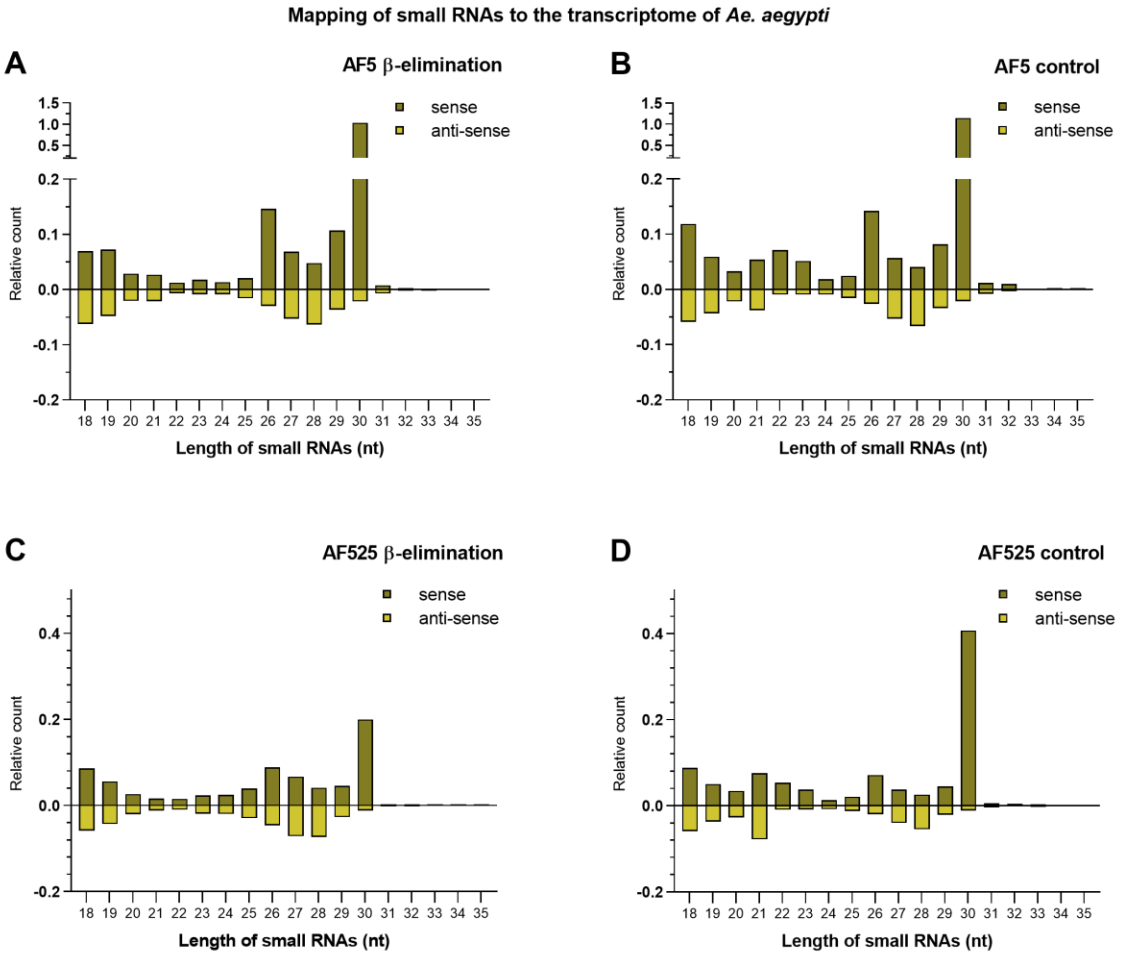

Figure S13: Length distribution of small RNAs from SFV4-infected AF5 and AF525 cells mapping to the transcriptome of Aedes aegypti Liverpool AGWG, version AaegL5.2 (sequencing run I).

Left panel side (A, C) shows β-eliminated treated samples of SFV4-infected AF5 and AF525 cells, right panel side shows the results for untreated controls (B, D). X-axis displays the different lengths of small RNAs from 18 nt to 35 nt and y-axis displays the amount of small RNAs normalized to clean reads. Positive numbers are RNAs mapping to sense RNAs (dark yellow) while negative numbers map to anti-sense RNAs (light yellow). Two independent experiments were carried out and the results of one representative experiment are shown here.

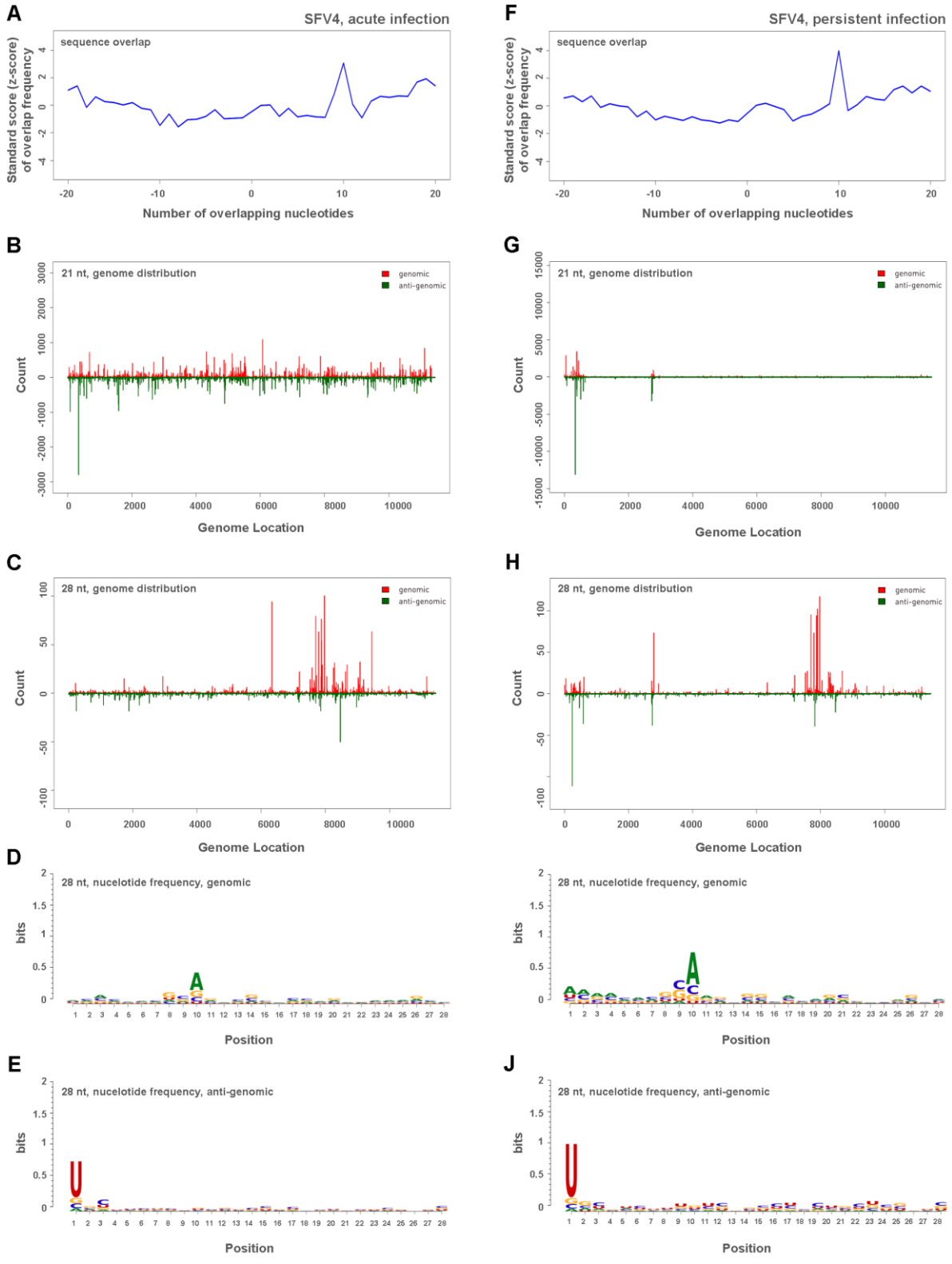

Figure S14: Small RNA sequencing data of SFV4 acute infection in AF5 cells (A-E) and persistent infection (F-J).
A, F: sense and anti-sense sequence overlap of vpiRNAs (25-29 nt). Length distribution along the SFV4 genome and anti-genome for 21 nt siRNA (B, G) or 28 nt piRNAs (C, H) (red: genome; green: antigenome). D, E, I, J: Relative nucleotide frequency and conservation per position of the 28 nt long vpiRNAs mapping to the SFV4 genome (D, I) or antigenome (E, J).

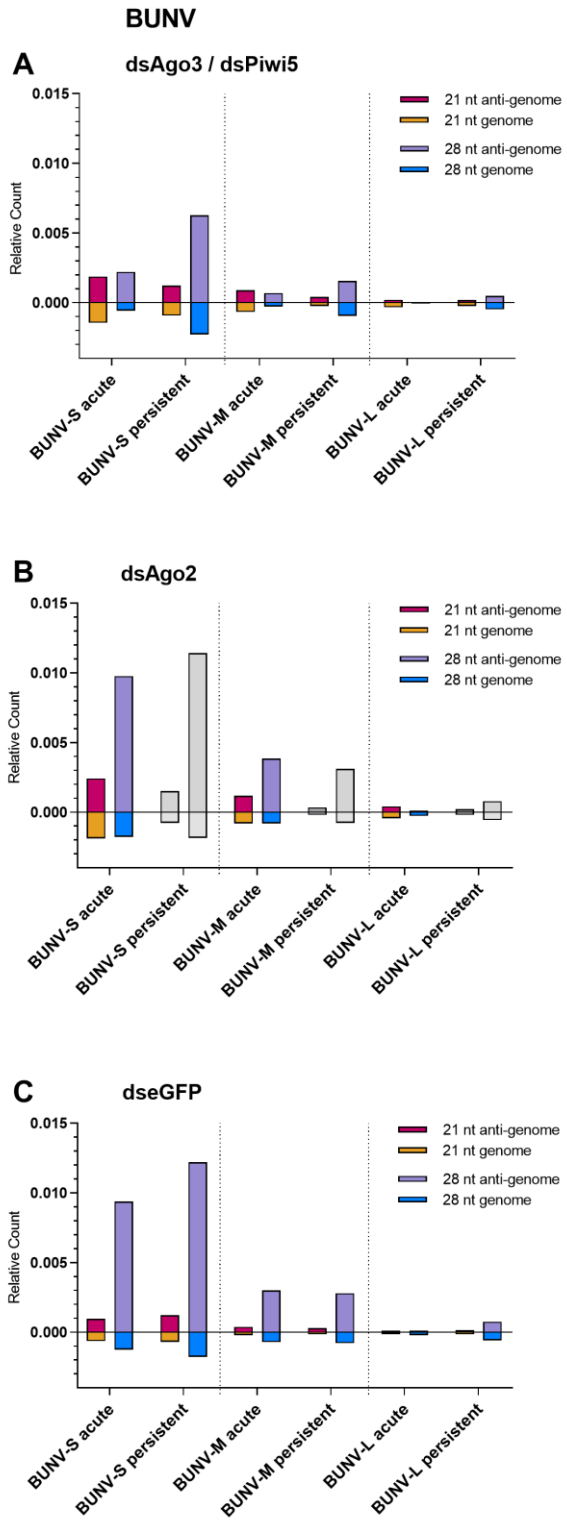

Figure S15: Distribution of 21 nt vsiRNAs and 28 nt vpiRNAs of BUNV infected AF5 cells transfected with dsRNA targeting different transcripts of RNAi pathway proteins.

Small RNA distribution determined by analysis of sequencing results of AF5 cells with either acute (MOI 5) or persistent BUNV infection, transfected with either dsAgo2 (B), dseGFP as control (C) or a combination of dsAgo3 and dsPiwi5 (A). X-axis: sequencing data of BUNV S, M and L segment for acute and persistent infection, y-axis: relative count of small RNAs normalized to total clean reads of the sequencing run. Relative count of 21 nt long vsiRNAs of the anti-genome (red) or genome (orange) or 28 nt long vpiRNAs of the anti-genome (purple) or genome (blue). Grey bars: Knockdown with dsAgo2 not sufficient, see associated data in Figure 32D.

List of figures

List of supplementary figures

List of tables